



THE HONG KONG  
POLYTECHNIC UNIVERSITY

香港理工大學

Pao Yue-kong Library

包玉剛圖書館

---

## Copyright Undertaking

This thesis is protected by copyright, with all rights reserved.

**By reading and using the thesis, the reader understands and agrees to the following terms:**

1. The reader will abide by the rules and legal ordinances governing copyright regarding the use of the thesis.
2. The reader will use the thesis for the purpose of research or private study only and not for distribution or further reproduction or any other purpose.
3. The reader agrees to indemnify and hold the University harmless from and against any loss, damage, cost, liability or expenses arising from copyright infringement or unauthorized usage.

If you have reasons to believe that any materials in this thesis are deemed not suitable to be distributed in this form, or a copyright owner having difficulty with the material being included in our database, please contact [lbsys@polyu.edu.hk](mailto:lbsys@polyu.edu.hk) providing details. The Library will look into your claim and consider taking remedial action upon receipt of the written requests.

“Syntheses and Characterization of ruthenium  $\eta^2$ -dihydrogen  
and  $\eta^2$ -silane complexes”

A Thesis Submitted to

The Department of Applied Biology and Chemical Technology

for the degree of Master of Philosophy

at

The Hong Kong Polytechnic University

by

Siu-Man, NG

July, 1998



## ***Declaration***

I hereby declare that this thesis summarized my own work carried out since my registration for the Degree of Master of Philosophy in September, 1995; and that has not been previously included in a thesis, dissertation or report submitted to this or any other institution for a degree, diploma or other qualification.

---

Siu-Man, NG

July, 1998

## *Acknowledgements*

I would like to express my deepest gratitude to my supervisor Dr. C. P. Lau for his advice and patience throughout the course of my study. His guidance, encouragement and devoted attitude in research has made my study a truly rewarding experience.

Thanks are also expressed to Dr. G. Jia of the Department of Chemistry, The Hong Kong University of Science and Technology for many fruitful discussions over the area of acidity of non-classical dihydrogen complexes and Dr. W. T. Wong of The University of Hong Kong for solving the crystal structures of some of the ruthenium complexes.

I am deeply in debt to Dr. C. H. Yeung for his expertise knowledge and assistance in performing the  $^{29}\text{Si}$  NMR.

I also want to thank all my postgraduate colleagues and the undergraduate students in Dr. Lau's group, especially Mr. W. C. Chan who introduced to me the interesting chemistry of ruthenium. Sincere thanks are due to Mr. Y. Z. Chen, Mr. Y. Q. Fang, Ms. M. Y. Hung, Mr. C. C. Mak and Mr. C. Q. Yin, all of whom have made my study in FG 703 more pleasant. Special thanks are expressed to Mr. H. S. Chu for his valuable discussions and assistance.

I am obliged to the staff and the technical service crew of the Chemical Technology section of the Department of Applied Biology and Chemical Technology, The Hong Kong Polytechnic University for their assistance throughout my postgraduate study, especially thanks to Mr. Y. K. Au , Ms. P. S. Chan and Mr. W. K. Kwan for their assistance in running the MS and NMR. spectra respectively.

Lastly but not the least, I am greatly indebted to my parents and the whole family for their support, forbearance, patience and concern while I was engaged in this research project.

Finally, I would like to acknowledge the Research Degree Committee of The Hong Kong Polytechnic University for the awarding of a Studentship.

Abstract of thesis entitled "Syntheses and Characterization of ruthenium  $\eta^2$ -  
dihydrogen and  $\eta^2$ -silane complexes"

submitted by Siu-Man. NG

for the degree of Master of Philosophy

at the Hong Kong Polytechnic University

in July, 1998.

## *Abstract*

Protonation of  $[\text{R}^{\text{Cn}}\text{RuH}(\text{L})(\text{L}')]^+$  ( $\text{R}^{\text{Cn}} = 1,4,7\text{-triazacyclononane}$  and  $1,4,7\text{-trimethyl-}1,4,7\text{-triazacyclononane}$ ,  $(\text{L})(\text{L}') = (\text{PPh}_3)_2$ ,  $\text{dppe}$ , and  $(\text{CO})(\text{PPh}_3)$ ) and  $\text{TpRuH}(\text{dppe})$  ( $\text{Tp} = \text{hydrotris}(\text{pyrazolyl})\text{borato}$ ) produced the corresponding dicationic dihydrogen complexes  $[\text{R}^{\text{Cn}}\text{Ru}(\text{H}_2)(\text{L})(\text{L}') ]^{2+}$  and new monocationic dihydrogen complex  $[\text{TpRu}(\text{H}_2)(\text{dppe})]^+$ , respectively.  $\text{p}K_{\text{a}}$  measurements indicate that the dicationic  $\eta^2\text{-H}_2$  complexes are more acidic than their monocationic Tp and Cp counterparts.  $[\text{Me}^{\text{Cn}}\text{Ru}(\text{H}_2)(\text{CO})(\text{PPh}_3)]^{2+}$  was found to be more acidic than  $[\text{H}^{\text{Cn}}\text{Ru}(\text{H}_2)(\text{CO})(\text{PPh}_3)]^{2+}$ , probably due to stronger H—H interaction in the latter complex. It is also noted that triazacyclononane and hydrotris(pyrazolyl)borato dihydrogen complexes with pseudo aqueous  $\text{p}K_{\text{a}}$  values well above that of  $\text{H}_3\text{O}^+$  can be deprotonated by  $\text{H}_2\text{O}$  to form the corresponding monohydride complexes in organic/aqueous mixed solvents. It is believed that deprotonation of the dihydrogen ligands in these complexes is assisted by strong solvation of  $\text{H}^+$  by  $\text{H}_2\text{O}$ .

No silane complex was observed in the reaction of  $[\text{TpRu}(\text{H}_2)(\text{PPh}_3)_2]^+$  with silane, although the  $\eta^2\text{-H}_2$  ligand had undoubtedly been displaced. The silane complex had probably been formed, but it was readily attacked by nucleophilic species such as the counterion  $\text{BF}_4^-$  or water in the solvent. It was found that ruthenium solvent hydride complex  $[\text{TpRuH}(\text{CH}_3\text{CN})(\text{PPh}_3)]$  reacted with silanes  $\text{HSiR}_3$  ( $\text{R}_3 = \text{HPh}_2, \text{HEt}_2, \text{Ph}_3, \text{Et}_3, \text{H}_2\text{Ph}$  and  $(\text{OEt})_3$ ) to yield the silane complexes  $[\text{TpRuH}(\text{HSiR}_3)(\text{PPh}_3)]$  which, instead of equilibrating between the  $\eta^2\text{-silane}$  and  $\eta^2\text{-}$

H<sub>2</sub> tautomeric forms, interchanged the H atoms rapidly, and rendering them equivalent. The silane complex [TpRuH(HSiR<sub>3</sub>)(PPh<sub>3</sub>)] is analogous to the dihydrogen hydride complex TpRuH(H<sub>2</sub>)(PPh<sub>3</sub>) which we have recently reported.



# Table of Contents

|   |     |
|---|-----|
| Abstract  | i   |
| Tablet of Contents  | iii |
| List of Figures   | v   |
| List of Tables  | x   |
| List of Schemes   | xi  |
| Abbreviations   | xii |
| <br>  |     |
| Chapter One   |     |
| Introduction  | 1   |
| <br>  |     |
| Chapter Two   |     |
| Syntheses, characterization and reactivity of ruthenium $\eta^2$ -dihydrogen complexes                            | 18  |
| <br>  |     |
| 2.1 Introduction  | 18  |
| <br>  |     |
| 2.2 Experimental  | 18  |
| 2.2.1 Materials   | 18  |
| 2.2.2 Instrumentation   | 19  |
| 2.2.3 Syntheses   | 20  |
| 2.2.3.1 Hydrido complexes   | 20  |
| 2.2.3.2 Dihydrogen Complexes and Their Isotopomers  | 21  |
| 2.2.3.3 Solvento complex  | 25  |
| 2.2.4 Acidity Measurement   | 26  |
| 2.2.5 Crystallographic Analysis   | 27  |
| <br>  |     |
| 2.3 Results and Discussion  | 29  |
| 2.3.1 Synthesis and Characterization of $[\text{R}^{\text{Cn}}(\text{H}_2)(\text{L})(\text{L}') ]^{2+}$ Complexes | 29  |
| 2.3.2 Synthesis and Characterization of $[\text{TpRu}(\text{H}_2)(\text{L})(\text{L}') ]^+$ Complexes             | 40  |
| 2.3.3 Comparison of the Abilities of Cp, Tp, and $\text{R}^{\text{Cn}}$ in Stabilizing Dihydrogen Complexes       | 41  |
| 2.3.4 Acidity of the Dihydrogen Complexes   | 42  |
| 2.3.5 Comments on the Acidity   | 45  |
| 2.3.6 Reactions of Dihydrogen Complexes with Water  | 50  |
| <br>  |     |
| Chapter Three   |     |
| Syntheses, characterization and reactivity of ruthenium $\eta^2$ -silane complexes                                | 53  |
| <br>  |     |
| 3.1 Introduction  | 53  |

|   |     |
|---|-----|
| 3.2 Experimental  | 54  |
| 3.2.1 Materials   | 54  |
| 3.2.2 Instrumentation   | 55  |
| 3.2.3 Syntheses   | 55  |
| 3.2.4 NMR studies of reactions of the ruthenium complexes                                   | 59  |
| 3.3 Results and Discussion  | 62  |
| 3.3.1 Reactions of Tp dihydrogen complexes with silane                                      | 62  |
| 3.3.2 Synthesis of $\text{TpRu}(\text{PPh}_3)_2\text{H}_2\text{SiR}_3$                      | 66  |
| 3.3.3 Characterization and Structure of $\text{TpRu}(\text{PPh}_3)_2\text{H}_2\text{SiR}_3$ | 69  |
| 3.3.4 Reactivity of $\text{TpRu}(\text{PPh}_3)_2\text{H}_2\text{SiR}_3$                     | 72  |
| 3.3.5 Reaction of $\text{TpRuCl}(\text{CH}_3\text{CN})(\text{PPh}_3)_2$ with diphenylsilane | 73  |
| Chapter Four  | 74  |
| Conclusion  | 74  |
| Reference   | 76  |
| Appendix  | 84  |
| Publication   | 161 |

## List of Figures

|                |   |     |
|----------------|---|-----|
| Figure 2.1     | The molecular structure of $[\text{H}^{\text{Cn}}\text{RuH}(\text{PPh}_3)_2]\text{BF}_4$ ( <b>1</b> )   | 32  |
| Figure 2.2     | The molecular structure of $[\text{H}^{\text{Cn}}\text{Ru}(\text{H}_2\text{O})(\text{PPh}_3)_2](\text{BF}_4)_2$ ( <b>9</b> ).   | 37  |
| Figure 2.3 (a) | The $^{31}\text{P}$ NMR spectra of $[\text{M}^{\text{Cn}}\text{RuH}(\text{CO})(\text{PPh}_3)]^+$ and $[\text{H}^{\text{Cn}}\text{RuH}(\text{CO})(\text{PPh}_3)]^+$ in $\text{CD}_2\text{Cl}_2$ at $-35\text{ }^\circ\text{C}$   | 49  |
| Figure 2.3 (b) | The $^{31}\text{P}$ NMR spectra of $([\text{M}^{\text{Cn}}\text{RuH}(\text{CO})(\text{PPh}_3)]^+ \text{ and } [\text{H}^{\text{Cn}}\text{RuH}(\text{CO})(\text{PPh}_3)]^+ + \text{HBF}_4 \cdot \text{Et}_2\text{O})$ in $\text{CD}_2\text{Cl}_2$ at $-80\text{ }^\circ\text{C}$ | 49  |
| Figure 2.4     | Infra-red spectrum of $[\text{H}^{\text{Cn}}\text{RuH}(\text{PPh}_3)_2]\text{BF}_4$ ( <b>1</b> ) in KBr disc  | 84  |
| Figure 2.5     | 400 MHz $^1\text{H}$ -NMR spectrum of $[\text{H}^{\text{Cn}}\text{RuH}(\text{PPh}_3)_2]\text{BF}_4$ ( <b>1</b> )  | 85  |
| Figure 2.6     | 161 MHz $^{31}\text{P}\{^1\text{H}\}$ -NMR spectrum of $[\text{H}^{\text{Cn}}\text{RuH}(\text{PPh}_3)_2]\text{BF}_4$ ( <b>1</b> )   | 86  |
| Figure 2.7     | FAB mass spectrum of $[\text{H}^{\text{Cn}}\text{RuH}(\text{PPh}_3)_2]\text{BF}_4$ ( <b>1</b> )   | 87  |
| Figure 2.8     | Infra-red spectrum of $[\text{H}^{\text{Cn}}\text{RuH}(\text{CO})(\text{PPh}_3)]\text{BF}_4$ ( <b>2</b> ) in KBr disc   | 88  |
| Figure 2.9     | 400 MHz $^1\text{H}$ -NMR spectrum of $[\text{H}^{\text{Cn}}\text{RuH}(\text{CO})(\text{PPh}_3)]\text{BF}_4$ ( <b>2</b> )   | 89  |
| Figure 2.10    | 161 MHz $^{31}\text{P}\{^1\text{H}\}$ -NMR spectrum of $[\text{H}^{\text{Cn}}\text{RuH}(\text{CO})(\text{PPh}_3)]\text{BF}_4$ ( <b>2</b> )  | 90  |
| Figure 2.11    | FAB mass spectrum of $[\text{H}^{\text{Cn}}\text{RuH}(\text{CO})(\text{PPh}_3)]\text{BF}_4$ ( <b>2</b> )  | 91  |
| Figure 2.12    | Infra-red spectrum of $\text{TpRuH}(\text{dppe})$ ( <b>14</b> ) in KBr disc   | 92  |
| Figure 2.13    | 400 MHz $^1\text{H}$ -NMR spectrum of $\text{TpRuH}(\text{dppe})$ ( <b>14</b> )   | 93  |
| Figure 2.14    | 161 MHz $^{31}\text{P}\{^1\text{H}\}$ -NMR spectrum of $\text{TpRuH}(\text{dppe})$ ( <b>14</b> )  | 94  |
| Figure 2.15    | FAB mass spectrum of $\text{TpRuH}(\text{dppe})$ ( <b>14</b> )  | 95  |
| Figure 2.16    | 400 MHz $^1\text{H}$ -NMR spectrum of $[\text{H}^{\text{Cn}}\text{Ru}(\text{H}_2)(\text{PPh}_3)_2](\text{BF}_4)_2$ ( <b>5</b> )   | 96  |
| Figure 2.17    | 161 MHz $^{31}\text{P}\{^1\text{H}\}$ -NMR spectrum of $[\text{H}^{\text{Cn}}\text{Ru}(\text{H}_2)(\text{PPh}_3)_2](\text{BF}_4)_2$ ( <b>5</b> )  | 97  |
| Figure 2.18    | 400 MHz $^1\text{H}$ -NMR spectrum of $[\text{H}^{\text{Cn}}\text{Ru}(\text{HD})(\text{PPh}_3)_2](\text{BF}_4)_2$ ( <b>5-d</b> <sub>1</sub> )   | 98  |
| Figure 2.19    | 400 MHz $^1\text{H}$ -NMR spectrum of $[\text{H}^{\text{Cn}}\text{Ru}(\text{H}_2)(\text{CO})(\text{PPh}_3)](\text{BF}_4)_2$ ( <b>6</b> )  | 99  |
| Figure 2.20    | 161 MHz $^{31}\text{P}\{^1\text{H}\}$ -NMR spectrum of $[\text{H}^{\text{Cn}}\text{Ru}(\text{H}_2)(\text{CO})(\text{PPh}_3)](\text{BF}_4)_2$ ( <b>6</b> )   | 100 |

|             |   |     |
|-------------|---|-----|
| Figure 2.21 | 400 MHz $^1\text{H}$ -NMR spectrum of $[\text{CnRu}(\text{HD})(\text{CO})(\text{PPh}_3)](\text{BF}_4)_2$ ( <b>6-d<sub>1</sub></b> )                           | 101 |
| Figure 2.22 | 400 MHz $^1\text{H}$ -NMR spectrum of $[\text{CnRu}(\text{H}_2)(\text{dppe})](\text{CF}_3\text{SO}_3)_2$ ( <b>7</b> )   | 102 |
| Figure 2.23 | 161 MHz $^{31}\text{P}\{^1\text{H}\}$ -NMR spectrum of $[\text{CnRu}(\text{H}_2)(\text{dppe})](\text{CF}_3\text{SO}_3)_2$ ( <b>7</b> )                        | 103 |
| Figure 2.24 | 400 MHz $^1\text{H}$ -NMR spectrum of $[\text{CnRu}(\text{HD})(\text{dppe})](\text{CF}_3\text{SO}_3)_2$ ( <b>7-d<sub>1</sub></b> )                            | 104 |
| Figure 2.25 | 400 MHz $^1\text{H}$ -NMR spectrum of $[\text{CnRu}(\text{H}_2)(\text{CO})(\text{PPh}_3)](\text{PF}_6)(\text{CF}_3\text{SO}_3)$ ( <b>8</b> )                  | 105 |
| Figure 2.26 | 161 MHz $^{31}\text{P}\{^1\text{H}\}$ -NMR spectrum of $[\text{CnRu}(\text{H}_2)(\text{CO})(\text{PPh}_3)](\text{PF}_6)(\text{CF}_3\text{SO}_3)$ ( <b>8</b> ) | 106 |
| Figure 2.27 | 400 MHz $^1\text{H}$ -NMR spectrum of $[\text{CnRu}(\text{HD})(\text{CO})(\text{PPh}_3)](\text{PF}_6)(\text{CF}_3\text{SO}_3)$ ( <b>8-d<sub>1</sub></b> )     | 107 |
| Figure 2.28 | 400 MHz $^1\text{H}$ -NMR spectrum of $[\text{TpRu}(\text{H}_2)(\text{dppe})]\text{BF}_4$ ( <b>19</b> )   | 108 |
| Figure 2.29 | 161 MHz $^{31}\text{P}\{^1\text{H}\}$ -NMR spectrum of $[\text{TpRu}(\text{H}_2)(\text{dppe})]\text{BF}_4$ ( <b>19</b> )                                      | 109 |
| Figure 2.30 | 400 MHz $^1\text{H}$ -NMR spectrum of $[\text{TpRu}(\text{HD})(\text{dppe})]\text{BF}_4$ ( <b>19-d<sub>1</sub></b> )  | 110 |
| Figure 2.31 | 400 MHz $^1\text{H}$ -NMR spectrum of $[\text{TpRu}(\text{H}_2)(\text{CO})(\text{PPh}_3)]\text{BF}_4$ ( <b>20</b> )   | 111 |
| Figure 2.32 | 161 MHz $^{31}\text{P}\{^1\text{H}\}$ -NMR spectrum of $[[\text{TpRu}(\text{H}_2)(\text{CO})(\text{PPh}_3)]\text{BF}_4$ ( <b>20</b> )                         | 112 |
| Figure 2.33 | 400 MHz $^1\text{H}$ -NMR spectrum of $[\text{TpRu}(\text{HD})(\text{CO})(\text{PPh}_3)]\text{BF}_4$ ( <b>20-d<sub>1</sub></b> )                              | 113 |
| Figure 2.34 | 400 MHz $^1\text{H}$ -NMR spectrum of $[\text{CnRu}(\text{H}_2\text{O})(\text{PPh}_3)_2](\text{BF}_4)_2$ ( <b>9</b> )   | 114 |
| Figure 2.35 | 161 MHz $^{31}\text{P}\{^1\text{H}\}$ -NMR spectrum of $[\text{CnRu}(\text{H}_2\text{O})(\text{PPh}_3)_2](\text{BF}_4)_2$ ( <b>9</b> )                        | 115 |
| Figure 2.36 | FAB mass spectrum of $[\text{CnRu}(\text{H}_2\text{O})(\text{PPh}_3)_2](\text{BF}_4)_2$ ( <b>9</b> )  | 116 |

|               |  |     |
|---------------|--|-----|
| Figure 2.37   | The $^1\text{H}$ -NMR spectra of $[\text{H}^{\text{Cn}}\text{RuH}(\text{PPh}_3)_2]\text{BF}_4$ ( <b>1</b> ) and $\text{RuHCl}(\text{dppe})_2 + \text{HBF}_4 \cdot \text{Et}_2\text{O}$ in $\text{CD}_2\text{Cl}_2$   | 117 |
| Figure 2.38   | The $^1\text{H}$ -NMR spectra of $[\text{H}^{\text{Cn}}\text{RuH}(\text{CO})(\text{PPh}_3)_2]\text{BF}_4$ ( <b>2</b> ) and $\text{HBF}_4 \cdot \text{Et}_2\text{O}$ in $\text{CD}_2\text{Cl}_2$ -80 °C   | 118 |
| Figure 2.39   | The $^1\text{H}$ -NMR spectra of $[\text{Me}^{\text{Cn}}\text{RuH}(\text{dppe})](\text{CF}_3\text{SO}_3)$ ( <b>3</b> ) and $\text{RuHCl}(\text{dppe})_2 + \text{HBF}_4 \cdot \text{Et}_2\text{O}$ in $\text{CD}_2\text{Cl}_2$  | 119 |
| Figure 2.40   | The $^1\text{H}$ -NMR spectra of $[\text{H}^{\text{Cn}}\text{RuH}(\text{CO})(\text{PPh}_3)_2]\text{PF}_6$ ( <b>4</b> ) and $\text{HBF}_4 \cdot \text{Et}_2\text{O}$ in $\text{CD}_2\text{Cl}_2$ -30 °C   | 120 |
| Figure 2.41   | The $^1\text{H}$ -NMR spectra of $\text{TpRuH}(\text{PPh}_3)_2$ ( <b>12</b> ) and $\text{CpRuH}(\text{dppm}) + \text{HBF}_4 \cdot \text{Et}_2\text{O}$ in $\text{CD}_2\text{Cl}_2$   | 121 |
| Figure 2.42   | The $^1\text{H}$ -NMR spectra of $\text{TpRuH}(\text{CH}_3\text{CN})(\text{PPh}_3)$ ( <b>13</b> ) and $\text{CpRuH}(\text{PPh}_3)_2 + \text{HBF}_4 \cdot \text{Et}_2\text{O}$ in $\text{CD}_2\text{Cl}_2$ -35 °C   | 122 |
| Figure 2.43   | The $^1\text{H}$ -NMR spectra of $\text{TpRuH}(\text{dppe})$ ( <b>14</b> ) and $\text{CpRuH}(\text{dppm}) + \text{HBF}_4 \cdot \text{Et}_2\text{O}$ in $\text{CD}_2\text{Cl}_2$  | 123 |
| Figure 2.44   | The $^{31}\text{P}\{^1\text{H}\}$ -NMR spectra of $\text{TpRuH}(\text{CO})(\text{PPh}_3)$ ( <b>15</b> ) and $[\text{H}^{\text{Cn}}\text{RuH}(\text{CO})(\text{PPh}_3)_2]\text{PF}_6$ ( <b>4</b> ) + $\text{HBF}_4 \cdot \text{Et}_2\text{O}$ in $\text{CD}_2\text{Cl}_2$ | 124 |
| Figure 3.1    | Infra-red spectrum of $\text{TpRuH}(\text{HSiEt}_3)(\text{PPh}_3)$ ( <b>21a</b> ) in KBr disc  | 125 |
| Figure 3.2(a) | 400 MHz $^1\text{H}$ -NMR spectrum of $\text{TpRuH}(\text{HSiEt}_3)(\text{PPh}_3)$ ( <b>21a</b> )  | 126 |
| Figure 3.2(b) | Expanded upfield region of Figure 3.2(a)   | 127 |
| Figure 3.3    | 161 MHz $^{31}\text{P}\{^1\text{H}\}$ -NMR spectrum of $\text{TpRuH}(\text{HSiEt}_3)(\text{PPh}_3)$ ( <b>21a</b> )   | 128 |
| Figure 3.4    | 79 MHz $^{29}\text{Si}\{^1\text{H}\}$ -NMR spectrum of $\text{TpRuH}(\text{HSiEt}_3)(\text{PPh}_3)$ ( <b>21a</b> )   | 129 |
| Figure 3.5    | FAB mass spectrum of $\text{TpRuH}(\text{HSiEt}_3)(\text{PPh}_3)$ ( <b>21a</b> )   | 130 |
| Figure 3.6    | Infra-red spectrum of $\text{TpRuH}(\text{HSi}(\text{EtO})_3)(\text{PPh}_3)$ ( <b>21b</b> ) in KBr disc  | 131 |
| Figure 3.7(a) | 400 MHz $^1\text{H}$ -NMR spectrum of $\text{TpRuH}(\text{HSi}(\text{EtO})_3)(\text{PPh}_3)$ ( <b>21b</b> )  | 132 |

|                |  |     |
|----------------|--|-----|
| Figure 3.7(b)  | Expanded upfield region of Figure 3.7(a)   | 133 |
| Figure 3.8     | 161 MHz $^{31}\text{P}\{^1\text{H}\}$ -NMR spectrum of $\text{TpRuH}(\text{HSi}(\text{EtO})_3)(\text{PPh}_3)$ ( <b>21b</b> ) | 134 |
| Figure 3.9     | 79 MHz $^{29}\text{Si}\{^1\text{H}\}$ -NMR spectrum of $\text{TpRuH}(\text{HSi}(\text{EtO})_3)(\text{PPh}_3)$ ( <b>21b</b> ) | 135 |
| Figure 3.10    | FAB mass spectrum of $\text{TpRuH}(\text{HSi}(\text{EtO})_3)(\text{PPh}_3)$ ( <b>21b</b> )                                   | 136 |
| Figure 3.11    | Infra-red spectrum of $\text{TpRuH}(\text{HSiPh}_3)(\text{PPh}_3)$ ( <b>21c</b> ) in KBr disc                                | 137 |
| Figure 3.12(a) | 400 MHz $^1\text{H}$ -NMR spectrum of $\text{TpRuH}(\text{HSiPh}_3)(\text{PPh}_3)$ ( <b>21c</b> )                            | 138 |
| Figure 3.12(b) | Expanded upfield region of Figure 3.12(a)  | 139 |
| Figure 3.13    | 161 MHz $^{31}\text{P}\{^1\text{H}\}$ -NMR spectrum of $\text{TpRuH}(\text{HSiPh}_3)(\text{PPh}_3)$ ( <b>21c</b> )           | 140 |
| Figure 3.14    | 79 MHz $^{29}\text{Si}\{^1\text{H}\}$ -NMR spectrum of $\text{TpRuH}(\text{HSiPh}_3)(\text{PPh}_3)$ ( <b>21c</b> )           | 141 |
| Figure 3.15    | FAB mass spectrum of $\text{TpRuH}(\text{HSiPh}_3)(\text{PPh}_3)$ ( <b>21c</b> )   | 142 |
| Figure 3.16    | Infra-red spectrum of $\text{TpRuH}(\text{H}_2\text{SiEt}_2)(\text{PPh}_3)$ ( <b>21d</b> ) in KBr disc                       | 143 |
| Figure 3.17(a) | 400 MHz $^1\text{H}$ -NMR spectrum of $\text{TpRuH}(\text{H}_2\text{SiEt}_2)(\text{PPh}_3)$ ( <b>21d</b> )                   | 144 |
| Figure 3.17(b) | Expanded upfield region of Figure 3.17(a)  | 145 |
| Figure 3.18    | 161 MHz $^{31}\text{P}\{^1\text{H}\}$ -NMR spectrum of $\text{TpRuH}(\text{H}_2\text{SiEt}_2)(\text{PPh}_3)$ ( <b>21d</b> )  | 146 |
| Figure 3.19    | 79 MHz $^{29}\text{Si}\{^1\text{H}\}$ -NMR spectrum of $\text{TpRuH}(\text{H}_2\text{SiEt}_2)(\text{PPh}_3)$ ( <b>21d</b> )  | 147 |
| Figure 3.20    | FAB mass spectrum of $\text{TpRuH}(\text{H}_2\text{SiEt}_2)(\text{PPh}_3)$ ( <b>21d</b> )                                    | 148 |
| Figure 3.21    | Infra-red spectrum of $\text{TpRuH}(\text{H}_2\text{SiPh}_2)(\text{PPh}_3)$ ( <b>21e</b> ) in KBr disc                       | 149 |
| Figure 3.22(a) | 400 MHz $^1\text{H}$ -NMR spectrum $\text{TpRuH}(\text{H}_2\text{SiPh}_2)(\text{PPh}_3)$ ( <b>21e</b> )                      | 150 |
| Figure 3.22(b) | Expanded upfield region of Figure 3.22(a)  | 151 |

|                |   |     |
|----------------|---|-----|
| Figure 3.23    | 161 MHz $^{31}\text{P}\{^1\text{H}\}$ -NMR spectrum of $\text{TpRuH}(\text{H}_2\text{SiPh}_2)(\text{PPh}_3)$ ( <b>21e</b> ) | 152 |
| Figure 3.24    | 79 MHz $^{29}\text{Si}\{^1\text{H}\}$ -NMR spectrum of $\text{TpRuH}(\text{H}_2\text{SiPh}_2)(\text{PPh}_3)$ ( <b>21e</b> ) | 153 |
| Figure 3.25    | FAB mass spectrum of $\text{TpRuH}(\text{H}_2\text{SiPh}_2)(\text{PPh}_3)$ ( <b>21e</b> )                                   | 154 |
| Figure 3.26    | Infra-red spectrum of $\text{TpRuH}(\text{H}_3\text{SiPh})(\text{PPh}_3)$ ( <b>21f</b> )<br>in KBr disc                     | 155 |
| Figure 3.27(a) | 400 MHz $^1\text{H}$ -NMR spectrum $\text{TpRuH}(\text{H}_3\text{SiPh})(\text{PPh}_3)$ ( <b>21f</b> )                       | 156 |
| Figure 3.27(b) | Expanded upfield region of Figure 3.27(a)   | 157 |
| Figure 3.28    | 161 MHz $^{31}\text{P}\{^1\text{H}\}$ -NMR spectrum of $\text{TpRuH}(\text{H}_3\text{SiPh})(\text{PPh}_3)$ ( <b>21f</b> )   | 158 |
| Figure 3.29    | 79 MHz $^{29}\text{Si}\{^1\text{H}\}$ -NMR spectrum of $\text{TpRuH}(\text{H}_3\text{SiPh})(\text{PPh}_3)$ ( <b>21f</b> )   | 159 |
| Figure 3.30    | FAB mass spectrum of $\text{TpRuH}(\text{H}_3\text{SiPh})(\text{PPh}_3)$ ( <b>21f</b> )                                     | 160 |

## *List of Tables*

|         |   |    |
|---------|---|----|
| Table 1 | Crystal Data and Refinement Details for $[\text{H}^{\text{Cn}}\text{RuH}(\text{PPh}_3)_2]\text{BF}_4$ ( <b>1</b> )                                  | 33 |
| Table 2 | Selected Bond Distances (Å) and Angles (deg) for $[\text{H}^{\text{Cn}}\text{RuH}(\text{PPh}_3)_2]\text{BF}_4$ ( <b>1</b> )                         | 34 |
| Table 3 | Crystal Data and Refinement Details for $[\text{H}^{\text{Cn}}\text{Ru}(\text{H}_2\text{O})(\text{PPh}_3)_2](\text{BF}_4)_2$ ( <b>9</b> )           | 38 |
| Table 4 | Selected Bond Distances (Å) and Angles (deg) for $[\text{H}^{\text{Cn}}\text{Ru}(\text{H}_2\text{O})(\text{PPh}_3)_2](\text{BF}_4)_2$ ( <b>9</b> ). | 39 |
| Table 5 | Acidity Measurements of Dihydrogen Complexes in $\text{CD}_2\text{Cl}_2$  | 44 |
| Table 6 | Spectroscopic Properties and Acidities of Hydride Complexes   | 46 |
| Table 7 | NMR and IR Spectroscopic Data for $\text{TpRu}(\text{PPh}_3)_2\text{H}_2\text{SiR}_3$ ( <b>21a-f</b> )  | 67 |



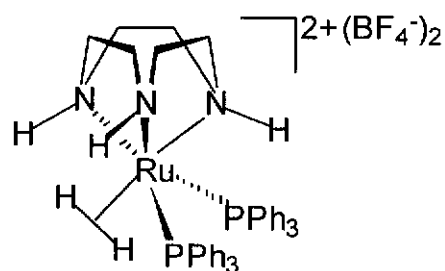
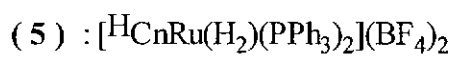
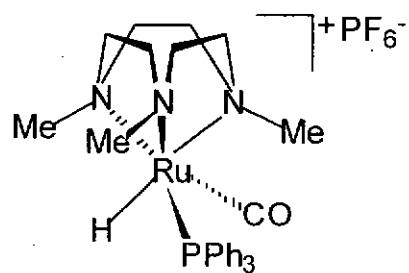
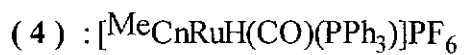
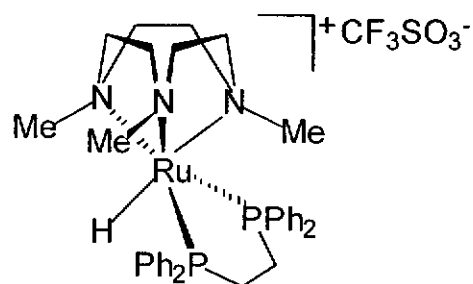
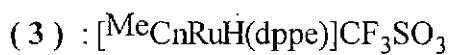
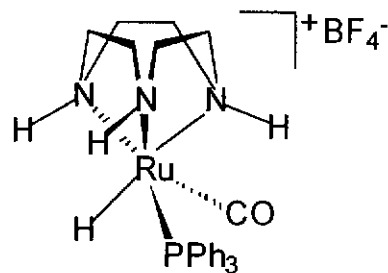
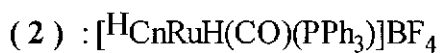
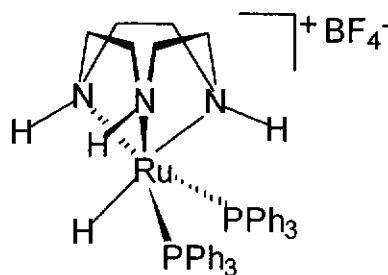
## *List of Schemes*

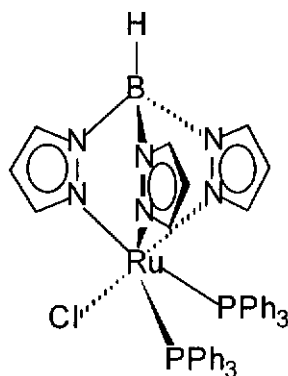
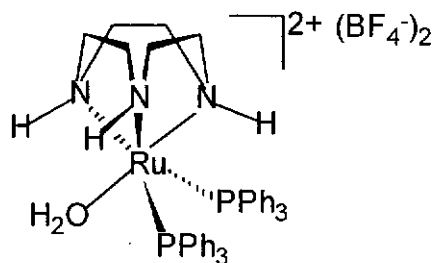
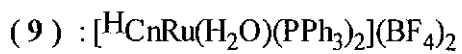
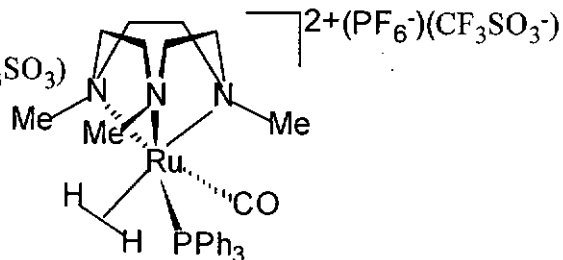
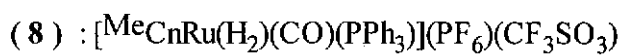
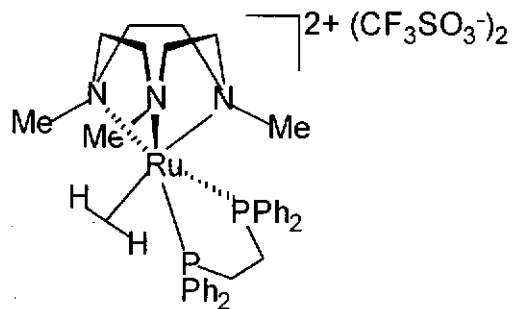
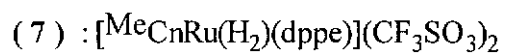
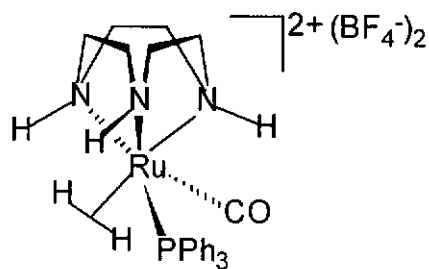
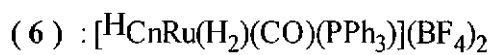
|          |  |    |
|----------|--|----|
| Scheme 1 | Reaction scheme of preparation of hydrido complex<br>$[\text{}^{\text{H}}\text{CnRuH}(\text{PPh}_3)_2]\text{BF}_4$ ( <b>1</b> )  | 30 |
| Scheme 2 | Reactions between the dihydrogen complexes ( <b>17,18 &amp; 20</b> )<br>and silanes  | 63 |
| Scheme 3 | Reaction scheme of preparation of $\text{TpRuCl}(\eta^2\text{-H}_2\text{SiPh}_3)(\text{PPh}_3)$ ( <b>21d</b> )<br>from $\text{TpRuCl}(\text{CH}_3\text{CN})(\text{PPh}_3)$ ( <b>11</b> ) | 73 |

## Abbreviations

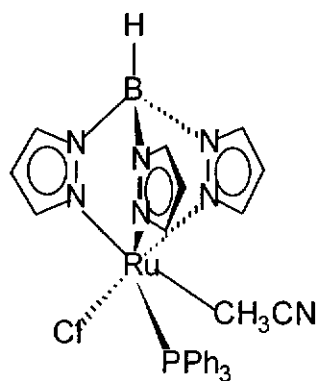
|  |  |
|--|--|
| Me :   | methyl                                       |
| Et :   | ethyl  |
| <sup>i</sup> Pr :                              | isopropyl                                    |
| <sup>n</sup> Pr :                              | n-propyl                                     |
| <sup>n</sup> Bu :                              | n-butyl                                      |
| CH <sub>3</sub> CN :                           | acetonitrile                                 |
| EtOH :   | ethanol                                      |
| NEt <sub>3</sub> :                             | triethylamine                                |
| THF :  | tetrahydrofuran                              |
| Cp :   | cyclopentadienyl                             |
| Cp* :  | pentamethylcyclopentadienyl                  |
| COD :  | 1,5-cyclooctadiene                           |
| pz :   | pyrazole                                     |
| H <sub>2</sub> Bpz <sub>2</sub> <sup>-</sup> : | dihydrobis (1-pyrazolyl) borate              |
| TP :   | hydrotris (1-pyrazolyl) borate               |
| <sup>3,5-Me</sup> TP :                         | hydrotris [1-(3,5-dimethylpyrazolyl)] borate |
| <sup>3,5-tBu</sup> TP :                        | hydrotris [1-(3-t-butylpyrazolyl)]borate     |
| <sup>R</sup> Cn :                              | 1,4,7-triazacyclononane derivatives          |
| <sup>Me</sup> Cn :                             | 1,4,7-trimethyl-1,4,7-triazacyclononane.     |
| <sup>H</sup> Cn :                              | 1,4,7-triazacyclononane                      |
| PMe <sub>3</sub> :                             | trimethylphosphine                           |
| PEt <sub>3</sub> :                             | triethylphosphine                            |
| P(OMe) <sub>3</sub> :                          | trimethylphosphite                           |
| PMePh <sub>2</sub> :                           | methyldiphenylphosphine                      |
| PPh <sub>3</sub> :                             | triphenylphosphine                           |
| PCy <sub>3</sub> :                             | tricyclohexylphosphine                       |
| <sup>i</sup> Pr <sub>3</sub> :                 | tri-isopropylphosphine                       |
| dppe :   | 1,2-bis(diphenylphosphino)ethane             |
| dppp :   | 1,3-bis(diphenylphosphino)propane            |
| bpy :  | 2,2'-bipyridine                              |
| phen :   | 1,10-phenanthroline                          |
| IR :   | infra-red                                    |
| FT-IR :  | Fourier transform infra-red                  |
| NMR :  | nuclear magnetic resonance spectroscopy      |
| EI-MS :  | electron impact mass spectroscopy            |
| FAB-MS :                                       | fast atom bombardment mass spectroscopy      |
| nba :  | 3-nitrobenzylalcohol                         |

|       |                   |
|-------|-------------------|
| TMS : | tetramethylsilane |
| sh :  | sharp             |
| br :  | broad             |
| vs :  | very strong       |
| med : | medium            |
| w :   | weak              |
| s :   | singlet           |
| d :   | doublet           |
| t :   | triplet           |
| m :   | multiplet         |

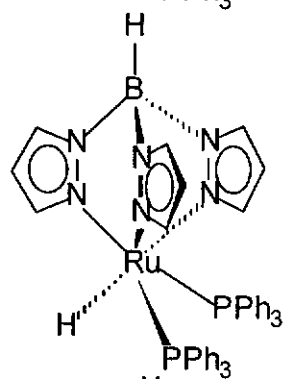




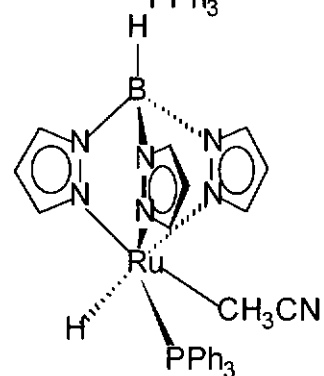
(11) :  $\text{TpRuCl}(\text{CH}_3\text{CN})(\text{PPh}_3)$



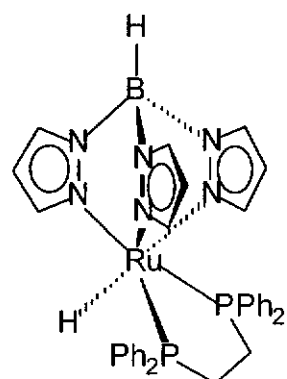
(12) :  $\text{TpRuH}(\text{PPh}_3)_2$



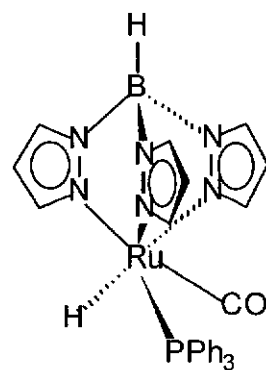
(13) :  $\text{TpRuH}(\text{CH}_3\text{CN})(\text{PPh}_3)$



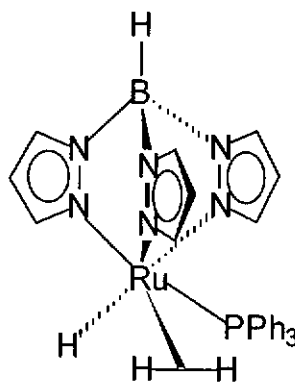
(14) :  $\text{TpRuH}(\text{dppe})$



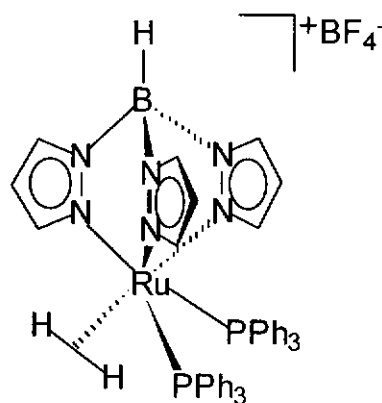
(15) :  $\text{TpRuH}(\text{CO})(\text{PPh}_3)$



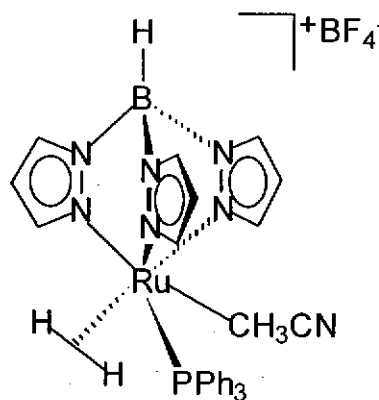
(16) :  $\text{TpRuH}(\text{H}_2)(\text{PPh}_3)$



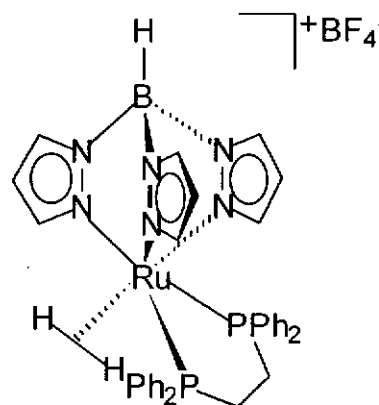
(17) :  $[\text{TpRu}(\text{H}_2)(\text{PPh}_3)_2]\text{BF}_4$

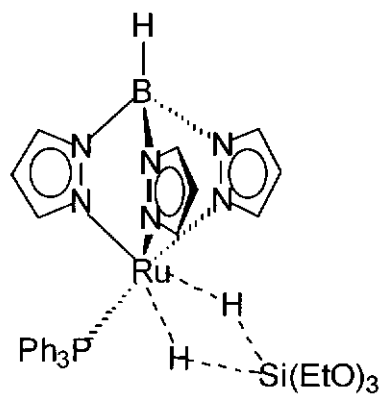
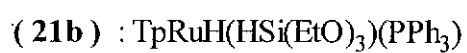
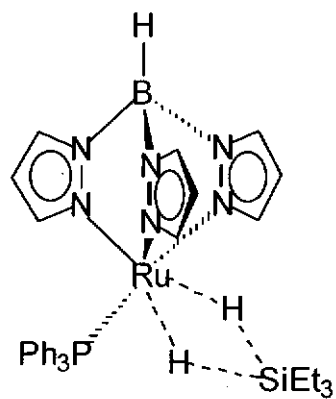
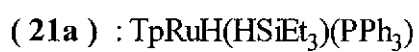
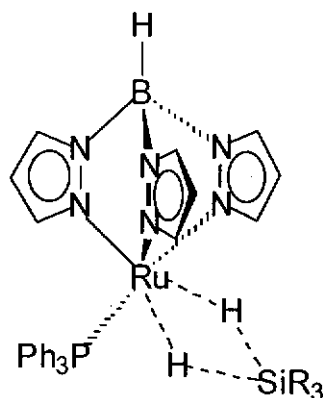
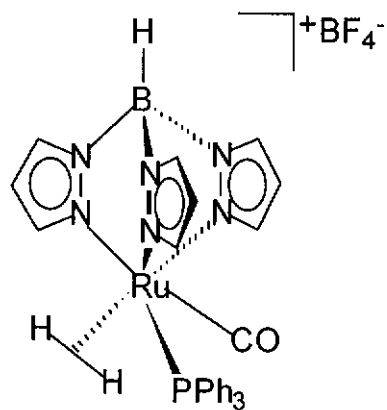
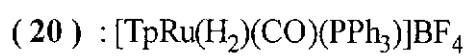


(18) :  $[\text{TpRu}(\text{H}_2)(\text{CH}_3\text{CN})(\text{PPh}_3)]\text{BF}_4$



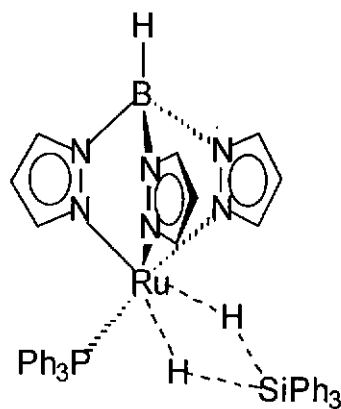
(19) :  $[\text{TpRu}(\text{H}_2)(\text{dppe})]\text{BF}_4$



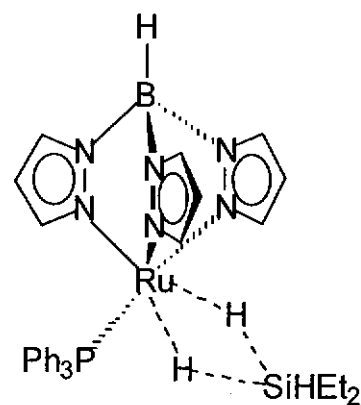




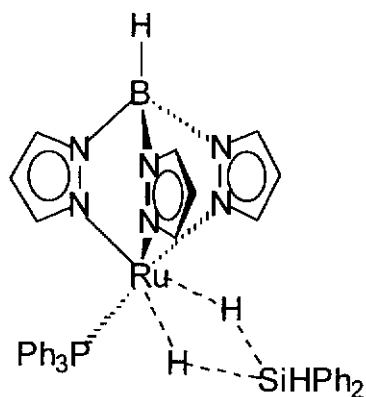
(21c) :  $\text{TpRuH}(\text{HSiPh}_3)(\text{PPh}_3)$



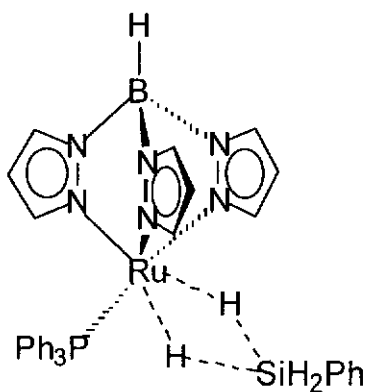
(21d) :  $\text{TpRuH}(\text{H}_2\text{SiEt}_2)(\text{PPh}_3)$



(21e) :  $\text{TpRuH}(\text{H}_2\text{SiPh}_2)(\text{PPh}_3)$



(21f) :  $\text{TpRuH}(\text{H}_3\text{SiPh})(\text{PPh}_3)$



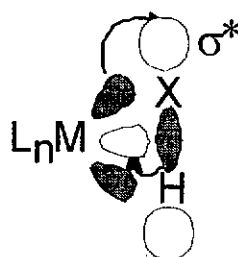
# *Chapter One*

## *Introduction*

Recent developments in coordination chemistry have demonstrated that certain  $\sigma$  bonds can coordinate to transition metals in an  $\eta^2$ -fashion without bond cleavage by the formation of three-centre two-electron bonds, giving rise to the so-called “ $\sigma$  complexes”. The first  $\sigma$  complex  $[\text{Cp}_2\text{Ti}(\text{H}_2\text{BH}_2)]^1$  was found in the 1960s, but it did not attract much attention at that time. The  $\eta^2$ -coordination of  $\sigma$  bonds not only is of fundamental importance from a structural point of view but also has significant implications for the activation of  $\sigma$  bonds in transition-metal-catalyzed transformation. Since we are beginning to recognize the key role of them in chemical reactions, there is an ever growing number of examples of nondestructive  $\sigma$  bond coordination to transition metals in the chemical literature.<sup>2</sup> Nowadays, a variety of well-characterized complexes are known to contain  $\sigma$ -coordinated ligands such as  $(\eta^2\text{-H}_2)$ ,<sup>3</sup> and  $(\eta^2\text{-HSiR}_3)$ .<sup>4</sup> To date, the formal relationship of  $\eta^2$ -dihydrogen complexes with the intramolecular agostic C—H species is well established,<sup>5</sup> in the meantime, transition metal complexes can be obtained with a variety of  $\sigma$ -coordinated X—H fragments, and their mode of bonding can be understood by a common and quite general model.

The simplest ligand that forms exclusively  $\sigma$  complex with transition metals is the dihydrogen molecule. The bonding model for  $\eta^2$ -( $\sigma$ - coordination) of H—X can be described in terms of two components: donation of electron density from the

$\sigma$ -bonding orbital of the ligand into an empty  $d_\sigma$  orbital of the metal and back-donation of electron density from a filled  $d_\pi$  orbital of metal into the  $\sigma^*$ -antibonding orbital of the ligand. The  $\sigma$  to  $M(d_\sigma)$  donation weakens but does not break the X—H bond because the resulting three-centre-two-electron ( $3c - 2e$ ) orbital has bonding character over all three centres. On the other hand, the  $M(d_\pi)$  to ( $\sigma^*$ ) back-donation populates the  $\sigma^*$ -antibonding orbital and thus can break the X—H bond if the back-donation is sufficiently strong.



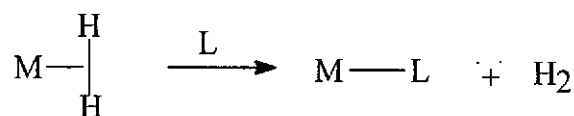
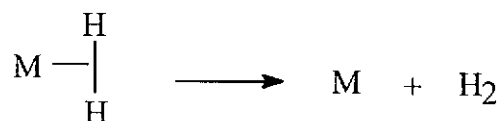
The relative stability of  $\sigma$  complex is controlled by the electronic and steric effect of the coordinated ligands. When varying the ancillary ligands and  $\pi$ -back-bonding capability of the metal-centre, the coordination of the complex will change from the non-classical  $\eta^2$ -( $\sigma$ -complex) to the classical one. For example, increasing the basicity of the ancillary ligands should promote  $M(d_\pi)$  to ( $\sigma^*$ ) back-donation and thereby ultimately lead to the cleavage of the X—H bond.

The first non-classical  $\eta^2$ -dihydrogen complex  $[W(\eta^2-H_2)(CO)_3(PCy_3)_2]$  was reported by Kubas<sup>6</sup> and co-workers at 1984. Recent years have witnessed considerable interest in transition-metal  $\eta^2$ -dihydrogen complexes, their establishment has opened the possibility of activating dihydrogen without oxidative addition, and these complexes represent intermediates or transition states in a number of important catalytic processes such as hydrogenation, hydrogenolysis, and

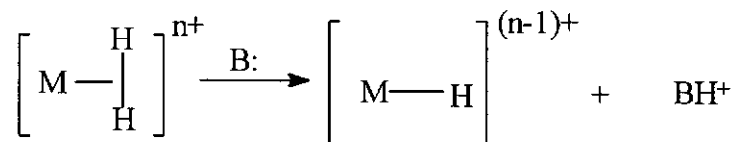
hydroformylation. The  $\eta^2$ -dihydrogen coordination not only is of fundamental interest from a structural point of view but also has significance in metal-catalyzed transformations involving dihydrogen. In this respect,  $\eta^2$ -dihydrogen complexes have been found to be involved in the mechanistic pathway in homogeneous catalysis including hydrogenation of alkenes<sup>7</sup> and alkynes,<sup>8</sup> hydrogenation of ketones,<sup>9</sup> dehydrogenation of alcohols,<sup>10</sup> dimerization of alkynes,<sup>11</sup> and H/D isotopic exchange.<sup>12</sup>

The followings are the features of  $\eta^2$ -dihydrogen metal complexes:<sup>13</sup>

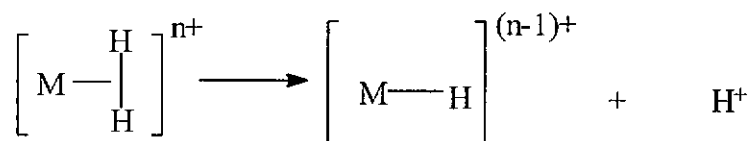
(i) facile dissociation and substitution lability;



(ii) heterolytic cleavage by base ( B =base );



(iii) high acidity,



These features render the  $\eta^2$ -dihydrogen complexes potentially valuable catalytic species. For example, coordinate unsaturation can be generated by dissociation of the labile dihydrogen ligand. Furthermore, heterolytic cleavage of acidic dihydrogen ligand by a base to give metal monohydride, which is one of the most interesting features of this class of compounds, opens the possibility of unique reactivity patterns of these complexes including catalysis and selective proton transfer to an ancillary ligand. Several enzymatic systems found in nature such as hydrogenases and nitrogenases are believed to involve the heterolytic activation of dihydrogen at a metal centre during sequential proton-electron transfer steps.<sup>14</sup>

In the past few years, there have been numerous efforts in defining the factors affecting the acidity properties of dihydrogen complexes, especially dihydrogen complexes of the type  $[\text{Cp}'\text{Ru}(\text{H}_2)(\text{PP})]^+$  ( $\text{Cp}' = \text{Cp}, \text{Cp}^*$ ;  $\text{PP} = \text{diphosphines}$ ),<sup>15,16</sup>  $[\text{MH}(\text{H}_2)(\text{PP})]^+$  ( $\text{M} = \text{Fe}, \text{Ru}, \text{Os}$ ;  $\text{PP} = \text{diphosphines}$ ),<sup>17,18</sup>  $[\text{MCl}(\text{H}_2)(\text{PP})]^+$  ( $\text{M} = \text{Fe}, \text{Ru}, \text{Os}$ ;  $\text{PP} = \text{diphosphines}$ ),<sup>18,19</sup> and  $[\text{M}(\text{L})(\text{H}_2)(\text{PP})_2]^{2+}$  ( $\text{M} = \text{Fe}, \text{Ru}, \text{Os}$ ;  $\text{PP} = \text{diphosphines}$ ;  $\text{L} = \text{CO}, \text{CH}_3\text{CN}$ ).<sup>18,20</sup> Deprotonation of dihydrogen ligands with various bases have been reported for other complexes,<sup>21</sup> for example,  $[\text{IrH}(\text{H}_2)(\text{bq})(\text{PPh}_3)_2]^+$  ( $\text{bq} = 7,8\text{-benzoquinolate}$ ) by  $\text{BuLi}$ ,  $[\text{Os}(\text{H}_2)(\text{NH}_3)_5]^{5+}$  by  $\text{NaOMe}$ , and  $[\text{Os}(\text{H}_2)(\text{CO})(\text{bpy})(\text{PPh}_3)_2]^{2+}$  by  $\text{Et}_2\text{O}$ . These studies showed that acidity of dihydrogen complexes can vary widely depending on the ligands and metals.

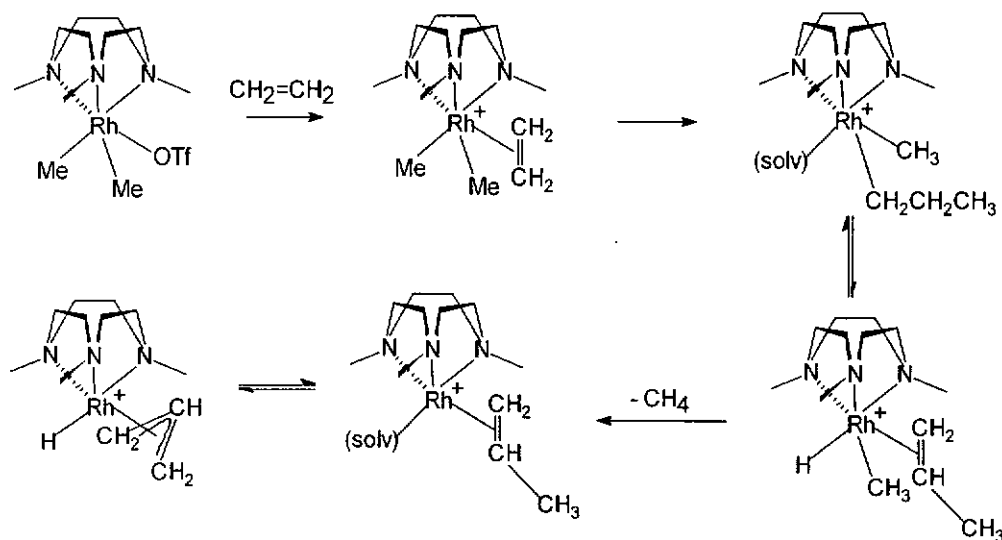
After the discovery of the first  $\eta^2$ -dihydrogen complex, a large number of isolable  $\eta^2$ -dihydrogen complexes have been prepared, the majority of which have been found to be singly charged cationic species. While the plethora of monocationic

complexes may be due to the common synthetic route of protonating a neutral metal hydride, an underlying aspect may be that the positive charge confers additional stability on the dihydrogen complexes. In contrast, the numbers of well-characterized dicationic complexes are limited.

Recently, there have been several interesting reports on the synthesis and reactivity of dicationic dihydrogen complexes. The dicationic complexes  $[\text{Os}(\text{H}_2)(\text{NH}_3)_5]^{2+}$  and  $[\text{Os}(\text{H}_2)(\text{en})_2(\text{L})]^{2+}$  were first reported by Taube,<sup>22</sup> other noted examples included  $[\text{Os}(\text{H}_2)(\text{CH}_3\text{CN})_3(\text{P}^i\text{Pr}_3)_2]^{2+}$ ,<sup>23</sup>  $[\text{Os}(\text{H}_2)(\text{CH}_3\text{CN})(\text{dppe})_2]^{2+}$ ,<sup>20</sup>  $[\text{M}(\text{H}_2)(\text{CO})(\text{dppp})_2]^{2+}$  (M = Ru, Os),<sup>18</sup>  $[\text{M}(\text{H}_2)(\text{CO})(\text{bpy})(\text{PR}_3)_2]^{2+}$  (M = Ru, Os),<sup>21k</sup> and , most recently,  $[\text{Fe}(\text{H}_2)(\text{dppe})_2(\text{L})]^{2+}$  (L = CO, CH<sub>3</sub>CN).<sup>18</sup> In my research, monocationic hydrido ruthenium complexes containing neutral <sup>R</sup>Cn were prepared, and formation of the corresponding dicationic dihydrogen complexes was the result of the protonation of these hydrido complexes.

The macrocyclic 1,4,7-triazacyclononane derivatives <sup>R</sup>Cn,<sup>24</sup> (where <sup>H</sup>Cn = 1,4,7-triazacyclononane, <sup>Me</sup>Cn = 1,4,7-trimethyl-1,4,7-triazacyclononane) have been used extensively in inorganic and organic chemistry, they are ‘hard’, facial tri-amine chelating ligands. Some Werner-type coordination chemistry of these pure σ-donor ligands with rhodium (e.g. <sup>Me</sup>CnRhCl<sub>3</sub>) was originally reported by Wieghardt and co-workers.<sup>25</sup> More recently, Flood et al have extensively studied the aspects of organometallic chemistry in the coordination sphere of rhodium bounded with 1,4,7-trimethyl-1,4,7-triazacyclononane. The <sup>Me</sup>Cn-containing compounds that have been

examined are  $^{\text{Me}}\text{CnRhMe}_{3-n}\text{X}_n$  ( $n = 0-3$ ;  $\text{X} = \text{H}, \text{Cl}, \text{Br}$  and  $\text{OTf}$ ). Flood has also revealed the key role of  $^{\text{Me}}\text{CnRhMe}_2(\text{OTf})$  in olefin metathesis.<sup>26j</sup>



In comparison with that of rhodium, the chemistry of ruthenium complexes of  $^{\text{R}}\text{Cn}$  is still in its infancy. But recent studies by Che have witnessed the rich oxidation chemistry of high-valent ruthenium-oxo complexes of macrocyclic amines. Some of these ruthenium  $^{\text{R}}\text{Cn}$  complexes show intriguing reactivities, for example,  $[\text{MeCnRu}^{\text{VI}}(\text{O})_2(\text{O}_2\text{CCF}_3)]\text{ClO}_4$  and  $[\text{MeCnRu}^{\text{VI}}(\text{O})(\text{bpy})][\text{ClO}_4]_2$  are active oxidants for organic oxidation.<sup>26g,h</sup>

Cyclopentadienyls,<sup>27</sup> hydrotris(pyrazolyl)borates<sup>28,29</sup> and 1,4,7-triazacyclononane derivatives ( $^{\text{R}}\text{Cn}$ )<sup>24,26</sup> are very useful ligands in organometallic chemistry and homogeneous catalysis. The three ligands are similar in that they all coordinate to the metals in a facial geometry, and are formally 6e donors on ionic model. They are different in their  $\pi$ -accepting ability, with cyclopentadienyls being the strongest and 1,4,7-triazacyclononane derivatives the weakest. It is therefore expected that the three ligands should show differences in stabilizing dihydrogen

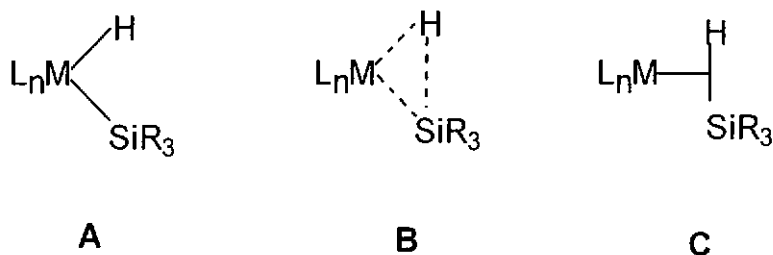
ligands and in affecting the acidity of the resulting dihydrogen and hydride complexes. However, such comparison has not been made yet. While numerous complexes of the type  $[(C_5R_5)Ru(H_2)(L)(L')]^+$  have been reported,<sup>15,16,30</sup> only a few  $[TpRu(H_2)(L)(L')]^+$  complexes are known,<sup>29a,b,i</sup> and the isostructural complexes  $[^R CnRu(H_2)(L)(L')]^{2+}$  are virtually unknown. The  $pK_a$  values of complexes of the type  $[(C_5R_5)Ru(H_2)(L)(L')]^+$  have been reported,<sup>15,16</sup> but that of the isostructural Tp and  $^R Cn$  complexes have not been well studied. In my research, dihydrogen complexes of ruthenium supported by 1,4,7-triazacyclononane and 1,4,7-trimethyl-1,4,7-triazacyclononane ligands have been synthesized and their chemical properties studied. Furthermore, the acidity measurements of  $[^R CnRu(H_2)(L)(L')]^{2+}$  and  $[TpRu(H_2)(L)(L')]^+$  have also been performed. These studies enable us to evaluate how the acidity of dihydrogen complexes change when they change from monocationic to dicationic.

Besides  $\eta^2-H_2$ , the chemistry of  $\sigma$ -bound silane ligands has also been intensively investigated. These silane ligands, which enable the investigation of a large range of  $\sigma$ -coordinated metal complex fragments, up to complete oxidative addition with cleavage of the Si—H bond and formation of silyl(hydrido) complexes, have thus widened our general understanding of the bonding of  $\sigma$  bound ligands.

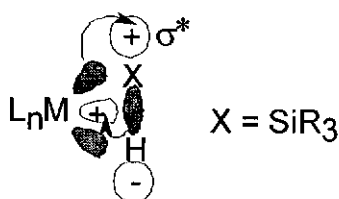
Transition metal silyl hydride complexes have been proposed as intermediates in many catalytic reactions, such as hydrosilylation of olefins<sup>31</sup> silane alcoholysis<sup>32</sup> and the polymerization of organosilanes.<sup>33</sup> The bonding in transition metal silyl hydride complexes has classically been described by either of two



structures, **A** (oxidative addition) or **C** (adducts formation). However, there are many complexes that cannot be accurately described by either **A** or **C** and are thus best represented by an intermediate structure such as **B**.

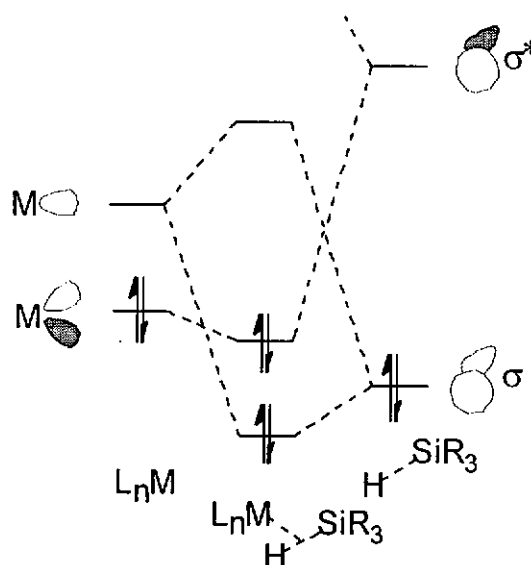


The metal centre fragment can react with a Si—H bond to give a  $\sigma$  complex, in which the Si—H bond acts as a  $2e^-$  donor. The Si—H bond is coordinated side-on to the metal centre, this gives rise to a three-centre-two electron bond. In analogy to the  $\sigma/\pi$  bonding formalism for ethene bonding to a transition metal, in silane bonding to a transition metal, electron density is transferred from an occupied  $\sigma$  orbital of the Si—H bond into an unoccupied metal  $d_\pi$  orbital. By a synergistic interaction, electron density also transfers from an occupied metal  $d_\pi$  orbital to the  $\sigma^*$  of the Si—H bond.



The M-(Si-H) can be strengthened by the backbonding of the  $d_\pi$  electrons on the metal into the Si—H bond  $\sigma^*$  orbital. Modest backbonding accounts for the stability of many  $\sigma$  complexes, but strong backbonding can lead to Si—H bond

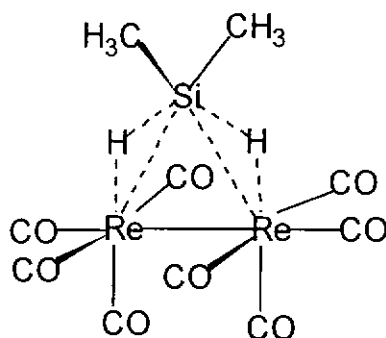
scission in the process known as oxidative addition to give compound of type Si-M-H as A.



The oxidative addition of a Si—H  $\sigma$  bond is one of the key steps in the mechanism of transition metal catalyzed hydrosilylation. There are numerous examples of the activation of Si—H  $\sigma$  bonds by  $M(L_n)$  centres and of complex formation. These reveal that the bonding in silane complexes corresponds to a late step in the oxidative addition to the transition metal centre. The  $^1J(\text{SiH})$  coupling constants and the elongation of the Si—H interatomic distances (from X-ray and neutron scattering investigations) provide a measure of the extent of the oxidative addition in  $\sigma$ -coordinated M-H-SiR<sub>3</sub> complexes.

The first silane  $\sigma$  complex<sup>34</sup> was formed from  $(\text{CH}_3)_2\text{SiH}_2$  and  $[\text{Re}_2(\text{CO})_{10}]$ . The reduction of proton coupling constant of the CH<sub>3</sub> proton to Si—H from 4.2 Hz in the free silane to 1.5 Hz in silane-rhenium complex provides an evidence of a  $\sigma$ -silane complex. The first mononuclear  $\sigma$ -silane complex was mentioned at an ACS Meeting and reported in 1970 only as a news item in *C & E News*.<sup>35</sup> However, this

field did not develop significantly at that time, it may have been caused by the misconception that such relatively weak M-(SiH) interaction would not have usefully large effects on the reactivity of the Si—H bond.



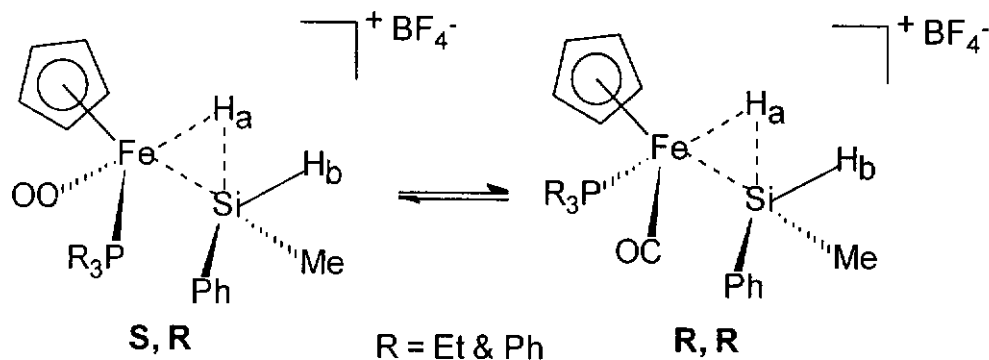
After the discovery of the distinctive properties of  $\eta^2$ -dihydrogen complexes<sup>6</sup> in the mid-80s, extensive studies on other  $\sigma$  complexes, such as the agostic species concerning C—H activation, have been carried out. During the same period, Schubert et al<sup>36</sup> have prepared a homologous series of manganese silane complexes which have the general formula  $\text{Cp}'\text{Mn}(\text{HSiX}_3)(\text{CO})(\text{L})$  and some of their structures have been carefully characterized by neutron diffraction. They have described the changes in structure and bonding which result from systematic variations in the substituents on the silicon and the Cp ring, as well as variations of the ligand L. It was found that both steric and electronic factors play important roles in determining whether the silane be oxidatively added to the metal centre, and the extent of Si—H bond breaking in the  $\eta^2$ -silane complexes. Extended Huckel calculation by Rabaa and Sailard<sup>37</sup> of these type of complexes showed that the three centre Mn-(H-Si) interaction can be viewed as a  $\sigma$  Si—H bond coordination to the  $d^6$   $\text{CpMnL}_2$  fragment. They also made generalization for other  $d^n$   $\text{L}_n\text{MHSiR}_3$  complexes in which, when the Si—H bond is fully broken, the addition is not oxidative, but the

bonding be better described as having a formally  $\text{H}^-$  and a formally  $\text{SiR}_3^+$  ligand coordinated to a metal atom which has the same formal oxidation state as in the free  $\text{ML}_n$  fragment.

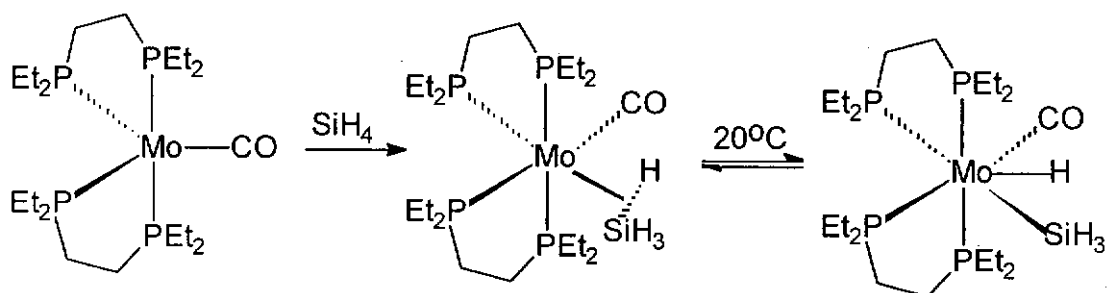
While there are numerous examples of neutral transition metal silane complexes, cationic complexes of this type are quite rare. During the investigations of silane alcoholysis catalyzed by a cationic Ir complex, Luo and Crabtree<sup>32</sup> suggested that cationic silane adducts and  $[\text{Ir}(\text{Et}_2\text{HSiSiHEt}_2)(\text{H})_2(\text{PPh}_3)_2]\text{SbF}_6$ , detected spectroscopically at low temperature, were related to the intermediate species in the catalytic cycle. The extremely high activity of  $[\text{Ir}(\text{HSiEt}_3)_2(\text{H})_2(\text{PPh}_3)_2]\text{SbF}_6$  in silane alcoholysis could be accounted for by the Lewis acidity of the metal centre which renders the bound Si—H group more polarized and significantly increase the electrophilic character of the silicon, thus making it very susceptible to nucleophilic attack by an alcohol and hence increase the rate of the reaction.

Recently, Brookhart<sup>38</sup> introduced a general and convenient method for the generation of cationic iron  $\eta^2$ -silane complexes,  $[\text{CpFe}(\text{HSiR}_3)(\text{CO})(\text{L})]^+$ , which are stabilized through the use of the non-coordinating counterion  $\text{BAr}'_4^-$  ( $\text{Ar}' = (\text{CF}_3)_2\text{C}_6\text{H}_3$ ). These species are easily formed by displacement of  $\text{H}_2$  from the cationic  $\eta^2\text{-H}_2$  complex by free silane. Diastereomeric iron silane complexes  $[\text{CpFe}(\text{H}_2\text{SiMePh})(\text{CO})(\text{PR}_3)]\text{BAr}'_4$  (where, R = Et and Ph) have been generated,

these complexes exhibit dynamic behavior that results from interconversion of the diastereomers.<sup>38</sup>

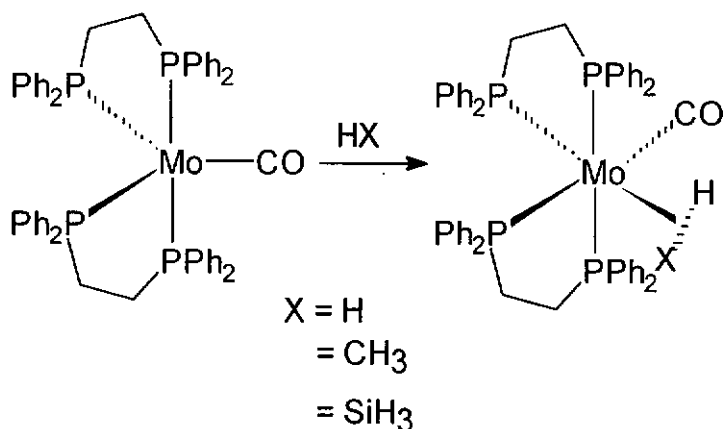


Moreover, Luo and Kubas<sup>39</sup> have succeeded in the synthesis, isolation, and structural characterization of a  $\eta^2$ -silane complex as formed by reaction of silane with the electronically and coordinatively unsaturated  $16 e^- \text{Mo}^0$  complexes of the type  $\text{Mo}(\text{CO})(\text{R}_2\text{PC}_2\text{H}_4\text{PR}_2)_2$ . When the R group in the unsaturated Mo complex is an ethyl group, it reacts with silane and an equilibrium of two tautomers exists in solution at room temperature.



With the phenyl phosphine analogs, only side-on  $\eta^2$ -coordination is observed both in solution and in the solid state. Moreover, all Si—H, H—H and agostic C—H bonds are capable of binding to this metal centre  $\text{Mo}(\text{CO})(\text{Ph}_2\text{PC}_2\text{H}_4\text{PPh}_2)_2$  in an  $\eta^2$ -

fashion. This is the first example of a system which provides a unique opportunity to study the differences between the common features among the three prototypes of  $\sigma$  complexes<sup>40</sup>.

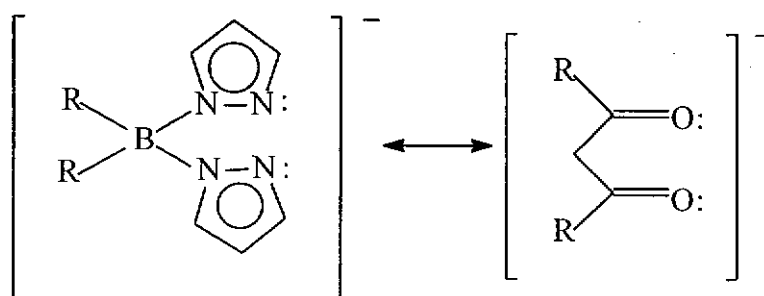


The work of Kubas on  $\sigma$ -complexes raises the possibility of having more than one  $\sigma$ -bonded groups attached to a metal centre. Complex of the general formula ' $\text{ML}_n(\text{H}_2\text{SiR}_3)$ ', where ' $\text{H}_2\text{SiR}_3$ ' stands for  $(\text{SiR}_3)(\eta^2\text{-H}_2)$  or  $(\text{H})(\eta^2\text{-HSiR}_3)$ , is interesting because it can form one tautomer containing a  $\eta^2\text{-H}_2$  or another one containing a  $\eta^2\text{-HSiR}_3$  ligand. For example, the complex  $\text{OsCl}(\text{SiEt}_3)(\text{H}_2)(\text{CO})(\text{P}^i\text{Pr}_3)_2$  has been characterized as a dihydrogen complex by Oro et al,<sup>41</sup> it is formulated as  $[\text{ML}_n(\text{SiR}_3)(\eta^2\text{-H}_2)]$ . On the other hand, Crabtree<sup>32</sup> reported a  $[\text{ML}_n(\text{H})(\eta^2\text{-HSiR}_3)]$  structure for the complex  $[\text{Ir}(\eta^2\text{-HSiR}_3)_2(\text{H})_2(\text{PPh}_3)_2]^+$ . Recently, ab Initio MO calculation on the model system of  $[\text{OsCl}(\text{CO})(\text{PH}_3)_2\text{'H}_2\text{SiH}_3\text{'}]$  has been performed by Lledos and co-workers,<sup>42</sup> the possible existence of two stable species,  $[\text{OsCl}(\text{SiH}_3)(\eta^2\text{-H}_2)(\text{CO})(\text{PH}_3)_2]$  and  $[\text{OsCl}(\text{H})(\eta^2\text{-HSiH}_3)(\text{CO})(\text{PH}_3)_2]$ , which are very close in energy has been postulated.

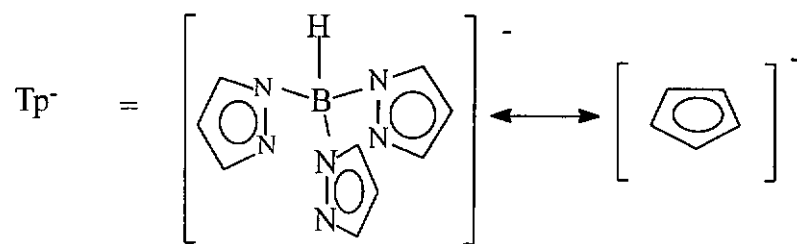
Coordination of  $\eta^2$ -silane ligands have been found on many transition metals and in different ligand environments. However, most of these known complexes contain cyclopentadienyl ( $Cp^-$ ) and / or phosphine ligands,<sup>36,38,43</sup> but very few complexes supported by nitrogen donor ligands have been reported.<sup>44</sup> It is noted that nitrogen donors are among the various ligands that exert poor trans effect / influence and it can be easily labilized by common ligands like phosphine.

The poly(pyrazolyl)borate ( $H_nB(pz)_{4-n}$ ) is one of the ligands containing nitrogen donors. This type of ligands have found wide application in coordination chemistry, and their complexes with most metals or metalloids in the periodic table have been prepared.<sup>28a</sup>

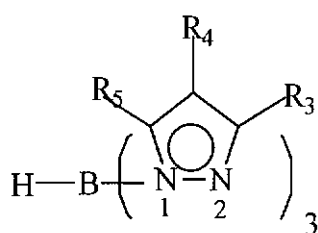
Throughout the years, poly(pyrazolyl)borates have been compared to  $\beta$ -diketonates of its bidentate form ( $R_2Bpz_2^-$ ):



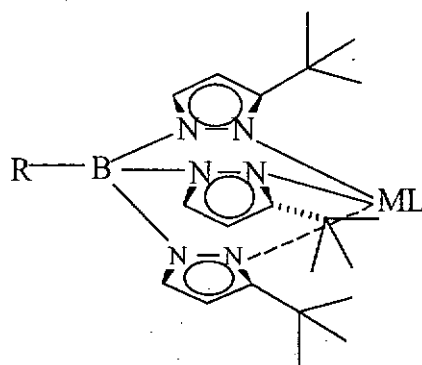
or to cyclopentadienyl ligands  $Cp^-$  /  $Cp^*$  of its tridentate form  $Tp^-$ :



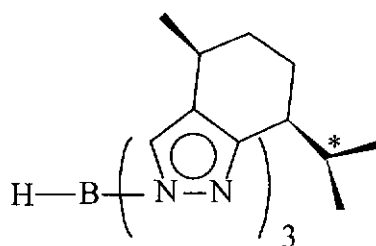
Both  $\text{Cp}^-$  and  $\text{Tp}^-$  are uni-negative charged, six-electron donating and facial tridentate ligand. Moreover, the pyrazolyl groups in  $\text{Tp}^-$  contains three C—H bonds which can be substituted by various substituents, such as alkyl, aryl,  $\text{NR}_2$  and  $\text{ArS}$ :



Such substitution can produce a highly screened metal centre:



For instance, the cone angles of  $\text{Tp}^-$ ,  $^{3,5\text{-Me}}\text{Tp}^-$  and  $^{3,5\text{-tBu}}\text{Tp}^-$  are  $184^\circ$ ,  $224^\circ$ , and  $244^\circ$  respectively. Optically active poly(pyrazolyl)borate ligands can be generated by attachment of chiral substituents.<sup>28a</sup>





The ligand hydrotris(1-pyrazolyl)borate has been extensively used in this research. Its potassium salt can be easily synthesized by direct reaction of potassium borohydride with pyrazole. Due to the ready availability of hydrotris(1-pyrazolyl)borate ligand, considerable amount of work with this ligand has been reported.<sup>29</sup>

A number of  $\eta^2$ -dihydrogen complexes bearing hydrotris(1-pyrazolyl)borate ligand have been synthesized and characterized by our group.<sup>29b</sup> Some of these complexes such as  $[\text{TpRu}(\text{H}_2)(\text{PPh}_3)_2]\text{BF}_4$  (**17**) and  $[\text{TpRu}(\text{H}_2)(\text{CH}_3\text{CN})(\text{PPh}_3)]\text{BF}_4$  (**18**) were shown to be involved in the catalytic hydrogenation of unsaturated hydrocarbon.<sup>29b</sup> In the light of the similarity in the bonding modes of the  $\eta^2$ - $\text{H}_2$  and the  $\eta^2$ - $\text{HSiR}_3$  ligands in  $\eta^2$ -dihydrogen complexes and the  $\eta^2$ -silane complexes, respectively, it is interesting to synthesize and to study the chemical properties of Tp ruthenium complexes containing  $\eta^2$ -silane ligands. These complexes are analogous to the Tp ruthenium  $\eta^2$ -dihydrogen complexes. The first attempt to synthesize the Tp ruthenium  $\eta^2$ -silane complexes was by reacting **17** with triethylsilane, it was expected that simple ligand substitution of  $\eta^2$ - $\text{H}_2$  with  $\eta^2$ - $\text{HSiR}_3$  would give the  $\eta^2$ -silane complexes  $[\text{TpRu}(\eta^2\text{-HSiR}_3)(\text{PPh}_3)_2]\text{BF}_4$ . But unfortunately, the expected  $\eta^2$ -silane complexes were not obtained, probably due to the instability of the  $\eta^2$ - $\text{HSiR}_3$  ligand in  $[\text{TpRu}(\eta^2\text{-HSiR}_3)(\text{PPh}_3)_2]\text{BF}_4$  towards nucleophiles such as  $\text{BF}_4^-$  and adventitious  $\text{H}_2\text{O}$  in the solvent. It was later found that ruthenium hydrido solvento complex  $[\text{TpRuH}(\text{CH}_3\text{CN})(\text{PPh}_3)]$  (**13**) reacted with silane  $\text{HSiR}_3$  ( $\text{R}_3 = \text{Et}_3, (\text{OEt})_3, \text{Ph}_3, \text{HEt}_2, \text{HPh}_2, \text{and H}_2\text{Ph}$ ) to yield the silane complexes  $[\text{TpRu}(\text{PPh}_3)(\text{H}_2\text{SiR}_3)]$

(**21**) which, instead of equilibrating between the  $\eta^2$ -silane and  $\eta^2$ -H<sub>2</sub> tautomeric forms (eq. 1), interchanged the H atoms rapidly, and rendering them equivalent. (eq.

2) The silane complex **21** is analogous to the dihydrogen hydride complex [TpRuH(H<sub>2</sub>)(PPh<sub>3</sub>)] (**16**) that we have recently reported.<sup>29a</sup>



## *Chapter Two*

### *Syntheses, characterization and reactivity of ruthenium $\eta^2$ - dihydrogen complexes*

#### **2.1 Introduction**

Knowledge about the acidity of dihydrogen complexes may help to understand mechanisms of stoichiometric and/or catalytic reactions involving heterolytic cleavage of dihydrogen bond,<sup>45</sup> and to design new catalytic processes. The most interesting examples involving heterolytic cleavage of dihydrogen reported recently include intramolecular protonation of alkyl ligands by dihydrogen ligands in the hydrogenation reactions,<sup>7,8</sup> intramolecular protonation of vinylidene ligands by dihydrogen ligands to form carbyne complexes,<sup>8</sup> and transition metal catalyzed H/D exchange reactions.<sup>12</sup>

In this chapter, the preparation of some ruthenium hydrido and dihydrogen complexes containing Tp and <sup>R</sup>Cn are described. The acidity of these dihydrogen complexes have been measured, and differences in stability and acidity between the Cp, Tp and <sup>R</sup>Cn dihydrogen complexes are also discussed.

#### **2.2 Experimental**

##### *2.2.1 Materials*

All reactions were carried out under a dry N<sub>2</sub> atmosphere using Schlenk techniques. All solvents were distilled and degassed prior to use. Dichloromethane and acetonitrile were distilled from calcium hydride; tetrahydrofuran, diethyl ether and

hexane were distilled from sodium benzophenone ketyl. Deuterated dichloromethane was dried on P<sub>2</sub>O<sub>5</sub> and vacuum transferred to a flask fitted with a rubber septum. Deuterated Tetrahydrofuran was dried on calcium hydride and vacuum transferred to a flask fitted with a rubber septum. 1,4,7-triazacyclononane, 1,4,7-trimethyl-1,4,7-triazacyclononane were prepared as reported.<sup>25a</sup> The complexes RuHCl(PPh<sub>3</sub>)<sub>3</sub>,<sup>46</sup> <sup>Me</sup>CnRuCl<sub>3</sub>,<sup>47</sup> RuHCl(CO)(PPh<sub>3</sub>)<sub>3</sub>,<sup>48</sup> [<sup>Me</sup>CnRuH(dppe)]CF<sub>3</sub>SO<sub>3</sub>,<sup>26d</sup> [<sup>Me</sup>CnRuH(CO)(PPh<sub>3</sub>)]PF<sub>6</sub>,<sup>26d</sup> TpRuH(PPh<sub>3</sub>)<sub>2</sub>,<sup>29b</sup> [TpRu(H<sub>2</sub>)(CH<sub>3</sub>CN)(PPh<sub>3</sub>)]BF<sub>4</sub>,<sup>29b</sup> [TpRu(H<sub>2</sub>)(PPh<sub>3</sub>)<sub>2</sub>]<sup>29b</sup> BF<sub>4</sub>,<sup>29b</sup> TpRuH(CH<sub>3</sub>CN)(PPh<sub>3</sub>),<sup>29b</sup> and TpRuH(CO)(PPh<sub>3</sub>)<sup>29a</sup> were synthesized according to literature methods. HBF<sub>4</sub>.Et<sub>2</sub>O (56%) and aqueous HBF<sub>4</sub> (50%) were purchased from Fluka, CF<sub>3</sub>SO<sub>3</sub>H was purchased from Aldrich and was used as received.

### 2.2.2 Instrumentation

Infrared spectra were obtained as KBr disc from a Nicolet Magna 750 FT IR spectrophotometer. <sup>1</sup>H NMR spectra were taken on a Bruker DPX 400 spectrometer. Chemical shifts were referenced to the residue peaks of the deuterated solvents(CD<sub>2</sub>HCl<sub>2</sub> δ 5.32 ppm, C<sub>4</sub>D<sub>7</sub>H δ 1.85 ppm, δ 3.70 ppm). <sup>31</sup>P{<sup>1</sup>H} NMR spectra were recorded on a Bruker DPX 400 spectrometer at 161.70 MHz. <sup>31</sup>P chemical shifts were externally referenced to 85% H<sub>3</sub>PO<sub>4</sub>. T<sub>1</sub> relaxation measurements were carried out in CD<sub>2</sub>Cl<sub>2</sub> at 400 MHz by the inversion-recovery method using a standard 180-τ-90 pulse sequence. Fast Atom Bombardment Mass Spectrometry was carried out with a Finnigan MAT 95S mass spectrometer using 3-nitrobenzyl alcohol as matrix. Elemental analyses were performed by M-H-W Laboratories, Phoenix, Arizona, U.S.A.

## 2.2.3 Syntheses

### 2.2.3.1 Hydrido complexes

**[<sup>1</sup>H]CnRuH(PPh<sub>3</sub>)<sub>2</sub>]BF<sub>4</sub> (1).** A mixture of RuHCl(PPh<sub>3</sub>)<sub>3</sub> (0.50 g, 0.54 mmol), 1,4,7-triazacyclononane (0.20 g, 1.55 mmol) and NaBF<sub>4</sub> (0.10 g, 0.91 mmol) in 100 mL of THF was stirred under nitrogen for 2 h. The mixture was filtered through celite, and the filtrate was concentrated to about 5 mL. Diethyl ether (10 mL) was added to precipitate out a yellow solid which was filtered out. The solid was washed with diethyl ether and vacuum dried at room temperature. Yield: 0.36 g (79%). Anal. Calcd for C<sub>42</sub>H<sub>46</sub>BN<sub>3</sub>F<sub>4</sub>P<sub>2</sub>Ru: C, 59.86; H, 5.50; N, 4.99. Found: C, 59.10; H, 5.73; N, 5.03. IR (KBr, cm<sup>-1</sup>): ν(Ru-H) 1958 (w). <sup>1</sup>H NMR (400 MHz, CD<sub>2</sub>Cl<sub>2</sub>): δ -15.98 (t, 1H, <sup>2</sup>J(HP) = 38.3 Hz, Ru-H), 2.29-3.44 (m, 2H, N-H and 12H, NCH<sub>2</sub>), 5.24 (s, 1H, N-H), 7.19-7.43 (m, 30 H of PPh<sub>3</sub>). <sup>31</sup>P{<sup>1</sup>H} NMR (161.70 MHz, CD<sub>2</sub>Cl<sub>2</sub>): δ 67.4 (s). FAB MS (m/z): 756 [M-BF<sub>4</sub>]<sup>+</sup>, 494 [M-BF<sub>4</sub>-PPh<sub>3</sub>]<sup>+</sup>.

**[<sup>1</sup>H]CnRuH(CO)(PPh<sub>3</sub>)]BF<sub>4</sub> (2).** A mixture of RuHCl(CO)(PPh<sub>3</sub>)<sub>3</sub> (2.50 g, 2.69 mmol) and 1,4,7-triazacyclononane (0.50 g, 3.87 mmol) in 250 mL of 2-methoxyethanol was refluxed under nitrogen for 18 h. The mixture was filtered, and the filtrate was concentrated to about 40 mL. Sodium tetrafluoroborate (0.66 g, 6.00 mmol) was added, and the resulting mixture was filtered to afford the crude product which was washed with ethanol and diethyl ether. It was then extracted with 20 mL of dichloromethane, and the solvent of the extract was removed to yield a white solid. Yield: 0.44 g (27%). Anal. Calcd for C<sub>25</sub>H<sub>31</sub>BN<sub>3</sub>OF<sub>4</sub>PRu: C, 49.36; H, 5.14; N, 6.91. Found: C, 49.10; H, 5.23; N, 6.78. IR (KBr, cm<sup>-1</sup>): ν(CO) 1920 (vs), ν(Ru-H) 1997 (w). <sup>1</sup>H NMR (400 MHz, CD<sub>2</sub>Cl<sub>2</sub>): δ -12.83 (d, 1H, <sup>2</sup>J(HP) = 28.8 Hz, Ru-H), 2.81 (s,

1H, N-H), 2.45-3.40 (m, 12H, NCH<sub>2</sub>), 3.90 (s, 1H, N-H), 5.12 (s, 1H, N-H), 7.34-7.58 (m, 15H of PPh<sub>3</sub>). <sup>31</sup>P{<sup>1</sup>H} NMR (161.70 MHz, CD<sub>2</sub>Cl<sub>2</sub>): δ 68.1 (s). FAB MS (m/z): 522 [M-BF<sub>4</sub>]<sup>+</sup>.

**TpRuH(dppe) (14).** A 1,4-dioxane solution (100 mL) of TpRuH(PPh<sub>3</sub>)<sub>2</sub> (0.50 g, 0.60 mmol) and dppe (0.30 g, 0.75 mmol) was stirred under nitrogen at 100 °C for 16 h. The solution was cooled and concentrated to about 5 mL. Diethyl ether (10 mL) was added to give a yellow solid which was filtered out. The solid was washed with diethyl ether and then dried under vacuum. Yield: 0.35 g (82%). Anal. Calcd for C<sub>35</sub>H<sub>35</sub>BN<sub>6</sub>P<sub>2</sub>Ru: C, 58.89; H, 4.94; N, 11.78. Found: C, 58.88; H, 5.10; N, 11.54. IR (KBr, cm<sup>-1</sup>): ν(Ru-H) 1909 (w), ν(B-H) 2470 (br). <sup>1</sup>H NMR (400 MHz, CD<sub>2</sub>Cl<sub>2</sub>): δ -14.23 (t, 1H, <sup>2</sup>J(HP) = 28.0 Hz, Ru-H), 2.09-2.49 (m, 4H, CH<sub>2</sub>CH<sub>2</sub>), 5.34 [t, 1H, H(pz)], 5.58 (d, 1H, H(pz)], 5.90 [t, 2H, H(pz')], 7.03 [d, 2H, H(pz')], 7.47 [d, 1H, H(pz)], 7.61 [d, 2H, H(pz')] (pz = pyrazolyl group trans to hydride, pz' = pyrazolyl groups trans to dppe; all coupling constants for pyrazolyl proton resonances were about 2 Hz); 6.86, 6.98, 7.13, 7.35, 7.89 (m, 20 H of dppe phenyl groups). <sup>31</sup>P{<sup>1</sup>H} NMR (161.70 MHz, CD<sub>2</sub>Cl<sub>2</sub>): δ 90.0 (s). FAB MS (m/z): 714 [M]<sup>+</sup>.

### 2.2.3.2 Dihydrogen Complexes and Their Isotopomers.

The carbonyl dihydrogen complexes **6**, **8** and **20** are unstable with respect to loss of H<sub>2</sub> at room temperature. It is also difficult to obtain dihydrogen complexes **5**, **7** and **19** in pure form because they are usually contaminated by their corresponding aquo complexes. These dihydrogen complexes were therefore only characterized in situ.

The complexes [ $^{\text{H}}\text{CnRu}(\text{H}_2)(\text{PPh}_3)_2](\text{BF}_4)_2$  (**5**), [ $^{\text{Me}}\text{CnRu}(\text{H}_2)(\text{dppe})](\text{CF}_3\text{SO}_3)_2$  (**7**) and [ $\text{TpRu}(\text{H}_2)(\text{dppe})\text{BF}_4$ ] (**19**) were prepared as follows. In a typical experiment, a sample (10 mg) of a metal hydride was loaded into a 5 mm NMR tube, which was then capped with a rubber septum. The tube was evacuated and then filled with nitrogen for three cycles. Dichloromethane- $d_2$  (0.4 mL) was added to dissolve the sample, followed by addition of 5  $\mu\text{L}$  of  $\text{HBF}_4\cdot\text{Et}_2\text{O}$  or  $\text{CF}_3\text{SO}_3\text{H}$ . The solution was immediately analyzed by NMR spectroscopy.

**[ $^{\text{H}}\text{CnRu}(\text{H}_2)(\text{PPh}_3)_2](\text{BF}_4)_2$  (**5**).**  $^1\text{H}$  NMR (400 MHz,  $\text{CD}_2\text{Cl}_2$ ):  $\delta$  -9.04 [br, 2H, Ru-( $\text{H}_2$ )], 2.35-4.29 (m, 2H, N- $\text{H}$  and 12H,  $\text{NCH}_2$ ), 5.84 (s, 1H, N- $\text{H}$ ), 7.26-7.44 (m, 30H of  $\text{PPh}_3$ ).  $^{31}\text{P}\{^1\text{H}\}$  NMR (161.70 MHz,  $\text{CD}_2\text{Cl}_2$ ):  $\delta$  39.5 (s).  $T_1$  (400 MHz,  $\text{CD}_2\text{Cl}_2$ ), ms (temperature): 22 (273 K), 21 (263 K), 20 (253 K), 20 (243 K), 21 (233 K), 23 (223 K), 27 (213 K), 34 (203 K). A  $\ln T_1$  vs  $1000/T$  plot gave a  $T_1(\text{min})$  of 20 ms at 250 K.

**[ $^{\text{Me}}\text{CnRu}(\text{H}_2)(\text{dppe})](\text{CF}_3\text{SO}_3)_2$  (**7**).**  $^1\text{H}$  NMR (400 MHz,  $\text{CD}_2\text{Cl}_2$ ):  $\delta$  -9.79 [br, 2H, Ru-( $\text{H}_2$ )], 1.93 (m, 2H,  $\text{NCH}_2$ ), 2.56-2.69 (m, 4H,  $\text{PCH}_2$ ), 2.79-2.81 (m, 6H,  $\text{NCH}_2$ ), 7.48-7.62 (m, 20H of  $\text{PPh}_3$ ).  $^{31}\text{P}\{^1\text{H}\}$  NMR (161.70 MHz,  $\text{CD}_2\text{Cl}_2$ ):  $\delta$  57.4 (s).  $T_1$  (400 MHz,  $\text{CD}_2\text{Cl}_2$ ), ms (temperature): 29 (313 K), 27 (303 K), 26 (293 K), 25 (283 K), 25 (273 K), 24 (263 K), 25 (253 K), 26 (243 K), 28 (233 K), 31 (223 K), 37 (213 K), 47 (203 K). A  $\ln T_1$  vs  $1000/T$  plot gave a  $T_1(\text{min})$  of 24 ms at 266 K.

**[ $\text{TpRu}(\text{H}_2)(\text{dppe})\text{BF}_4$ ] (**19**).**  $^1\text{H}$  NMR (400 MHz,  $\text{CD}_2\text{Cl}_2$ ):  $\delta$  -9.28 [br, 2H, Ru-( $\text{H}_2$ )], 2.82-2.96 (m, 4H,  $\text{PCH}_2$ ), 5.25 [t, 1H, H( $\text{pz}$ )], 5.52 [d, 1H, H( $\text{pz}$ )], 6.09 [t,

2H, H(pz')], 6.82 [d, 2H, H(pz')], 7.51 [d, 1H, H(pz)], 7.79 [d, 2H, H(pz')] (pz = pyrazolyl group trans to H<sub>2</sub>, pz' = pyrazolyl groups trans to dppe; all coupling constants for pyrazolyl proton resonances were about 2 Hz); 6.63, 7.06, 7.30, 7.53 (m, 20H of dppe phenyl groups). <sup>31</sup>P{<sup>1</sup>H} NMR (161.70 MHz, CD<sub>2</sub>Cl<sub>2</sub>): δ 45.7 (s). T<sub>1</sub> (400 MHz, CD<sub>2</sub>Cl<sub>2</sub>), ms (temperature): 22 (293 K), 20 (283 K), 18 (273 K), 17 (263 K), 15 (253 K), 14 (243 K), 14 (233 K), 13 (228 K), 15 (218 K), 16 (213 K). A T<sub>1</sub> vs 1000/T plot gave a T<sub>1</sub>(min) of 14 ms at 230 K.

The corresponding HD isotopomers were prepared analogously except that DBF<sub>4</sub>, which was prepared by mixing HBF<sub>4</sub>·Et<sub>2</sub>O with D<sub>2</sub>O in a volume ratio of 3:1, was used instead of HBF<sub>4</sub>·Et<sub>2</sub>O or CF<sub>3</sub>SO<sub>3</sub>H. The η<sup>2</sup>-HD signals were observed after nulling the η<sup>2</sup>-H<sub>2</sub> peaks by the inversion-recovery method.

**[<sup>H</sup>CnRu(HD)(PPh<sub>3</sub>)<sub>2</sub>]<sup>2+</sup>**. <sup>1</sup>H NMR (400 MHz, CD<sub>2</sub>Cl<sub>2</sub>): δ -9.06 [tt, <sup>1</sup>J(HD) = 29.4 Hz, <sup>2</sup>J(HP) = 6.3 Hz, Ru-(HD)]

**[<sup>Me</sup>CnRu(HD)(dppe)]<sup>2+</sup>**. <sup>1</sup>H NMR (400 MHz, CD<sub>2</sub>Cl<sub>2</sub>): δ -9.85 [tt, <sup>1</sup>J(HD) = 29.4 Hz, <sup>2</sup>J(HP) = 8.0 Hz, Ru-(HD)].

**[TpRu(HD)(dppe)]<sup>+</sup>**. <sup>1</sup>H NMR (400 MHz, CD<sub>2</sub>Cl<sub>2</sub>): δ -9.34 [t, <sup>1</sup>J(HD) = 32.5 Hz, Ru-(HD)].

The CO-containing dihydrogen complexes **6**, **8** and **20** were prepared as follows. In a typical experiment, a sample (10 mg) of the metal hydride was loaded into



a 5 mm NMR tube, which was then capped with a rubber septum. The tube was evacuated and filled with nitrogen for three cycles. Dichloromethane- $d_2$  (0.4 mL) was added to dissolve the sample. The solution was cooled to  $-78\text{ }^\circ\text{C}$ , and  $5\text{ }\mu\text{L}$  of  $\text{HBF}_4$  was added through a microsyringe. The tube was loaded into the NMR probe precooled to  $-30\text{ }^\circ\text{C}$  (**6** and **8**) or  $-80\text{ }^\circ\text{C}$  (**20**), and the sample was immediately analyzed by NMR spectroscopy.

$[\text{CnRu}(\text{H}_2)(\text{CO})(\text{PPh}_3)](\text{BF}_4)_2$  (**6**).  $^1\text{H}$  NMR (400 MHz,  $\text{CD}_2\text{Cl}_2$ ):  $\delta$  -7.25 [br, 2H, Ru- $(\text{H}_2)$ ], 1.26-5.58 (m, 3H, N- $H$  and 12H,  $\text{NCH}_2$ ), 7.48-7.61 (m, 15H of  $\text{PPh}_3$ ).  $^{31}\text{P}\{^1\text{H}\}$  NMR (161.70 MHz,  $\text{CD}_2\text{Cl}_2$ ):  $\delta$  45.7 (s).  $T_1$  (400 MHz,  $\text{CD}_2\text{Cl}_2$ ), ms (temperature): 15 (263 K), 13 (253 K), 14 (243 K), 18 (233 K), 19 (223 K), 20 (213 K). A  $\ln T_1$  vs  $1000/T$  plot gave a  $T_1(\text{min})$  of 14 ms at 248 K.

$[\text{MeCnRu}(\text{H}_2)(\text{CO})(\text{PPh}_3)](\text{PF}_6)(\text{CF}_3\text{SO}_3)$  (**8**).  $^1\text{H}$  NMR (400 MHz,  $\text{CD}_2\text{Cl}_2$ ):  $\delta$  -7.63 [br, 2H, Ru- $(\text{H}_2)$ ], 1.26-4.52 (m, 9H,  $\text{NCH}_3$  and 12H,  $\text{NCH}_2$ ), 7.41-7.66 (m, 15H of  $\text{PPh}_3$ ).  $^{31}\text{P}\{^1\text{H}\}$  NMR (161.70 MHz,  $\text{CD}_2\text{Cl}_2$ ):  $\delta$  32.2 (s).  $T_1$  (400 MHz,  $\text{CD}_2\text{Cl}_2$ ), ms (temperature): 41 (258 K), 28 (253 K), 17 (248 K), 15 (243 K), 14 (238 K), 15 (223 K), 17 (215 K), 20 (203 K). A  $\ln T_1$  vs  $1000/T$  plot gave a  $T_1(\text{min})$  of 12 ms at 224 K.

$[\text{TpRu}(\text{H}_2)(\text{CO})(\text{PPh}_3)]\text{BF}_4$  (**20**).  $^1\text{H}$  NMR (400 MHz,  $\text{CD}_2\text{Cl}_2$ ):  $\delta$  -6.84 [br, 2H, Ru- $(\text{H}_2)$ ], 5.89 [br, 1H, H(pz)], 6.05 [br, 1H, H(pz)], 6.31 [br, 1H, H(pz)], 6.40 [br, 1H, H(pz)], 6.66 [br, 1H, H(pz)], 7.76 [br, 2H, H(pz)], 7.85 1H, H(pz)], 7.94 [br, 1H, H(pz)].  $^{31}\text{P}\{^1\text{H}\}$  NMR (161.70 MHz,  $\text{CD}_2\text{Cl}_2$ ):  $\delta$  45.7 (s).  $T_1$  (400 MHz,  $\text{CD}_2\text{Cl}_2$ ), ms

(temperature): 13 (243 K), 12 (238 K), 11 (233 K), 11 (223 K), 12 (218 K), 13 (213 K), 14 (208), 47 (203 K). A  $\ln T_1$  vs  $1000/T$  plot gave a  $T_1$ (min) of 12 ms at 224 K.

The corresponding HD isotopomers were prepared analogously except that  $\text{DBF}_4$  was used in place of  $\text{HBF}_4 \cdot \text{Et}_2\text{O}$ . The  $\eta^2$ -HD signals were observed after nulling the  $\eta^2$ - $\text{H}_2$  peaks by the inversion-recovery method.

$[\text{H}^{\text{CnRu}}(\text{HD})(\text{CO})(\text{PPh}_3)]^{2+}$ .  $^1\text{H}$  NMR (400 MHz,  $\text{CD}_2\text{Cl}_2$ ):  $\delta$  -7.29 [t,  $^1J(\text{HD}) = 31.8$  Hz, Ru-(HD)].

$[\text{Me}^{\text{CnRu}}(\text{HD})(\text{CO})(\text{PPh}_3)]^{2+}$ .  $^1\text{H}$  NMR (400 MHz,  $\text{CD}_2\text{Cl}_2$ ):  $\delta$  -7.65 [t,  $^1J(\text{HD}) = 31.0$  Hz, Ru-(HD)].

$[\text{TpRu}(\text{HD})(\text{CO})(\text{PPh}_3)]^+$ .  $^1\text{H}$  NMR (400 MHz,  $\text{CD}_2\text{Cl}_2$ ):  $\delta$  -6.87 [t,  $^1J(\text{HD}) = 33.3$  Hz, Ru-(HD)].

### 2.2.3.3 Solvento complex

$[\text{H}^{\text{CnRu}}(\text{H}_2\text{O})(\text{PPh}_3)_2](\text{BF}_4)_2$  (**9**). A sample of **1** (0.20 g, 0.24 mmol) was added to a two-necked round bottom flask which was evacuated and flushed with nitrogen. Degassed THF (10 mL) was syringed into the flask, followed by addition of 5 equiv of aqueous tetrafluoroboric acid (50  $\mu\text{L}$ ,  $\text{HBF}_4$ , 8M). After the mixture was stirred at room temperature for 5 min, 0.5 mL of degassed water was added to the mixture, and the resulting solution was stirred for a further 30 min. Addition of degassed hexane (20 mL) led to the precipitation of a yellow solid, which was then

filtered out and washed with diethyl ether (2 X 5 mL). Finally, it was collected and dried under vacuum. Yield: 0.13 g (58%). Anal. Calcd for  $C_{42}H_{47}B_2N_3F_8OP_2Ru$ : C, 53.30; H, 5.01; N, 4.44. Found: C, 52.11; H, 4.92; N, 4.21.  $^1H$  NMR (400 MHz,  $CD_2Cl_2$ ):  $\delta$  1.26 (s, 2H,  $H_2O$ ), 2.43-4.03 (m, 3H, N-H and 12H,  $NCH_2$ ), 7.19-7.75 (m, 30 H of  $PPh_3$ ).  $^{31}P\{^1H\}$  NMR (161.70 MHz,  $CD_2Cl_2$ ):  $\delta$  38.7 (s).

#### 2.2.4 Acidity Measurement.

$pK_a$  values of **5**, **7**, and **17-20** were estimated by studying the equilibrium shown in eq. 5. All measurements were carried out at room temperature except that of **18** (-30 °C) and **20** (-80 °C). In a typical experiment, appropriate amounts of  $[L_nRuH]^{(n-1)+}$  and  $L'_nRuH$  were dissolved in  $CD_2Cl_2$  in an NMR tube, and then limited amount of  $HBf_4 \cdot Et_2O$  was added.  $^{31}P$  and  $^1H$  NMR spectra were taken. Relative molar concentrations of the equilibrated species were estimated from the  $^1H$  NMR integrations of the hydride signals.

The  $pK_a$  values of the two  $R^{Cn}$  carbonyl dihydrogen complexes **6** and **8** were estimated by use of the equilibrium depicted in eq. 6. In a typical experiment, appropriate amount of  $HBf_4 \cdot Et_2O$  was added to a  $CD_2Cl_2$  solution of the metal hydride in an NMR tube. NMR spectra were recorded at -80 °C, and the relative molar concentrations of  $HBf_4 \cdot Et_2O$ ,  $Et_2O$ , the metal hydride and the dihydrogen complex were estimated based on the  $^1H$  NMR integrations.

### 2.2.5 Crystallographic Analysis

$[\text{H}^{\text{Cn}}\text{RuH}(\text{PPh}_3)_2]\text{BF}_4 \cdot 2\text{CH}_2\text{Cl}_2$  (**1**). Suitable crystals for X-ray diffraction study were obtained by layering of hexane on a dichloromethane solution of  $[\text{H}^{\text{Cn}}\text{RuH}(\text{PPh}_3)_2]\text{BF}_4$ . A red block crystal of dimension 0.22x0.23x0.29 mm was mounted in a glass capillary and used for X-ray structure determination. All measurements were made on a Marresearch image plate scanner with graphite monochromated Mo K $\alpha$  radiation. The crystal system is orthorhombic and the space group  $P2_12_12_1$  (#19). The data were collected at 25 °C using the  $\omega$  scan technique to a maximum  $2\theta$  value of 51.2°. A total of 4741 intensity measurements were made using the  $\omega$  scan technique. The linear coefficient,  $\mu$ , for Mo K $\alpha$  radiation is 6.8 cm $^{-1}$ . Azimuthal scans of several reflections indicated no need for an absorption correction. The data were corrected for Lorentz and polarization effects. The structure was solved by heavy-atom Patterson methods and expanded using Fourier techniques using the TEXSAN program package. Some non-hydrogen atoms were refined anisotropically, while the rest were refined isotropically. The final cycle of Full-matrix least square refinements was based on 3178 observed reflection ( $I > 3.00\sigma(I)$ ) and 328 variable parameters and converged with unweighted and weighted agreement factors  $R = 7.2\%$ ,  $R_w = 9.9\%$  with GOF = 3.41. The data:parameter ratio was 9.69:1 and residual electron density/hole 0.63/-0.52 eÅ $^{-3}$ . Further crystallographic details and selected bond distances and angles are given in Tables 1 and 2, respectively.

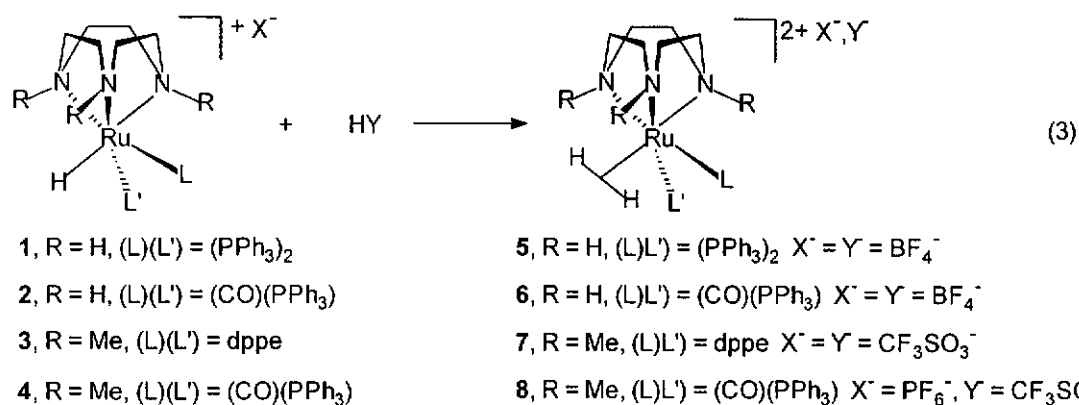
$[\text{H}^{\text{Cn}}\text{Ru}(\text{H}_2\text{O})(\text{PPh}_3)_2](\text{BF}_4)_2$  (**9**). Suitable crystals for X-ray diffraction study were obtained by layering of hexane on a dichloromethane solution of  $[\text{H}^{\text{Cn}}\text{Ru}(\text{H}_2\text{O})(\text{PPh}_3)_2](\text{BF}_4)_2$ . A red block crystal of dimension 0.12x0.16x0.26 mm was

mounted in a glass capillary and used for X-ray structure determination. All measurements were made on a Marresearch image plate scanner with graphite monochromated Mo K $\alpha$  radiation. The crystal system is orthorhombic and the space group *P1* (#2). The data were collected at 25 °C using the  $\omega$  scan technique to a maximum  $2\theta$  value of 50.6°. A total of 5388 intensity measurements were made using the  $\omega$  scan technique. The linear coefficient,  $\mu$ , for Mo K $\alpha$  radiation is 4.7 cm<sup>-1</sup>. Azimuthal scans of several reflections indicated no need for an absorption correction. The data were corrected for Lorentz and polarization effects. The structure was solved by heavy-atom Patterson methods and expanded using Fourier techniques using the TEXSAN program package. Some non-hydrogen atoms were refined anisotropically, while the rest were refined isotropically. The final cycle of Full-matrix least square refinements was based on 2725 observed reflection ( $I > 3.00\sigma(I)$ ) and 212 variable parameters and converged with unweighted and weighted agreement factors  $R = 0.177$ ,  $R_w = 0.242$  with GOF = 5.08. The data:parameter ratio was 12.85:1 and residual electron density/hole 1.77/-1.44 eÅ<sup>-3</sup>. Further crystallographic details and selected bond distances and angles are given in Tables 3 and 4, respectively.

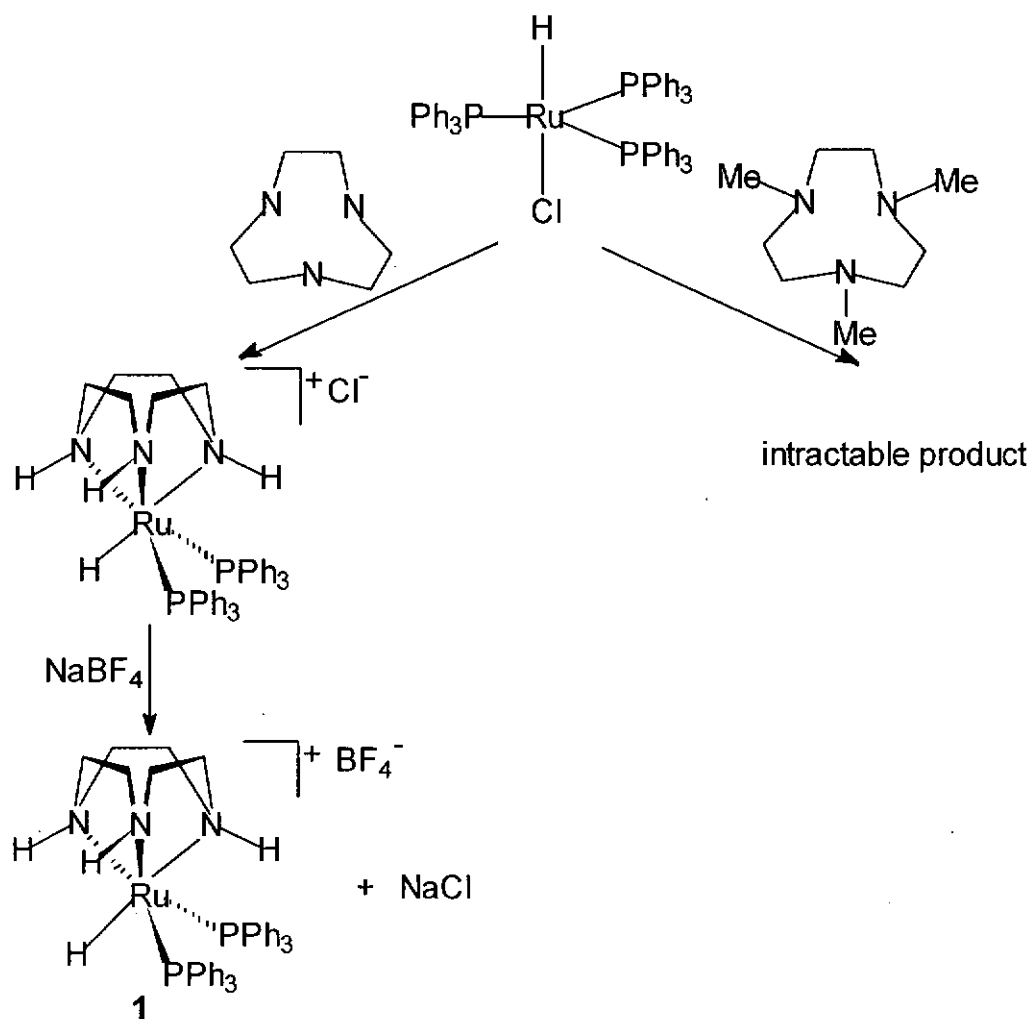
## 2.3 Results and Discussion

### 2.3.1 Synthesis and Characterization of $[\text{R}^{\text{Cn}}(\text{H}_2)(\text{L})(\text{L}')]\text{X}^{2+}$ Complexes.

The dihydrogen complexes  $[\text{R}^{\text{Cn}}\text{Ru}(\text{H}_2)(\text{L})(\text{L}')]\text{X}^{2+}$  (**5-8**) were synthesized by protonation of the corresponding monohydride complexes **1-4** with  $\text{HBF}_4 \cdot \text{Et}_2\text{O}$  or  $\text{CF}_3\text{SO}_3\text{H}$  (eq. 3).



The starting monohydride complexes  $[\text{Me}^{\text{Cn}}\text{RuH}(\text{dppe})]\text{CF}_3\text{SO}_3$  (**3**)<sup>26d</sup> and  $[\text{Me}^{\text{Cn}}\text{RuH}(\text{CO})(\text{PPh}_3)]\text{PF}_6$  (**4**)<sup>26d</sup> are known compounds. The monohydride complex  $[\text{H}^{\text{Cn}}\text{RuH}(\text{PPh}_3)_2]\text{BF}_4$  (**1**) was prepared by reacting  $\text{H}^{\text{Cn}}$  with  $\text{RuHCl}(\text{PPh}_3)_3$  in the presence of  $\text{NaBF}_4$  (scheme 1). Preparation of the analogous complex  $[\text{Me}^{\text{Cn}}\text{RuH}(\text{PPh}_3)_2]\text{BF}_4$  was attempted by using  $\text{Me}^{\text{Cn}}$  in place of  $\text{H}^{\text{Cn}}$ . However, the preparation was not successful and some intractable materials were obtained. Failure of the reaction is probably due to large steric interaction between triphenylphosphine and the sterically more demanding  $\text{Me}^{\text{Cn}}$  ligand. The complex  $[\text{H}^{\text{Cn}}\text{RuH}(\text{CO})(\text{PPh}_3)]\text{BF}_4$  (**2**) was prepared by refluxing a mixture of  $\text{H}^{\text{Cn}}$  and  $\text{RuHCl}(\text{CO})(\text{PPh}_3)_3$  in 2-methoxyethanol, followed by precipitation with  $\text{NaBF}_4$ . Similar procedure has been used previously for the preparation of  $[\text{Me}^{\text{Cn}}\text{RuH}(\text{CO})(\text{PPh}_3)]\text{PF}_6$  (**4**).<sup>26d</sup>



Scheme 1

The new monohydride complexes can be readily characterized by their NMR, IR and elemental analysis. The structure of complex **1** has also been confirmed by X-ray diffraction. The molecular structure of the cation  $[\text{H}^{\text{Cn}}\text{RuH}(\text{PPh}_3)_2]^+$  is shown in Figure 2.1. Crystallographic details and selected bond distances and angles are given in Tables 1 and 2, respectively.

The structure **1** could be described as a distorted octahedron with the hydride trans to N(2). The distortion can be attributed to the coordination geometry of the  $\text{H}^{\text{Cn}}$  ligand. The N-Ru-N angles and Ru-N bond distances in complex **1** are very similar to

those observed for related complexes such as [<sup>Me</sup>CnR(PMe<sub>3</sub>)(P(OMe)<sub>3</sub>(C≡CPh)]PF<sub>6</sub>,<sup>26a</sup> [<sup>Me</sup>CnRu(PMe<sub>3</sub>)(η<sup>3</sup>-PhC<sub>3</sub>CHPh)]PF<sub>6</sub>,<sup>26a</sup> [<sup>Me</sup>CnRuH(η<sup>4</sup>-COD)]PF<sub>6</sub><sup>26e</sup> and [<sup>Me</sup>CnRu(η<sup>5</sup>-C<sub>8</sub>H<sub>11</sub>)]PF<sub>6</sub>.<sup>26e</sup> The bond Ru-N(2) (2.30(1) Å) is slightly longer than Ru-N(1) (2.20(1) Å) and Ru-N(3) (2.19(1) Å), presumably due to the trans influence of the hydride ligand. The P(1)-Ru-P(2) angle (96.4°) is smaller than that observed for CpRuH(PPh<sub>3</sub>)<sub>2</sub> (101.4°)<sup>49a</sup> and comparable to that observed for CpRuH(PMe<sub>3</sub>)<sub>2</sub>.<sup>49b,c</sup>



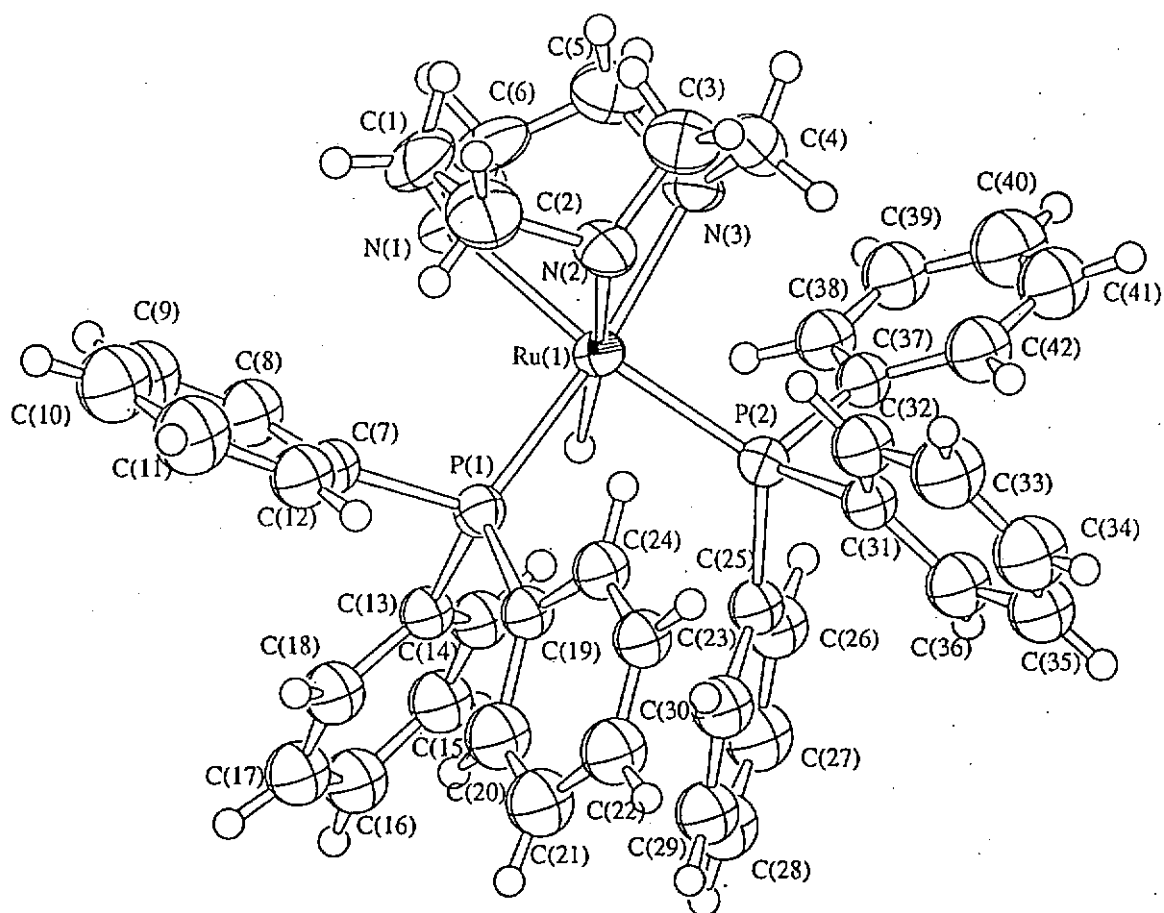


Figure 2.1. The molecular structure of  $[\text{}^1\text{H}\text{CnRuH}(\text{PPh}_3)_2]\text{BF}_4$  (**1**).

**Table 1. Crystal Data and Refinement Details for  $[\text{H}^{\text{Cn}}\text{RuH}(\text{PPh}_3)_2]\text{BF}_4 \cdot 2\text{CH}_2\text{Cl}_2$** 

|   |   |
|---|---|
| formula                                 | $\text{C}_{44}\text{H}_{47}\text{BCl}_4\text{F}_4\text{N}_3\text{P}_2\text{Ru}$ |
| fw                                      | 1009.51   |
| color and habit                         | red block   |
| crys dimens (mm)                        | 0.22x0.23x0.29  |
| crys sys                                | orthorhombic  |
| space group                             | $P2_12_12_1$ (#19)  |
| a, Å                                    | 10.598(1)   |
| b, Å                                    | 20.046(1)   |
| c, Å                                    | 21.973(1)   |
| V, Å <sup>3</sup>                       | 4668.1(4)   |
| Z                                       | 4   |
| $d_{\text{calc}}$ , g cm <sup>-3</sup>  | 1.436   |
| F(000)                                  | 2060.00   |
| radiation                               | Mo K $\alpha$ ( $\lambda = 0.71073$ Å)  |
| $\mu$ (MoK $\alpha$ ), cm <sup>-1</sup> | 6.83  |
| T, °C                                   | 25.0  |
| diffractometer                          | Marresearch Image Plate Scanner   |
| $2\theta_{\text{max}}$ , deg            | 3.0 to 50.0   |
| scan type                               | $\omega$  |
| explosure (min)                         | 5   |
| reflections collected                   | 28766   |
| unique reflections                      | 4741  |
| observed reflections                    | 3178 ( $F > 3.0 \sigma(F)$ )  |
| absorption correction                   | inter-image scaling   |
| no. of parameter refined                | 328   |
| final R indices (obs. data)             | $R = 7.2\%$ , $R_w = 9.9\%$   |
| goodness of fit                         | 3.41  |
| data to parameter ratio                 | 9.69  |
| largest difference peak                 | 0.63 eÅ <sup>-3</sup>   |
| largest difference hole                 | -0.52 eÅ <sup>-3</sup>  |

**Table 2. Selected Bond Distances (Å) and Angles (deg) for  $[\text{CnRuH}(\text{PPh}_3)_2]\text{BF}_4 \cdot 2\text{CH}_2\text{Cl}_2$**

---

| Interatomic Distance (Å)    |          |              |          |              |          |
|-----------------------------|----------|--------------|----------|--------------|----------|
| Ru-P(1)                     | 2.286(4) | Ru-P(2)      | 2.270(4) | Ru-N(1)      | 2.20(1)  |
| Ru-N(2)                     | 2.30(1)  | Ru-N(3)      | 2.19(1)  | Ru-H         | 1.8(2)   |
| Intramolecular Angles (deg) |          |              |          |              |          |
| P(1)-Ru-P(2)                | 96.4(1)  | P(1)-Ru-N(1) | 93.8(4)  | P(1)-Ru-N(2) | 102.2(4) |
| P(1)-Ru-N(3)                | 172.8(4) | P(1)-Ru-H    | 95(5)    | P(2)-Ru-N(1) | 164.5(4) |
| P(2)-Ru-N(2)                | 110.8(4) | P(2)-Ru-N(3) | 90.6(3)  | P(2)-Ru-H    | 85(6)    |
| N(1)-Ru-N(2)                | 78.2(6)  | N(1)-Ru-N(3) | 79.0(5)  | N(1)-Ru-H    | 82(6)    |
| N(2)-Ru-N(3)                | 76.9(5)  | N(2)-Ru-H    | 154(6)   | N(3)-Ru-H    | 83(6)    |

Protonation of the monohydride complexes **1-4** with  $\text{HBF}_4 \cdot \text{Et}_2\text{O}$  or  $\text{CF}_3\text{SO}_3\text{H}$  produced the dihydrogen complexes **5-8** (eq.3). The dihydrogen complex  $[\text{}^1\text{H}\text{CnRu}(\text{H}_2)(\text{PPh}_3)_2](\text{BF}_4)_2$  (**5**), isolated as yellow solid by addition of  $\text{Et}_2\text{O}$  to a  $\text{CH}_2\text{Cl}_2$  solution of  $[\text{}^1\text{H}\text{CnRuH}(\text{PPh}_3)_2]\text{BF}_4$  acidified with slightly excess of  $\text{HBF}_4 \cdot \text{Et}_2\text{O}$ , was contaminated by a small amount of the aquo complex  $[\text{}^1\text{H}\text{CnRu}(\text{H}_2\text{O})(\text{PPh}_3)_2](\text{BF}_4)_2$ . Apparently, the aquo complex was formed by displacement of  $\eta^2\text{-H}_2$  in **5** by adventitious water in the solvents. Similar contamination problem was encountered in the preparation of the dihydrogen complex  $[\text{}^{\text{Me}}\text{CnRu}(\text{H}_2)(\text{dppe})](\text{CF}_3\text{SO}_3)_2$  (**7**). But it will be seen (*vide infra*) that in the absence of acid, water acts as a base to deprotonate the  $\eta^2\text{-H}_2$  in **5** or **7**. The dihydrogen complexes **5** and **7** are stable in the solid state at room temperature; but in solution, the  $\eta^2\text{-H}_2$  ligand is displaced by strongly coordinating solvent such as acetonitrile. The very acidic CO-containing dihydrogen complexes **6** and **8** are unstable with respect to loss of  $\text{H}_2$ , both in solid state and in solution, at room temperature. These complexes were prepared by acidification at  $-30^\circ\text{C}$  with excess  $\text{HBF}_4 \cdot \text{Et}_2\text{O}$ , and were characterized in situ with NMR spectroscopy.

The existence of the  $\eta^2\text{-H}_2$  moieties in complexes **5-8** was confirmed by variable-temperature  $T_1$  measurements and the observation of large  $^1J(\text{HD})$  coupling constants for the corresponding isotopomers which were prepared by acidification of **1-4** with  $\text{DBF}_4$  or  $\text{CF}_3\text{SO}_3\text{D}$ . In particular, the  $^1J(\text{HD})$  coupling constants for the isotopomers were observed in the range of 29.4 to 31.8 Hz and  $T_1(\text{min})$  values in the range of 12 to 24 ms at 400 MHz. The changes in the  $^1J(\text{HD})$  and  $T_1(\text{min})$  are rather small especially in view of the fact that the electronic properties of the ligands have been changed drastically. It is also interesting to note that the  $^1J(\text{HD})$  for

$[\text{H}^1\text{CnRu}(\text{HD})(\text{CO})(\text{PPh}_3)]^{2+}$  (31.8 Hz) is slightly larger than that of  $[\text{Me}^1\text{CnRu}(\text{HD})(\text{CO})(\text{PPh}_3)]^{2+}$  (30.0 Hz), but the  $T_1(\text{min})$  for  $[\text{H}^1\text{CnRu}(\text{H}_2)(\text{CO})(\text{PPh}_3)]^{2+}$  (14 ms) is slightly longer than that of  $[\text{Me}^1\text{CnRu}(\text{H}_2)(\text{CO})(\text{PPh}_3)]^{2+}$  (12 ms). The shorter  $T_1(\text{min})$  for  $[\text{Me}^1\text{CnRu}(\text{H}_2)(\text{CO})(\text{PPh}_3)]^{2+}$  is undoubtedly caused by the extra relaxation due to the methyl groups.<sup>50</sup>

Complexes **5-8** provide additional examples of *dicationic* dihydrogen complexes. In contrast to the abundance of isolable monocationic dihydrogen complexes, well characterized dicationic dihydrogen complexes are still very limited in numbers. Reported dicationic dihydrogen complexes were mainly those of the osmium complexes such as  $[\text{Os}(\text{H}_2)(\text{NH}_3)_5]^{2+}$ ,<sup>22a</sup>  $[\text{Os}(\text{H}_2)(\text{en})_2(\text{L})]^{2+}$ ,<sup>22b</sup> *trans*- $[\text{Os}(\text{H}_2)(\text{dppe})_2(\text{CH}_3\text{CN})]^{2+}$ ,<sup>20</sup>  $[\text{Os}(\text{H}_2)(\text{CO})(\text{bpy})(\text{PPh}_3)_2]^{2+}$  (bpy = 2,2'-dipyridyl),  $[\text{Os}(\text{H}_2)(\text{CO})(\text{bpy})_2]^{2+}$ ,<sup>21k</sup> and  $[\text{Os}(\text{H}_2)(\text{CO})(\text{dppp})_2]^{2+}$ .<sup>18</sup> Dicationic dihydrogen complexes of other metals are limited to *trans*- $[\text{Fe}(\text{H}_2)(\text{L})(\text{dppe})_2]^{2+}$  (L = CO, CNH)<sup>51</sup> and  $[\text{Ru}(\text{H}_2)(\text{CO})(\text{dppp})_2]^{2+}$ .<sup>18</sup> Very recently, Luther and Heinekey reported the synthesis, characterization and reactivity of the dicationic dihydrogen complexes  $[\text{Os}(\text{H}_2)(\text{CO})(\text{bpy})(\text{PMePh}_2)_2]^{2+}$ ,  $[\text{Os}(\text{H}_2)(\text{CO})(\text{phen})(\text{PPh}_3)_2]^{2+}$  and  $[\text{Ru}(\text{H}_2)(\text{CO})(\text{bpy})(\text{PPh}_3)_2]^{2+}$ .<sup>52</sup>

As stated before, during the preparation of the dihydrogen complex  $[\text{H}^1\text{CnRu}(\text{H}_2)(\text{PPh}_3)_2](\text{BF}_4)_2$  (**5**) via the protonation of  $[\text{H}^1\text{CnRuH}(\text{PPh}_3)_2]\text{BF}_4$  (**1**), the product was always contaminated by small amount of the aquo complex  $[\text{H}^1\text{CnRu}(\text{H}_2\text{O})(\text{PPh}_3)_2](\text{BF}_4)_2$  (**9**). It was later found that addition of excess  $\text{HBF}_4$  to **1**, followed by introduction of water, gave **9** as the sole product. This aquo complex can

be readily characterized by NMR, and elemental analysis. The structure of complex **9** has also been confirmed by X-ray diffraction. The molecular structure of the cation  $[\text{CnRu}(\text{H}_2\text{O})(\text{PPh}_3)_2]^{2+}$  is shown in Figure 2.2. Crystallographic details and selected bond distances and angles are given in Tables 3 and 4, respectively.

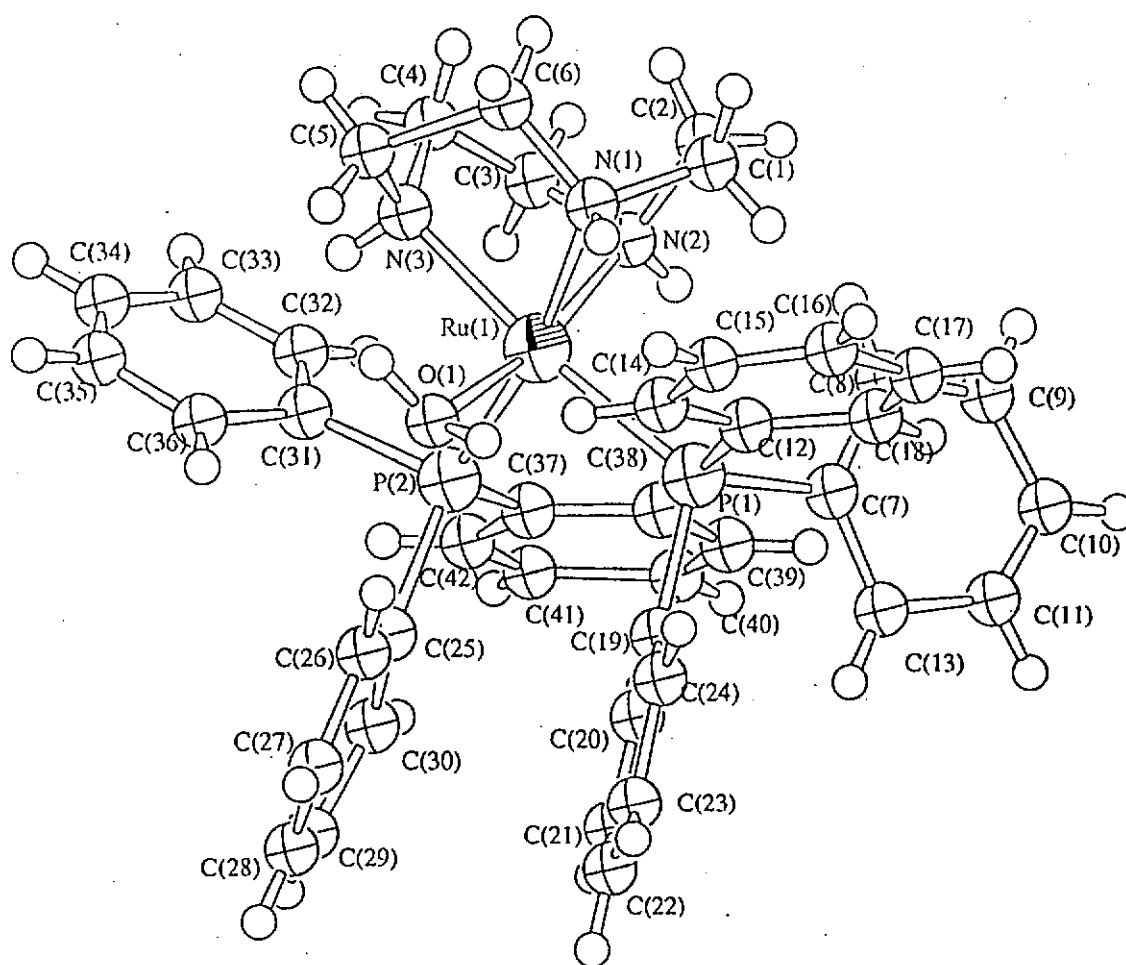


Figure 2.2. The molecular structure of  $[\text{CnRu}(\text{H}_2\text{O})(\text{PPh}_3)_2](\text{BF}_4)_2$  (**9**).

**Table 3. Crystal Data and Refinement Details for  $[\text{H}^{\text{Cn}}\text{Ru}(\text{H}_2\text{O})(\text{PPh}_3)_2](\text{BF}_4)_2$** 

|  |   |
|--|---|
| formula                                    | $\text{C}_{42}\text{H}_{47}\text{B}_2\text{F}_8\text{N}_3\text{P}_2\text{Ru}$ |
| fw   | 946.48  |
| color and habit                            | red blocok  |
| crys dimens (mm)                           | 0.12x0.16x0.26  |
| crys sys                                   | triclinic   |
| space group                                | $P1(\#2)$   |
| a, Å                                       | 11.199(1)   |
| b, Å                                       | 11.938(1)   |
| c, Å                                       | 18.163(1)   |
| V, Å <sup>3</sup>                          | 2332.1(3)   |
| Z  | 2   |
| $d_{\text{cacl}}$ , g cm <sup>-3</sup>     | 1.348   |
| F(000)                                     | 968.00  |
| radiation                                  | Mo K $\alpha$ ( $\lambda = 0.716069$ Å)                                       |
| $\mu(\text{MoK}\alpha)$ , cm <sup>-1</sup> | 4.71  |
| T, °C                                      | 25.0  |
| diffractometer                             | Marresearch Image Plate Scanner   |
| $2\theta_{\text{max}}$ , deg               | 50.6  |
| scan type                                  | $\omega$  |
| explosure (min)                            | 5   |
| reflections collected                      | 5388  |
| observed reflections                       | 2725 ( $F > 3.0 \sigma(F)$ )  |
| absorption correction                      | inter-image scaling   |
| no. of parameter refined                   | 212   |
| final R indices (obs. data)                | $R = 17.7\%$ , $R_w = 24.2\%$   |
| goodness of fit                            | 5.08  |
| data to parameter ratio                    | 12.85   |
| largest difference peak                    | $1.77\text{e}\text{Å}^{-3}$   |
| largest difference hole                    | $-1.44\text{e}\text{Å}^{-3}$  |

**Table 4. Selected Bond Distances (Å) and Angles (deg) for  $[\text{CnRu}(\text{H}_2\text{O})(\text{PPh}_3)_2](\text{BF}_4)_2$**

---

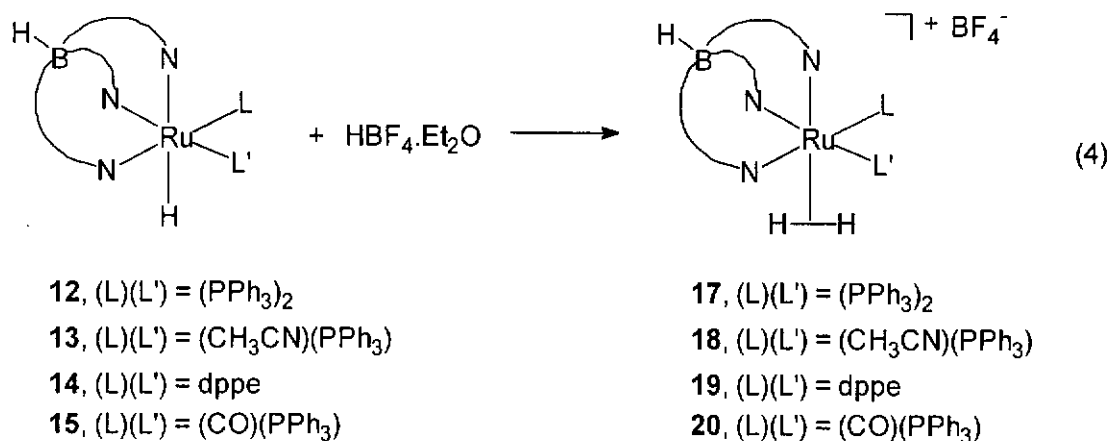
| Interatomic Distance (Å)    |          |              |           |              |          |
|-----------------------------|----------|--------------|-----------|--------------|----------|
| Ru-P(1)                     | 2.385(9) | Ru-P(2)      | 2.375(10) | Ru-N(1)      | 2.20(3)  |
| Ru-N(2)                     | 2.10(3)  | Ru-N(3)      | 2.17(3)   | Ru-O         | 2.20(5)  |
| Intramolecular Angles (deg) |          |              |           |              |          |
| P(1)-Ru-P(2)                | 98.9(3)  | P(1)-Ru-N(1) | 90.9(8)   | P(1)-Ru-N(2) | 99.5(7)  |
| P(1)-Ru-N(3)                | 171.1(9) | P(1)-Ru-O    | 87(1)     | P(2)-Ru-N(1) | 170.1(8) |
| P(2)-Ru-N(2)                | 97.3(7)  | P(2)-Ru-N(3) | 90.0(9)   | P(2)-Ru-O    | 85(6)    |
| N(1)-Ru-N(2)                | 82(1)    | N(1)-Ru-N(3) | 80(1)     | N(1)-Ru-O    | 86(1)    |
| N(2)-Ru-N(3)                | 79(1)    | N(2)-Ru-O    | 166(1)    | N(3)-Ru-O    | 91(1)    |



The structure of  $[\text{H}^{\text{Cn}}\text{Ru}(\text{H}_2\text{O})(\text{PPh}_3)_2](\text{BF}_4)_2$  (**9**) could be described as a distorted octahedron with the  $\text{H}_2\text{O}$  trans to N(2). The distortion can be attributed to the coordination geometry of the  $\text{H}^{\text{Cn}}$  ligand. The N-Ru-N and P-Ru-P are very similar to those observed for complex **1**. The Ru-N(2) bond (2.10(1) Å) is slightly shorter than Ru-N(1) (2.20(1) Å) and Ru-N(3) (2.17(1) Å), presumably due to the smaller trans influence of the aquo ligand than that of the phosphines.

### 2.3.2 Synthesis and Characterization of $[\text{TpRu}(\text{H}_2)(\text{L})(\text{L}')]^+$ Complexes.

The dihydrogen complexes  $[\text{TpRu}(\text{H}_2)(\text{PPh}_3)_2]\text{BF}_4$  (**17**) and  $[\text{TpRu}(\text{H}_2)(\text{CH}_3\text{CN})(\text{PPh}_3)]\text{BF}_4$  (**18**) were recently synthesized by our group from protonation reactions of the corresponding monohydride complexes with  $\text{HBF}_4 \cdot \text{Et}_2\text{O}$ .<sup>29b</sup> With similar strategy, the new dihydrogen complexes  $[\text{TpRu}(\text{H}_2)(\text{dppe})]\text{BF}_4$  (**19**) and  $[\text{TpRu}(\text{H}_2)(\text{CO})(\text{PPh}_3)]\text{BF}_4$  (**20**) were prepared (eq. 4). Like **5** and **7**, the isolated **19** was contaminated by a small amount of the aquo complex  $[\text{TpRu}(\text{H}_2\text{O})(\text{dppe})]\text{BF}_4$ . It should be mentioned that the CO-containing dihydrogen complex **20** is unstable with respect to loss of  $\text{H}_2$  at room temperature, therefore the acidification had to be carried out at  $-30\text{ }^\circ\text{C}$  and **20** was not isolated, but was studied in situ.



The existence of the  $\eta^2\text{-H}_2$  moiety in [TpRu(H<sub>2</sub>)(dppe)]BF<sub>4</sub> (**19**) was confirmed by observation of a  $T_1(\text{min})$  value of 14 ms for **19** and a large  $^1J(\text{HD})$  coupling constant of 32.5 Hz for the corresponding isotopomer [TpRu(HD)(dppe)]BF<sub>4</sub> which was prepared by acidification of **14** with DBF<sub>4</sub>. Similarly, the existence of the  $\eta^2\text{-H}_2$  moiety in **20** is evidenced by short  $T_1(\text{min})$  of this complex and large  $^1J(\text{HD})$  coupling constant (33.3 Hz) of the corresponding isotopomer [TpRu(HD)(CO)(PPh<sub>3</sub>)]BF<sub>4</sub>.

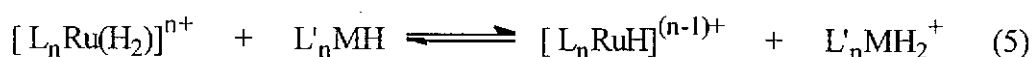
### 2.3.3 Comparison of the Abilities of Cp, Tp, and <sup>R</sup>Cn in Stabilizing Dihydrogen Complexes.

Although Cp, Tp and <sup>R</sup>Cn are isoelectronic and all adopt facial geometry, their abilities to stabilize dihydrogen ligands are different. For example, while [CpRuH<sub>2</sub>(PPh<sub>3</sub>)<sub>2</sub>]<sup>+</sup> is a classical dihydride complex, both [TpRu(H<sub>2</sub>)(PPh<sub>3</sub>)<sub>2</sub>]<sup>+</sup> and [<sup>H</sup>CnRu(H<sub>2</sub>)(PPh<sub>3</sub>)<sub>2</sub>]<sup>2+</sup> are molecular dihydrogen complexes. Subtle differences in the Tp and <sup>R</sup>Cn complexes are also noted. Although the <sup>R</sup>Cn dihydrogen complexes **5-8** are dicationic and the Tp dihydrogen complexes **17-20** are monocationic,  $^1J(\text{HD})$  couplings of the isotopomers of the <sup>R</sup>Cn complexes are consistently smaller than those of the Tp counterparts. This is probably the result of <sup>R</sup>Cn being better  $\sigma$ -donors than Tp, and the

latter being able to act as a  $\pi$ -accepting ligand. In consonance with the trends in  $^1J(\text{HD})$  couplings, we have observed that the  $\eta^2\text{-H}_2$  ligands in the Tp complexes **17-20** are much more readily displaced by water, in the absence of  $\text{H}_2$  pressure, than those in **5-8**. Reactions of these complexes with water warrant further discussion later.

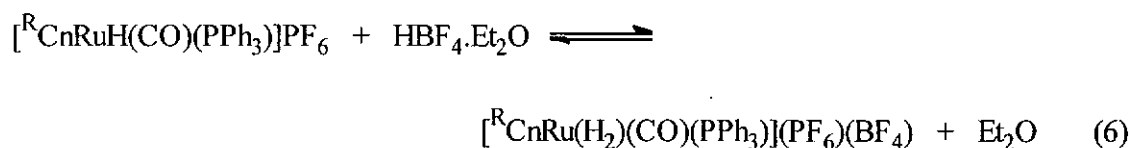
#### 2.3.4 Acidity of the Dihydrogen Complexes.

Attempt has been made to rank the relative acidity of the dihydrogen complexes. A useful approach to do so is to measure the pseudo aqueous  $\text{p}K_a$  values.<sup>6-10</sup> In this approach, equilibrium constants for the reactions of  $\text{L}_n\text{MH}$  (precursors to dihydrogen complexes) and an acid with known aqueous  $\text{p}K_a$  value are determined in non-aqueous solutions. The pseudo aqueous  $\text{p}K_a$  of the dihydrogen complexes are then calculated in reference to the aqueous  $\text{p}K_a$  of the acid. The pseudo aqueous  $\text{p}K_a$  values of **5**, **7**, **17**, **18**, and **19** were estimated by studying the equilibrium shown in eq. 5 with  $^1\text{H}$  NMR in  $\text{CD}_2\text{Cl}_2$ , using the hydride complexes  $\text{RuHCl}(\text{dppe})_2$ ,  $\text{CpRuH}(\text{PPh}_3)_2$ , and  $\text{CpRuH}(\text{dppm})$  as the bases. The pseudo aqueous  $\text{p}K_a$  values of  $[\text{RuCl}(\text{H}_2)(\text{dppe})_2]^+$ ,<sup>9b</sup>  $[\text{CpRuH}_2(\text{PPh}_3)_2]^+$ ,<sup>6b</sup> and  $[\text{CpRu}(\text{H}_2)(\text{dppm})]^+$ <sup>6b</sup> have been determined previously in  $\text{CD}_2\text{Cl}_2$  using similar method. The equilibrium mixture could be conveniently obtained by protonation with a limited amount of  $\text{HBF}_4\cdot\text{Et}_2\text{O}$  of a mixture of  $[\text{L}_n\text{RuH}]^{(n-1)+}$  and  $\text{L}'_n\text{MH}$ .



All the equilibria were obtained at room temperature, except in the case of  $[\text{TpRu}(\text{H}_2)(\text{CH}_3\text{CN})(\text{PPh}_3)]^+$ , which was carried out at  $-30\text{ }^\circ\text{C}$ . The relative concentrations of the dihydrogen complexes and the metal hydrides in equilibrium were estimated from integrations of the upfield hydride signals in the  $^1\text{H}$  NMR spectra, and therefore the equilibrium constants can be estimated based on the known  $\text{p}K_a$  values of  $\text{L}'_n\text{MH}_2^+$ . The pseudo aqueous  $\text{p}K_a$  value of the Tp carbonyl dihydrogen complex  $[\text{TpRu}(\text{H}_2)(\text{CO})(\text{PPh}_3)]\text{BF}_4$  (**20**) was determined in a similar manner at  $-80^\circ\text{C}$ , using  $[\text{H}^1\text{CnRu}(\text{H})(\text{CO})(\text{PPh}_3)]\text{BF}_4$  (**2**) as the base.

The  $\text{p}K_a$  values of the  $^R\text{Cn}$  carbonyl dihydrogen complexes **6** and **8** could not be estimated by use of eq. 5 because they are much more acidic than the  $\text{L}'_n\text{MH}_2^+$  complexes. The  $\text{p}K_a$  values of **6** and **8** were estimated by studying the protonation reactions of **2** and **4** with  $\text{HBF}_4 \cdot \text{Et}_2\text{O}$  (eq. 6)



using  $^1\text{H}$  NMR at  $-80\text{ }^\circ\text{C}$ . The relative molar concentrations of  $\text{HBF}_4 \cdot \text{Et}_2\text{O}$ ,  $\text{Et}_2\text{O}$ , the ruthenium carbonyl hydrides, and the carbonyl dihydrogen complexes were estimated based on the  $^1\text{H}$  NMR integrations. The  $\text{p}K_a$  values of **6** and **8** were estimated to be  $-1.3$  and  $-2.6$ , respectively, taking the  $\text{p}K_a$  of  $\text{HBF}_4 \cdot \text{Et}_2\text{O}$  as  $-2.4$ .<sup>53</sup> Details on the acidity measurements are summarized in Table 5.

**Table 5. Acidity Measurements of Dihydrogen Complexes in CD<sub>2</sub>Cl<sub>2</sub><sup>a</sup>**

| M(H <sub>2</sub> )   | B   | Keq                | pK <sub>a</sub> (M(H <sub>2</sub> )) |
|--|---|--------------------|--------------------------------------|
| [ <sup>H</sup> CnRu(H <sub>2</sub> )(PPh <sub>3</sub> ) <sub>2</sub> ](BF <sub>4</sub> ) <sub>2</sub> ( <b>5</b> )             | RuHCl(dppe) <sub>2</sub>                                  | 31.6               | 4.5                                  |
| [ <sup>H</sup> CnRu(H <sub>2</sub> )(CO)(PPh <sub>3</sub> )](BF <sub>4</sub> ) <sub>2</sub> ( <b>6</b> )                       | Et <sub>2</sub> O   | 0.07 <sup>b</sup>  | -1.3                                 |
| [ <sup>Me</sup> CnRu(H <sub>2</sub> )(dppe) <sub>2</sub> ](CF <sub>3</sub> SO <sub>3</sub> ) <sub>2</sub> ( <b>7</b> )         | RuHCl(dppe) <sub>2</sub>                                  | 166                | 3.8                                  |
| [ <sup>Me</sup> CnRu(H <sub>2</sub> )(CO)(PPh <sub>3</sub> )](PF <sub>6</sub> )(CF <sub>3</sub> SO <sub>3</sub> ) ( <b>8</b> ) | Et <sub>2</sub> O   | 1.56 <sup>b</sup>  | -2.6                                 |
| [TpRu(H <sub>2</sub> )(PPh <sub>3</sub> ) <sub>2</sub> ](BF <sub>4</sub> ) ( <b>17</b> )                                       | CpRuH(dppm)   | 0.303              | 7.6                                  |
| [TpRu(H <sub>2</sub> )(CH <sub>3</sub> CN)(PPh <sub>3</sub> )]BF <sub>4</sub> ( <b>18</b> )                                    | CpRuH(PPh <sub>3</sub> ) <sub>2</sub>                     | 0.277 <sup>c</sup> | 8.9                                  |
| [TpRu(H <sub>2</sub> )(dppe)]BF <sub>4</sub> ( <b>19</b> )   | CpRuH(dppm)   | 0.179              | 7.9                                  |
| [TpRu(H <sub>2</sub> )(CO)(PPh <sub>3</sub> )]BF <sub>4</sub> ( <b>20</b> )  | [ <sup>H</sup> CnRuH(CO)(PPh <sub>3</sub> )] <sup>+</sup> | 0.498 <sup>b</sup> | -0.6                                 |

<sup>a</sup>pK<sub>a</sub> values (on the pseudo aqueous scale) of the dihydrogen complexes are estimated by means of the equation: pK<sub>a</sub>(M(H<sub>2</sub>)) = pKeq + pK<sub>a</sub>(HB<sup>+</sup>); Keq is the equilibrium constant of eq. 5 or the reciprocal of the equilibrium constant of eq. 6. <sup>b</sup>At -80 °C. <sup>c</sup>-30 °C.

### 2.3.5 Comments on the Acidity .

It should be stressed that the pseudo aqueous  $pK_a$  values of complexes **5-8** and **17-20** are obtained based on the assumption that the differences in the  $pK_a$  values of the dihydrogen complexes and the reference acids are the same in water and  $CD_2Cl_2$ . Since the assumption has not been confirmed yet, the pseudo aqueous  $pK_a$  values of the complexes may be different from the true aqueous  $pK_a$  values and should not be treated too seriously. However, the pseudo aqueous  $pK_a$  values can still provide valuable information in the trend of the acidity of the complexes. For comparison, the pseudo aqueous  $pK_a$  values of the new dihydrogen complexes and related  $[(\eta^5-C_5R_5)RuH_2(L)(L')]^+$  complexes are listed in Table 6. In order to see the effect of H—H bonding on the acidity, the  $T_1(\text{min})$  and  $r(\text{HH})$  for the dihydrogen complexes, and  $^1J(\text{HD})$  for the HD isotopomers are also listed if available. The hydrogen-hydrogen separations  $r(\text{HH})$  were calculated according to the empirical equation (eq 7)<sup>19a</sup>

$$r(\text{HH}) = 1.42 - 0.0167J(\text{HD}) \quad (7)$$

which shows a linear relationship between  $J(\text{HD})$  and  $r(\text{HH})$  in a wide variety of  $\eta^2\text{-H}_2$  complexes whose  $J(\text{HD})$  values fall in the range 7 - 35 Hz. An essentially identical linear relationship is also predicted by quantum chemical calculation for complexes of the type  $[\text{Os}(\text{NH}_3)_4\text{L}(\text{H}_2)]^{2+}$  for a wide range of *trans* ligands L.<sup>54</sup>

**Table 6. Spectroscopic Properties and Acidities of Hydride Complexes**

| Complexes   | $T_1$ (min)<br>$\text{ms}^a$ (temp) | $^1J(\text{HD})$<br>Hz | $d(\text{HH})$<br>$\text{\AA}^b$ | $\text{p}K_a^c$   | reference |
|---|-------------------------------------|------------------------|----------------------------------|-------------------|-----------|
| $[\text{H}^{\text{Cn}}\text{Ru}(\text{H}_2)(\text{PPh}_3)_2](\text{BF}_4)_2$ ( <b>5</b> )                                 | 20 (250 K)                          | 29.4                   | 0.93                             | 4.5               | this work |
| $[\text{H}^{\text{Cn}}\text{Ru}(\text{H}_2)(\text{CO})(\text{PPh}_3)](\text{BF}_4)_2$ ( <b>6</b> )                        | 14 (248 K)                          | 31.8                   | 0.89                             | -1.3 <sup>d</sup> | this work |
| $[\text{Me}^{\text{Cn}}\text{Ru}(\text{H}_2)(\text{dppe})](\text{CF}_3\text{SO}_3)_2$ ( <b>7</b> )                        | 24 (266 K)                          | 29.4                   | 0.93                             | 3.8               | this work |
| $[\text{Me}^{\text{Cn}}\text{Ru}(\text{H}_2)(\text{CO})(\text{PPh}_3)](\text{PF}_6)(\text{CF}_3\text{SO}_3)$ ( <b>8</b> ) | 12 (224 K)                          | 31.0                   | 0.92                             | -2.6 <sup>d</sup> | this work |
| $[\text{TpRu}(\text{H}_2)(\text{PPh}_3)_2]\text{BF}_4$ ( <b>17</b> )  | 21 (240 K)                          | 32.0                   | 0.89                             | 7.6               | this work |
| $[\text{TpRu}(\text{H}_2)(\text{CH}_3\text{CN})(\text{PPh}_3)]\text{BF}_4$ ( <b>18</b> )                                  | 16 (231 K)                          | 33.0                   | 0.87                             | 8.9 <sup>e</sup>  | this work |
| $[\text{TpRu}(\text{H}_2)(\text{dppe})]\text{BF}_4$ ( <b>19</b> )   | 14 (230 K)                          | 32.5                   | 0.88                             | 7.9               | this work |
| $[\text{TpRu}(\text{H}_2)(\text{CO})(\text{PPh}_3)]\text{BF}_4$ ( <b>20</b> )   | 12 (224 K)                          | 33.3 <sup>d</sup>      | 0.86                             | -0.6 <sup>d</sup> | this work |
| $[\text{CpRuH}_2(\text{PPh}_3)_2]^+$  |                                     |                        | 8.3                              | 8.3               | 16b       |
| $[\text{CpRu}(\text{H}_2)(\text{dppm})]^+$  |                                     | 21.9                   | 1.05                             | 7.1               | 16b       |
| $[\text{Cp}^*\text{Ru}(\text{H}_2)(\text{dppm})]^+$   | 18(220K)                            | 20.9                   | 1.07                             | 9.2               | 16b       |
| $[\text{CpRu}(\text{H}_2)(\text{dppe})]^+$  |                                     | 24.9                   | 1.00                             | 7.0               | 16b       |

<sup>a</sup> At 400 MHz. <sup>b</sup> Calculated based on  $^1J(\text{HD})$  values as described in ref 19a. <sup>c</sup>  $\text{p}K_a$  values were determined in  $\text{CD}_2\text{Cl}_2$ , but reported on pseudo aqueous scale. <sup>d</sup> Determined at -80 °C. <sup>e</sup> Determined at -30 °C.

It can be seen from Table 6 that isostructural and monocationic Tp and Cp ruthenium dihydrogen complexes have similar acidity. The dicationic  $^R\text{Cn}$  dihydrogen complexes **5** and **7** are significantly more acidic than their Tp and Cp analogues (by 3-4  $pK_a$  units difference). The carbonyl-containing  $^R\text{Cn}$  dihydrogen complexes  $[\text{MeCnRu}(\text{H}_2)(\text{CO})(\text{PPh}_3)]^{2+}$  ( $pK_a = -2.6$ ) and  $[\text{HCnRu}(\text{H}_2)(\text{CO})(\text{PPh}_3)]^{2+}$  ( $pK_a = -1.3$ ) are also more acidic than the analogous monocationic Tp complex  $[\text{TpRu}(\text{H}_2)(\text{CO})(\text{PPh}_3)]^+$  ( $pK_a = -0.6$ ), but to a smaller extent. Several highly acidic dicationic dihydrogen complexes have been reported, for example, the dicationic dihydrogen complex *trans*- $[\text{Os}(\text{H}_2)(\text{dppe})_2(\text{CH}_3\text{CN})]^{2+}$  has a pseudo aqueous  $pK_a$  value close to -2.<sup>20</sup> The complex  $[\text{Os}(\text{H}_2)(\text{CO})(\text{bpy})(\text{PPh}_3)_2]^{2+}$  can be deprotonated by diethyl ether.<sup>21k</sup> The dicationic dihydrogen complexes  $[\text{M}(\text{H}_2)(\text{CO})(\text{dppp})_2]^{2+}$  ( $\text{M} = \text{Ru}; \text{Os}$ ) were reported to have  $pK_a$  values close to -6.<sup>18</sup> It should be mentioned that dicationic dihydrogen complexes are not necessarily stronger acids than monocationic complexes, for example,  $[\text{Os}(\text{H}_2)(\text{NH}_3)_5]^{2+}$  was reported to be a weak acid and is stable to moderately strong base such as NaOMe. The high  $pK_a$  value of this complex is probably due to the strong electron donating effect of the  $\text{NH}_3$  ligands.<sup>22a</sup>

Within the  $^H\text{Cn}$ ,  $^{\text{Me}}\text{Cn}$  and the Tp dihydrogen complex series, substitution of phosphine group for CO leads to a 5-8 unit decrease in the  $pK_a$  value. The observation is very similar to that observed for  $[\text{RuCl}(\text{H}_2)(\text{L})(\text{PMP})]^+$  ( $\text{L} = \text{CO}, \text{PPh}_3$ ).<sup>55</sup> The same trend has also been observed for classical hydride complexes. For example,  $\text{MnH}(\text{CO})_5$  has a  $pK_a(\text{CH}_3\text{CN})$  of 15.1<sup>56</sup> vs 20.4 for  $\text{MnH}(\text{CO})(\text{PPh}_3)$ ;<sup>57</sup>  $\text{CpCrH}(\text{CO})_3$  has a  $pK_a(\text{CH}_3\text{CN})$  of 13.3<sup>58</sup> vs 21.8 for  $\text{CpCrH}(\text{CO})_2(\text{PPh}_3)$ ,<sup>59</sup> and  $\text{HCo}(\text{CO})_4$  has a  $pK_a$  of 8.3<sup>56</sup> vs 15.4 for  $\text{HCo}(\text{CO})_3(\text{PPh}_3)$ .<sup>56</sup> These observations may indicate that the inductive



effect of the ligands is very important in determining the acidity of the dihydrogen complexes.

It is well established that the acidity of hydride complexes are strongly influenced by the metals as well as the auxiliary ligands.<sup>60,61</sup> With a few exceptions, the acidity of isostructural classic hydride complexes decreases as ligands become more electron-donating, and as the metal is replaced successively by heavier metals in the same group. The relative acidity of most of the complexes studied in this work are consistent with the trend. However, exception is observed for complexes **6** and **8**. It might be expected that complex **8** should be less acidic than complex **6** because <sup>Me</sup>Cn is more electron-donating than <sup>H</sup>Cn, as reflected from the <sup>1</sup>J(HD) coupling constants of the corresponding isotopomers of complexes **6** and **8**. In fact, complex **8** was found to be more acidic than complex **6** based on the equilibrium study as described before. The more acidic nature of complex **8** compared to complex **6** is further supported by the fact that the complex [<sup>H</sup>CnRuH(CO)(PPh<sub>3</sub>)]<sup>+</sup> is preferentially protonated when a mixture of [<sup>H</sup>CnRuH(CO)(PPh<sub>3</sub>)]<sup>+</sup> and [<sup>Me</sup>CnRuH(CO)(PPh<sub>3</sub>)]<sup>+</sup> was treated with a limited amount of HBF<sub>4</sub>·OEt<sub>2</sub>. (Fig 2.3)

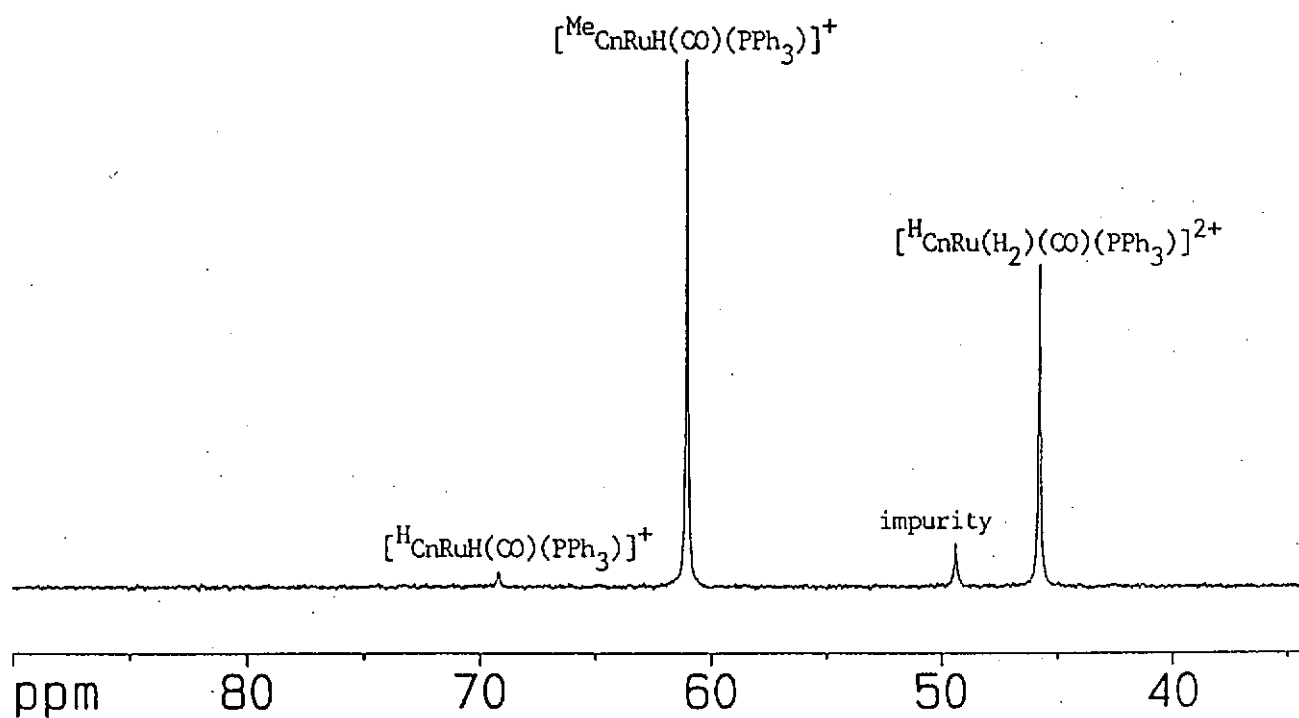
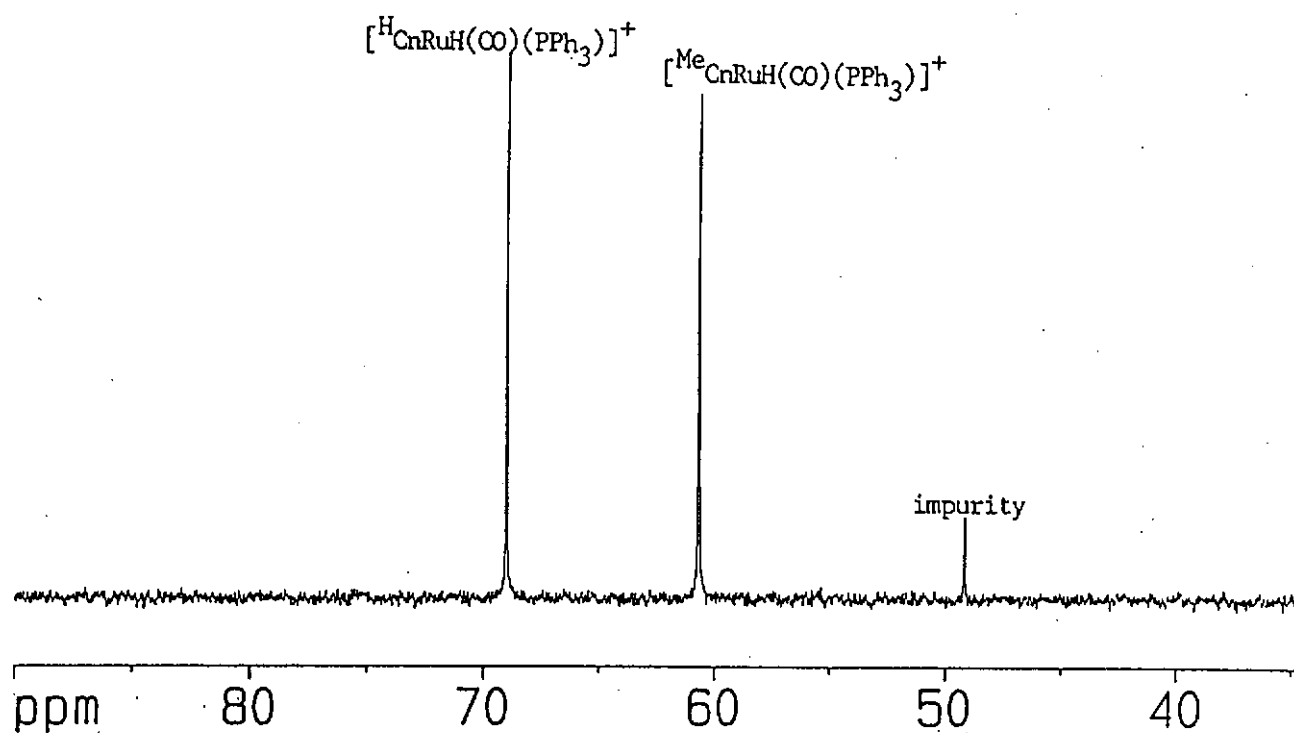


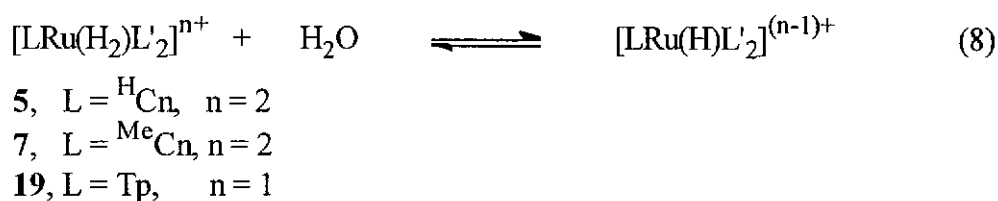
Figure 2.3. The  $^{31}\text{P}$  NMR spectra of (a)  $[\text{}^{\text{Me}}\text{CnRuH}(\text{CO})(\text{PPh}_3)]^+$  and  $[\text{}^{\text{H}}\text{CnRuH}(\text{CO})(\text{PPh}_3)]^+$  in  $\text{CD}_2\text{Cl}_2$  at  $-35\text{ }^\circ\text{C}$  and (b) ( $[\text{}^{\text{Me}}\text{CnRuH}(\text{CO})(\text{PPh}_3)]^+$  and  $[\text{}^{\text{H}}\text{CnRuH}(\text{CO})(\text{PPh}_3)]^+$ ) +  $\text{HBF}_4 \cdot \text{Et}_2\text{O}$  in  $\text{CD}_2\text{Cl}_2$  at  $-80\text{ }^\circ\text{C}$

It is not apparent why the  $^{\text{Me}}\text{Cn}$  complex **8** is more acidic than the  $^{\text{H}}\text{Cn}$  complex **6**. It is possible that the H-H bond strength in **6** and **8** may play some role in determining the relative acidity. The more electron donating  $^{\text{Me}}\text{Cn}$  ligand in **8** renders the H-H interaction weaker than that in complex **6** which contains the less donating  $^{\text{H}}\text{Cn}$  ligand, and the weaker H-H interaction may make a dihydrogen complex more acidic than may be suggested by the general trend in the acidity of classic hydride complexes. Morris *et al.* has recently proposed that dramatic reduction of  $\text{p}K_{\text{a}}$  value of *trans*- $[\text{RuCl}(\text{H}_2)(\text{dppe})_2]^+$  vs that of *trans*- $[\text{RuH}(\text{H}_2)(\text{dppe})_2]^+$  could be attributed to a lower H-H bond strength in the former. The high acidity of the trihydride complex  $[\text{RuH}_3(\text{dppf})_2]^+$  (dppf = 1,1'-bis(diphenylphosphino)ferrocene) compared to that of  $[\text{RuH}(\text{H}_2)(\text{dppe})_2]^+$  is also in accord with this idea.<sup>19b</sup>

### 2.3.6 Reactions of Dihydrogen Complexes with Water.

The roles of the dihydrogen complexes  $[\text{TpRu}(\text{H}_2)(\text{PPh}_3)_2]^+$  (**17**) and  $[\text{TpRu}(\text{H}_2)(\text{CH}_3\text{CN})(\text{PPh}_3)]^+$  (**18**) in olefin hydrogenation reactions have been discussed in a recent publication of our group.<sup>29b</sup> It was noted that their catalytic activities are greatly enhanced when the reactions were performed in THF/ $\text{H}_2\text{O}$  mixed solvents instead of anhydrous THF. The enhancement effect is attributed to deprotonation of  $\eta^2\text{-H}_2$  by  $\text{H}_2\text{O}$  to generate the active metal hydride species. The deprotonation reaction with water has been demonstrated with NMR study with complex **17**. It is somewhat surprising to find out in the present study that the pseudo aqueous  $\text{p}K_{\text{a}}$  of complexes **17** (7.6) and **18** (8.9) are significantly higher than that of  $\text{H}_3\text{O}^+$  (-1.74).<sup>62</sup> As  $\text{H}_2\text{O}$  is a very weak base, it is not expected that  $\text{H}_2\text{O}$  should be basic enough to deprotonate these dihydrogen complexes.

In order to see if deprotonation by water would also occur on other dihydrogen complexes with pseudo aqueous  $pK_a$  values significantly higher than that of  $H_3O^+$ , the reactivities of complexes  $[TpRu(H_2)(dppe)]BF_4$  (**19**,  $pK_a = 7.9$ ),  $[^H CnRu(H_2)(PPh_3)_2](BF_4)_2$  (**5**,  $pK_a = 4.5$ ) and  $[^{Me} CnRu(H_2)(dppe)](CF_3SO_3)_2$  (**7**,  $pK_a = 3.8$ ) toward water have been tested. (eq. 8)



In the absence of  $H_2$  pressure, like complex **17**,  $H_2O$  displaced the  $\eta^2-H_2$  ligand in **19** to give  $[TpRu(H_2O)(dppe)] BF_4$ . The reaction took a different route under  $H_2$  pressure in  $CD_2Cl_2/H_2O$  biphasic medium. When 50-100  $\mu L$  of  $H_2O$  was added to a 0.4 mL  $CD_2Cl_2$  solution of **19** in a Wilmad pressure valved NMR tube, phase separation occurred. The  $^1H$  NMR spectrum of the  $CD_2Cl_2$  phase showed that some of the  $\eta^2-H_2$  was displaced by  $H_2O$  via simple ligand substitution reaction. But after pressurizing the tube with 15 atm of  $H_2$ , most of the dihydrogen complex was reformed, partial deprotonation of  $\eta^2-H_2$  by  $H_2O$  took place, as evidenced by the appearance of the ruthenium hydride signal in the  $^1H$  NMR spectrum.

The dihydrogen complexes **5** and **7** are more stable with respect to loss of  $H_2$  at room temperature, thus deprotonation studies with  $H_2O$  can be carried out in the absence of  $H_2$  atmosphere in  $CD_2Cl_2$ . It was shown that the dihydrogen complexes

were deprotonated completely to form the monohydride complexes. The observation is probably not surprising, as complexes **5** and **7** are more acidic than their Tp analogues.

Deprotonation of  $\eta^2\text{-H}_2$  in complexes **5**, **7**, **17** and **19**, which have pseudo aqueous  $\text{p}K_{\text{a}}$  values above 3, in biphasic conditions, is probably due to the strong solvation of  $\text{H}^+$  by  $\text{H}_2\text{O}$ . It is also likely that the difference in the  $\text{p}K_{\text{a}}$  values of the dihydrogen complexes in aqueous solution may not be as large as the pseudo aqueous  $\text{p}K_{\text{a}}$  values may imply.

## Chapter Three

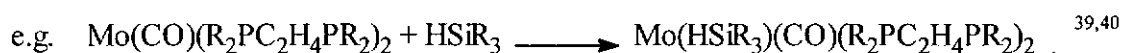
### *Syntheses, characterization and reactivity of ruthenium $\eta^2$ -silane complexes*

#### 3.1 Introduction

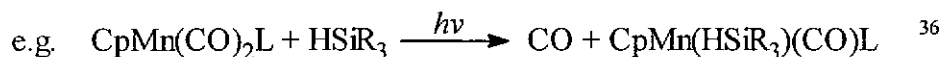
In recent years, the chemistry of metal- $\sigma$ -silane complexes has been extensively studied.<sup>4</sup> However, there is no report on ruthenium- $\sigma$ -silane complexes containing hydrotris(1-pyrazolyl)borate ligand (Tp). This chapter describes the preparation of some ruthenium- $\sigma$ -silane complexes supported by Tp ligand.

There are several common methods for the preparation of metal-silane complex:

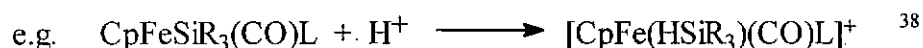
(i) reaction between an unsaturated transition metal centre and free silane,



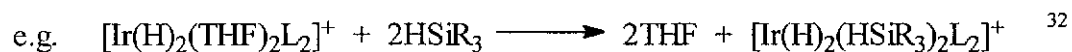
(ii) photochemical reaction of a carbonyl-containing complex with free silane;



(iii) protonation of transition metal silyl complex;



(iv) displacement of the labile ligands (e.g. solvento and  $\eta^2$ -dihydrogen ligands) by free silane.



The last preparative method was employed for the preparation of Tp  $\sigma$ -silane complexes in this research. The reactions between free silanes and the  $\eta^2$ -dihydrogen complexes (17, 18 & 20) bearing hydrotris(1-pyrazolyl)borato ligand were first attempted, but the expected  $\eta^2$ -silane complex  $[\text{TpRu}(\eta^2\text{-HSiR}_3)(\text{PPh}_3)_2]\text{BF}_4$  was not obtained. The solvento hydrido complex  $\text{TpRuH}(\text{CH}_3\text{CN})(\text{PPh}_3)_2$  (13) was then used in place of the dihydrogen complexes, it was found to react with a variety of silanes, leading to the formation of the corresponding hydrido  $\sigma$ -silane complexes  $\text{TpRu}(\text{PPh}_3)_2(\text{H}_2\text{SiR}_3)$  (21a-21f).

## **3.2 Experimental**

### *3.2.1 Materials*

All reactions were carried out under a dry  $\text{N}_2$  atmosphere using standard Schlenk techniques. All solvents were distilled and degassed prior to use. Dichloromethane and acetonitrile were distilled from calcium hydride; tetrahydrofuran, diethyl ether and hexane were distilled from sodium benzophenone ketyl. Deuterated dichloromethane was dried on  $\text{P}_2\text{O}_5$  and vacuum transferred to a flask fitted with a rubber septum for storage. Deuterated tetrahydrofuran was dried on calcium hydride and vacuum transferred to a flask fitted with a rubber septum for storage. The complexes  $[\text{TpRu}(\text{H}_2)(\text{PPh}_3)_2]\text{BF}_4$ ,<sup>29b</sup>  $\text{TpRuH}(\text{CH}_3\text{CN})(\text{PPh}_3)_2$ ,<sup>29b</sup>  $\text{TpRuH}(\text{PPh}_3)_2$ ,<sup>29b</sup>  $\text{TpRuH}(\text{H}_2)(\text{PPh}_3)_2$ ,<sup>29b</sup>  $\text{TpRuCl}(\text{CH}_3\text{CN})(\text{PPh}_3)_2$ ,<sup>29b</sup>  $[\text{TpRu}(\text{H}_2)(\text{CH}_3\text{CN})(\text{PPh}_3)]\text{BF}_4$ ,<sup>29b</sup>  $\text{TpRu}(\text{CH}_3)(\text{CO})(\text{PPh}_3)_2$ <sup>29a</sup> and  $\text{TpRuH}(\text{CO})(\text{PPh}_3)_2$ ,<sup>29a</sup> were synthesized according to literature methods. Triethylsilane, triethoxysilane, triphenylsilane, diethylsilane,

diphenylsilane, phenylsilane, and  $\text{HBF}_4 \cdot \text{Et}_2\text{O}$  were purchased from Fluka and were used as received.

### 3.2.2 Instrumentation

Infrared spectra were obtained from a Nicolet Magna 750 FT IR spectrophotometer.  $^1\text{H}$  NMR spectra were taken from a Bruker DPX 400 spectrometer; chemical shift were referenced to the proton residue of the deuterated solvents ( $\text{CDHCl}_2$   $\delta$  5.32 ppm;  $\text{C}_4\text{D}_7\text{H}$   $\delta$  1.85 ppm,  $\delta$  3.70 ppm).  $^{31}\text{P}\{^1\text{H}\}$  NMR spectra were taken on a Bruker DPX-400 spectrometer at 161.98 MHz.  $^{31}\text{P}$  Chemical shifts were externally referenced to 85%  $\text{H}_3\text{PO}_4$  in  $\text{D}_2\text{O}$  ( $\delta$  0.00 ppm).  $^{29}\text{Si}\{^1\text{H}\}$  NMR spectra were taken on a Bruker DPX-400 spectrometer at 79.50 MHz.  $^{29}\text{Si}$  Chemical shifts were externally referenced to TMS in  $\text{CDCl}_3$  ( $\delta$  0.00 ppm). Relaxation time  $T_1$  measurements were carried out in  $\text{THF-}d_8$  at 400 MHz by inversion-recovery method using standard  $180^\circ$ - $\tau$ - $90^\circ$  pulse sequence. High-pressure NMR studies were performed using a Wilmad pressure-valved NMR tube, the maximum pressure used was 15 atm (room temperature). FAB MS was carried out with a Finnigan MAT 95S mass spectrometer using 3-nitrobenzyl alcohol as matrix.

### 3.3.3 Syntheses

**$\text{TpRuH}(\text{HSiEt}_3)(\text{PPh}_3)$  (21a).** A THF solution (10 mL) of  $\text{TpRuH}(\text{CH}_3\text{CN})(\text{PPh}_3)$  (**13**) (0.2 g, 0.32 mmol) and  $\text{HSiEt}_3$  (0.3 mL, 4 mmol) was stirred under nitrogen at 80 °C for 4 h. The solution was cooled and the solvent was removed by vacuum. Hexane (10 mL) was added to the system and it was then cooled to -30 °C to give an orange solid which was filtered out. The solid was further washed with precooled hexane (5 mL) and then dried under vacuum. Yield: 0.09g (41%). IR



(KBr,  $\text{cm}^{-1}$ ):  $\nu(\text{Ru-H})$  2044 (w),  $\nu(\text{B-H})$  2461 (br).  $^1\text{H}$  NMR (400 MHz,  $\text{THF-}d_8$ , 20  $^\circ\text{C}$ ):  $\delta$  -11.62 (d, 2H,  $^2J(\text{HP}) = 22.8$  Hz,  $^{29}\text{Si}$  satellite,  $^1J(\text{HSi}) = 23.3$  Hz, Ru-H,  $T_1 = 593$  ms), 0.79 (q, 6H,  $^3J(\text{HH}) = 7.8$  Hz,  $\text{CH}_2\text{CH}_3$ ), 1.14 (t, 9H,  $^3J(\text{HH}) = 7.8$  Hz,  $\text{CH}_2\text{CH}_3$ ), 5.88 [t, 2H, H(pz)], 6.12 (t, 1H, H(pz')), 7.37 [d, 2H, H(pz)], 7.64 [d, 1H, H(pz')], 7.73 [d, 2H, H(pz)], 8.00 [d, 1H, H(pz')] (pz = pyrazolyl groups trans to hydrides, pz' = pyrazolyl group trans to  $\text{PPh}_3$ ; all coupling constants for pyrazolyl proton resonances were about 2 Hz); 7.11 - 7.84 (m, 15H of  $\text{PPh}_3$  phenyl groups).  $^{31}\text{P}\{^1\text{H}\}$  NMR (161.70 MHz,  $\text{THF-}d_8$ , 20  $^\circ\text{C}$ ):  $\delta$  67.9 (s)  $^{29}\text{Si}\{^1\text{H}\}$  NMR (79.50 MHz,  $\text{THF-}d_8$ , 20  $^\circ\text{C}$ ):  $\delta$  24.7 (s) FAB MS (m/z): 576  $[\text{M-HSiEt}_3]^+$ .

**$\text{TpRuH}(\text{HSi}(\text{EtO})_3)(\text{PPh}_3)$  (21b).** This complex was prepared by using the same procedure as for the preparation of **21a**, except that  $\text{HSi}(\text{EtO})_3$  was used. The yield of the orange solid obtained was 0.11 g (46%). IR (KBr,  $\text{cm}^{-1}$ ):  $\nu(\text{Ru-H})$  2057 (w),  $\nu(\text{B-H})$  2472 (br).  $^1\text{H}$  NMR (400 MHz,  $\text{THF-}d_8$ , 20  $^\circ\text{C}$ ):  $\delta$  -11.41 (d, 2H,  $^2J(\text{HP}) = 22.4$  Hz,  $^{29}\text{Si}$  satellite,  $^1J(\text{HSi}) = 52.8$  Hz, Ru-H,  $T_1 = 688$  ms), 1.06 (t, 9H,  $^3J(\text{HH}) = 7.8$  Hz,  $\text{OCH}_2\text{CH}_3$ ), 3.97 (q, 6H,  $^3J(\text{HH}) = 7.8$  Hz,  $\text{OCH}_2\text{CH}_3$ ), 5.90 [t, 2H, H(pz)], 6.07 (t, 1H, H(pz')), 7.07 [d, 2H, H(pz)], 7.61 [d, 1H, H(pz')], 7.76 [d, 2H, H(pz)], 8.51 [d, 1H, H(pz')] (pz = pyrazolyl groups trans to hydrides, pz' = pyrazolyl group trans to  $\text{PPh}_3$ ; all coupling constants for pyrazolyl proton resonances were about 2 Hz); 6.06 - 7.87 (m, 15H of  $\text{PPh}_3$  phenyl groups).  $^{31}\text{P}\{^1\text{H}\}$  NMR (161.70 MHz,  $\text{THF-}d_8$ , 20  $^\circ\text{C}$ ):  $\delta$  66.4 (s)  $^{29}\text{Si}\{^1\text{H}\}$  NMR (79.50 MHz,  $\text{THF-}d_8$ , 20  $^\circ\text{C}$ ):  $\delta$  -0.72 (s) FAB MS (m/z): 576  $[\text{M-HSi}(\text{EtO})_3]^+$ .

**TpRuH(HSiPh<sub>3</sub>)(PPh<sub>3</sub>) (21c).** This complex was prepared by using the same procedure as for the preparation of **21a**, except that HSiPh<sub>3</sub> was used. The yield of the orange solid obtained was 0.13 g (49%). IR (KBr, cm<sup>-1</sup>):  $\nu(\text{Ru-H})$  2040 (w),  $\nu(\text{B-H})$  2468 (br). <sup>1</sup>H NMR (400 MHz, THF-*d*<sub>8</sub>, 20 °C):  $\delta$  -10.11 (d, 2H, <sup>2</sup>*J*(HP) = 23.2 Hz, <sup>29</sup>Si satellite, <sup>1</sup>*J*(HSi) = 28.4 Hz, Ru-*H*, *T*<sub>1</sub> = 436 ms),  $\delta$  5.53 [t, 1H, H(pz)],  $\delta$  5.98 (t, 2H, H(pz')),  $\delta$  7.45 [d, 1H, H(pz')],  $\delta$  7.51 [d, 2H, H(pz)],  $\delta$  7.67 [d, 1H, H(pz')],  $\delta$  7.82 [d, 2H, H(pz)] (pz = pyrazolyl groups trans to hydrides, pz' = pyrazolyl group trans to PPh<sub>3</sub>; all coupling constants for pyrazolyl proton resonances were about 2 Hz);  $\delta$  5.89 - 7.69 (m, 30H of phenyl groups). <sup>31</sup>P{<sup>1</sup>H} NMR (161.70 MHz, THF-*d*<sub>8</sub>, 20 °C):  $\delta$  65.0 (s) <sup>29</sup>Si{<sup>1</sup>H} NMR (79.50 MHz, THF-*d*<sub>8</sub>, 20 °C):  $\delta$  26.9 (s) FAB MS (m/z): 576 [M-Ph<sub>3</sub>SiH]<sup>+</sup>.

**TpRuH(H<sub>2</sub>SiEt<sub>2</sub>)(PPh<sub>3</sub>) (21d).** This complex was prepared by using the same procedure as for the preparation of **21a**, except that H<sub>2</sub>SiEt<sub>2</sub> was used. The yield of the orange solid obtained was 0.13 g (61%). IR (KBr, cm<sup>-1</sup>):  $\nu(\text{Ru-H})$  2062 (w),  $\nu(\text{B-H})$  2469 (br). <sup>1</sup>H NMR (400 MHz, THF-*d*<sub>8</sub>, 20 °C):  $\delta$  -10.93 (dd, 2H, <sup>2</sup>*J*(HP) = 22.0 Hz, <sup>2</sup>*J*(HH) = 2.8 Hz, <sup>29</sup>Si satellite, <sup>1</sup>*J*(HSi) = 23.5 Hz, Ru-*H*, *T*<sub>1</sub> = 690 ms), 1.08 (m, 6H, CH<sub>2</sub>CH<sub>3</sub>), 1.21 (m, 4H, CH<sub>2</sub>CH<sub>3</sub>), 4.60 (m, 1H, Si-*H*) 5.92 [t, 2H, H(pz)], 6.14 [t, 1H, H(pz')], 7.08 [d, 2H, H(pz)], 7.68 [d, 1H, H(pz')], 7.78 [d, 2H, H(pz)], 7.87 [d, 1H, H(pz')] (pz = pyrazolyl groups trans to hydrides, pz' = pyrazolyl groups trans to PPh<sub>3</sub>; all coupling constants for pyrazolyl proton resonances were about 2 Hz); 7.22 - 7.56 (m, 15H of PPh<sub>3</sub> phenyl groups). <sup>31</sup>P{<sup>1</sup>H} NMR (161.70 MHz, THF-*d*<sub>8</sub>, 20 °C):  $\delta$  68.5 (s) <sup>29</sup>Si{<sup>1</sup>H} NMR (79.50 MHz, THF-*d*<sub>8</sub>, 20 °C):  $\delta$  16.9 (s) FAB MS (m/z): 576 [M-H<sub>2</sub>SiEt<sub>2</sub>]<sup>+</sup>.

**TpRuH(H<sub>2</sub>SiPh<sub>2</sub>)(PPh<sub>3</sub>) (21e).** This complex was prepared by using the same procedure as for the preparation of **21a**, except that H<sub>2</sub>SiPh<sub>2</sub> was used. The yield of the orange solid obtained was 0.14 g (58%). IR (KBr, cm<sup>-1</sup>):  $\nu$ (Ru-H) 2082 (w),  $\nu$ (B-H) 2470 (br). <sup>1</sup>H NMR (400 MHz, THF-*d*<sub>8</sub>, 20 °C):  $\delta$  -9.71 (dd, 2H, <sup>2</sup>*J*(HP) = 20.8 Hz, <sup>2</sup>*J*(HH) = 3.0 Hz, <sup>29</sup>Si satellite, <sup>1</sup>*J*(HSi) = 23.5 Hz, Ru-*H*, *T*<sub>1</sub> = 545 ms), 5.72 (dt, 1H, <sup>2</sup>*J*(HH) = 3.0 Hz, *J*(HH) = 10.6 Hz, Si-*H*) 5.80 [t, 1H, H(pz')], 5.97 [t, 2H, H(pz)], 7.13 [d, 2H, H(pz)], 7.35 [d, 1H, H(pz')], 7.60 [d, 1H, H(pz')], 7.84 [d, 2H, H(pz)] (pz = pyrazolyl groups trans to hydrides, pz' = pyrazolyl group trans to PPh<sub>3</sub>; all coupling constants for pyrazolyl proton resonances were about 2 Hz); 6.18 - 7.77 (m, 25H of phenyl groups). <sup>31</sup>P{<sup>1</sup>H} NMR (161.70 MHz, THF-*d*<sub>8</sub>, 20 °C):  $\delta$  65.6 (s) <sup>29</sup>Si{<sup>1</sup>H} NMR (79.50 MHz, THF-*d*<sub>8</sub>, 20 °C): 9.0 (s) FAB MS (*m/z*): 576 [M- H<sub>2</sub>SiPh<sub>2</sub>]<sup>+</sup>.

**TpRuH(H<sub>3</sub>SiPh)(PPh<sub>3</sub>) (21f).** This complex was prepared by using the same procedure as for the preparation of **21a**, except that H<sub>3</sub>SiPh was used. The yield of the orange solid obtained was 0.12 g (55%). IR (KBr, cm<sup>-1</sup>):  $\nu$ (Ru-H) 2029 (w),  $\nu$ (B-H) 2471 (br). <sup>1</sup>H NMR (400 MHz, THF-*d*<sub>8</sub>, 20 °C):  $\delta$  -10.32 (d, 2H, <sup>2</sup>*J*(HP) = 21.2 Hz, <sup>29</sup>Si satellite, <sup>1</sup>*J*(HSi) = 27.4 Hz, Ru-*H*, *T*<sub>1</sub> = 615 ms), 5.22 (d, 2H, *J*(HP) = 3.3 Hz, Hz Si-*H*) 5.98 [t, 1H, H(pz')], 5.99 [t, 2H, H(pz)], 7.08 [d, 1H, H(pz')], 7.37 [d, 2H, H(pz)], 7.67 [d, 1H, H(pz')], 7.84 [d, 2H, H(pz)] (pz = pyrazolyl groups trans to hydrides, pz' = pyrazolyl group trans to PPh<sub>3</sub>; all coupling constants for pyrazolyl proton resonances were about 2 Hz); 6.32 - 7.83 (m, 20H of phenyl groups). <sup>31</sup>P{<sup>1</sup>H} NMR (161.70 MHz, THF-*d*<sub>8</sub>, 20 °C):  $\delta$  67.2 (s) <sup>29</sup>Si{<sup>1</sup>H} NMR (79.50 MHz, THF-*d*<sub>8</sub>, 20 °C):  $\delta$  -17.2 (s) FAB MS (*m/z*): 576 [M- H<sub>3</sub>SiPh]<sup>+</sup>.

### 3.2.4 NMR studies of reactions of the ruthenium complexes

**[TpRu(PPh<sub>3</sub>)<sub>2</sub>(H<sub>2</sub>)]BF<sub>4</sub> (17)** (generated in situ by protonation of **TpRuH(PPh<sub>3</sub>)<sub>2</sub>** with HBF<sub>4</sub>.Et<sub>2</sub>O) with triethylsilane. A sample of 10 mg of **TpRuH(PPh<sub>3</sub>)<sub>2</sub>** (12) was loaded into a 5 mm NMR tube which was then capped with a rubber septum. The tube was evacuated and then filled with nitrogen for three cycles. Dichloromethane-*d*<sub>2</sub> (0.4 mL) was added to the tube to dissolve the sample, followed by the addition of 5 μL of tetrafluoroboric acid in ethereal solution (HBF<sub>4</sub>.Et<sub>2</sub>O 56%). Then 10 μL of triethylsilane was added and the tube was allowed to heat at 40 °C for ten hours. The solution was analyzed by NMR spectroscopy.

**[TpRu(H<sub>2</sub>)(CH<sub>3</sub>CN)(PPh<sub>3</sub>)]BF<sub>4</sub> (18)** (generated in situ by protonation of **TpRuH(CH<sub>3</sub>CN)(PPh<sub>3</sub>)** with HBF<sub>4</sub>.Et<sub>2</sub>O) with triethylsilane. A sample of 10 mg of **TpRuH(CH<sub>3</sub>CN)(PPh<sub>3</sub>)** (13) was loaded into a 5 mm NMR tube which was then capped with a rubber septum. The tube was evacuated and then filled with nitrogen for three cycles. Dichloromethane-*d*<sub>2</sub> (0.4 mL) was added to the tube to dissolve the sample. The solution was cooled to -78 °C, 5 μL of tetrafluoroboric acid and then 10 μL of triethylsilane were added through microsyringes. The tube was loaded into an NMR probe precooled to -60 °C and the sample was analyzed as it slowly warmed up to room temperature.

**[TpRu(H<sub>2</sub>)(CO)(PPh<sub>3</sub>)]BF<sub>4</sub> (20)** (generated in situ by protonation of **TpRuH(CO)(PPh<sub>3</sub>)** with **HBF<sub>4</sub>.Et<sub>2</sub>O**) with triethylsilane. The procedure for **18** was followed exactly, substituting **[TpRu(H<sub>2</sub>)(CO)(PPh<sub>3</sub>)]BF<sub>4</sub> (20)** for **18**.

**[TpRu-<sup>13</sup>CH<sub>4</sub>-(CO)(PPh<sub>3</sub>)]BF<sub>4</sub>** (generated in situ by protonation of **TpRu(CH<sub>3</sub>)(CO)(PPh<sub>3</sub>)** with **HBF<sub>4</sub>.Et<sub>2</sub>O**) with triethylsilane. A sample of 10 mg of **TpRu(CH<sub>3</sub>)(CO)(PPh<sub>3</sub>)** was loaded into a 5mm NMR tube which was then capped with a rubber septum. The tube was evacuated and then filled with nitrogen for three cycles. Dichloromethane-*d*<sub>2</sub> (0.4 mL) was added to the tube to dissolve the sample. The solution was cooled to -78 °C, 5 µl of tetrafluoroboric acid and then 10 µL of triethylsilane were added through microsyringes. The tube was loaded into an NMR probe precooled to -60 °C and the sample was analyzed as it slowly warmed up to room temperature.

**TpRuCl(CH<sub>3</sub>CN)(PPh<sub>3</sub>) (11)** with diphenylsilane. A sample of 10 mg of **TpRuCl(CH<sub>3</sub>CN)(PPh<sub>3</sub>) (11)** was loaded into a 5mm NMR tube which was then capped with a rubber septum. The tube was evacuated and then filled with nitrogen for three cycles. Tetrahydrofuran-*d*<sub>8</sub> (0.4 mL) was added to the tube to dissolve the sample, followed by the addition of 20 µL of diphenylsilane. The tube was heated at 60 °C for ten hours, after which the sample was analyzed by NMR spectroscopy. <sup>1</sup>H NMR indicated that **TpRuH(H<sub>2</sub>SiPh<sub>2</sub>)(PPh<sub>3</sub>) (21d)** was formed.

**TpRuH(HSiR<sub>3</sub>)(PPh<sub>3</sub>) (21) with acetonitrile.** A sample of 10 mg of TpRuH(HSiR<sub>3</sub>)(PPh<sub>3</sub>) (21) was loaded into a 5mm NMR tube which was then capped with a rubber septum. The tube was evacuated and then filled with nitrogen for three cycles. Tetrahydrofuran-*d*<sub>8</sub> (0.4 mL) was added to the tube to dissolve the sample followed by the addition of 20 μL of acetonitrile. The tube was allowed to heat at 60 °C for ten hours, after which the sample was analyzed by NMR spectroscopy. <sup>1</sup>H NMR indicated that 21 was converted to TpRuH(CH<sub>3</sub>CN)(PPh<sub>3</sub>) (13).

**TpRuH(HSiR<sub>3</sub>)(PPh<sub>3</sub>) (21) with hydrogen.** A sample of 10 mg of TpRuH(HSiR<sub>3</sub>)(PPh<sub>3</sub>) (21) was loaded into a 5mm Wilmad pressure NMR tube. The tube was evacuated and then filled with nitrogen for three cycles. Tetrahydrofuran-*d*<sub>8</sub> (0.3 mL) was added to the tube to dissolve the sample. The tube was then pressurised with 15 atm of H<sub>2</sub> and allowed to heat at 80 °C for ten hours, after which the sample was analyzed by NMR spectroscopy. <sup>1</sup>H NMR indicated the presence of TpRuH(H<sub>2</sub>)(PPh<sub>3</sub>) (16), and small amount of unreacted 21.

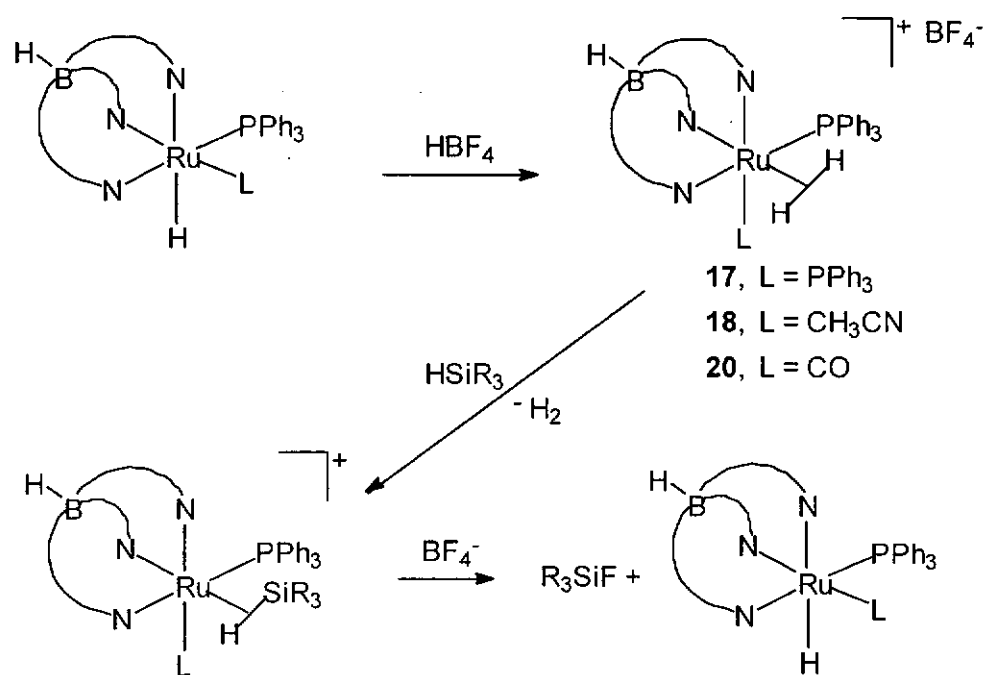
### **3.3 Results and Discussion**

#### *3.3.1 Reactions of Tp dihydrogen complexes with silane*

It is well documented that labile ligands in transition metal complexes can be displaced by free silanes to form the  $\eta^2$ -silane complexes.<sup>32,38</sup> While there are numerous examples of neutral transition metal  $\eta^2$ -silane complexes, cationic complexes of this type are rare. Crabtree spectroscopically observed the cationic  $\sigma$ -silane complex  $[(\text{IrH}_2(\eta^2\text{-HSiEt}_3)_2(\text{PPh}_3)_2)]\text{SbF}_6$  during his investigations of silane alcoholysis catalysed by  $[(\text{IrH}_2\text{S}_2(\text{PPh}_3)_2)]\text{SbF}_6$ .<sup>32</sup> A cationic ruthenium trichlorosilane complex  $[\text{CpRu}(\eta^2\text{-HSiCl}_3)(\text{PMe}_3)]\text{BAR}'_4$  ( $\text{BAR}'_4 = \text{B}(3,5\text{-}(\text{CF}_3)_2\text{C}_6\text{H}_3)_4$ ) has been prepared by protonation of  $\text{CpRu}(\text{SiCl}_3)(\text{PMe}_3)_2$  with  $[\text{H}(\text{Et}_2\text{O})_2][\text{BAR}'_4]$  in  $\text{CH}_2\text{Cl}_2$ .<sup>63</sup> Brookhart has recently developed a general method for the generation of cationic  $\eta^2$ -silane complexes  $[\text{CpFe}(\eta^2\text{-HSiR}_3)(\text{CO})\text{L}]^+$  ( $\text{L} = \text{PEt}_3, \text{PPh}_3; \text{R}_3 = \text{HPh}_2, \text{HMePh}, \text{HEt}_2, \text{H}_2\text{Ph}$ ) which are stabilized through the use of the non-nucleophilic counterion  $\text{BAR}'_4^-$ . These species are easily formed by displacement of the  $\eta^2\text{-H}_2$  ligand from the cationic  $\eta^2$ -dihydrogen complex  $[\text{CpFe}(\text{H}_2)(\text{CO})\text{L}]^+$  by the free silane.<sup>38</sup> In view of the rarity of cationic  $\eta^2$ -silane complexes and the fact that the hydrotris(pyrazolyl)borato (Tp) ligand has a high tendency of forming octahedral  $\eta^2$ -dihydrogen complex,<sup>29g,f</sup> the reactions of some of the Tp ruthenium  $\eta^2$ -dihydrogen complexes recently reported by our group<sup>29a,b</sup> with free silane were studied, in hope of obtaining stable cationic Tp-supported ruthenium  $\eta^2$ -silane complexes for further reactivity investigations.

However, in our work of reacting the  $\eta^2$ -dihydrogen complexes  $[\text{TpRu}(\text{H}_2)(\text{PPh}_3)_2]\text{BF}_4$  (17),  $[\text{TpRu}(\text{H}_2)(\text{CH}_3\text{CN})(\text{PPh}_3)]\text{BF}_4$  (18), and

[TpRu(H<sub>2</sub>)(CO)(PPh<sub>3</sub>)]BF<sub>4</sub> (**20**) with R<sub>3</sub>SiH (R<sub>3</sub> = Et<sub>3</sub>, (EtO)<sub>3</sub>, Ph<sub>3</sub>, HEt<sub>2</sub>, HPh<sub>2</sub> and H<sub>2</sub>Ph), it was found that the hydride complexes, TpRuH(PPh<sub>3</sub>)<sub>2</sub>, TpRuH(CH<sub>3</sub>CN)(PPh<sub>3</sub>) and TpRuH(CO)(PPh<sub>3</sub>) were produced, respectively; no silane complexes were formed. The formation of the hydride complexes can be accounted for by the reaction sequence depicted in Scheme 2. Substitution of the η<sup>2</sup>-H<sub>2</sub> ligand in the η<sup>2</sup>-dihydrogen complex for the silane molecule generates the σ-silane complex intermediate, which, due to the very high electrophilicity of the silicon centre of the η<sup>2</sup>-HSiR<sub>3</sub> ligand, is readily attacked by the nucleophile BF<sub>4</sub><sup>-</sup> to form the hydride complex TpRuH(L)(PPh<sub>3</sub>). It has been proposed that the extreme sensitivity of the electrophilic silicon centre of [CpFe(η<sup>2</sup>-HSiEt<sub>3</sub>)(CO)(PEt<sub>3</sub>)]BF<sub>4</sub> to nucleophile, even the traditionally non-nucleophilic counterion BF<sub>4</sub><sup>-</sup>, is responsible for the generation of the hydride complex CpRuH(CO)(PEt<sub>3</sub>), which in acidic medium, is protonated to give the η<sup>2</sup>-dihydrogen complex [CpFe(H<sub>2</sub>)(CO)(PEt<sub>3</sub>)]BF<sub>4</sub>.<sup>38</sup>



Scheme 2



Reaction of the transient 'CH<sub>4</sub>' complex [TpRu(CH<sub>4</sub>)(CO)(PPh<sub>3</sub>)]BF<sub>4</sub>, generated via protonation of TpRu(CH<sub>3</sub>)(CO)(PPh<sub>3</sub>) with HBF<sub>4</sub>·Et<sub>2</sub>O, with free silanes again led to the formation of the hydrido complex TpRuH(CO)(PPh<sub>3</sub>), no σ-silane complexes were detected.

The reactions of the η<sup>2</sup>-dihydrogen complexes **17**, **18**, and **20**, as well as the transient 'CH<sub>4</sub>' complex with free silanes seem to form unstable cationic η<sup>2</sup>-silane complexes, which, like [CpFe(η<sup>2</sup>-HSiEt<sub>3</sub>)](CO)(PEt<sub>3</sub>)]BF<sub>4</sub>, deteriorated to the metal hydride species due to nucleophilic attack of the η<sup>2</sup>-silane ligand by the counterion BF<sub>4</sub><sup>-</sup>. Since nucleophilic attack of the highly electrophilic silicon centre of η<sup>2</sup>-silane ligand is now a well-established reaction, it is believed that further research on the reactivities of Tp ruthenium η<sup>2</sup>-dihydrogen complexes toward free silanes is not likely to produce results of great interest, therefore this work is not further investigated.

The recent work of Kubas on coordination of Si—H, H—H, and agostic C—H σ-bonds to the same [Mo(R<sub>2</sub>PC<sub>2</sub>H<sub>4</sub>PR<sub>2</sub>)(CO)] fragment is exciting since it is the first system by which comparison between the coordination features of different σ-bonds to the same metal centre can be made. An alternative approach to this kind of comparison is the study of system that can tautomerize between different σ-complexes. A complex of the general formula L<sub>n</sub>M(H<sub>2</sub>SiR<sub>3</sub>), where 'H<sub>2</sub>SiR<sub>3</sub>' stands for (SiR<sub>3</sub>)(η<sup>2</sup>-H<sub>2</sub>) or (H)(η<sup>2</sup>-HSiR<sub>3</sub>), is a good example of such a system.

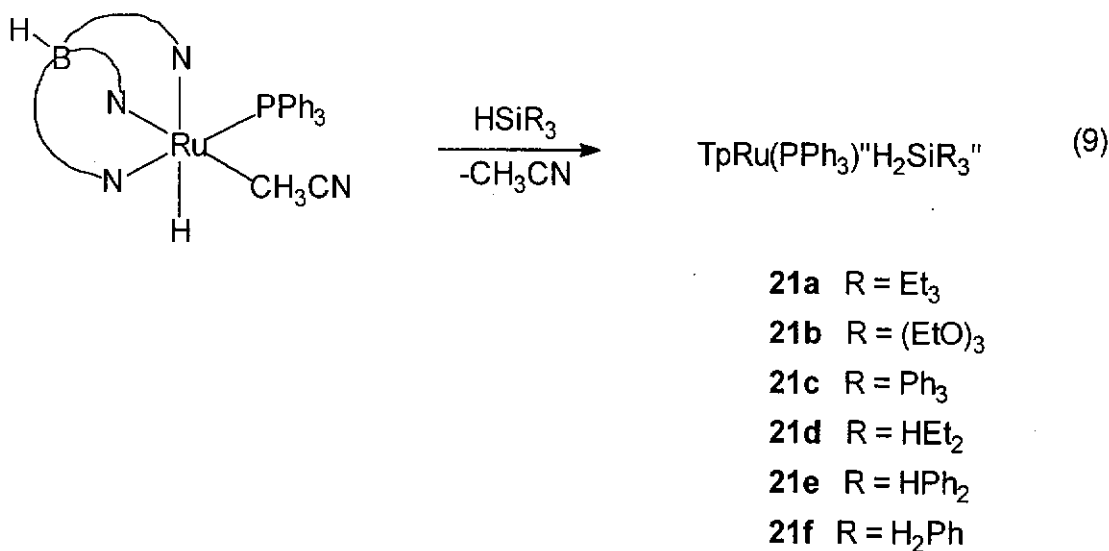
As has been mentioned above, Crabtree reported a  $L_nM(H)(\eta^2-HSiR_3)$  structure for the  $[(IrH_2(\eta^2-HSiEt_3)_2(PPh_3)_2)]SbF_6$  complex, which was an intermediate during the  $[(IrH_2S_2(PPh_3)_2)]SbF_6$  ( $S = THF, CH_3OH, H_2O, Me_2CO$ ) catalysed silane alcoholysis reaction.  $[(IrH_2(\eta^2-HSiEt_3)_2(PPh_3)_2)]SbF_6$  was stable only at low temperature and extremely sensitive to nucleophiles. Attempted isolation under a variety of conditions led to decomposition to the known  $[Ir_2(\mu-H)_3H_2(PPh_3)_4]SbF_6$ . On the other hand, reaction of  $OsHCl(CO)(P^iPr_3)_2$  with  $Et_3SiH$  was reported to give the  $\eta^2$ -dihydrogen silyl complex  $OsCl(SiEt_3)(H_2)(CO)(P^iPr_3)_2$  which was an intermediate in the hydrosilylation of phenylacetylene catalysed by  $OsHCl(CO)(P^iPr_3)_2$ .<sup>41</sup> Chaudret reported the preparation of a highly reactive  $\sigma$ -silane complex  $RuH_2(\eta^2-HSiPh_3)(H_2)(PCy_3)_2$  by substitution reaction of the bis-dihydrogen complex  $RuH_2(H_2)_2(PCy_3)_2$  with  $HSiPh_3$ .  $RuH_2(\eta^2-HSiPh_3)(H_2)(PCy_3)_2$  reacts instantaneously with  $H_2$  or  $N_2$  to give  $RuH_2(H_2)_2(PCy_3)_2$  or  $RuH_2(N_2)_2(PCy_3)_2$  together with free  $Ph_3SiH$ .<sup>64</sup> Recently, ab initio MO calculation at the MP2 and MP4 levels on the  $[OsCl(CO)(PH_3)'H_2SiH_3']$  model system predicts the existence of two stable octahedral species of very close energy: a dihydrogen complex  $[OsCl(SiH_3)(H_2)(CO)(PH_3)]$  and a  $\sigma$ -silane complex  $[OsClH(\eta^2-HSiH_3)(CO)(PH_3)]$ .<sup>42</sup>

We have recently reported the synthesis of  $TpRuH(H_2)(PPh_3)$  (**16**) by heating a THF solution of  $TpRuH(CH_3CN)(PPh_3)$  under 40 atm of  $H_2$ .  $^1H$ -NMR study revealed rapid fluxionality between the hydride and  $\eta^2-H_2$  ligands down to  $-110$  °C.<sup>29a</sup> In view of the analogy between  $\eta^2$ -dihydrogen complexes and  $\sigma$ -silane complexes and the delicate balance between the  $L_nM(H)(\eta^2-HSiR_3)$  and

$L_nM(SiR_3)(H_2)$  structures, it is interesting to study the reactions of  $TpRuH(CH_3CN)(PPh_3)$  with free silanes.

### 3.3.2 Synthesis of $TpRu(PPh_3)'H_2SiR_3'$ (**21**)

Reactions of  $TpRuH(CH_3CN)(PPh_3)$  (**13**) with free silanes  $HSiR_3$  in THF produce  $TpRu(PPh_3)'H_2SiR_3'$  ( $R_3 = Et_3$  (**21a**),  $(EtO)_3$  (**21b**),  $Ph_3$  (**21c**),  $HEt_2$  (**21d**),  $HPh_2$  (**21e**),  $H_2Ph$  (**21f**)) (eq. 9) for which NMR and IR data are collected in Table 7.



The complexes  $TpRu(PPh_3)'H_2SiR_3'$  are excellent model compounds for comparing the coordinating features of the two structures:  $L_nM(H)(\eta^2-HSiR_3)$  and  $L_nM(SiR_3)(H_2)$ . The facial coordination of Tp (*vide infra*) in  $TpRu(PPh_3)'H_2SiR_3'$  guarantee cis-dispositions of the hydride and  $\eta^2$ -silane ligands in one of the possible structures and of the silyl and  $\eta^2$ - $H_2$  ligands in the other.

**Table 7. NMR and IR Spectroscopic Data for TpRu(PPh<sub>3</sub>)'H<sub>2</sub>SiR<sub>3</sub>' 21a-f**

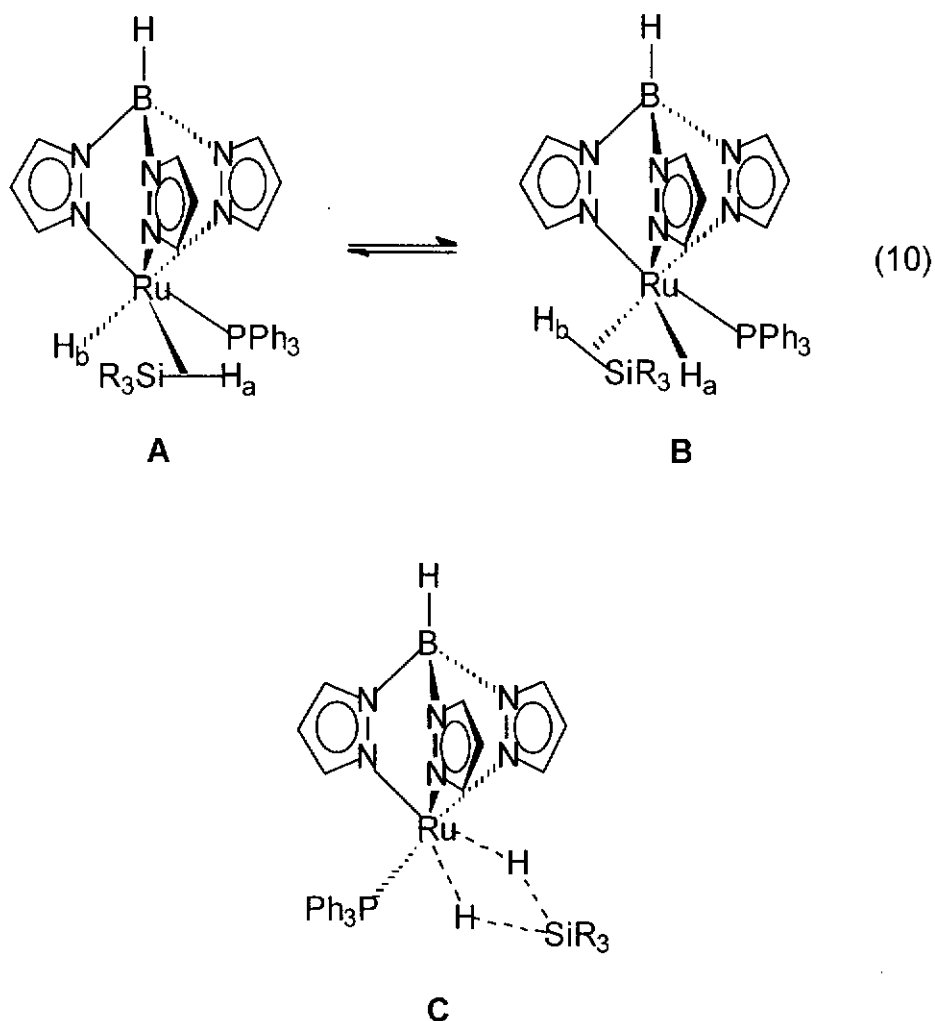
|   | $\delta(^1\text{H})$<br>(ppm) <sup>a</sup>  | $^1J(\text{SiH})^b$<br>(Hz) | $\delta(^{31}\text{P}\{^1\text{H}\})$<br>(ppm) <sup>a</sup> | $\delta(^{29}\text{Si}\{^1\text{H}\})$<br>(ppm) <sup>a</sup> | $\nu(\text{Ru-H})$<br>(KBr, cm <sup>-1</sup> ) | $\nu(\text{B-H})$<br>(KBr, cm <sup>-1</sup> ) |
|---|---|-----------------------------|---|--|--|---|
| (21a)<br>R <sub>3</sub> =Et <sub>3</sub>  | -11.62 (d, 2H, $^2J(\text{HP}) = 22.8$ Hz, Ru-H, $T_1 = 593$ ms), 0.79 (q, 6H, CH <sub>2</sub> CH <sub>3</sub> ), 1.14 (t, 9H, CH <sub>2</sub> CH <sub>3</sub> ), 9H of Tp, <sup>c</sup> 5.88 (t, 2H), 6.12 (t, 1H), 7.37 (d, 2H), 7.64 (d, 1H), 7.73 (d, 2H), 8.00 (d, 1H), 7.11 - 7.84 (m, 15H of PPh <sub>3</sub> )  | 23.3                        | 67.9 (s)  | 24.7   | 2044(w)  | 2461(br)                                      |
| (21b)<br>R <sub>3</sub> =EtO <sub>3</sub> | -11.41 (d, 2H, $^2J(\text{HP}) = 22.4$ Hz, Ru-H, $T_1 = 688$ ms), 1.06 (t, 9H, OCH <sub>2</sub> CH <sub>3</sub> ), 3.97 (q, 6H, OCH <sub>2</sub> CH <sub>3</sub> ), 9H of Tp, <sup>c</sup> 5.90 (t, 2H), 6.07 (t, 1H), 7.07 (d, 2H), 7.61 (d, 1H), 7.76 (d, 2H), 8.51 (d, 1H); 6.06 - 7.87 (m, 15H of PPh <sub>3</sub> )  | 52.8                        | 66.4 (s)  | -0.72  | 2057(w)  | 2472(br)                                      |
| (21c)<br>R <sub>3</sub> =Ph <sub>3</sub>  | -10.11 (d, 2H, $^2J(\text{HP}) = 23.2$ Hz, Ru-H, $T_1 = 436$ ms), 9H of Tp, <sup>c</sup> 5.53 (t, 1H), 5.98 (t, 2H), 7.45 (d, 1H), 7.51 (d, 2H), 7.67 (d, 1H), 7.82 (d, 2H); 5.89 - 7.69 (m, 30H of Ph)   | 28.4                        | 65.0 (s)  | 26.9   | 2040(w)  | 2468(br)                                      |
| (21d)<br>R <sub>3</sub> =HEt <sub>2</sub> | -10.93 (dd, 2H, $^2J(\text{HP}) = 22.0$ Hz, $^2J(\text{HH}) = 2.8$ Hz, Ru-H, $T_1 = 690$ ms), 1.08 (m, 6H, CH <sub>2</sub> CH <sub>3</sub> ), 1.21 (m, 4H, CH <sub>2</sub> CH <sub>3</sub> ), 4.60 (m, 1H, Si-H) 9H of Tp, <sup>c</sup> 5.92 (t, 2H), 6.14 (t, 1H), 7.08 (d, 2H), 7.68 (d, 1H), 7.78 (d, 2H), 7.87 (d, 1H); 7.22 - 7.56 (m, 15H of PPh <sub>3</sub> ) | 23.5                        | 68.5 (s)  | 16.9   | 2062(w)  | 2469(br)                                      |

|       |   |      |          |       |         |          |
|-------|---|------|----------|-------|---------|----------|
| (21e) | -9.71 (dd, 2H, $^2J(\text{HP}) = 20.8$ Hz, $^2J(\text{HH}) = 3.0$ Hz, Ru- <i>H</i> , $T_1$ = 545 ms), 5.72 (dt, 1H, $^2J(\text{HH}) = 3.0$ Hz, $J(\text{HH}) = 10.6$ Hz Si- <i>H</i> ) 9H of Tp, <sup>c</sup> 5.80 (t, 1H), 5.97 (t, 2H), 7.13 (d, 2H), 7.35 (d, 1H, H), 7.60 (d, 1H), 7.84 (d, 2H); 6.18 - 7.77 (m, 25H of Ph) | 23.5 | 65.6 (s) | 9.0   | 2082(w) | 2470(br) |
| (21f) | -10.32 (d, 2H, $^2J(\text{HP}) = 21.2$ Hz, Ru- <i>H</i> , $T_1 = 615$ ms), 5.22 (d, 2H, $J(\text{HP}) = 3.3$ Hz, Hz Si- <i>H</i> ) 9H of Tp, <sup>c</sup> 5.98 (t, 1H), 5.99 (t, 2H), 7.08 (d, 1H), 7.37 (d, 2H), 7.67 (d, 1H), 7.84 (d, 2H); 6.32 - 7.83 (m, 20H of Ph)  | 27.4 | 67.2 (s) | -17.2 | 2029(w) | 2471(br) |

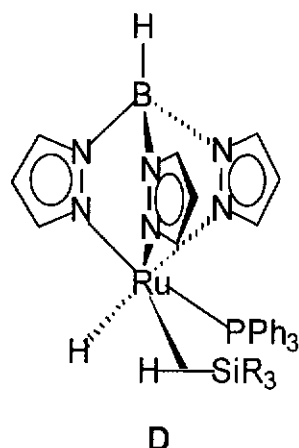
<sup>a</sup> in THF-*d*<sub>6</sub>. <sup>b</sup> obtaining from the <sup>29</sup>Si satellites of the hydride singal in <sup>1</sup>H NMR. <sup>c</sup> All coupling constants for pyrazolyl proton resonances were about 2 Hz.

### 3.3.3 Characterization and Structure of $\text{TpRu}(\text{PPh}_3)_2\text{H}_2\text{SiR}_3$

The  $^1\text{H}$  NMR spectrum of each of the complexes  $\text{TpRu}(\text{PPh}_3)_2\text{H}_2\text{SiR}_3$  (**21a-f**) shows a hydride signal, which integrates to two hydrogens, in the upfield region; it is coupled to the triphenylphosphine, with a coupling constant falling in the range of 20.8 - 23.2 Hz, which is typical for a cis-disposed phosphine ligand. For the secondary silane complexes **21d** and **21e**, the hydride signals show additional coupling to the normal Si-H hydrogens. It is important to note that all the hydride signals of **21a-f** are flanked by  $^{29}\text{Si}$  satellites. All the  $^1J(\text{Si-H})$  values, except that of **21b**, lie at the lower end of the range of values (20 - 70 Hz) found for the known  $\eta^2$ -silane complexes in which the silicon bears one or more substituents other than the hydrogen.<sup>40</sup> The Si-H coupling constants of our complexes, although low, unequivocally indicate the presence of the  $\eta^2$ -silane ligands. Therefore it seems adequate to assign the  $\eta^2$ -silane hydride structure  $\text{TpRuH}(\eta^2\text{-HSiR}_3)(\text{PPh}_3)_2$ , rather than the  $\eta^2\text{-H}_2$  silyl structure  $\text{TpRu}(\text{SiR}_3)(\eta^2\text{-H}_2)(\text{PPh}_3)_2$  to  $\text{TpRu}(\text{PPh}_3)_2\text{H}_2\text{SiR}_3$ . The rejection of the  $\eta^2\text{-H}_2$  structure is further supported by the relaxation time measurements which show that the room temperature  $T_1$  values of **21a-f** (436 - 690 ms) are well outside the range of  $T_1$  values for non-classical  $\eta^2$ -dihydrogen complexes.<sup>65</sup> The fact that only one hydride signal was observed even down to -110 °C can be explained in terms of rapid fluxionality between  $\text{H}_a$  and  $\text{H}_b$ , (eq. 10) or more appropriately by having  $\text{TpRu}(\text{PPh}_3)_2\text{H}_2\text{SiR}_3$  to adopt the structure **C**. This bonding mode of silane is reminiscent of the  $\eta^2\text{-BH}_4$  ligand.<sup>66</sup>



The existence of a rapid equilibrium between structure **A** and **B**, or the adoption of structure **C** for  $\text{TpRu}(\text{PPh}_3)\text{H}_2\text{SiR}_3$  is in accord with the observation of two groups of resonances (3 peaks in each group) for the pyrazole protons of the Tp ligand in the range 5.80 - 8.00 ppm in the  $^1\text{H}$  NMR spectrum. Each peak in one of the groups integrates to 2H, while every one in the other group corresponds to 1H. This 6 peak pattern for Tp protons is consistent with two of the pyrazole rings being trans to two identical ligands. Should all three pyrazole rings of the Tp ligand in  $\text{TpRu}(\text{PPh}_3)\text{H}_2\text{SiR}_3$  be trans to three different ligands as in the non-dynamic structure **D**, a 9 peak pattern would have been observed for the Tp protons.



The  $^{29}\text{Si}\{^1\text{H}\}$  NMR spectra of **21a-f**, which show singlets and are therefore devoid of silicon-phosphorous couplings, are also supportive of the presence of  $\eta^2$ -silane ligands in  $\text{TpRu}(\text{PPh}_3)(\text{H}_2\text{SiR}_3)$ . It is generally true that metal-silyl complexes containing phosphine ligands show silicon-phosphorous coupling,<sup>67</sup> which, in phosphine-containing  $\eta^2$ -silane complexes, are rarely observable.<sup>40, 43</sup>

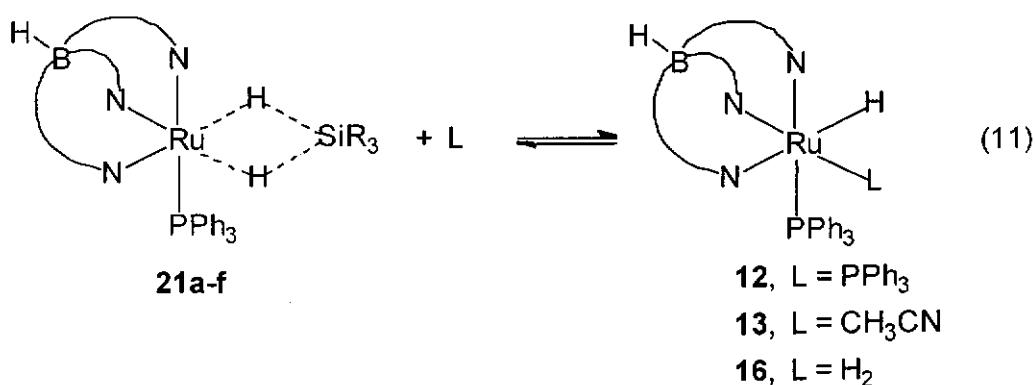
Finally, it is worth commenting on the denticity of the Tp ligands in **21a-f**. Although it is well known that the tendency for hydrotris(pyrazolyl)borate to adopt a facial tridentate coordination mode is very strong, and reduced denticity is usually only observed in cases where it is disfavoured by the electronic nature of the metal, e.g.,  $d^8\text{-ML}_4$  square-planar geometry,<sup>68</sup> bidentate coordinations of hydrotris(pyrazolyl)borate ligand to  $d^6$  Ru(II) and Os(II) centres has recently been reported.<sup>69</sup> The  $\kappa^2$ -Tp Ru(II) and Os(II) complexes were prepared by displacement of a phosphine and a halo ligands from the precursor complex with hydrotris(pyrazolyl)borate at room temperature. Thermolysis of these  $\kappa^2$ -Tp complexes via loss of a phosphine ligand gives the conventional tridentate Tp complexes. A common spectroscopic feature of the  $\kappa^2$ -Tp Ru(II) and Os(II)



complexes is that the  $\nu(\text{B-H})$  are shifted to lower frequencies ( $\sim 2440 \text{ cm}^{-1}$ ) compared to those of the  $\kappa^3\text{-Tp}$  complexes which are usually above  $2460 \text{ cm}^{-1}$ . Perusal of Table 7 reveals that the  $\nu(\text{B-H})$  of **21a** - **21f** are all above  $2460 \text{ cm}^{-1}$ , these complexes were prepared by thermo displacement of  $\text{CH}_3\text{CN}$  from  $\text{TpRuH}(\text{CH}_3\text{CN})(\text{PPh}_3)$  (**13**) which already contained a tridentate hydrotris(pyrazolyl)borate ligand, therefore it is very unlikely that the denticity of hydrotris(pyrazolyl)borate would decrease from 3 to 2 during the reactions, these facts are taken together, it is probably true that tridentate coordination Tp in **21a** - **21f** is maintained.

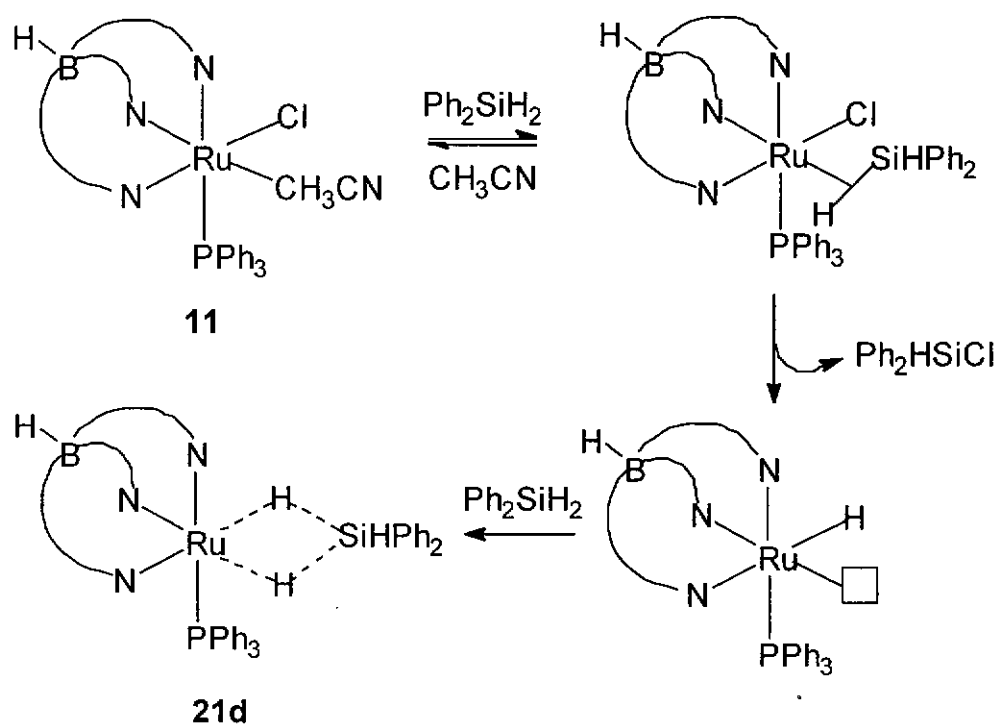
### 3.3.4 Reactivity of $\text{TpRu}(\text{PPh}_3)\text{H}_2\text{SiR}_3$

The  $\eta^2$ -silane complexes **21a-f** react reversibly with triphenylphosphine, acetonitrile, and pressurized  $\text{H}_2$ , to give  $\text{TpRuH}(\text{PPh}_3)_2$  (**12**),  $\text{TpRuH}(\text{CH}_3\text{CN})(\text{PPh}_3)$  (**13**), and  $\text{TpRuH}(\text{H}_2)(\text{PPh}_3)$  (**16**), respectively. (eq. 11) While the dihydrogen complex **16** can be used in place of **13** for preparation of the  $\eta^2$ -silane complexes **21a-f**, it was found that reaction of **12** with excess free silanes only led to partial formation of **21a-f**, probably due to the stronger coordination of the phosphine ligand.



### 3.3.5 Reaction of $\text{TpRuCl}(\text{CH}_3\text{CN})(\text{PPh}_3)$ with diphenylsilane.

Surprisingly, it was found that reaction of  $\text{TpRuCl}(\text{CH}_3\text{CN})(\text{PPh}_3)$  (**11**) with the diphenylsilane did not give the chloro  $\eta^2$ -silane complexes  $\text{TpRuCl}(\eta^2\text{-H}_2\text{SiPh}_2)(\text{PPh}_3)$ , but rather **21d** was formed. The formation of **21d** from **11** can best be explained by the mechanism depicted in Scheme 3. The main feature of the scheme is the SiH/RuCl redistribution process that leads to the severance of the Ru—Cl bond and the formation of the Ru—H bond. It has been suggested that the Si—Cl bond energy is high enough to allow SiH/IrCl redistribution which causes the iridium complex  $\text{IrCl}(\text{CO})(\text{PPh}_3)_2$  to react with triorganosilanes to give the hydrido complex and the chlorotriorganosilanes.<sup>70</sup> Yamamoto has recently reported facile transfer of a chloro ligand bonded to the Rh centre onto the Si atom bonded to the same metal centre, even in the rigid octahedral coordination.<sup>71</sup>



Scheme 3

## Chapter Four

### Conclusion

Like Cp and Tp, the macrocyclic facially chelating ligand  $^R\text{Cn}$  (where  $^H\text{Cn} = 1,4,7\text{-triazacyclononane}$ ,  $^{\text{Me}}\text{Cn} = 1,4,7\text{-trimethyl-}1,4,7\text{-triazacyclononane}$ ), are shown to be a good ligands for the preparation of ruthenium  $\eta^2$ -dihydrogen complexes.

Some ruthenium hydrido complexes containing  $^R\text{Cn}$  were prepared in this work, these hydrido complexes were prepared by reacting the hydrido precursors ( $\text{RuHCl}(\text{PPh}_3)_3$  and  $\text{RuHCl}(\text{CO})(\text{PPh}_3)_3$ ) with free  $^R\text{Cn}$ . Protonation of these hydrido complexes produced the first dihydrogen complexes supported by triazacyclononane ligands. These complexes are also new members of the still very small family of dicationic dihydrogen complexes. Triazacyclononane ligands seem to have similar properties as the hydrotris(pyrazolyl)borates in stabilizing dihydrogen ligands.

The acidity of Tp and  $^R\text{Cn}$  dihydrogen complexes have been measured and it was found that the dicationic  $^R\text{Cn}$  dihydrogen complexes are more, and in some cases significantly more acidic than their hydrotris(pyrazolyl)borato and cyclopentadienyl analogues, which are monocationic. Water can deprotonate  $^R\text{Cn}$  and Tp dihydrogen complexes with pseudo aqueous  $\text{p}K_a$  values significantly larger than that of  $\text{H}_3\text{O}^+$ , probably due to strong solvation of  $\text{H}^+$  by  $\text{H}_2\text{O}$ .

The second part of this work concerns the chemistry of  $\eta^2$ -silane complexes. The reactions between free silanes and the  $\eta^2$ -dihydrogen complexes (17, 18 and 20)

bearing hydrotris(1-pyrazolyl)borato ligand were first attempted, but the expected  $\eta^2$ -silane complex  $[\text{TpRu}(\eta^2\text{-HSiR}_3)(\text{PPh}_3)_2]\text{BF}_4$  was not obtained, probably due to nucleophilic attack of the  $\eta^2$ -silane ligand by the counterion  $\text{BF}_4^-$  to give the metal hydride.

The  $\eta^2$ -silane complexes  $\text{TpRu}(\text{PPh}_3)_2(\text{H}_2\text{SiR}_3)$  (**21a-f**) have been synthesized via reaction of  $\text{TpRuH}(\text{CH}_3\text{CN})(\text{PPh}_3)$  (**13**) with free silanes. The NMR spectroscopic data indicate that the “ $\text{H}_2\text{SiR}_3$ ” moiety in **21a-f** is  $(\text{H})(\eta^2\text{-HSiR}_3)$  rather than  $(\text{SiR}_3)(\eta^2\text{-H}_2)$ . The chemical equivalence of the two hydrogen atoms is attributed to rapid fluxionality between the two, i.e.,  $\text{TpRu}(\text{PPh}_3)_2(\text{H}_a)(\eta^2\text{-H}_b\text{SiR}_3) \leftrightarrow \text{TpRu}(\text{PPh}_3)_2(\text{H}_b)(\eta^2\text{-H}_a\text{SiR}_3)$  or better to the adoption of a  $\eta^2\text{-BH}_4$ -type bonding mode by the “ $\text{H}_2\text{SiR}_3$ ” moiety to the metal centre. **21a-f** react reversibly with  $\text{PPh}_3$ ,  $\text{CH}_3\text{CN}$ , and pressurized  $\text{H}_2$  to give  $\text{TpRuH}(\text{PPh}_3)_2$ ,  $\text{TpRuH}(\text{PPh}_3)(\text{CH}_3\text{CN})$ , and  $\text{TpRuH}(\text{H}_2)(\text{PPh}_3)$ , respectively. Reaction of the chloro complex  $\text{TpRuCl}(\text{PPh}_3)(\text{CH}_3\text{CN})$  with  $\text{H}_2\text{SiPh}_2$  did not give the chloro  $\eta^2$ -silane complexes  $\text{TpRuCl}(\text{PPh}_3)(\eta^2\text{-H}_2\text{SiPh}_2)$ , but rather **21d** was formed. The formation of **21d** is best explained by a reaction sequence which include a SiH/RuCl redistribution step.

## Reference

1. Noth, R.; Hartwimmer, R. *Chem. Ber.* **1960**, *93*, 2238.
2. Crabtree, R. H. *Angew. Chem. Int. Ed. Eng.* **1993**, *32*, 789.
3. (a) Kubas, G. J. *Comments Inorg. Chem.* **1988**, *7*, 17. (b) Kubas, G. J. *Acc. Chem. Res.* **1988**, *21*, 120. (c) Crabtree, R. H. *Acc. Chem. Res.* **1990**, *23*, 95. (d) Banister, J. A.; Lee, P. D.; Poliakoff, M. *Organometallics* **1995**, *14*, 3876.
4. (a) Graham, W. A. G. *J. Organomet. Chem.* **1986**, *300*, 81. (b) Schubert, U. *Adv. Organomet. Chem.* **1990**, *30*, 151.
5. (a) Shilov, A. E. *Activation of Saturated Hydrocarbons by Transition Metal complexes*, D. Reidel Publishing: Dordcht, **1984**. (b) Crabtree, R. H. *Chem. Rev.* **1985**, *85*, 245. (c) Jones, W. D.; Feher, F. J. *Acc. Chem. Res.* **1989**, *22*, 91.
6. Kubas, G. J.; Ryan, R. R.; Swanson, B. I.; Wasserman, H. J. *J. Am. Chem. Soc.* **1984**, *106*, 541.
7. Esteruelas, M. A.; Oro, L. A.; Valreo, C. *Organometallics* **1992**, *11*, 3362.
8. Marinelli, G.; Rachidi, I. E.-I.; Streib, W. E.; Eisenstein, O.; Caulton, K. G. *J. Am. Chem. Soc.* **1989**, *111*, 2346.
9. Harman, W. D.; Halpern, H. J. *J. Am. Chem. Soc.* **1990**, *10*, 462.
10. Morton, D.; Cole-Hamilton, D. J. *J. Chem. Soc., Chem. Commun.* **1988**, 1154.
11. Bianchini, C.; Peruzzini, M.; Zanobini, F.; Frediani, P.; Albinat, A. *J. Am. Chem. Soc.* **1991**, *113*, 5453.
12. Albeniz, A. C.; D. Heinekey, M.; Crabtree, R. H. *Inorg. Chem.* **1991**, *30*, 3632.
13. Heinekey, D. M.; Oldman Jr, W. J. *Chem. Rev.* **1993**, *93*, 913.

14. Volbeda, A.; Charon, M. H.; Piras, C.; Hatchikan, E.C.; Frey, M.; Fontecilla-Camps, J. C. *Nature* **1995**, *373*, 580.
15. (a) Chinn, M. S.; Heinekey, D. M. *J. Am. Chem. Soc.* **1990**, *112*, 5166. (b) Chinn, M. S.; Heinekey, D. M. *J. Am. Chem. Soc.* **1987**, *109*, 5865.
16. (a) Jia, G.; Lough, A. J.; Morris, R. H. *Organometallics* **1992**, *11*, 161. (b) Jia, G.; Morris, R. H. *J. Am. Chem. Soc.* **1991**, *113*, 875. (c) Jia, G.; Morris, R. H.; Schweitzer, C. T. *Inorg. Chem.* **1991**, *31*, 593. (d) Jia, G.; Morris, R. H. *Inorg. Chem.* **1990**, *29*, 581.
17. Cappellani, E. P.; Drouin, S. D.; Jia, G.; Maltby, P. A. Morris, R. H.; Schweitzer, C. T. *J. Am. Chem. Soc.* **1994**, *116*, 3375.
18. Rocchini, E.; Mezzetti, A.; Rügger, H.; Burckhardt, U.; Gramlich, V.; Del Zotto, A.; Martinuzzi, P.; Rigo, P. *Inorg. Chem.* **1997**, *36*, 711.
19. (a) Maltby, P. A.; Schlaf, M.; Steinbeck, M.; Lough, A. J.; Morris, R. H.; Klooster, W. T.; Koetzle, T. F.; Srivastava, R. C. *J. Am. Chem. Soc.* **1996**, *118*, 5396. (b) Chin, B.; Lough, A. J.; Morris, R. H.; Schweitzer, C. T.; D'Agostino, C. *Inorg. Chem.* **1994**, *33*, 6278.
20. Schlaf, M.; Lough, A. J.; Maltby, P. A.; Morris, R. H. *Organometallics* **1996**, *15*, 2270.
21. See for examples: (a) Lough, A. J.; Park, S.; Ramchandran, R.; Morris, R. H. *J. Am. Chem. Soc.* **1994**, *116*, 8356. (b) Schlaf, M.; Lough, A. J.; Morris, R. H. *Organometallics* **1993**, *12*, 3808. (c) Crabtree, R. H.; Lavin, M. *J. Chem. Soc., Chem. Commun.* **1985**, 794. (d) Crabtree, R. H.; Lavin, M.; Bonneviot, L. *J. Am. Chem. Soc.* **1986**, *108*, 4032. (e) Baker, M. V.; Field, L. D.; Young, D. J. *J. Chem. Soc., Chem. Commun.* **1988**, 546. (f) Van Der Sluys, L. S.; Miller, M. M.; Kubas,

- G. J.; Caulton, K. G. *J. Am. Chem. Soc.* **1991**, *113*, 2513. (g) Bianchini, C.; Perez, P. J.; Peruzzini, M.; Zanobini, F.; Vacca, A. *Inorg. Chem.* **1991**, *30*, 279. (h) Sellman, D.; Käppler, J.; Moll, M. *J. Am. Chem. Soc.* **1993**, *115*, 1830. (i) Mudalige, D. C.; Rettig, S. J.; James, B. R.; Cullen, W. R. *J. Chem. Soc., Chem. Commun.* **1993**, 830. (j) Bianchini, C.; Linn, K.; Masi, D.; Peruzzini, M.; Polo, A.; Vacca, A.; Zanobini, F. *Inorg. Chem.* **1993**, *32*, 2366. (k) Heinekey, D.M.; Luther, T. A. *Inorg. Chem.* **1996**, *35*, 4396. (l) Heinekey, D. M.; Voges, M. H.; Barnhart, D. M. *J. Am. Chem. Soc.* **1996**, *118*, 10792.
22. (a) Harman, W. D.; Taube, H. *J. Am. Chem. Soc.* **1990**, *112*, 2261. (b) Li, Z. W.; Taube, H. *J. Am. Chem. Soc.* **1991**, *113*, 8946.
23. Smith, K.-T.; Tilset, M.; Kuhlmann, R.; Caulton, K. G. *J. Am. Chem. Soc.* **1995**, *117*, 9473.
24. Flood's notation is adopted with slight modification.  $^{\text{H}}\text{Cn} = 1,4,7$ -triazacyclononane,  $^{\text{Me}}\text{Cn} = 1,4,7$ -trimethyl-1,4,7-triazacyclononane.
25. (a) Wieghardt, K.; Chaudhuri, P.; Nuber, B.; Weiss, J.; *Inorg. Chem.* **1982**, *21*, 3086. (b) Chaudhuri, P.; Wieghardt, K. *Prog. Inorg. Chem.* **1987**, *35*, 329.
26. For recent work on  $^{\text{R}}\text{Cn}$  complexes, see for examples: (a) Yang, S. M.; Chen, M. C. W.; Cheung, K. K.; Che, C. M.; Peng, S. M. *Organometallics* **1997**, *16*, 2819. (b) Wang, L.; Sowa, J. R., Jr.; Wang, C.; Lu, R. S.; Gassman, P. G.; Flood, T. C. *Organometallics* **1996**, *15*, 4240. (c) Wang, L.; Wang, C.; Bau, R.; Flood, T. C. *Organometallics* **1996**, *15*, 491. (d) Yang, S. M.; Cheng, W. C.; Peng, S. M.; Cheung, K. K.; Che, C. M. *J. Chem. Soc., Dalton Trans.* **1995**, 2955. (e) Yang, S. M.; Cheng, W. C.; Cheung, K. K.; Che, C. M.; Peng, S. M. *J. Chem. Soc., Dalton Trans.* **1995**, 227. (f) Wang, C.; Ziler, J. W.; Flood, T. C. *J. Am. Chem. Soc.* **1995**,

- 117, 1647. (g) Cheng, W. C.; Yu, W. Y.; Cheung, K. K.; Che, C. M. *J. Chem. Soc., Dalton Trans.* **1994**, 57. (h) Cheng, W. C.; Yu, W. Y.; Cheung, K. K.; Che, C. M. *J. Chem. Soc., Chem. Commun.* **1994**, 1063. (i) Wang, L.; Lu, R. S.; Bau, R.; Flood, T. C. *J. Am. Chem. Soc.* **1993**, *115*, 6999. (j) Wang, C.; Flood, T. C. *J. Am. Chem. Soc.* **1992**, *114*, 3169. (k) Sun, N. Y.; Simpson, S. J. *J. Organomet. Chem.* **1992**, *434*, 341.
27. Crabtree, R. H. *The Organometallic Chemistry of the Transition Metals*, 2nd Ed, John Wiley & Sons: New York, 1994.
28. Reviews on Tp complexes: (a) Trofimenko, S. *Chem. Rev.* **1993**, *93*, 943. (b) Trofimenko, S. *Prog. Inorg. Chem.* **1986**, *34*, 115. (c) Trofimenko, S. *Chem. Rev.* **1972**, *72*, 497. (d) Trofimenko, S. *Acc. Chem. Res.* **1971**, *4*, 17.
29. For recent work on tris(pyrazolyl)borato dihydrogen complexes, see for examples: (a) Chen, Y. Z.; Chan, W. C.; Lau, C. P.; Chu, H. S.; Lee, H. L.; Jia, G. *Organometallics* **1997**, *16*, 1241. (b) Chan, W. C.; Lau, C. P.; Chen, Y. Z.; Fang, Y. Q.; Ng, S. M.; Jia, G. *Organometallics* **1997**, *16*, 34. (c) Bohanna, C.; Esteruelas, M. A.; Gómez, A. V.; López, A. M.; Martínez, M.-P. *Organometallics* **1997**, *16*, 4464. (d) Eckert, J.; Albinati, A.; Bucher, U. E.; Venanzi, L. M. *Inorg. Chem.* **1996**, *35*, 1292. (e) Vicente, C.; Shul'pin, G. G.; Moreno, B.; Sabo-Etienne, S.; Chaudret, B. *J. Mol. Catal. A: Chem.* **1995**, *98*, L5. (f) Moreno, B.; Sabo-Etienne, S.; Chaudret, B.; Rodriguez, A.; Jalon, F.; Trofimenko, S. *J. Am. Chem. Soc.* **1995**, *117*, 7441. (g) Moreno, B.; Sabo-Etienne, S.; Chaudret, B. *J. Am. Chem. Soc.* **1994**, *116*, 2635. (h) Heinekey, D. M.; Oldham, W. J., Jr. *J. Am. Chem. Soc.* **1994**, *116*, 3137. (i) Halcrow, M. A.; Chaudret, B.; Trofimenko, S. *J. Chem. Soc.*,



- Chem. Commun.* **1993**, 465. (j) Bucher, U. E.; Lengweiler, T.; Nanz, D.; von Philipsborn, W.; Vernanzi, L. M. *Angew. Chem. Int. Ed. Engl.* **1990**, *29*, 548.
30. (a) de los Ríos, I.; Tenorio, M. J.; Padilla, J.; Puerta, M. C.; Valerga, P. *Organometallics* **1996**, *15*, 4565. (b) Lemke, F. R.; Brammer, L. *Organometallics* **1995**, *14*, 3980. (c) Conroy-Lewis, F. M.; Simpson, S. J. *J. Chem. Soc., Chem. Commun.* **1986**, 506. (d) Conroy-Lewis, F. M.; Simpson, S. J. *J. Chem. Soc., Chem. Commun.* **1987**, 1675. (e) Wilczewski, T. *J. Organomet. Chem.* **1989**, *361*, 219. (f) Chinn, M. S.; Heinekey, D. M.; Payne, N. G.; Sofield, C. D. *Organometallics* **1989**, *8*, 1824. (g) Klooster, W. T.; Koetzle, T. F.; Jia, G.; Fong, T. P.; Morris, R. H.; Albinati, A. *J. Am. Chem. Soc.* **1994**, *116*, 7677.
31. (a) Brookhart, M.; Grant, B. E. *J Am Chem Soc.* **1993**, *115*, 2151. (b) Takahashi, T.; Hasegawa, M.; Suznki, N.; Sabari, M.; Rousset, C. J.; Fanwick, P. E.; Negishi, E. *J Am Chem. Soc.* **1991**, *113*, 8564
32. Lxo, X-L.; Crabtree, R. H. *J. Am. Chem. Soc.* **1989**, *111*, 2527
33. (a) Aitken, C.T.; Harrod, J. F.; Samuel, E. *J. Am. Chem. Soc.* **1986**, *108*, 4059. (b) Harrod, J. K.; Yun, S. S. *Organometallics* **1987**, *6*, 1381.
34. Hoyano, J. K.; Graham, W. A. G. *J. Am. Chem. Soc.* **1969**, *91*, 45
35. Graham, W. A. G; Bennett, M. *J. Chem Eng. New.* **1970**, *48* (24) 75.
36. a) Schubert, U.; Ackermann, K.; Worle, B. *J. Am. Chem. Soc.* **1982**, *104*, 7378. b) Schubert, U.; Bahr, K.; Muller, J. *J. Organomet. Chem.* **1987**, *327*, 357.
37. Rabaa, H.; Saillard, J-Y.; Schubert, U. *J. Organomet. Chem.* **1987**, *330*, 397
38. Scharrer, E.; Chang, S. Brookhart, M. *Organometallics* **1995**, *14*, 5686.
39. Luo, X-L.; Kubas, G. J.; Burns, C. J.; Bryan, J. C.; Unkefer, C. J. *J. Am. Chem. Soc.* **1995**, *117*, 1159.

40. Luo, X-L.; Kubas, G. J.; Burns, C. J.; Bryan, J. C.; Unkefer, C. J. *Organometallics* **1991**, *10*, 462.
41. Esteruelas, M. A.; Oro, L. A.; Valreo, C., *Organometallics* **1991**, *10*, 462.
42. Maseras, F.; Lledos, A. *Organometallics* **1996**, *15*, 1218.
43. Spaltenstein, E.; Palma, P.; Kreutzer, K. A.; Willoughby, C. A.; Davis, W. M.; Buchwald, S. L. *J. Am. Chem. Soc.* **1994**, *116*, 10308.
44. Procopio, L. J.; Carroll, P. J.; Berry, D. H. *J. Am. Chem. Soc.* **1994**, *116*, 177.
45. Jessop, P. G.; Morris, R. H. *Coord. Chem. Rev.* **1992**, *121*, 155.
46. Kono, H. *J. Organomet. Chem.* **1977**, *132*, 53.
47. Wieghardt, K.; Chaudhuri, P.; Nuber, B.; Weiss, J. *Inorg. Chem.* **1989**, *28*, 459.
48. Ahmad, N.; Levison, J. J.; Robinson, S. D.; Uttley, M. F. *Inorg. Synth.* **1974**, *15*, 48.
49. (a) Smith, K. T.; Rømming, C.; Tilset, M. *J. Am. Chem. Soc.* **1993**, *115*, 8681. (b) Lemke, F. R.; Brammer, L. *Organometallics* **1995**, *14*, 3980. (c) Brammer, L.; Klooster, W. T.; Lemke, F. R. *Organometallics* **1996**, *15*, 1721.
50. Desrosiers, P. J.; Cai, L.; Lin, Z.; Richards, R.; Halpern, J. *J. Am. Chem. Soc.* **1991**, *113*, 4173.
51. Forde, C. E.; Landau, S. E.; Morris, R. H. *J. Chem. Soc., Dalton Trans.* **1997**, 1663.
52. Luther, T-A.; Heinekey, D.M. *Inorg. Chem.* **1998**, *37*, 127.
53. Perdoncin, G.; Scorrano, G. *J. Am. Chem. Soc.* **1977**, *99*, 6983.
54. Hush, N. S. *J. Am. Chem. Soc.* **1997**, *119*, 1717.
55. Jia, G.; Lee, H. M.; Williams, I. D.; Lau, C. P.; Chen, Y. Z. *Organometallics* **1997**, *16*, 3941.
56. Moore, E. J.; Sullivan, J. M.; Norton, J. R. *J. Am. Chem. Soc.* **1986**, *108*, 2257.

57. Kristjánisdóttir, S. S.; Moody, A. E.; Weberg, R. T.; Norton, J. R. *Organometallics* **1988**, *7*, 1983.
58. Jordan, R. F.; Norton, J. R. *J. Am. Chem. Soc.* **1982**, *104*, 1255.
59. Parker, V. D.; Handoo, K. L.; Roness, F.; Tilset, M. *J. Am. Chem. Soc.* **1991**, *113*, 7493.
60. Kristjánisdóttir, S. S.; Norton, J. R. In *Transition Metal Hydrides*; Dedieu, A., Ed.; VCH: Weinheim, FRG, 1992.
61. (a) Angelici, R. J. *Acc. Chem. Res.* **1995**, *28*, 51. (b) Pearson, R. G. *Chem. Rev.* **1985**, *85*, 41.
62. Ritchie, C. D. *Physical Organic Chemistry, The Fundamental Concept*, Marcel Dekker, Inc.: New York 1990, p.238.
63. Lemke, F. R. *J. Am. Chem. Soc.* **1994**, *116*, 11183.
64. Sabo-etienne, S.; Hernandez, M.; Chung, G.; Chaudret, B. *New. J. Chem.* **1994**, *18*, 175.
65. Crabtree, R. H.; Lavin, M.; Bonnneviot, L. *J. Am. Chem. Soc.* **1986**, *108*, 4032.
66. (a) Oishi, Y.; Albright, T. A.; *Polyhedron*, **1995**, *14*, 2603. (b) Hartwig, F.; De Gala, S. R.; *J. Am. Chem. Soc.* **1994**, *116*, 3661.
67. (a) Johnson, T. J.; Coan, P. S.; Caulton, K. G. *Inorg. Chem.* **1993**, *32*, 4594. (b) Sun, J.; Lu, R. S.; Bau, R.; Yang, G. K. *Organometallics*. **1994**, *13*, 1317.
68. (a) Albinati, A.; Bovens, M.; Ruegger, H.; Venanzi, L. M. *Inorg. Chem.* **1997**, *36*, 5991. (b) Akita, M.; Ohta, K.; Takahashi, Y.; Hikichi, S.; Moro-oka, Y. *Organometallics* **1997**, *16*, 4121.

69. (a) Burns, I. D.; Hill, A. F.; White, A. J. P.; Williams, D. J.; Wilton-Ely, J. D. E. T. *Organometallics* **1998**, *17*, 1552. (b) Bohanna, C.; Esteruelas, M. A.; Gomez, A. V.; Lopez, A. M.; Martinez, M-P. *Organometallics* **1997**, *16*, 4464.
70. (a) Chalk, A. J. *J. Chem. Soc., Chem. Commun.* **1969**, 1207. (b) Chalk, A. J.; Harrod, J. F. *J. Am. Chem. Soc.* **1965**, *87*, 16.
71. Osakada, K.; Sarai, S.; Koizumi, T.; Yamamoto, T. *Organometallics* **1997**, *16*, 3980.

# Appendix

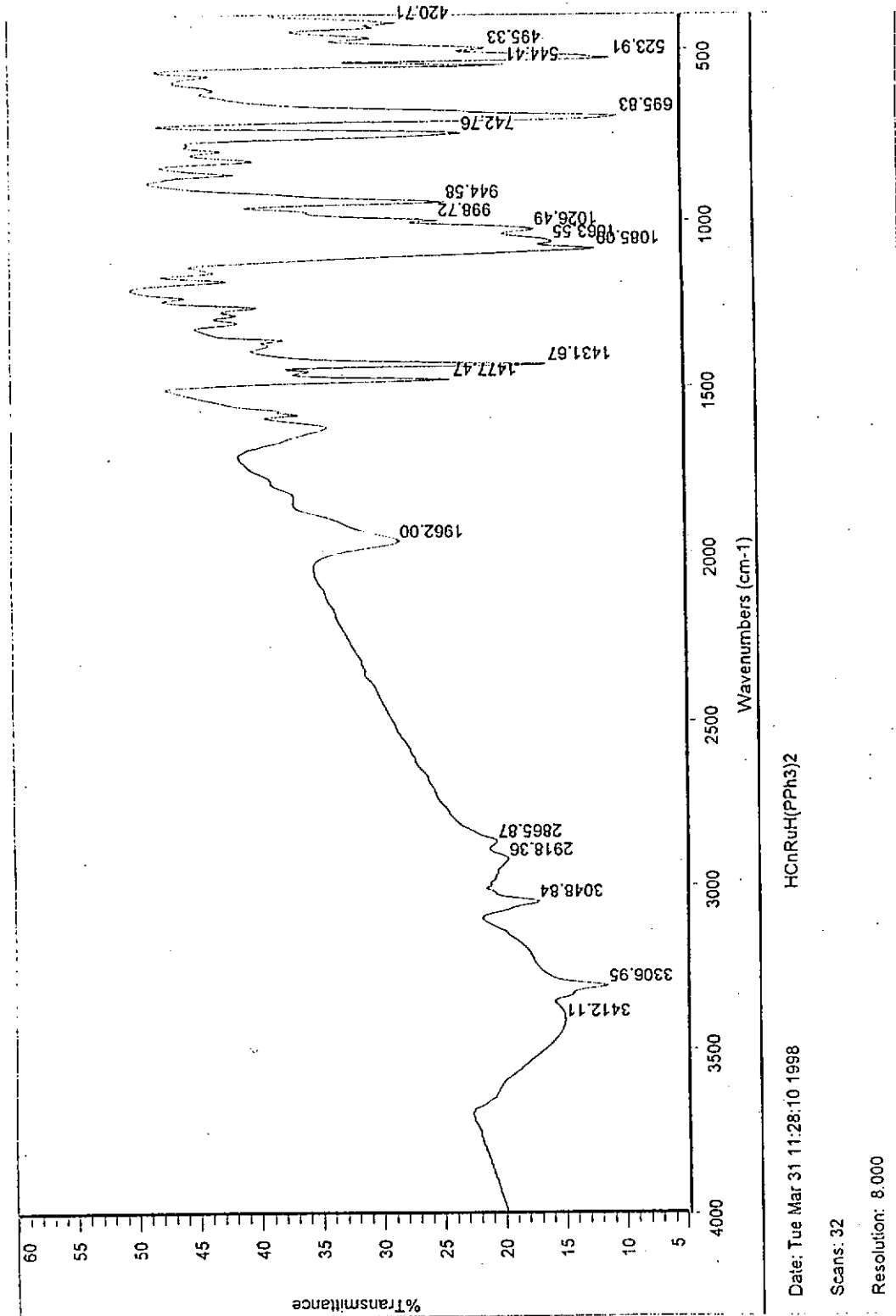
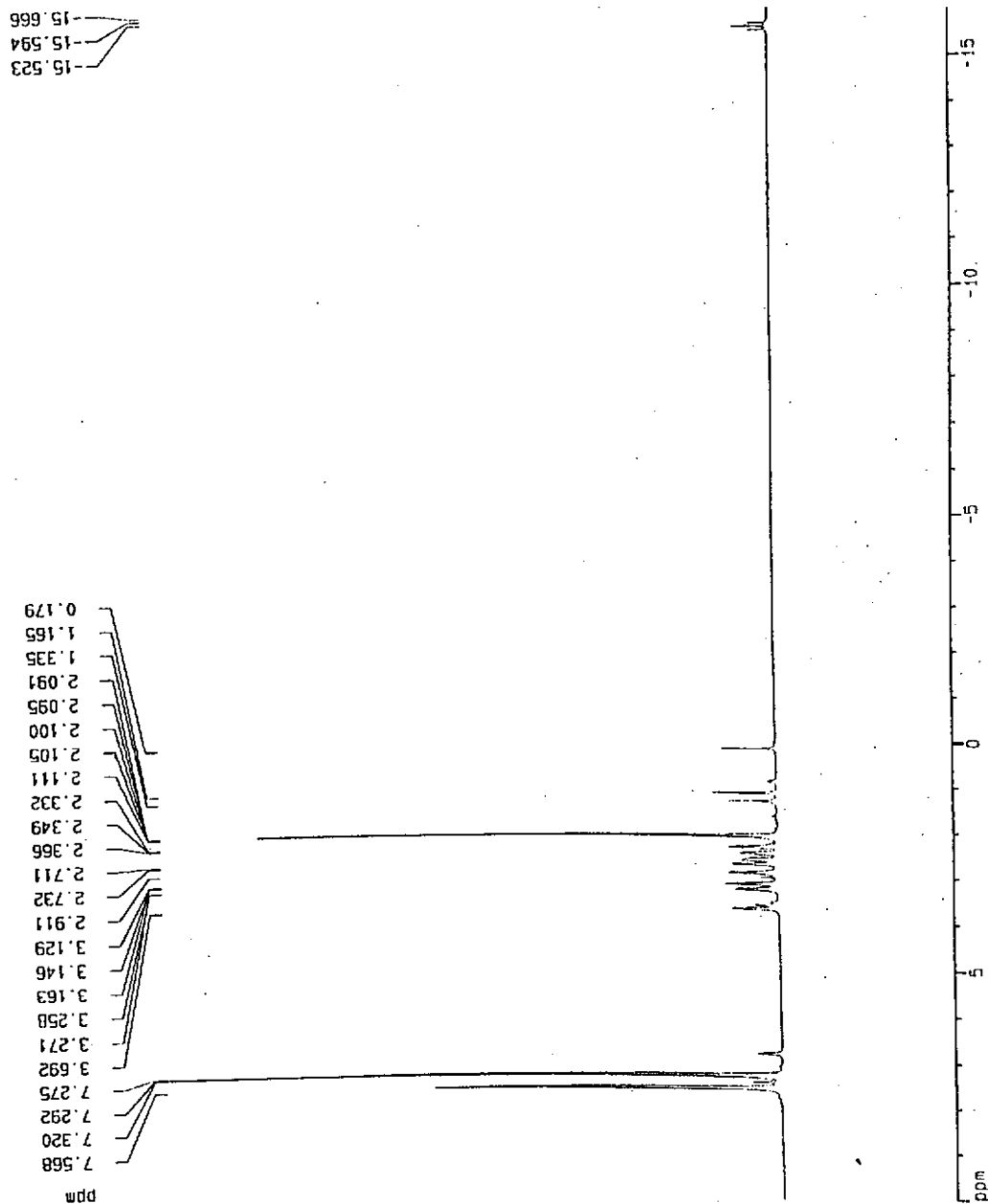


Figure 2.4 Infra-red spectrum of  $[\text{}^{119\text{m}}\text{TcRuH}(\text{PPh}_3)_2]\text{BF}_4$  (1) in KBr disc

$\text{HCnRuH}(\text{PPh}_3)_2$  in  $\text{CDCl}_2$



Current Data Parameters  
 NAME pen35ah  
 EXPNO 3  
 PROCNO 1

F2 - Acquisition Parameters  
 Date\_ 970110  
 Time 13.55  
 INSTRN gdx400  
 PROBHD 5 mm QNP 1H/  
 PULPROG zg30  
 TD 32768  
 SOLVENT Aceton  
 NS 64  
 DS 0  
 SWH 16025.641 Hz  
 FIDRES 0.489064 Hz  
 AQ 1.0224116 sec  
 RG 512  
 DW 31.200 usec  
 DE 4.50 usec  
 TE 300.0 K  
 PI 1.00000000 sec  
 P1 9.50 usec  
 DE 4.50 usec  
 SFO1 400.1275993 MHz  
 NUC1 1H  
 PL1 -6.00 dB

F2 - Processing parameters  
 SI 16384  
 SF 400.1259859 MHz  
 MDW EM  
 SSB 0  
 LB 0.30 Hz  
 GB 0  
 PC 1.00

1D NMR dict parameters  
 CX 20.00 cm  
 F1 10.000 ppm  
 F2 4001.30 Hz  
 F3 -16.000 ppm  
 F4 -6402.06 Hz  
 SCA1 1.30000 ppm/cm  
 SCA2 520.15855 Hz/cm

Figure 2.5. 400 MHz  $^1\text{H}$ -NMR spectrum of  $[\text{CnRuH}(\text{PPh}_3)_2]\text{BF}_4$  (1).

H<sub>2</sub>CnRUH (PPh<sub>3</sub>)<sub>2</sub> in CD<sub>2</sub>Cl<sub>2</sub>

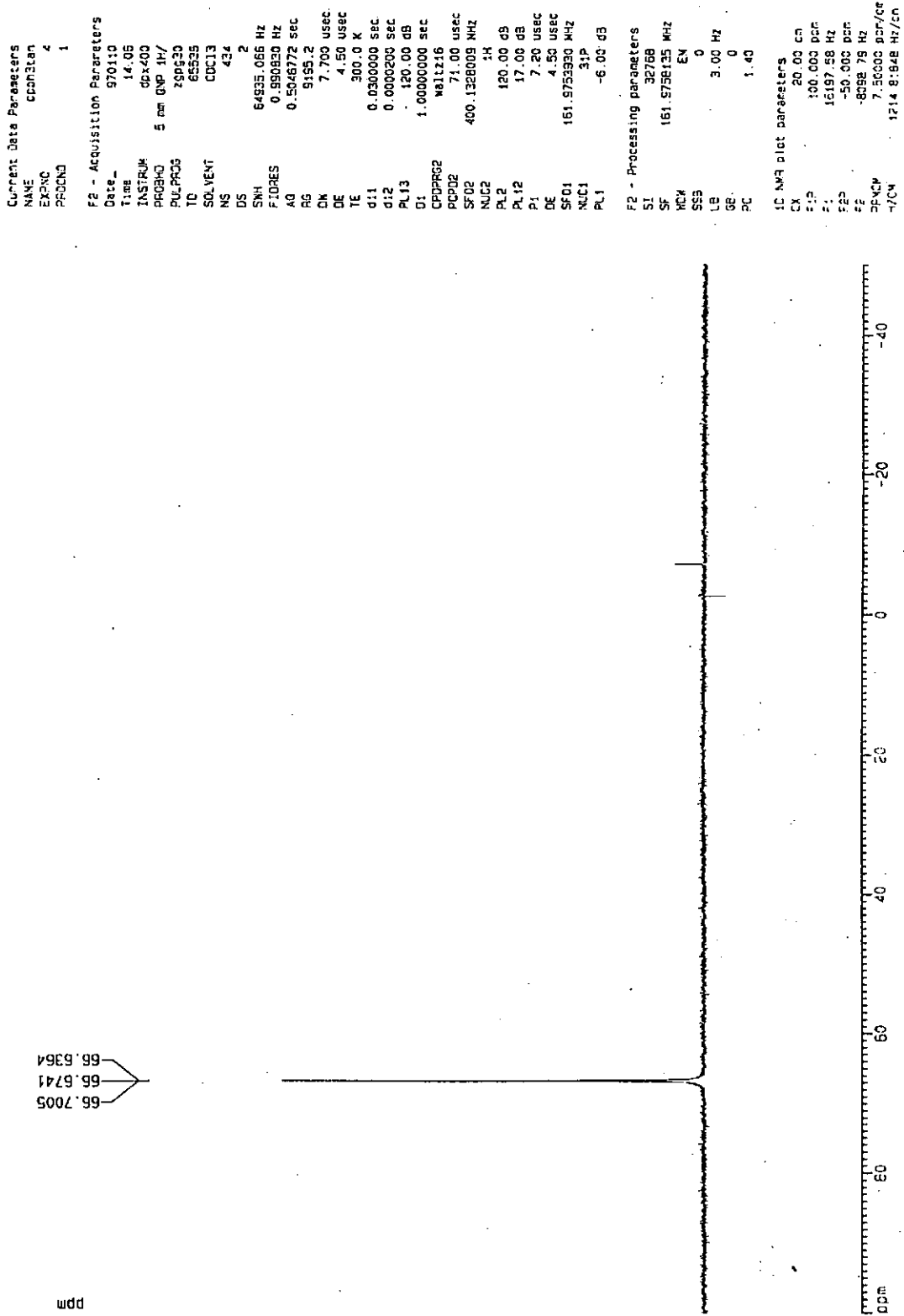


Figure 2.6 161 MHz <sup>31</sup>P{<sup>1</sup>H}-NMR spectrum of [H<sub>2</sub>CnRUH(PPh<sub>3</sub>)<sub>2</sub>]BF<sub>4</sub> (1).

SPEC: 97519  
 Samp: TACNRUP2H  
 Comm: FAB-mode  
 Mode: FAB +VE +LMR BSCAN (EXP) UP LR NETCDF  
 Oper: LI Ping/WAN/YK\_AU  
 Base: 0.0  
 Norm: 756.4  
 Peak: 3000.00 mmu  
 Accu: 1 > 14

12-May-97 Elapse: 00:00.0 1  
 Start: 14:00:18 15

Inlet :  
 Masses: 0 > 0  
 #peaks: 0

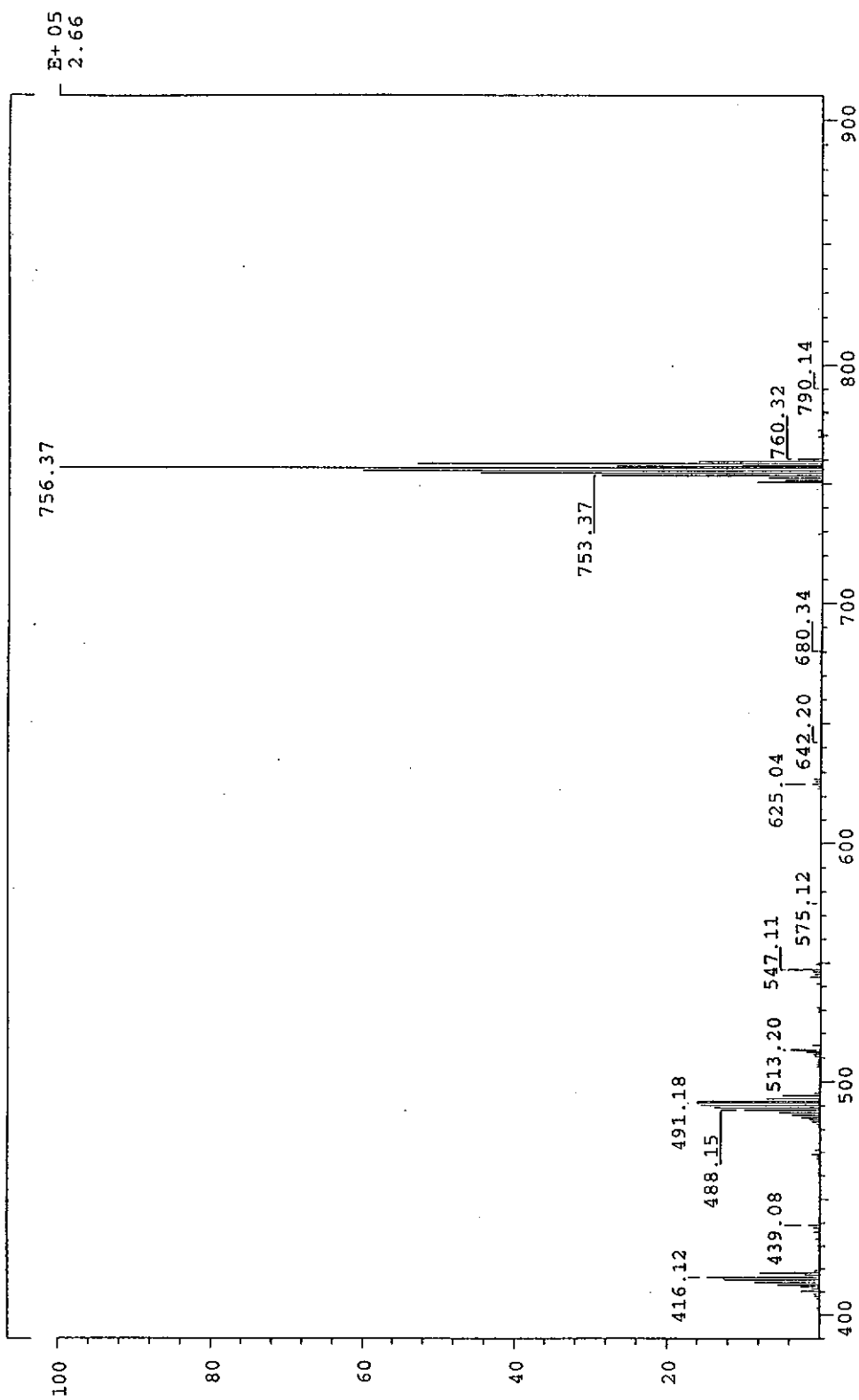


Figure 2.7 FAB mass spectrum of  $[^1\text{H}]\text{CnRuH}(\text{PPh}_3)_2]\text{BF}_4$  (**1**).



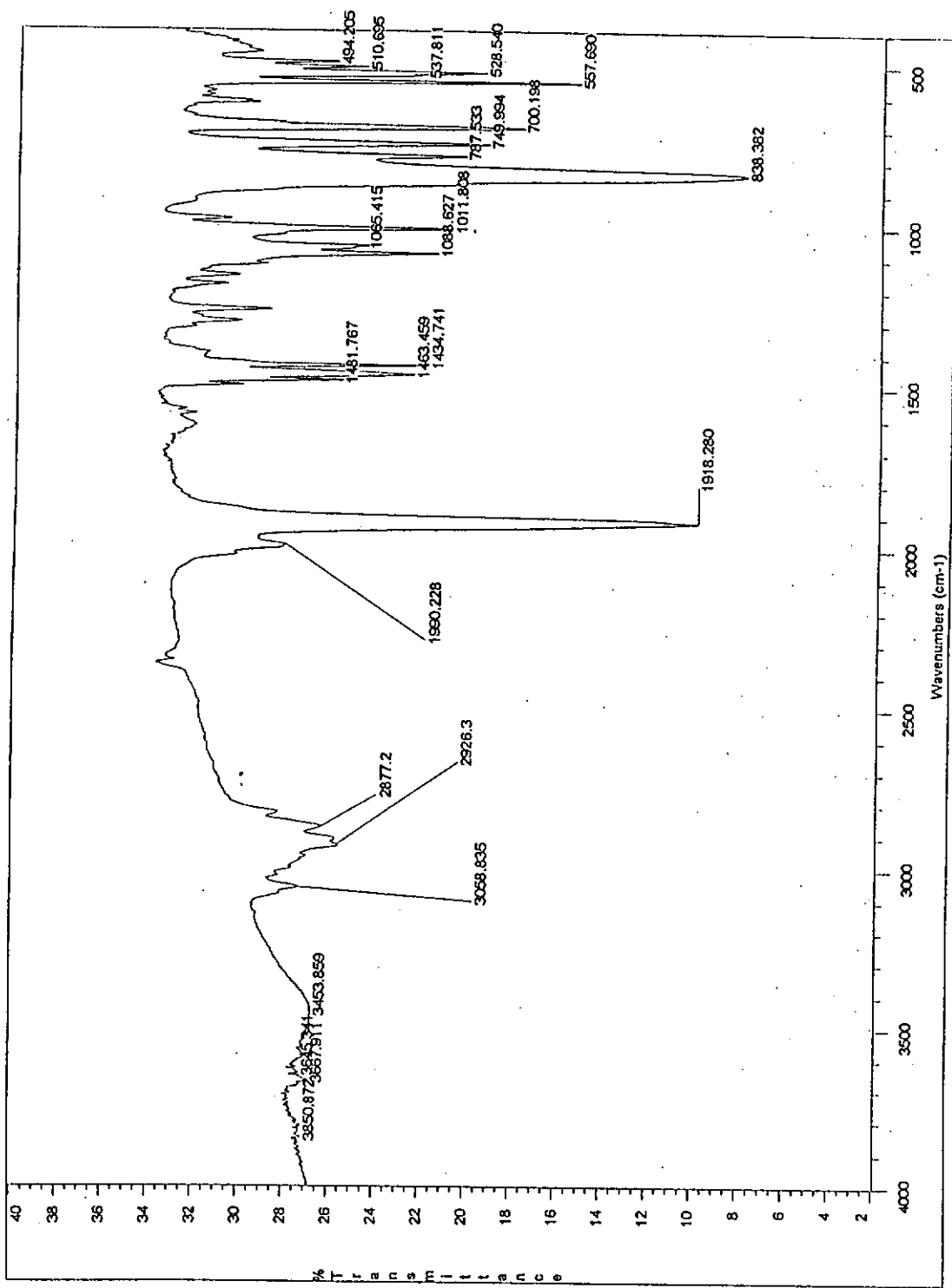


Figure 2.8 Infra-red spectrum of  $[\text{CnRuH(CO)(PPh}_3\text{)]BF}_4$  (2) in KBr disc

(H-tacn)Ru(PPh<sub>3</sub>)(CO)H in CD<sub>2</sub>Cl<sub>2</sub> (0.4ml), 20°C

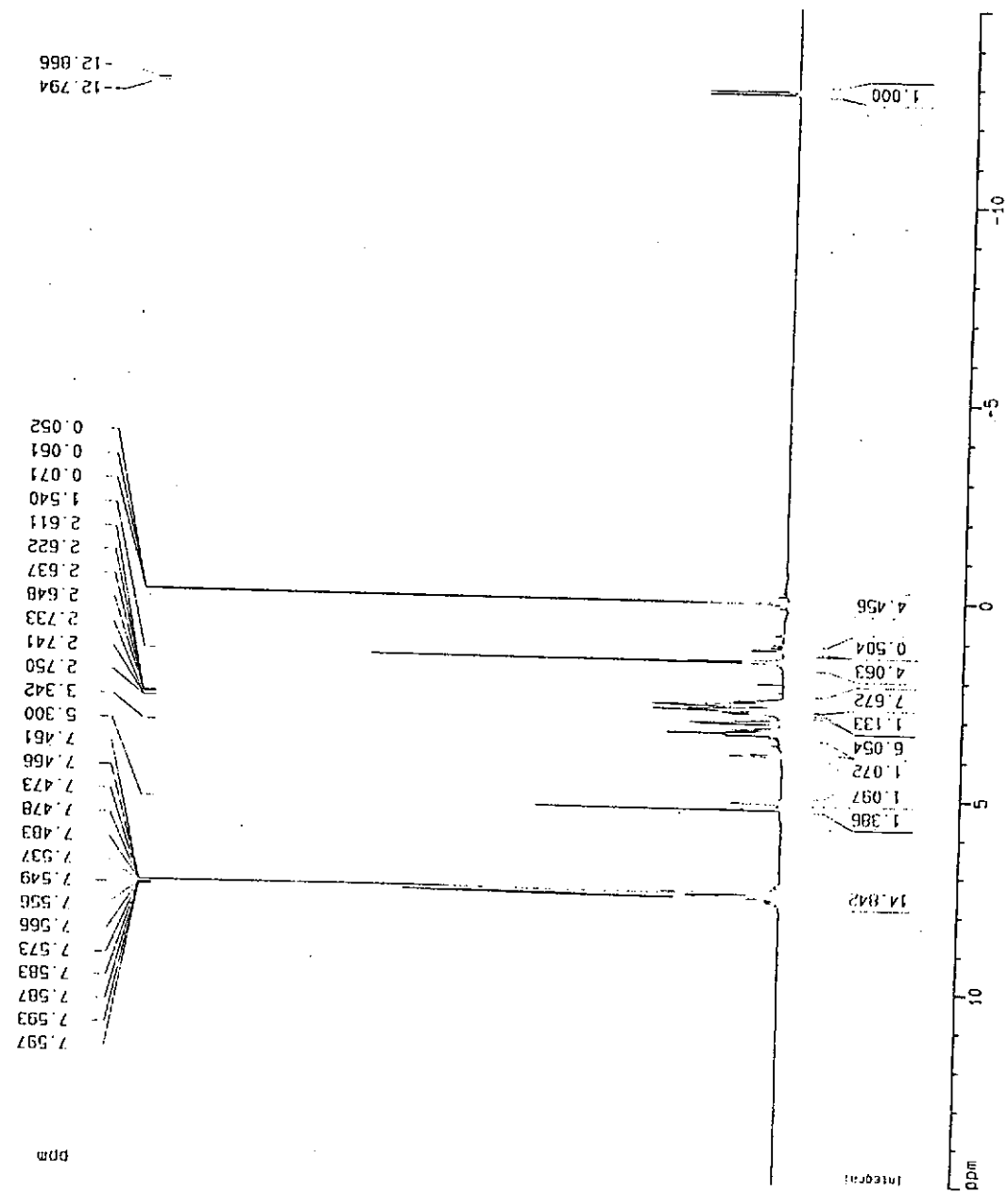


Figure 2.9. 400 MHz <sup>1</sup>H-NMR spectrum of [H-tacnRu(PPh<sub>3</sub>)(CO)H]BF<sub>4</sub> (2).

(H-tacn)Ru(PPh<sub>3</sub>)(CO)H in CD<sub>2</sub>C12(0.4ml). 20°C

```

Current Data Parameters
NAME          chltacn
EXPNO        1
PROCNO       1

F2 - Acquisition Parameters
Date_         970315
Time          22:51
INSTRUM      gpc400
PROBHD       5 mm GNP 1H/
PULPROG      zgpg30
TD           65536
SOLVENT      CDCl3
NS           400
DS           2
SWH          67535.665 Hz
FIDRES       0.1590830 Hz
AQ           0.5046772 sec
RG           9155.2
DN           7.700 USEC
DE           4.50 USEC
TE           300.2 K
S11          0.0300000 sec
S12          0.0000000 sec
PL13         120.00 dB
S1           1.0000000 sec
CPDPRG2      waltz15
PCPD2        71.00 usec
SFO2         400.1340013 MHz
NUC2         14
PL2          120.00 dB
PL12         17.00 dB
S1           6.00 USEC
DE           4.50 USEC
SFO1         161.8582953 MHz
NUC1         31P
PL1          -6.00 dB

F2 - Processing Parameters
SI           32768
SF           161.8758115 MHz
RG           EM
SSB          0
LB           3.00 Hz
GB           0
PC           1.40

1D NMR plot parameters
CX           50.00 cm
FID         100 000 DCF
F1          15197.58 Hz
F2          -186 000 DCF
F3          -25155.85 Hz
RFNOY       14 00000 CCF/CF
HZCM        2267 66138 Hz/CF
  
```

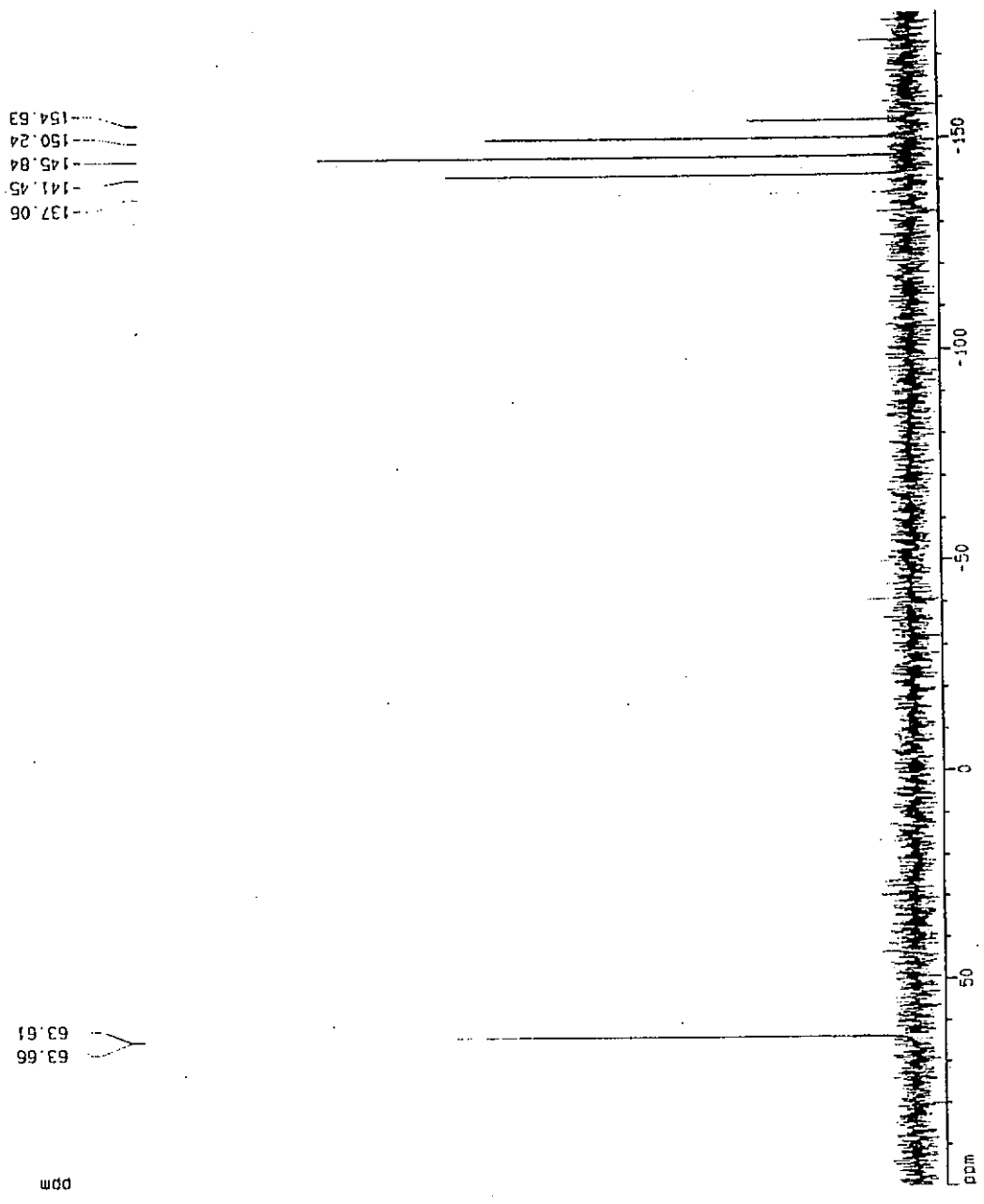


Figure 2.10. 161 MHz <sup>31</sup>P{<sup>1</sup>H}-NMR spectrum of [H-tacn]Ru(PPh<sub>3</sub>)(CO)H (2).

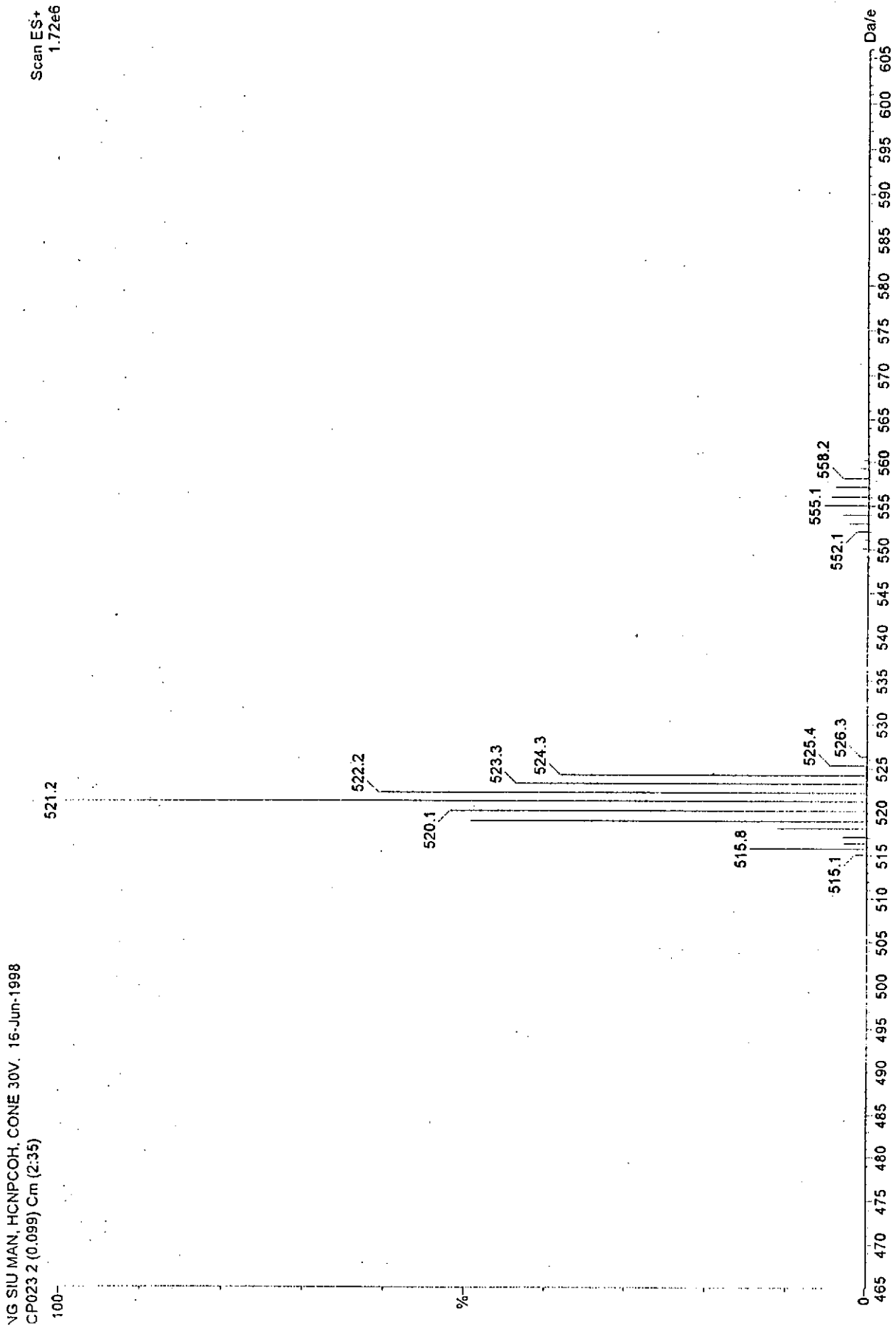


Figure 2.11 FAB mass spectrum of  $[^1\text{H}]\text{CnRuH}(\text{CO})(\text{PPh}_3)]\text{BF}_4$  (2).

TpRu(dppe)H in CDCl<sub>2</sub>

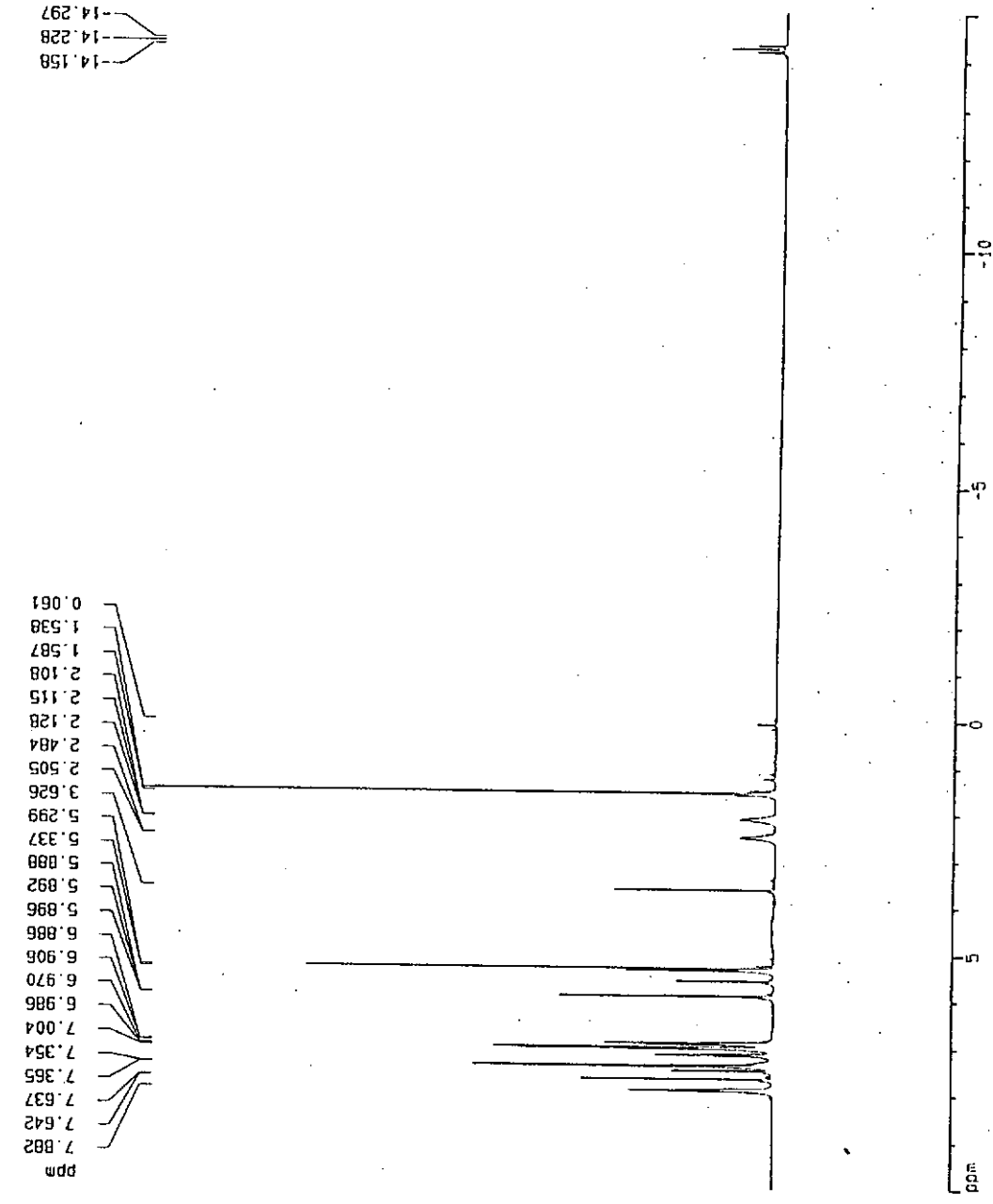


Figure 2.13. 400 MHz <sup>1</sup>H-NMR spectrum of TpRuH(dppe) (14).

Current Data Parameters  
 NAME tzc050eh  
 EXPNO 2  
 PROCNO 1

F2 - Acquisition Parameters  
 Date\_ 970223  
 Time 10.02  
 INSTRUM dpx400  
 PROBHD 5 mm QNP 1H/  
 PULPROG zgpg30  
 TO 32768  
 SOLVENT CDCl<sub>2</sub>  
 NS 40  
 DS 2  
 SWH 16025.641 Hz  
 FIDRES 0.489054 Hz  
 AQ 1.0224116 sec  
 RG 574.7  
 DW 31.200 usec  
 DE 4.50 usec  
 TE 300.0 K  
 C1 2.00000000 sec  
 P1 5.80 usec  
 DE 4.50 usec  
 SFO1 400.1306004 MHz  
 NUC1 1H  
 PL1 -6.00 dB

F2 - Processing parameters  
 SI 16384  
 SF 400.1307928 MHz  
 KCM 0  
 SSB 0  
 LB 0.00 Hz  
 GB 0  
 PC 1.00

1D NMR plot parameters  
 CX 20.00 cm  
 F1F 10.000 ppm  
 F1 4001.31 Hz  
 F2P -15.000 ppm  
 F2 -6001.55 Hz  
 PPMCM 1.25000 ppm/cm  
 HZCM 500.15351 Hz/cm

TpRuH(dppe) in CD<sub>2</sub>C1<sub>2</sub>

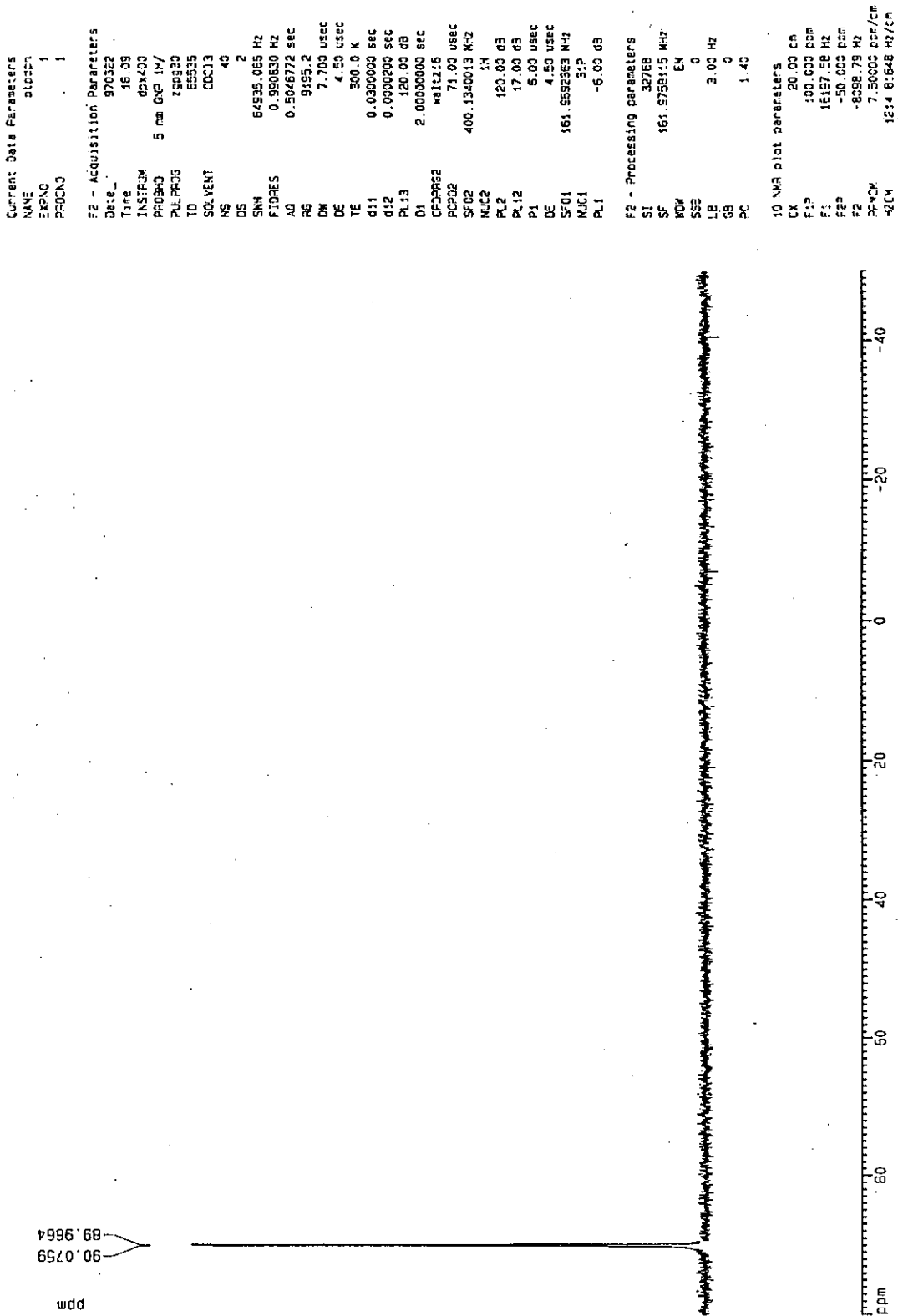


Figure 2.14. 161 MHz <sup>31</sup>P{<sup>1</sup>H}-NMR spectrum of TpRuH(dppe) (14).

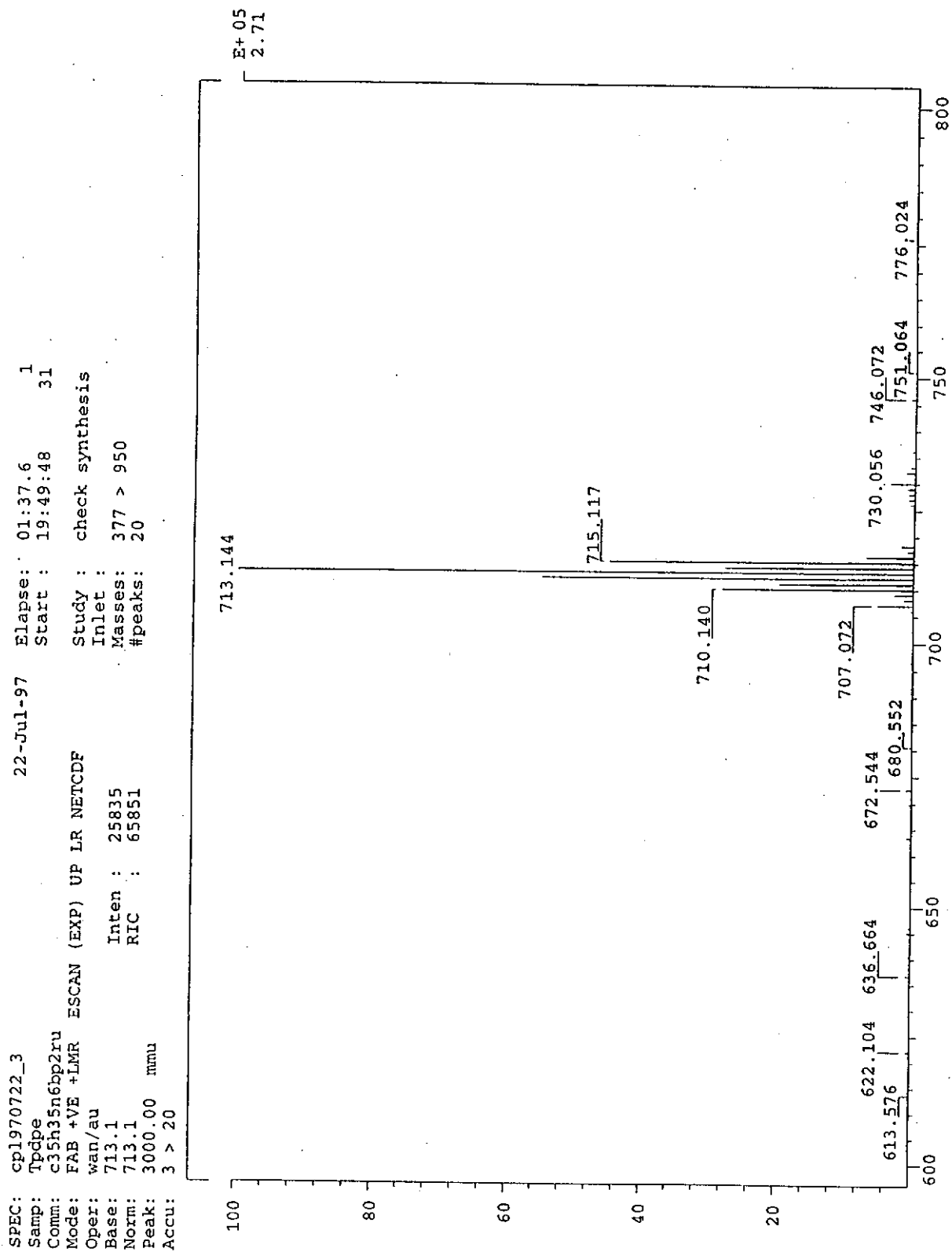


Figure 2.15 FAB mass spectrum of TpRuH(dppe) (14).

H<sub>2</sub>CnRu (H<sub>2</sub>) (PPh<sub>3</sub>)<sub>2</sub> in CD<sub>2</sub>C1<sub>2</sub>

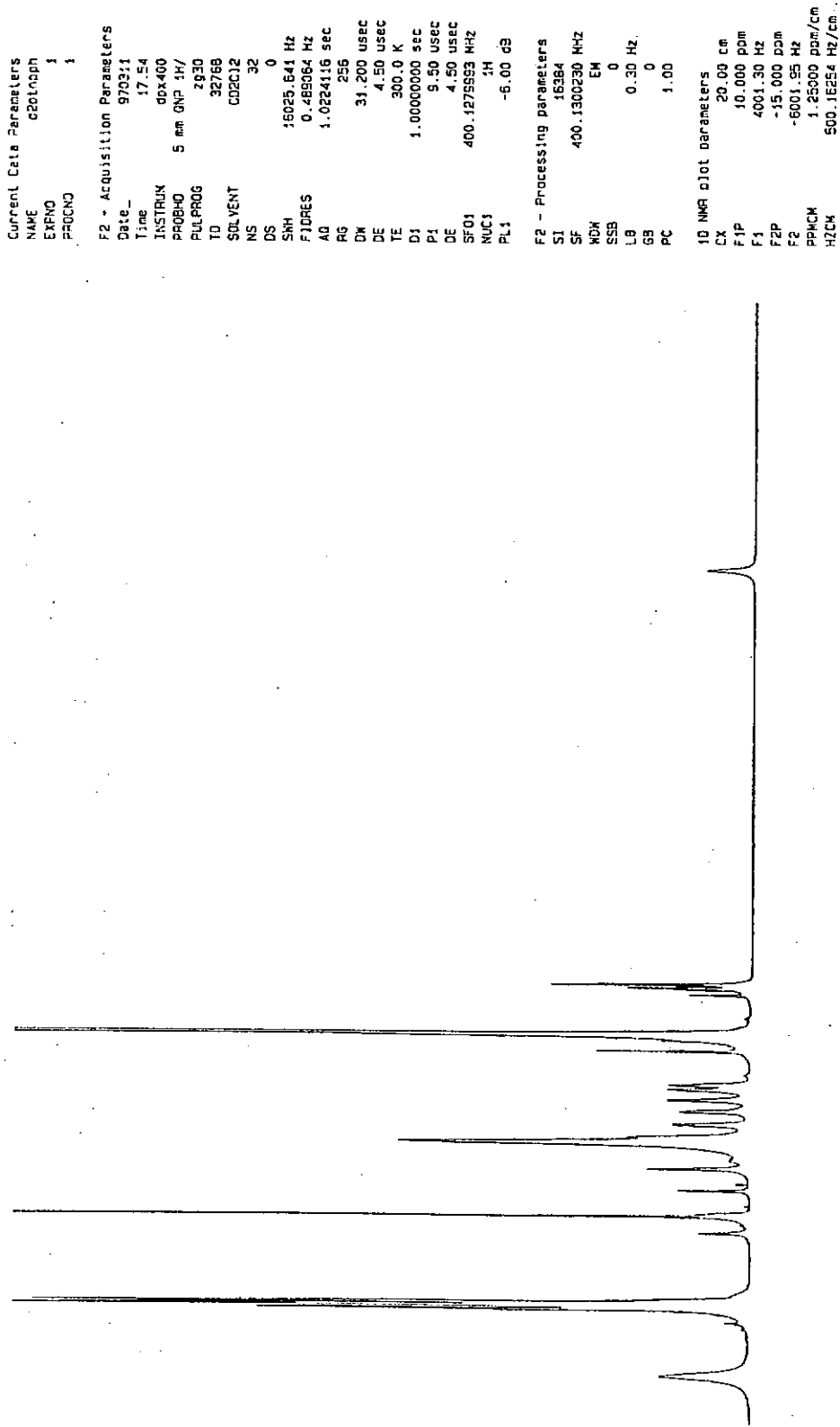


Figure 2.16. 400 MHz <sup>1</sup>H-NMR spectrum of [<sup>1</sup>H]CnRu(H<sub>2</sub>)(PPh<sub>3</sub>)<sub>2</sub>(BF<sub>4</sub>)<sub>2</sub>(5)



HCrRu (H2) (PPh3)2 in CDCl2

Current Data Parameters  
 NAME spantanh2  
 EXPNO 4  
 PROCNO 1

F2 - Acquisition Parameters

Date\_ 970120  
 Time 14.14  
 INSTRUM spect-400  
 PROBHD 5 mm QNP 1H/  
 PULPROG zgpg30  
 TD 65525  
 SOLVENT CDCl3  
 NS 255  
 DS 2  
 SWH 64535.065 Hz  
 FIDRES 0.390650 Hz  
 AQ 0.5626772 sec  
 RG 5195.2  
 DM 7.700 usec  
 DE 4.50 usec  
 TE 300.0 K  
 d11 0.030000 sec  
 d12 0.000200 sec  
 PL13 120.00 dB  
 D1 1.0000000 sec  
 CPDPRG2 waltz16  
 PCPD2 71.00 usec  
 SFO2 400.1328009 MHz  
 NUC2 1H  
 PL2 120.00 dB  
 PL12 17.00 dB  
 P1 7.20 usec  
 DE 4.50 usec  
 SFO1 161.5759350 MHz  
 NUC1 31P  
 PL1 -6.00 dB

F2 - Processing parameters

SI 32768  
 SF 161.575935 MHz  
 MCH EM  
 SSB 0  
 LB 3.00 Hz  
 GB 0  
 PC 1.40

10 NMR plot parameters

CX 20.00 cm  
 F1P 100.000 ppm  
 F1 16157.56 Hz  
 F2 -50.000 ppm  
 F2 -8058.78 Hz  
 PENCH 7.50000 per/ct  
 -ZC4 1214.81648 Hz/cr

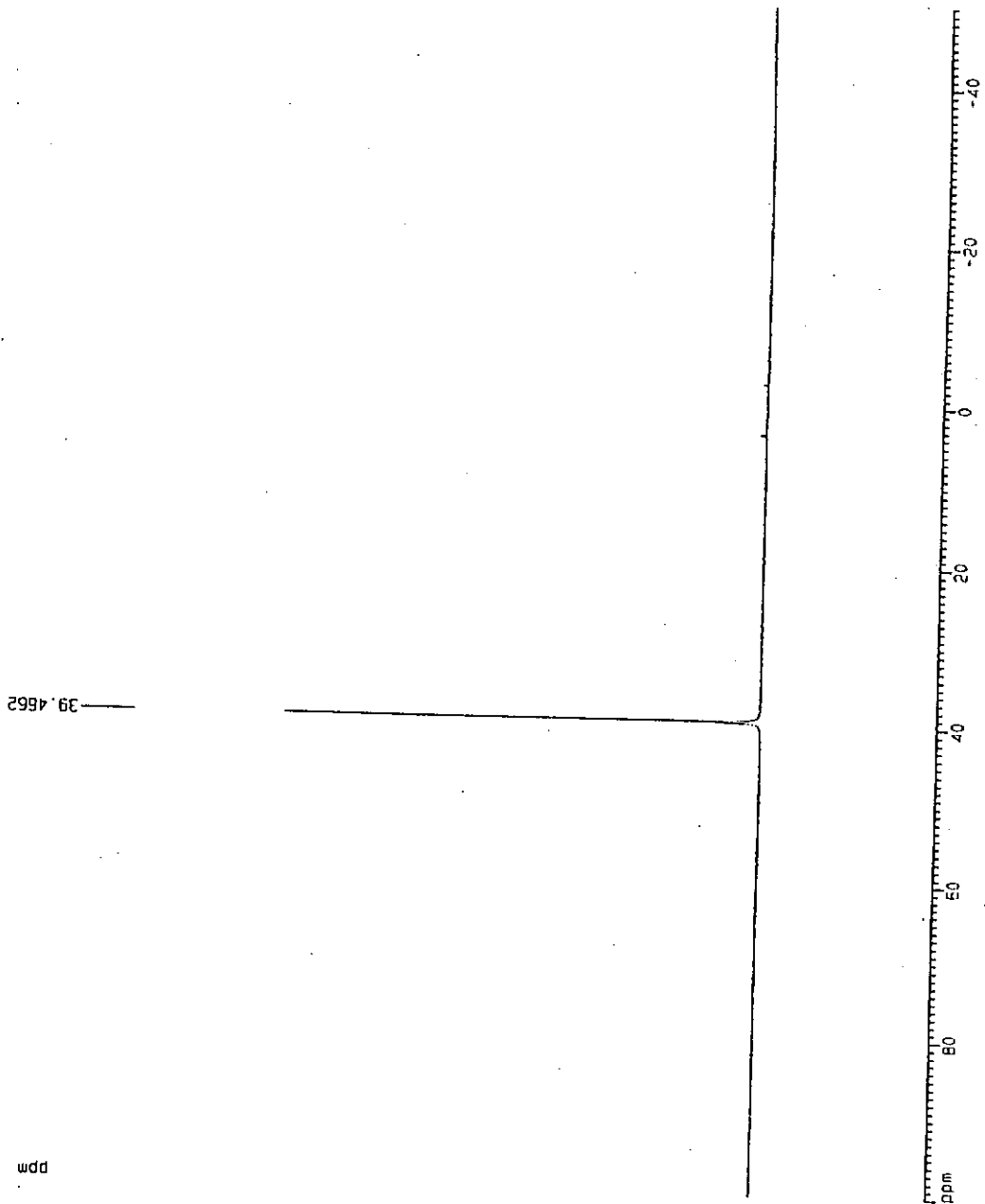


Figure 2.17. 161 MHz  $^{31}\text{P}\{^1\text{H}\}$ -NMR spectrum of  $[\text{CnRu}(\text{H}_2)(\text{PPh}_3)_2](\text{BF}_4)_2(5)$

${}^1\text{H}\text{-CnRu(HD)} (\text{PPh}_3)_2$  in  $\text{CDCl}_2$

Current Data Parameters  
NAME c2stnpph  
EXPNO 3  
PROCNO 1

F2 - Acquisition Parameters  
Date\_ 970311  
Time 18.48  
INSTRUM dop400  
PROBHD 5 mm QNP 1H/  
PULPROG zg30  
TD 32768  
SOLVENT  $\text{CDCl}_2$   
NS 1334  
DS 0  
SWH 16025.641 Hz  
FIDRES 0.489064 Hz  
AQ 1.0224116 sec  
RG 128  
DK 31.200 usec  
DE 4.50 usec  
TE 300.0 K  
D1 0.30000001 sec  
F1 9.50 usec  
DE 4.50 usec  
SFO1 400.1279993 MHz  
NUC1  ${}^1\text{H}$   
PL1 -6.00 dB

F2 - Processing parameters  
SI 15364  
SF 400.1300230 MHz  
WDW EM  
SSB 0  
LB 0.30 Hz  
GB 0  
PC 1.00

1D NMR plot parameters  
CX 20.00 cm  
F1P -8.000 ppm  
F1 -3201.04 Hz  
F2P -10.000 ppm  
F2 -4001.30 Hz  
PPH1M 0.10000 ppm/cm  
HZCM 40.01300 Hz/cm

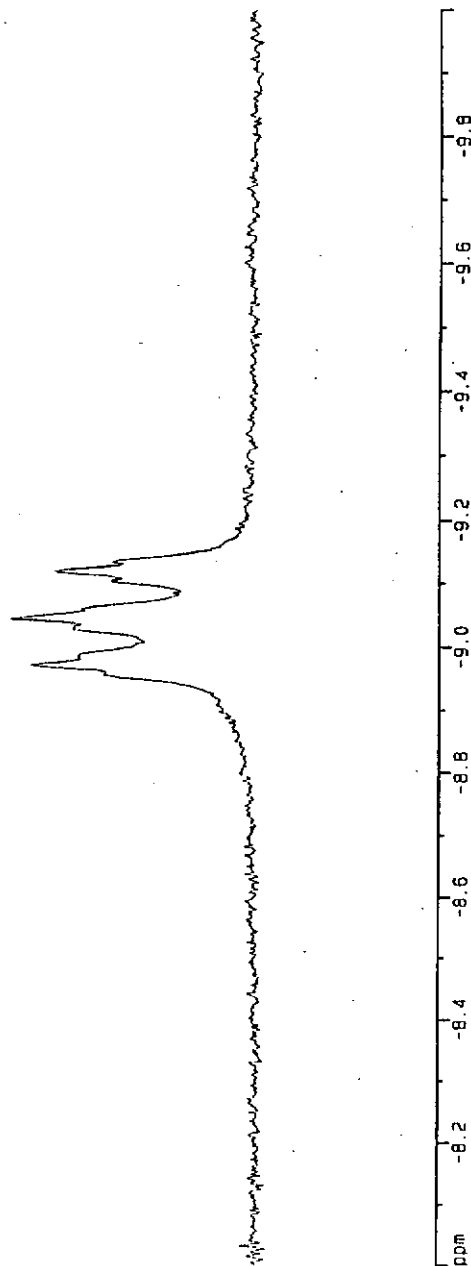


Figure 2.18. 400 MHz  ${}^1\text{H}$ -NMR spectrum of  $[\text{CnRu(HD)(PPh}_3)_2] (\text{BF}_4)_2$  ( $5\text{-}d_1$ )



(H-tacn)Ru(PPh<sub>3</sub>)(CO)H + HBF<sub>4</sub> (in ether, 0.002ml)  
 -60°C, in CD<sub>2</sub>Cl<sub>2</sub> (0.4ml)

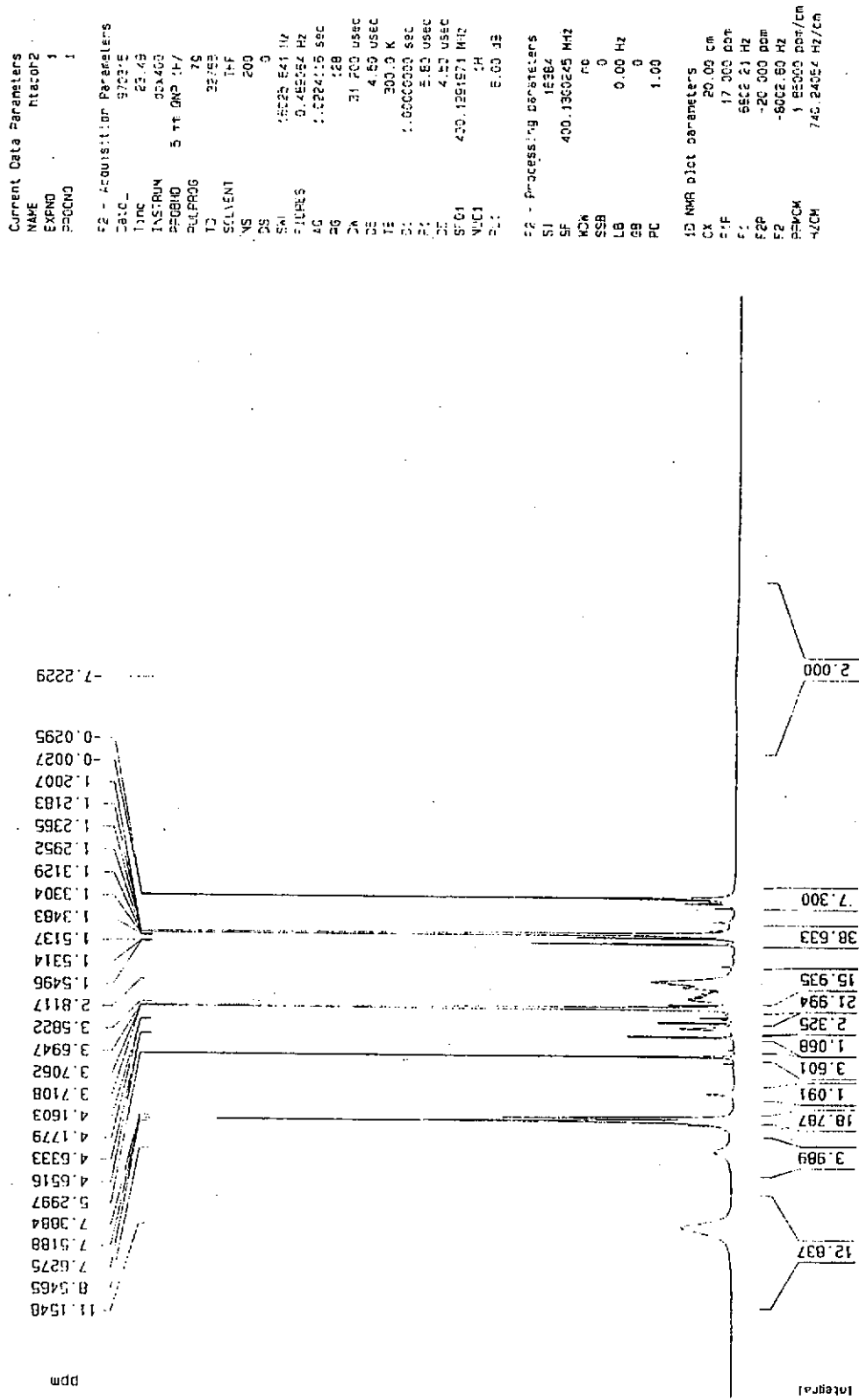


Figure 2.19. 400 MHz <sup>1</sup>H-NMR spectrum of [H-tacnRu(H<sub>2</sub>)(CO)(PPh<sub>3</sub>)](BF<sub>4</sub>)<sub>2</sub>(6)

(H-techn) Ru (PPh3) (CO)H + HBF4 (in ether, 0.002ml)  
 -60°C, in CD2Cl2 (0.4ml)

```

Current Data Parameters
NAME      ZPTACN2
EXPNO     1
PROCNO    1

F2 - Acquisition Parameters
Date_     970315
Time      25.45
INSTRUM   spect
PROBHD    EPR 5MP 1H/
PULPROG   zgpg30
RG         655.35
SOLVENT   CDCl3
NS         200
DS         2
SWH        64335.668 Hz
F2FREQ    161.950315 MHz
AQ         0.5246772 sec
RG         9155.2
DM         7.700 usec
DE         4.50 usec
TE         300.2 K
D1         0.0300000 sec
D12        0.0300000 sec
E113       120.00 dB
Z1         1.0000000 sec
SFOF2      161.950315 MHz
SFO2       400.1340013 MHz
NUC2        14
PL2         120.00 dB
PL12        17.00 dB
P1         15.00 usec
DE         4.50 usec
SFO1       161.5592363 MHz
NUC1        31P
PL1         -6.00 dB

F2 - Processing Parameters
SI         32768
SF         161.575927 MHz
RG         655.35
SOLVENT   CDCl3
LB         3.00 Hz
GB         0
PC         1.40

1D NMR plot parameters
CX         20.00 cm
F1P        100.000 ppm
F1         16197.58 Hz
F2P        -160.000 ppm
F2         -25155.84 Hz
PRN1CM    14.00000 ppm/cm
HZ1CM     2267.66069 Hz/cm
  
```

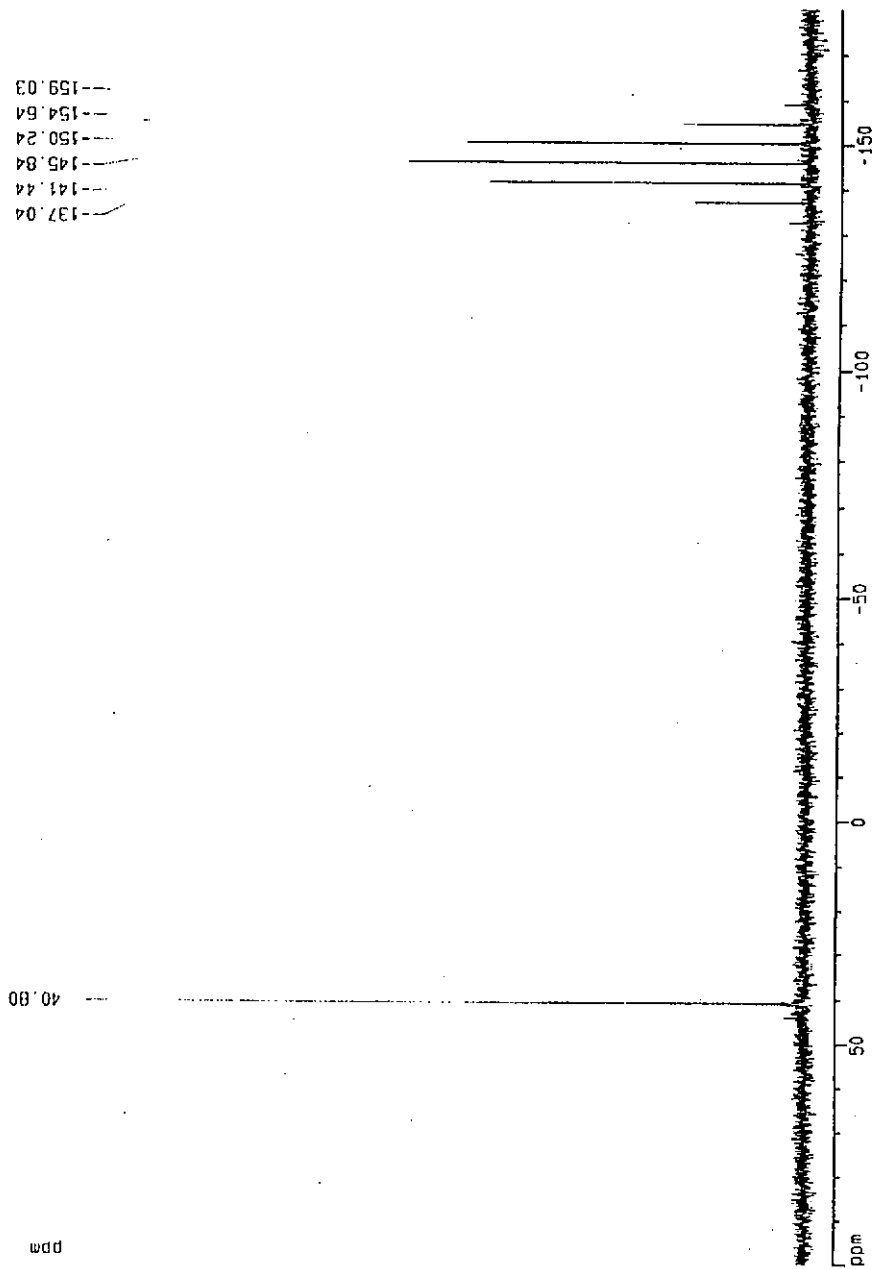


Figure 2.20. 161 MHz  $^{31}\text{P}\{^1\text{H}\}$ -NMR spectrum of  $[\text{CnRu}(\text{H}_2)(\text{CO})(\text{PPh}_3)](\text{BF}_4)_2(6)$

HcRu(HD)(CO)(PPh3) in CD2Cl2 in -55oC

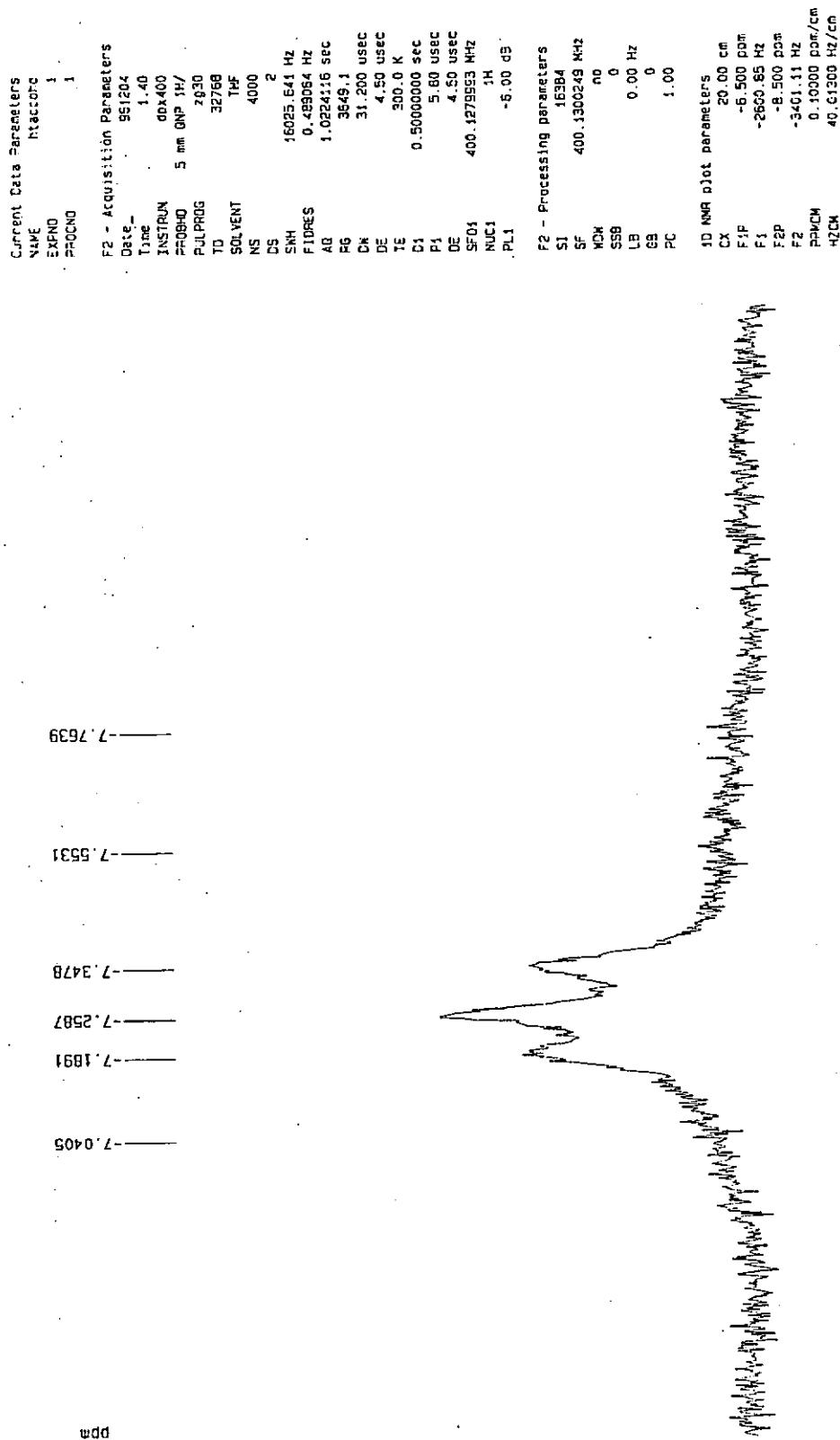


Figure 2.21. 400 MHz <sup>1</sup>H-NMR spectrum of [<sup>1</sup>HcRu(HD)(CO)(PPh<sub>3</sub>)](BF<sub>4</sub>)<sub>2</sub> (6-d<sub>1</sub>)

MeCnRu (H<sub>2</sub>) (dppe) in CDCl<sub>2</sub>

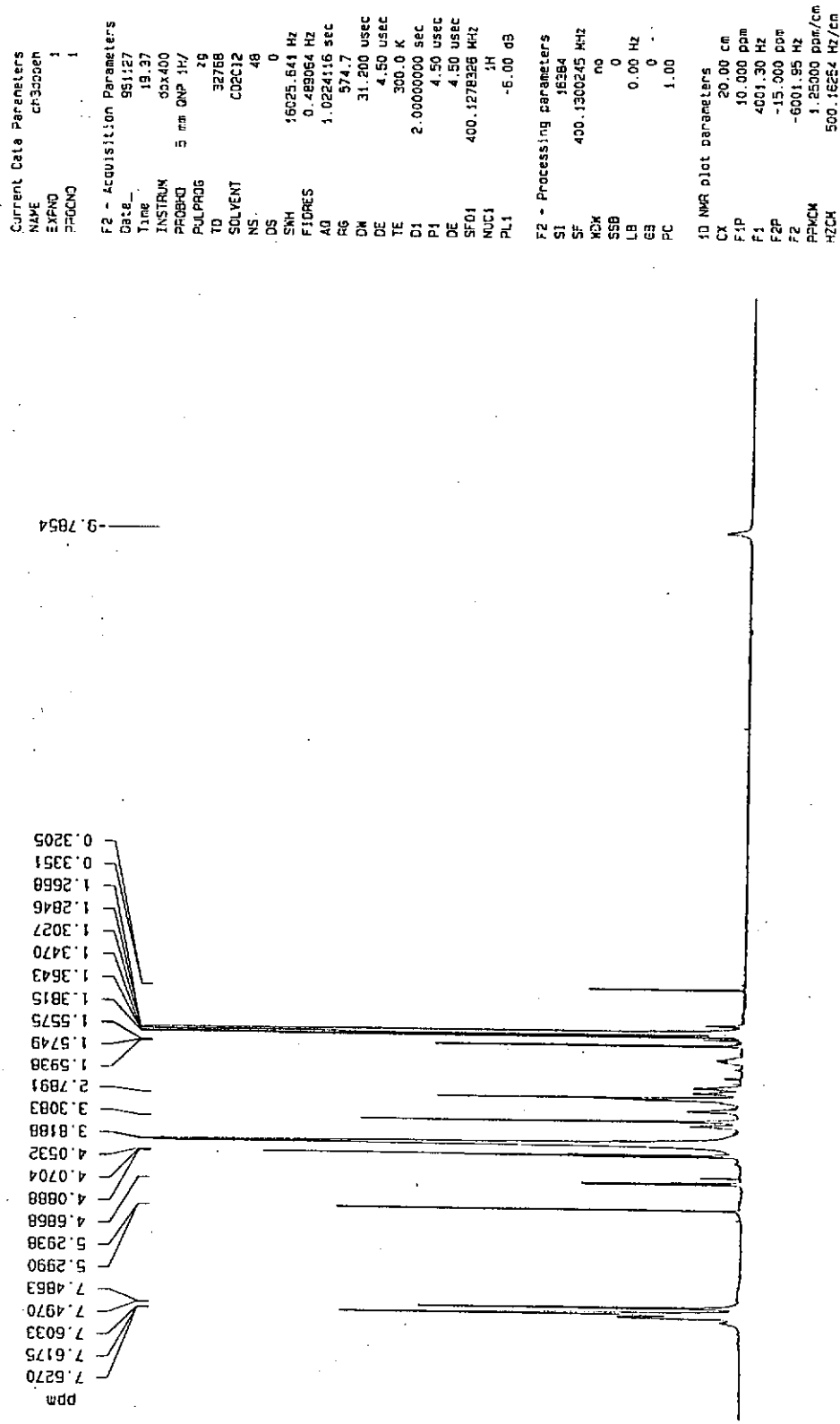


Figure 2.22. 400 MHz <sup>1</sup>H-NMR spectrum of [MeCnRu(H<sub>2</sub>)(dppe)](CF<sub>3</sub>SO<sub>3</sub>)<sub>2</sub>(7)

[(<sup>13</sup>C=Me)Ru(dppe)](CF<sub>3</sub>SO<sub>3</sub>)<sub>2</sub>(7) + HBF<sub>4</sub> (in ether, 0.007ml)  
 20°C, in CD<sub>2</sub>Cl<sub>2</sub> (0.4ml), under 1atm N<sub>2</sub>

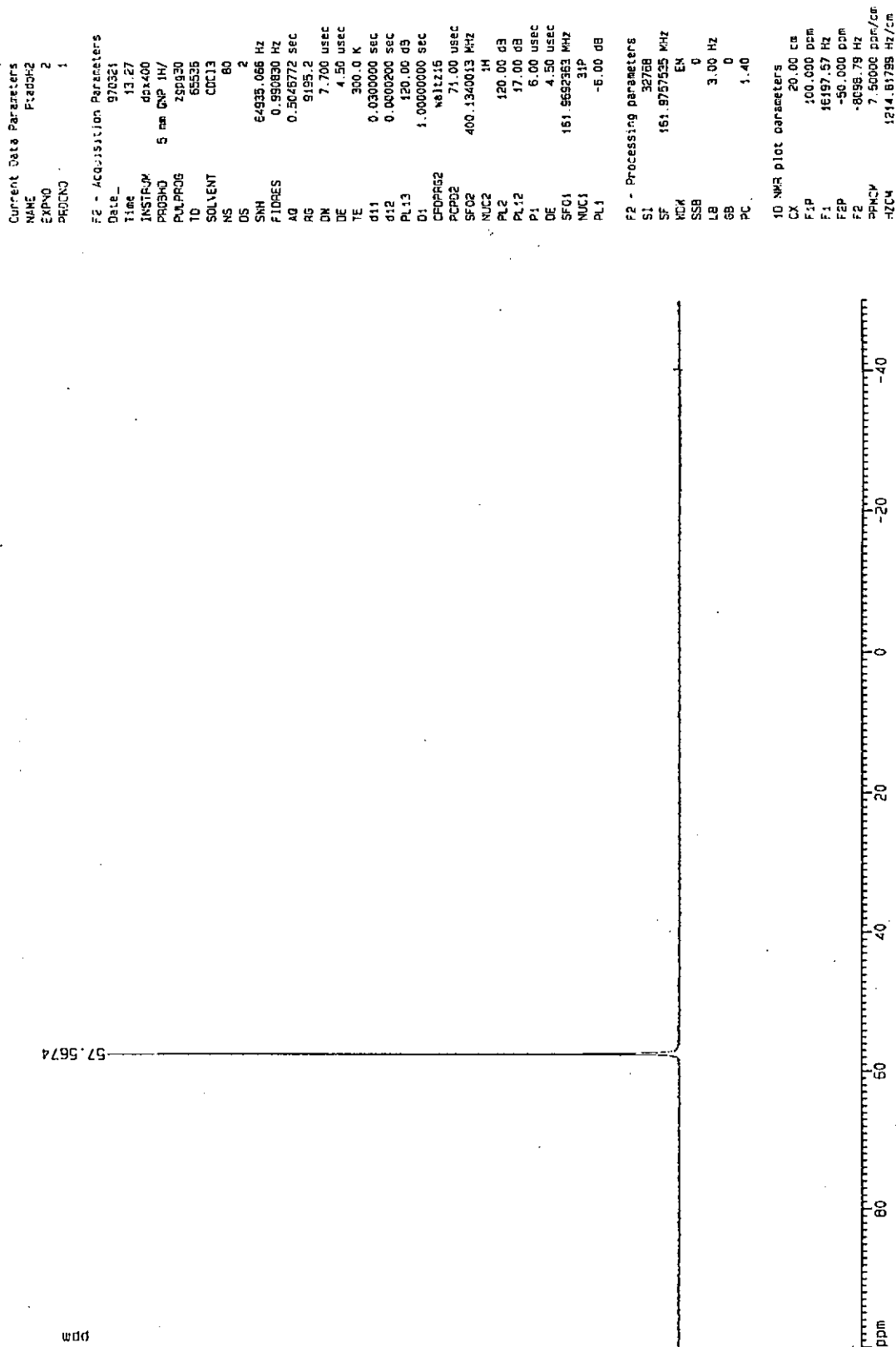


Figure 2.23. 161 MHz <sup>31</sup>P{<sup>1</sup>H}-NMR spectrum of [(<sup>13</sup>C=Me)Ru(H<sub>2</sub>)(dppe)](CF<sub>3</sub>SO<sub>3</sub>)<sub>2</sub>(7)

MeCnRu (HD) (dppe) in CD2Cl2, room Temp.

```

Current Data Parameters
NAME      CN33000
EXPNO    2
PROCNO    1

F2 - Acquisition Parameters
Date_     961128
Time      2.44
INSTRUM   spect
PROBHD    5 mm QNP 1H/
PULPROG   zg
TD         32768
SOLVENT   CDCl2
NS         3600
DS         0
SINH       16025.641 Hz
FIDRES     0.489064 Hz
AQ         1.0224115 sec
RG         574.7
DM         31.200 usec
DE         4.50 usec
TE         300.0 K
D1         0.80000001 sec
P1         4.50 usec
DE         4.50 usec
SFO1      400.1276326 MHz
NUC1      1H
PL1       -6.00 dB

F2 - Processing parameters
SI         16384
SF         400.1307913 MHz
WDW        no
SSB        0
LB         0.00 Hz
GB         0
PC         1.00

ID NMR dict parameters
CX         20.00 cm
F1P        -9.500 ppm
F1         -5461.11 Hz
F2P        -10.500 ppm
F2         -4201.37 Hz
PP4MCH     0.10000 ppm/cm
HZCK       40.01308 Hz/cm
  
```

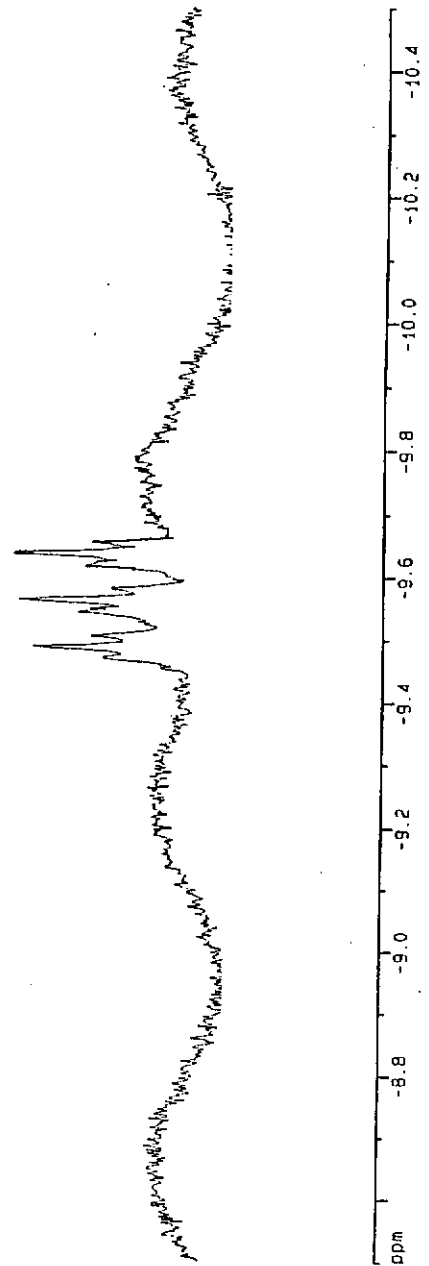


Figure 2.24. 400 MHz  $^1\text{H}$ -NMR spectrum of  $[\text{MeCnRu}(\text{HD})(\text{dppe})](\text{CF}_3\text{SO}_3)_2(7-d_1)$



(CH<sub>3</sub>-tach)/Ru (PPh<sub>3</sub>) (CO) (H<sub>2</sub>) = Ru-H (10mg) + HBF<sub>4</sub>-Ether (0.01ml)  
 -50°C in CDCl<sub>2</sub> (0.4ml)

Current Data Parameters  
 NAME tac0-h2  
 EXPNO 1  
 PROCNO 1

F2 - Acquisition Parameters  
 Date\_ 970311  
 Time 20.16  
 INSTRUM cca400  
 PRBHD 5 RT ONP 3H/  
 PULPROG zg  
 TD 32768  
 SOLVENT Aceton  
 NS 40  
 DS 0  
 SWH 15025.641 Hz  
 FIDRES 0.482954 Hz  
 AQ 1.0224116 sec  
 RG 35.9  
 DA 31.200 USEC  
 DE 4.50 USEC  
 TE 300.0 K  
 D1 2.0000000 sec  
 D2 5.00 USEC  
 DE 4.50 USEC  
 SFO1 400.1276326 MHz  
 NUC1 1H  
 PL1 -5.00 dB

F2 - Processing parameters  
 SI 16384  
 SF 400.1360245 MHz  
 CK no  
 SSB 0  
 LB 0.00 Hz  
 GB 0  
 PC 1.00

1D NMR plot parameters  
 CK 20.00 CF  
 F1 14.500 ppm  
 F2 5901.89 Hz  
 FZ -20.000 ppm  
 FZ 8002.60 Hz  
 SFO1 1.72500 ppm/cm  
 AZO1 650.22430 Hz/CF

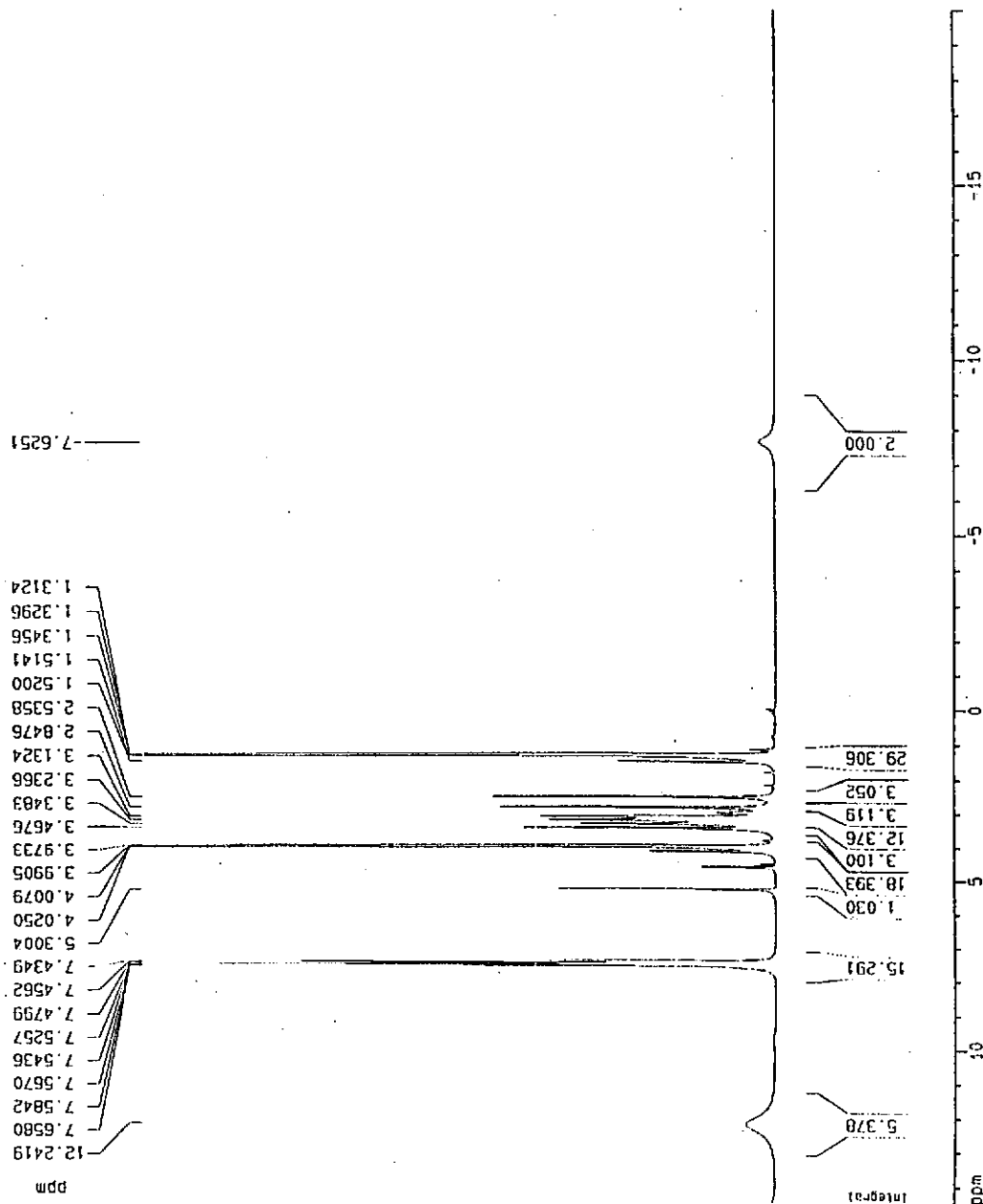


Figure 2.25. 400 MHz <sup>1</sup>H-NMR spectrum of [<sup>Me</sup>CnRu(H<sub>2</sub>)(CO)(PPh<sub>3</sub>)](PF<sub>6</sub>)(CF<sub>3</sub>SO<sub>3</sub>)  
 (8)

(CH<sub>3</sub>-tacn)Ru(PPh<sub>3</sub>)(CO)(H<sub>2</sub>) = Ru-H (10mg) + HBF<sub>4</sub>-Ether (0.01ml)  
 -60°C in CDCl<sub>2</sub> (0.4ml)

```

Current Data Parameters
NAME          C1aco-N2
EXPNO        1
PROCNO       1

F2 - Acquisition Parameters
Date_        970311
Time         20.08
INSTRUM      dpx400
PROBHD       5 mm QNP 1H/
PULPROG      zgpg30
TO          65335
SOLVENT      CDCl3
NS           60
DS           2
SINH         64535.065 Hz
FIDRES       0.590630 Hz
AQ           0.5046772 sec
RG           9165.2
DW           7.700 usec
DE           4.50 usec
TE           300.0 K
d11          0.0300000 sec
d12          0.0002000 sec
PL13         120.00 dB
d1           2.0000000 sec
CFDPRG2      waltz16
PCPD2        71.00 usec
SFO2         400.1340013 MHz
NUC2         1H
PL2          120.00 dB
PL12         17.00 dB
P1           6.00 usec
DE           4.50 usec
SFO1         161.5692363 MHz
NUC1         31P
PL1          -6.00 dB

F2 - Processing parameters
SI           32768
SF           161.5755951 MHz
RG           64
WDW          EM
SSB          0
LB           3.00 Hz
GB           0
PC           1.40

10 NMR plot parameters
CX           20.00 cm
F1P         100.000 pcm
F1          16197.56 Hz
F2P         -160.000 pcm
F2          -25155.61 Hz
FPCW        14.00000 Dcr/Cr
HZCW        2667.65545 Hz/Cr
  
```

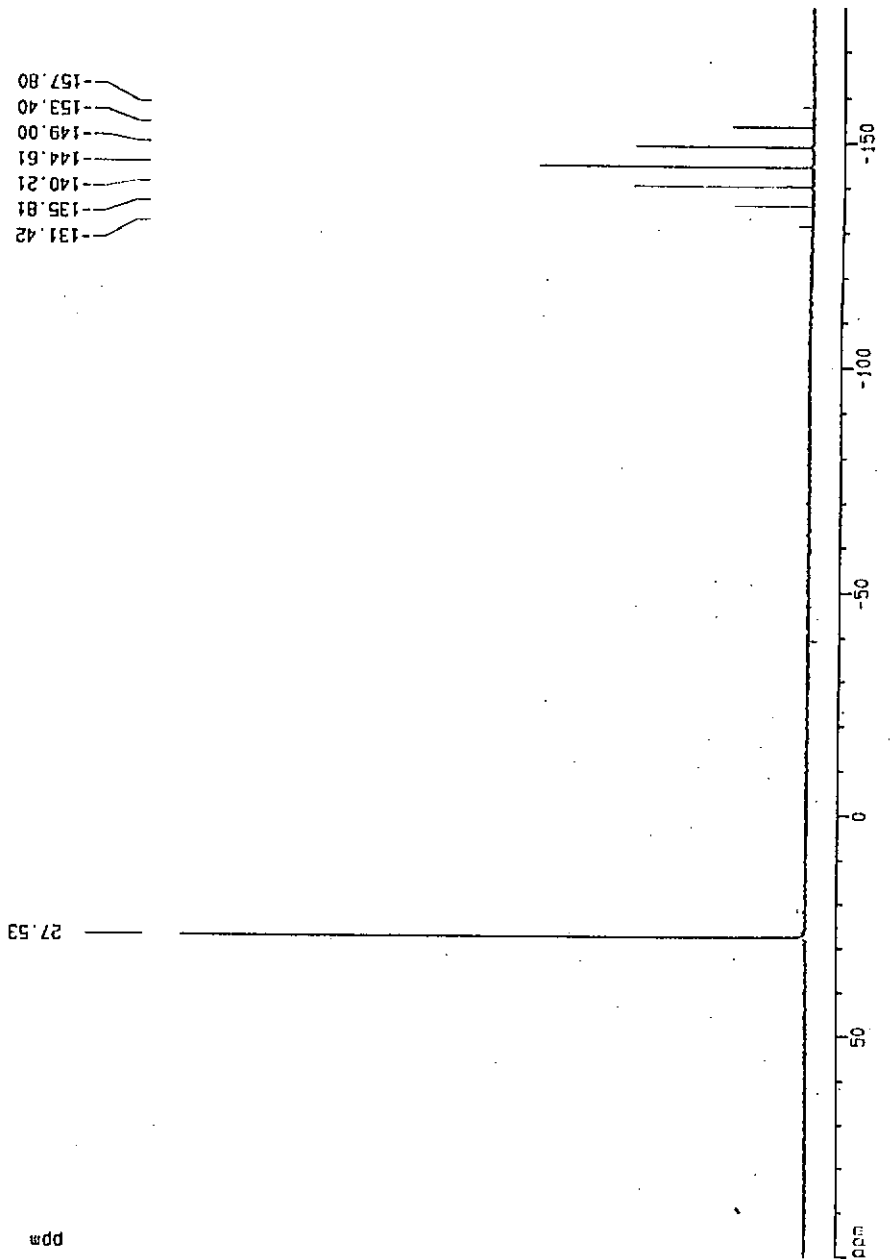


Figure 2.26. 161 MHz <sup>31</sup>P{<sup>1</sup>H}-NMR spectrum of [MeCnRu(H<sub>2</sub>)(CO)(PPh<sub>3</sub>)](PF<sub>6</sub>)(CF<sub>3</sub>SO<sub>3</sub>) (8)

MeCnRu (HD) (CO) (PPh3) in CD2Cl2 -55oC

```

Current Data Parameters
NAME      lactoh2
EXPNO    1
PROCNO   1

F2 - Acquisition Parameters
Date_    961123
Time     4.00
INSTRUM  dx400
PROBHD   5 mm QNP 1H/
PULPROG  zg
TD        32768
SOLVENT  Aceton
NS        120
DS        0
SWH       16025.641 Hz
FIDRES    0.469064 Hz
AQ         1.0224116 sec
RG         161
DK         31.200 usec
DE         4.50 usec
TE        300.0 K
D1         1.00000000 sec
P1         5.80 usec
DE         4.50 usec
SFO1      400.1278325 MHz
NUC1      1H
PL1       -6.00 dB

F2 - Processing parameters
SI        16384
SF        400.1288918 MHz
RG         64
WDW        0
SSB        0
LB         0.00 Hz
GB         0
PC         1.00

1D NMR plot parameters
CX        20.00 cm
F1P       -6.500 ppm
F1        -2600.84 Hz
F2P       -9.000 ppm
F2        -3601.16 Hz
PPMCK     0.12500 ppm/cm
HZCM      50.01611 Hz/cm
  
```

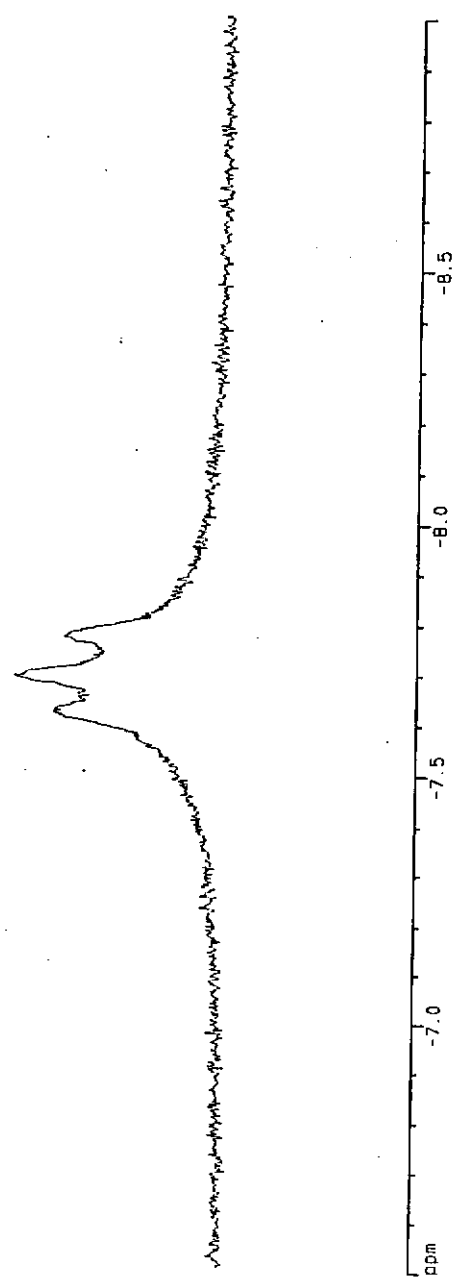


Figure 2.27. 400 MHz <sup>1</sup>H-NMR spectrum of [MeCnRu(HD)(CO)(PPh<sub>3</sub>)](PF<sub>6</sub>)(CF<sub>3</sub>SO<sub>3</sub>) (8-d<sub>1</sub>)

1pRu (F2) (dppf) in CDCl2

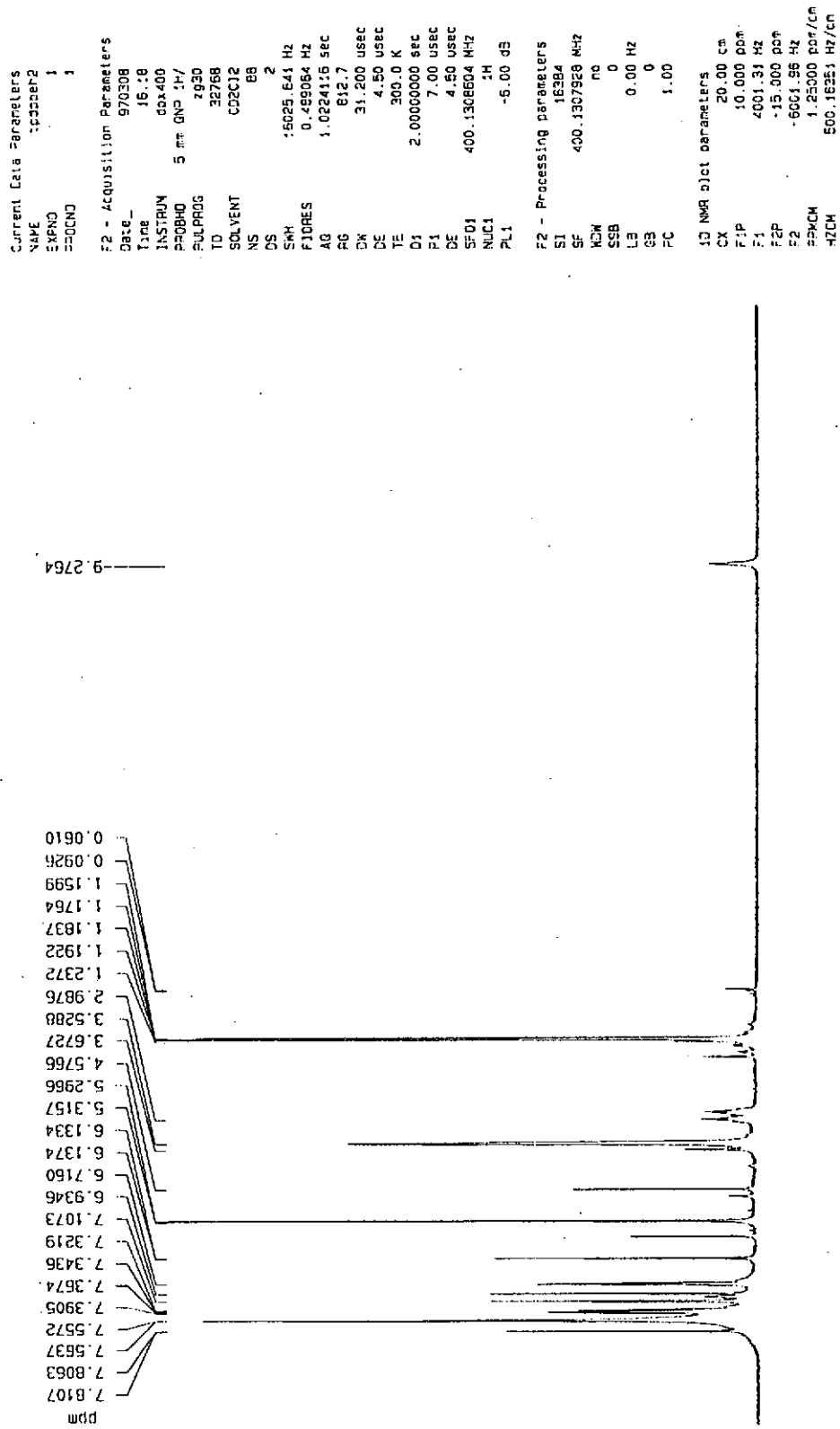


Figure 2.28. 400 MHz  $^1\text{H}$ -NMR spectrum of  $[\text{TpRu}(\text{H}_2)(\text{dppe})]\text{BF}_4$  (19)

TPRu (H2) (dppf) in CDCl3

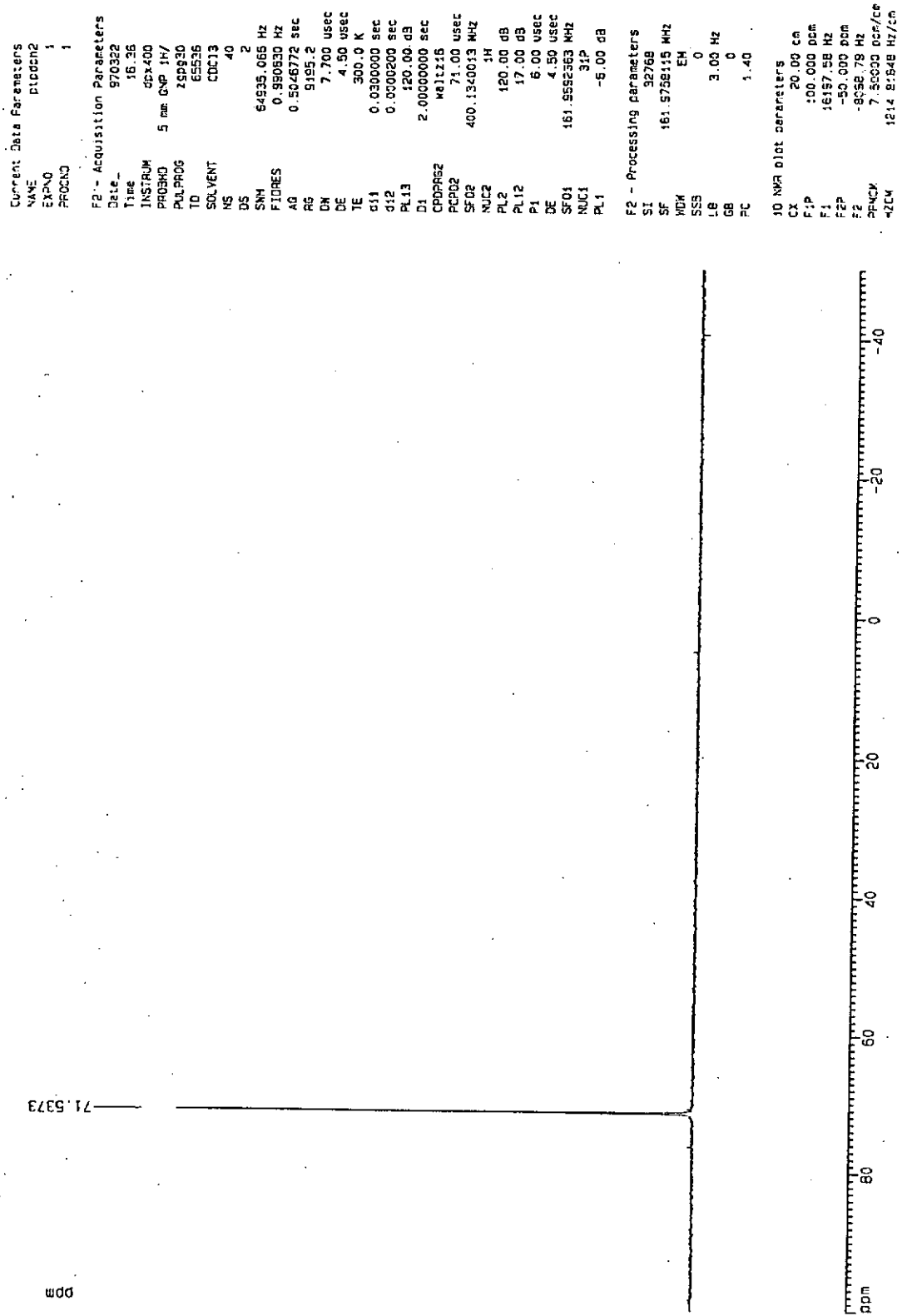


Figure 2.29. 161 MHz  $^{31}\text{P}\{^1\text{H}\}$ -NMR spectrum of  $[\text{TPRu}(\text{H}_2)(\text{dppf})]\text{BF}_4$  (19)

TpRu(HD) (dppe) in CD2Cl2

```

Current Data Parameters
NAME      :tpcd2bnc
EXPNO    : 1
PROCNO   : 1

F2 - Acquisition Parameters
Date_    : 951210
Time     : 23.43
INSTRUM  : cdx400
PROBHD   : 5 mm QNP 1H/
PULPROG  : zg30
TD       : 32768
SOLVENT  : Aceton
NS       : 215
DS       : 2
SWH       : 16025.641 Hz
FIDRES   : 0.489054 Hz
AQ       : 1.0224116 sec
RG       : 2289.8
DK       : 31.200 usec
DE       : 4.50 usec
TE       : 300.0 K
D1       : 1.00000000 sec
P1       : 5.80 usec
DE       : 4.50 usec
SFO1     : 400.1308004 MHz
NUC1     : 1H
PL1      : -6.00 dB

F2 - Processing parameters
SI       : 16384
SF       : 400.1300249 MHz
WDW      : no
SSB      : 0
LB       : 0.00 Hz
GB       : 0
PC       : 1.00

ID NMR plot parameters
CX       : 20.00 cm
F1P      : -8.500 ppm
F1       : -3461.11 Hz
F2P      : -10.500 ppm
F2       : -4201.37 Hz
PPMCK   : 0.10000 ppm/cm
GZCK    : 40.01300 Hz/cm
  
```

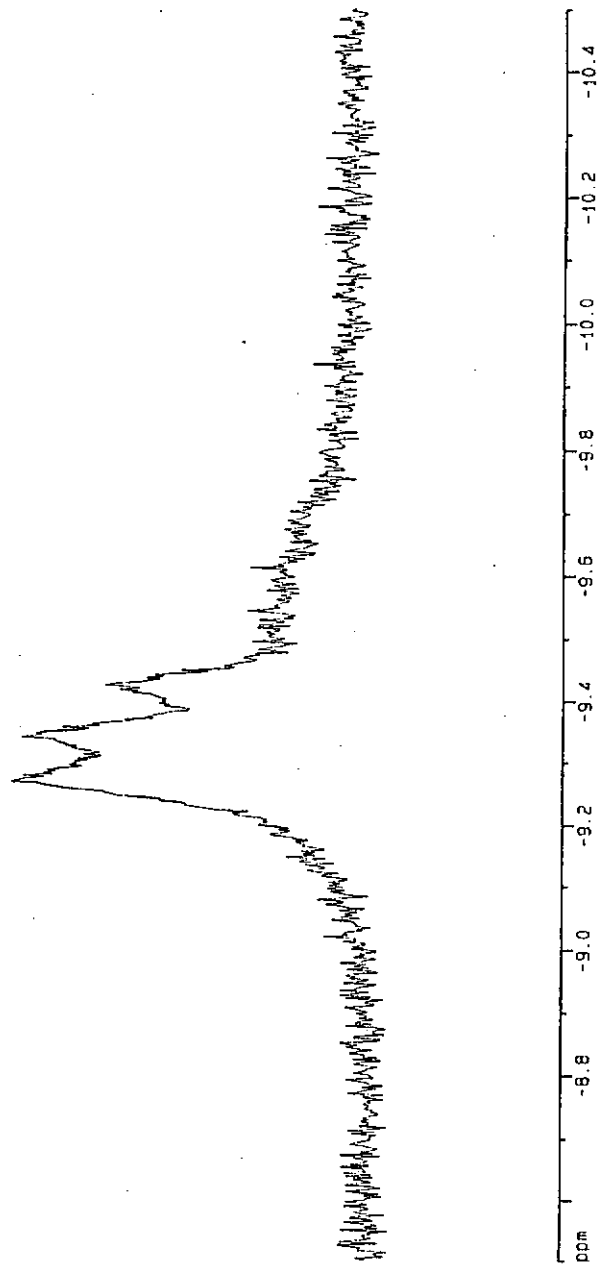


Figure 2.30. 400 MHz <sup>1</sup>H-NMR spectrum of [TpRu(HD)(dppe)]BF<sub>4</sub> (19-d<sub>1</sub>)

TpRu(H<sub>2</sub>)(CO)(PPh<sub>3</sub>) in CDCl<sub>2</sub> at -30°C

```

Current Data Parameters
NAME      TPCC10
EXPNO     8
PROCNO    1

F2 - Acquisition Parameters
Date_     970616
Time      17.32
INSTRUM   dx400
PROBHD    5 mm QNP 1H/
PULPROG   zgpg30
TD         32768
SOLVENT   CDCl2
NS         32
DS         0
SWH        16025.841 Hz
FIDRES     0.488064 Hz
AQ         1.0224116 sec
RG         71.8
CW         31.200 usec
DE         4.50 usec
TE         300.0 K
C1         1.00000000 sec
P1         9.50 usec
DE         4.50 usec
SFO1       400.1279993 MHz
NUC1       1H
PL1        -6.00 dB

F2 - Processing parameters
SI         16384
SF         400.1300150 MHz
WDW        EM
SSB        0
LB         0.30 Hz
GB         0
PC         1.00

1D NMR plot parameters
CX         20.00 cm
F1P        10.000 ppm
F1         4001.50 Hz
F2P        -20.000 ppm
F2         -8082.60 Hz
SFO1M      1.50000 ppm/cm
HZCM       600.19501 Hz/cm
  
```

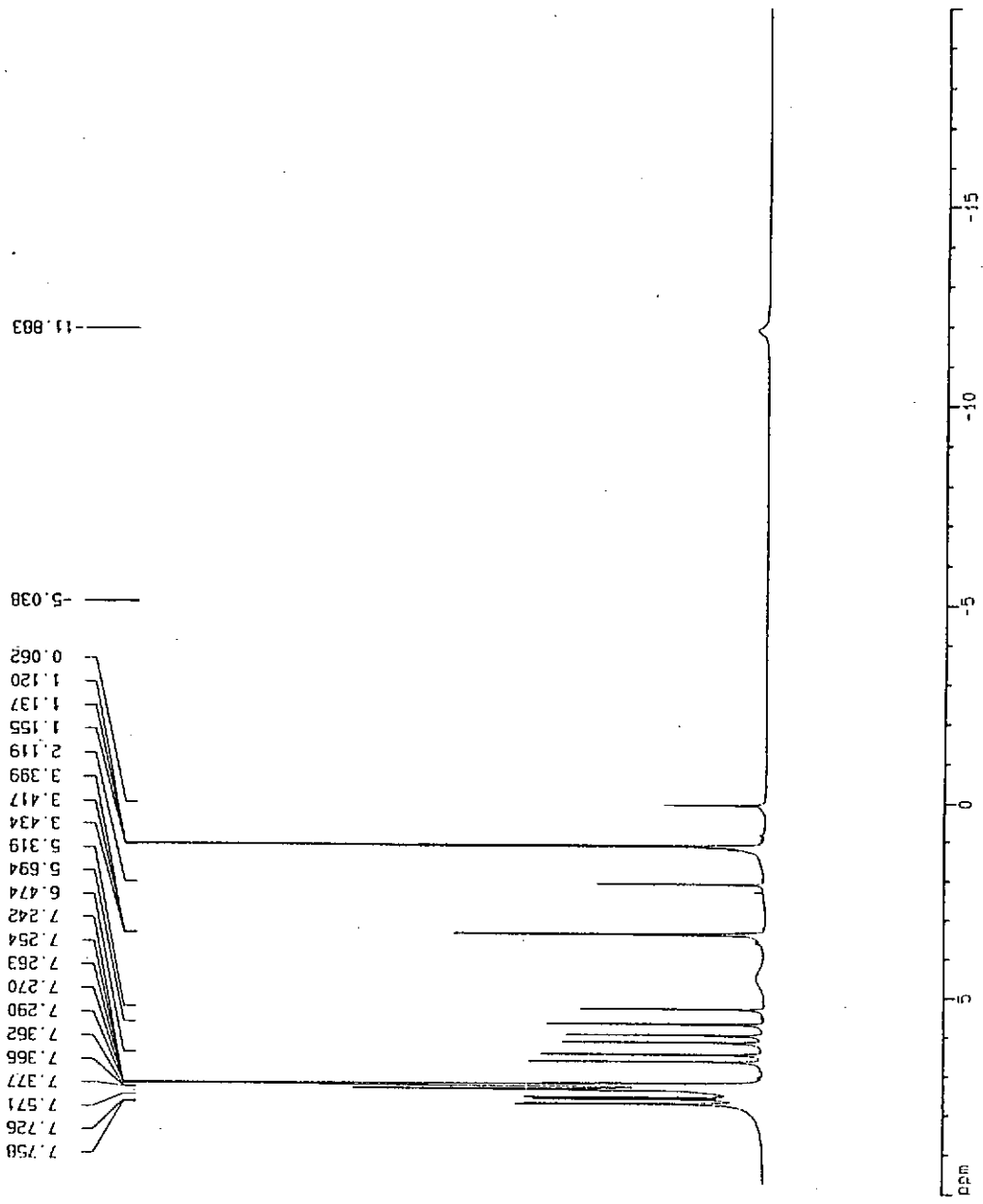


Figure 2.31. 400 MHz <sup>1</sup>H-NMR spectrum of [TpRu(H<sub>2</sub>)(CO)(PPh<sub>3</sub>)]BF<sub>4</sub> (20)

[[[PtRu(H<sub>2</sub>)(CO)(PPh<sub>3</sub>)<sub>3</sub>]]BF<sub>4</sub> (20)  
 -60°C, in CD<sub>2</sub>C1<sub>2</sub> (0.5ml)

```

Current Data Parameters
NAME          FIDOR2
EXPNO        1
PROCNO       1

F2 - Acquisition Parameters
Date_        970317
Time         11.53
INSTRUM      GDX400
PROBHD       5 mm GNP 1H/
PULPROG      zgpg30
TD           65535
SOLVENT      CDCl3
NS           120
DS           2
SMH          64935.065 Hz
FIDRES       0.980830 Hz
AQ           0.5248772 sec
RG           11585.2
DN           7.700 usec
DE           4.50 usec
TE           300.0 K
d11          0.0300000 sec
d12          0.0002000 sec
PL13         120.00 dB
D1           1.0000000 sec
CQPRG2       waltz16
PCPD2        71.00 usec
SF02         400.1340013 MHz
NUC2         1H
PL2          120.00 dB
PL12         17.00 dB
P1           6.00 usec
DE           4.50 usec
SF01         161.9582363 MHz
NUC1         31P
PL1          -6.00 dB

F2 - Processing Parameters
SI           32768
SF           161.9758113 MHz
PCX          EN
SSB          0
LB           3.00 Hz
GB           0
PC           1.40

1D NMR plot parameters
CX           20.00 cm
F1P         100.000 ppm
F1          16197.58 Hz
F2P         -50.000 ppm
F2          -8598.79 Hz
PFCYK       7.50000 pct/cm
AZCX        1214.51648 Hz/cx
  
```

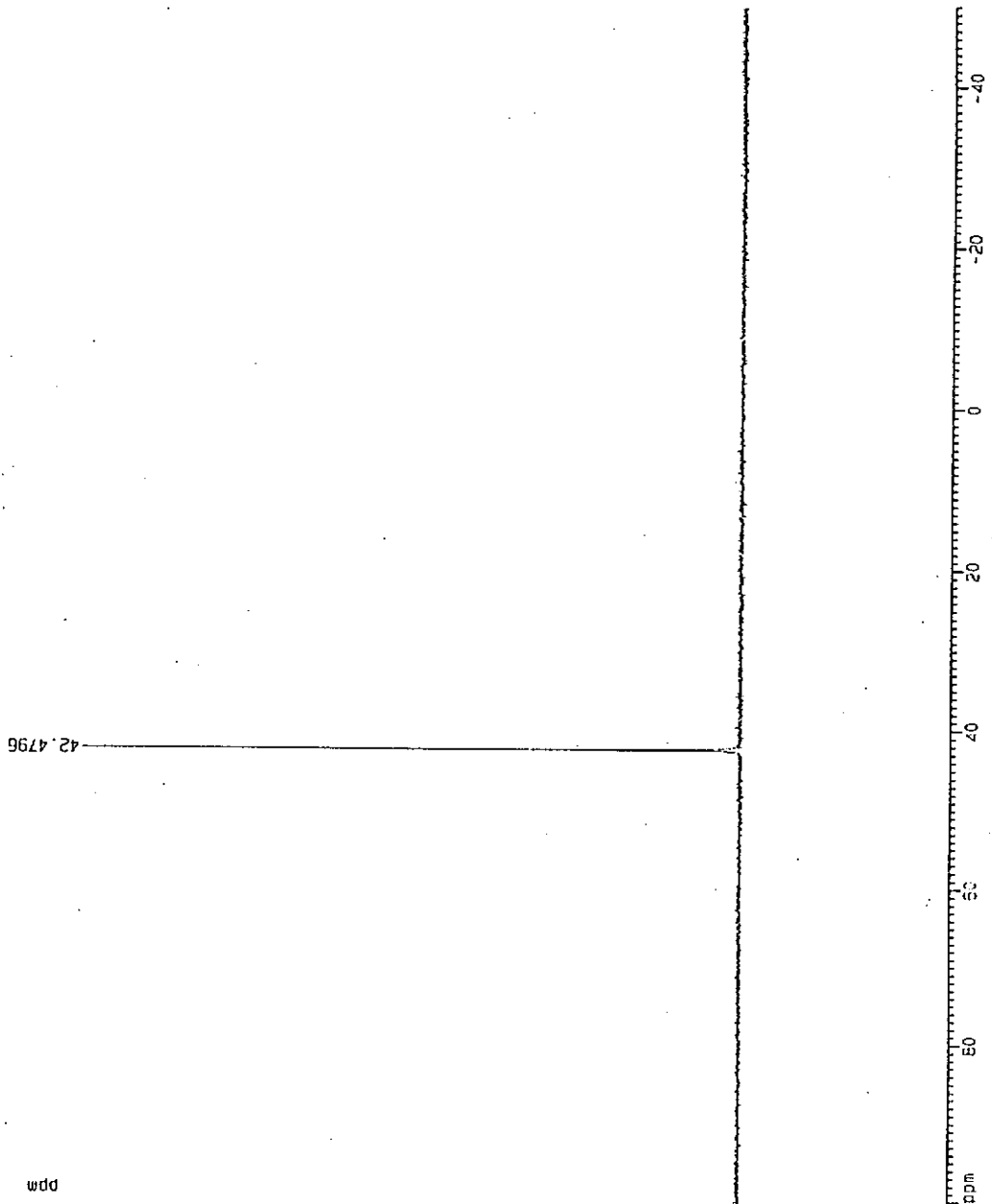


Figure 2.32. 161 MHz <sup>31</sup>P{<sup>1</sup>H}-NMR spectrum of [[[PtRu(H<sub>2</sub>)(CO)(PPh<sub>3</sub>)<sub>3</sub>]]BF<sub>4</sub> (20)



TpRuH(CO)(PPh<sub>3</sub>) + 2u<sub>3</sub>OBf<sub>4</sub> in CD<sub>2</sub>Cl<sub>2</sub> at -80°C

```

Current Data Parameters
NAME      TcCCFO
EXPNO    3
PROCNO   1

F2 - Acquisition Parameters
Date_    971021
Time     17.29
INSTRUM  cpz400
PROBHD   5 mm QNP 1H/
PULPROG  zg30
TD       32768
SOLVENT  CDCl3
NS       54
DS       0
SMH      16025.641 Hz
FIDRES   0.489054 Hz
AQ       1.0224116 sec
RG        128
DE       31.200 usec
TE       4.50 usec
D1       1.0000000 sec
DE       9.50 usec
DE       4.50 usec
SF01     400.1275953 MHz
NUC1     1H
PL1      -6.00 dB

F2 - Processing parameters
SI       16384
SF       400.1360111 MHz
RG       655
EM       0
SSB      0
LB       0.30 Hz
GB       0
PC       1.00

1D NMR list parameters
CX       20.00 cm
FIP      -4.000 bar
F1       -1600.52 Hz
F2P      -9.000 bar
F2       -3601.17 Hz
PASCAN   0.25000 bar/cm
HZCM     100.63250 Hz/cm
    
```

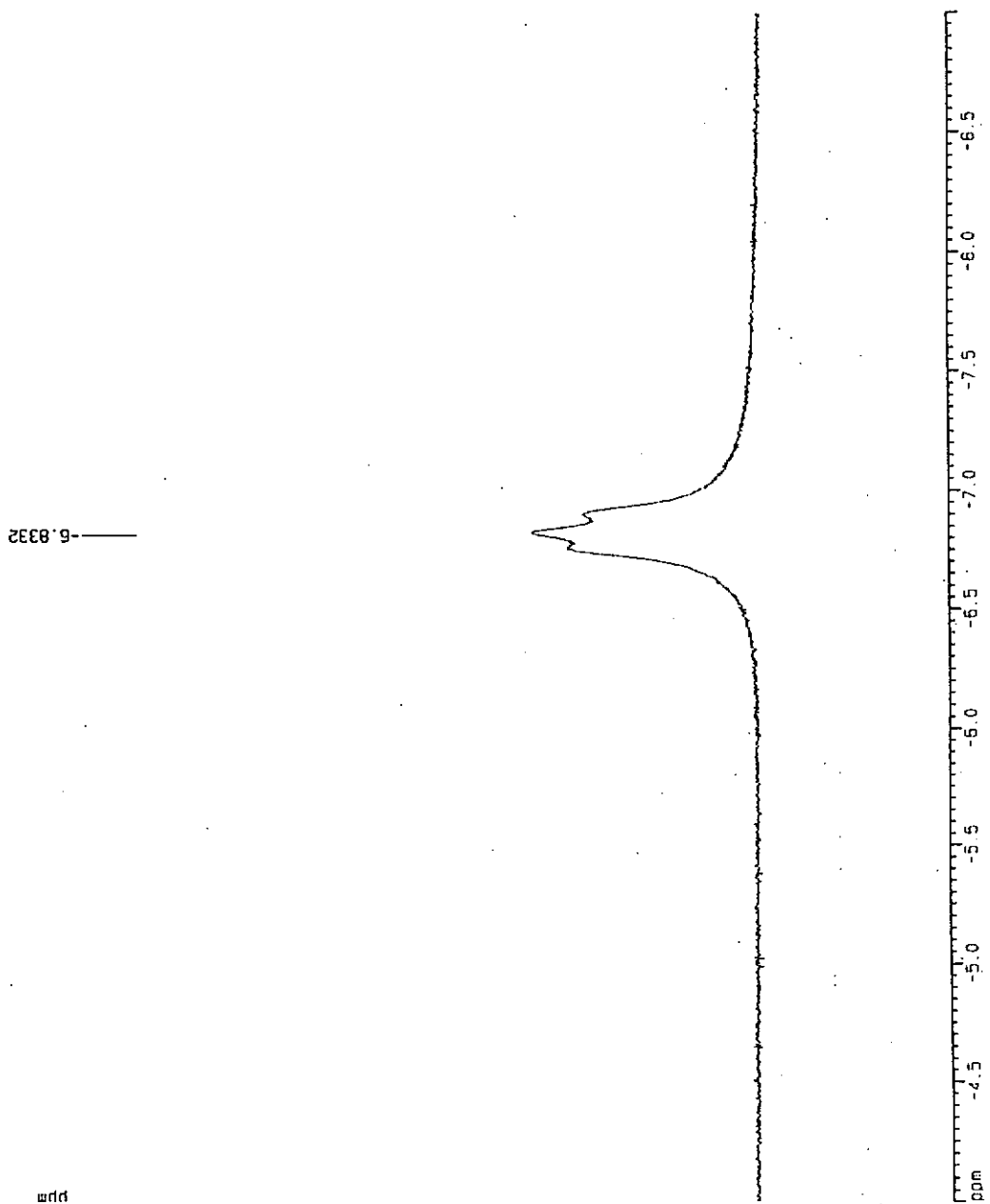


Figure 2.33. 400 MHz <sup>1</sup>H-NMR spectrum of [TpRu(HD)(CO)(PPh<sub>3</sub>)]BF<sub>4</sub> (20-d<sub>1</sub>)

H<sub>2</sub>O (H<sub>2</sub>O) (PPH<sub>3</sub>)<sub>2</sub> in CD<sub>2</sub>C1<sub>2</sub>

```

Current Data Parameters
NAME      HPE-20
EXPNO    2
PROCNO   1

F2 - Acquisition Parameters
Date_    990513
Time     15:40
INSTRUM  zg30400
PROBHD   5 mm QNP 1H/
PULPROG  zg30
TD        32768
SOLVENT  CD2C12
NS        256
DS        0
SWH       16025.641 Hz
FIDRES    0.489064 Hz
AQ        1.0224116 sec
RG         1145.4
CW        31.200 usec
DE        4.50 usec
TE        300.0 K
D1        1.00000000 sec
P1        9.50 usec
DE        4.50 usec
SF01      400.1278553 MHz
NUC1      1H
PL1       -6.00 dB

F2 - Processing parameters
SI        15384
SF        400.1300150 MHz
WDW       EM
SSB       0
LB        0.30 Hz
GB        0
PC        1.00

1D NMR plot parameters
CX        20.00 cm
ZP        9.000 ppm
F1        5261.04 Hz
F2P       -6.500 ppm
F2        -260.07 Hz
F2FCH     0.46500 ppm/cm
AQCM      :70.65525 Hz/cm
  
```

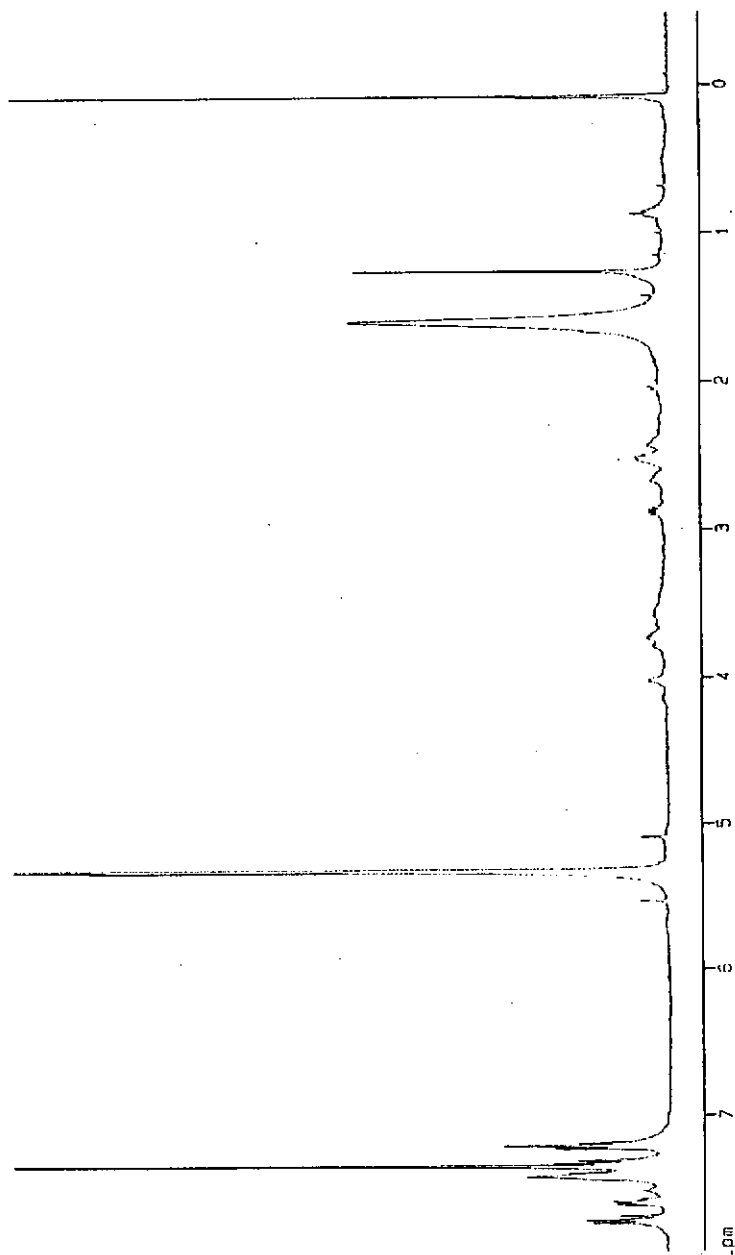


Figure 2.34. 400 MHz <sup>1</sup>H-NMR spectrum of [<sup>1</sup>H-CnRu(H<sub>2</sub>O)(PPh<sub>3</sub>)<sub>2</sub>](BF<sub>4</sub>)<sub>2</sub> (9)

HcN (H2O) (PPn3)2 in CD2Cl2

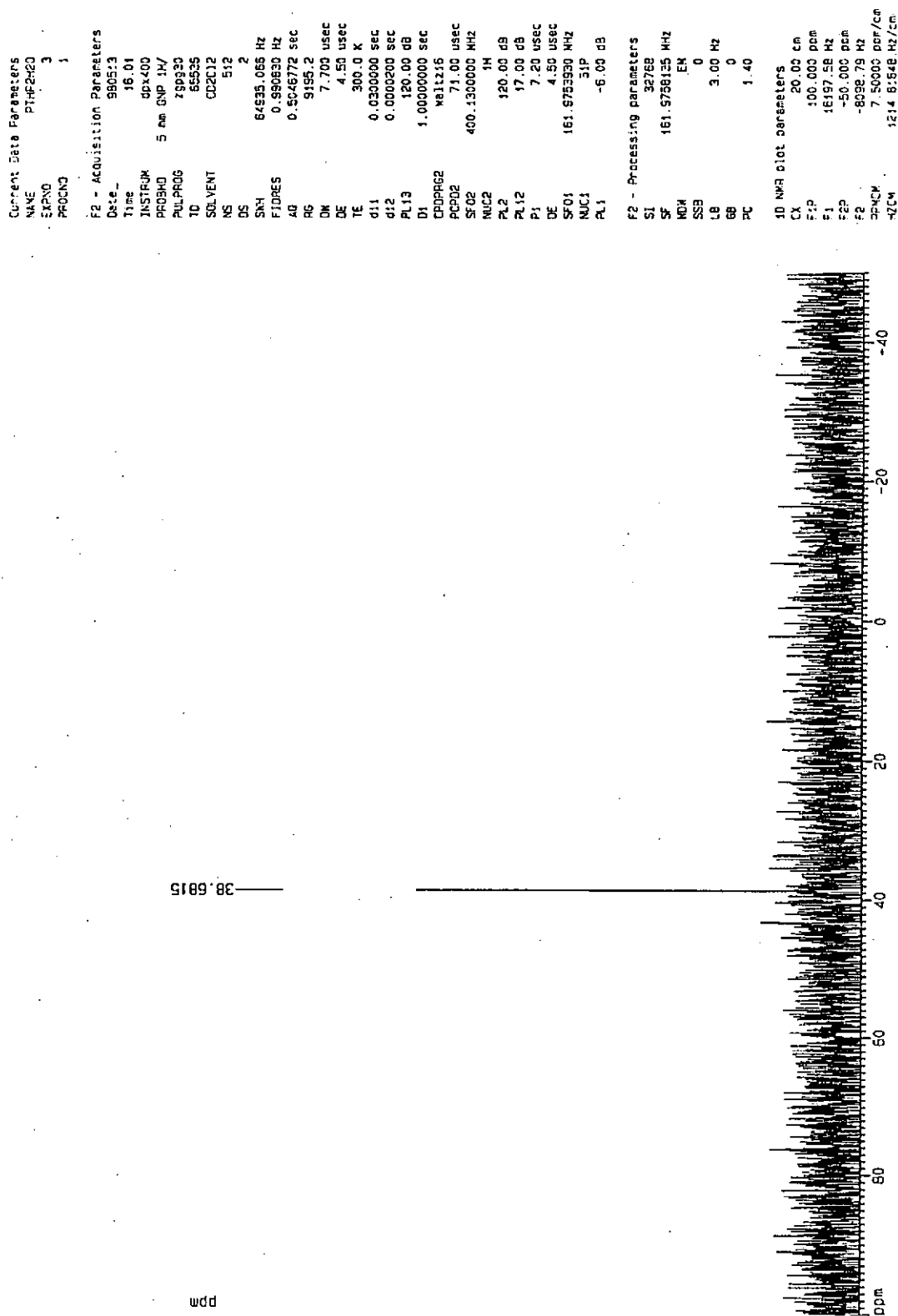


Figure 2.35. 161 MHz  $^{31}\text{P}\{^1\text{H}\}$ -NMR spectrum of  $[\text{HcNRu}(\text{H}_2\text{O})(\text{PPh}_3)_2](\text{BF}_4)_2$  (9)

SIU MAN, HCNP2H2O, CONE 30V, 16-Jun-1998  
022 13 (0.502) Cm (3:36)

Scan ES+  
1.58e5

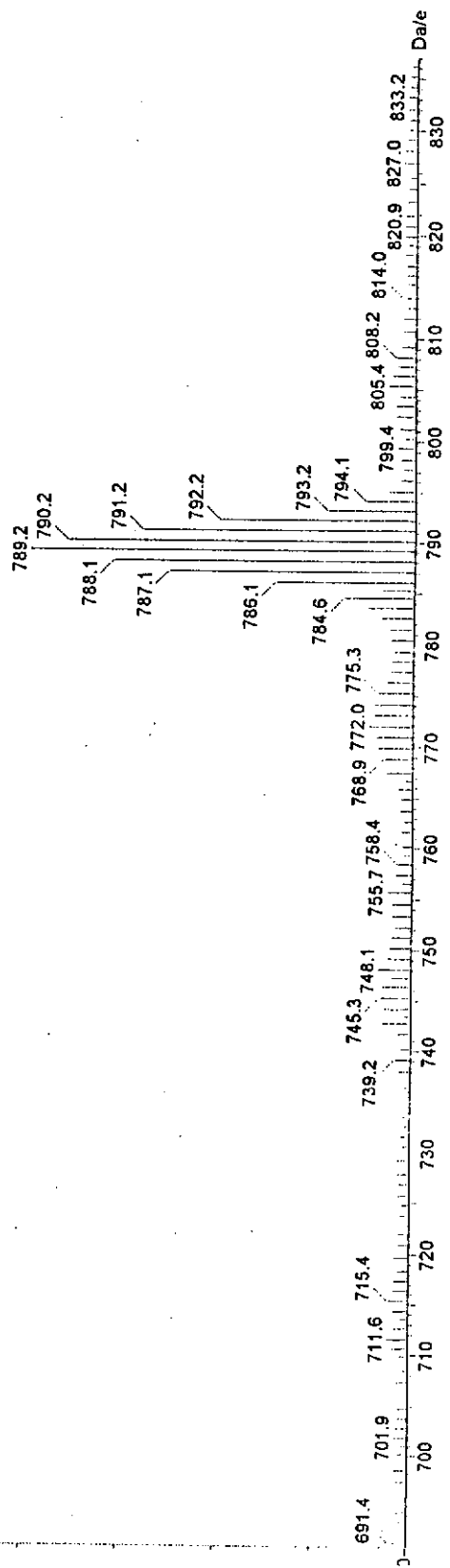


Figure 2.36. FAB mass spectrum of  $[^1\text{H}]\text{CnRu}(\text{H}_2\text{O})(\text{PPh}_3)_2](\text{BF}_4)_2$  (9)

$\text{HCnRuH}(\text{PPh}_3)_2 + \text{RuHC}(\text{dppp})_2$  in  $\text{CD}_2\text{Cl}_2$  after addition of 1.5  $\mu\text{l}$   $\text{HBF}_4$  for 0.5 hr

Current Data Parameters  
 NAME ptab2h  
 EXPNO 4  
 PROCNO 1

F2 - Acquisition Parameters  
 Date\_ 970501  
 Time 17.58  
 INSTRUM ddx400  
 PROBHD 5 mm QNP 1H/  
 PULPROG zg30  
 TD 32768  
 SOLVENT CDCl2  
 NS 320  
 DS 0  
 SWH 16025.641 Hz  
 FIDRES 0.489064 Hz  
 AQ 1.022415 sec  
 RG 181  
 DM 31.200 usec  
 DE 4.50 usec  
 TE 300.0 K  
 T1 1.0000000 sec  
 P1 9.50 usec  
 DE 4.50 usec  
 SFO1 400.1275993 MHz  
 NUC1 1H  
 PL1 -6.00 dB

F2 - Processing parameters  
 SI 16384  
 SF 400.1300150 MHz  
 XDW EM  
 SSB 0  
 LB 0.30 Hz  
 GB 0  
 PC 1.00

1D NMR pict parameters  
 CX 20.00 cm  
 F1P -8.000 ppm  
 F1 -3201.04 Hz  
 F2P -20.000 ppm  
 F2 -5002.60 Hz  
 PPMCM 0.60000 ppm/cm  
 HZCM 240.07800 Hz/cm

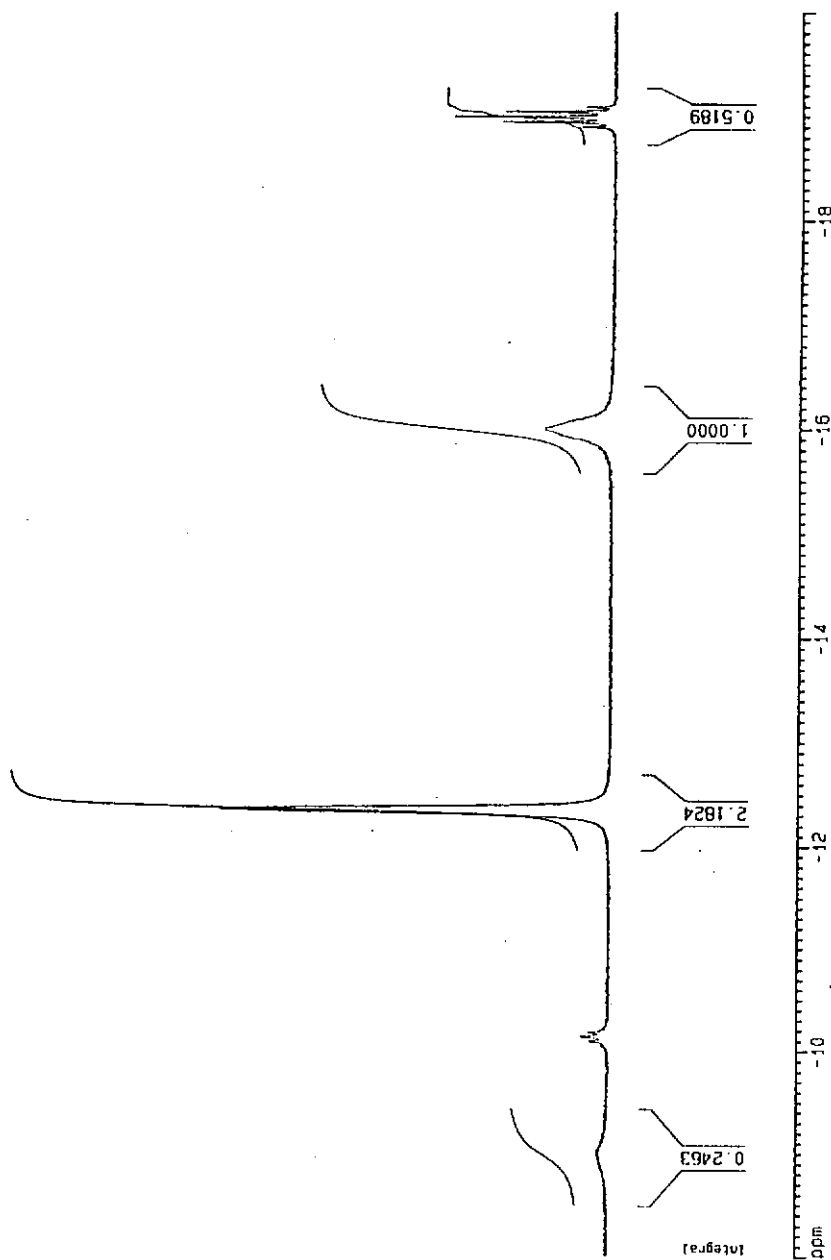


Figure 2.37. The  $^1\text{H}$ -NMR spectra of  $[\text{H}^+\text{CnRuH}(\text{PPh}_3)_2]\text{BF}_4$  (1) and  $\text{RuHCl}(\text{dppp})_2 + \text{HBF}_4 \cdot \text{Et}_2\text{O}$  in  $\text{CD}_2\text{Cl}_2$

HC≡RuH(CO) (PPh<sub>3</sub>)<sub>2</sub> + 0.5M HBF<sub>4</sub> in CD<sub>2</sub>Cl<sub>2</sub> at -80°C

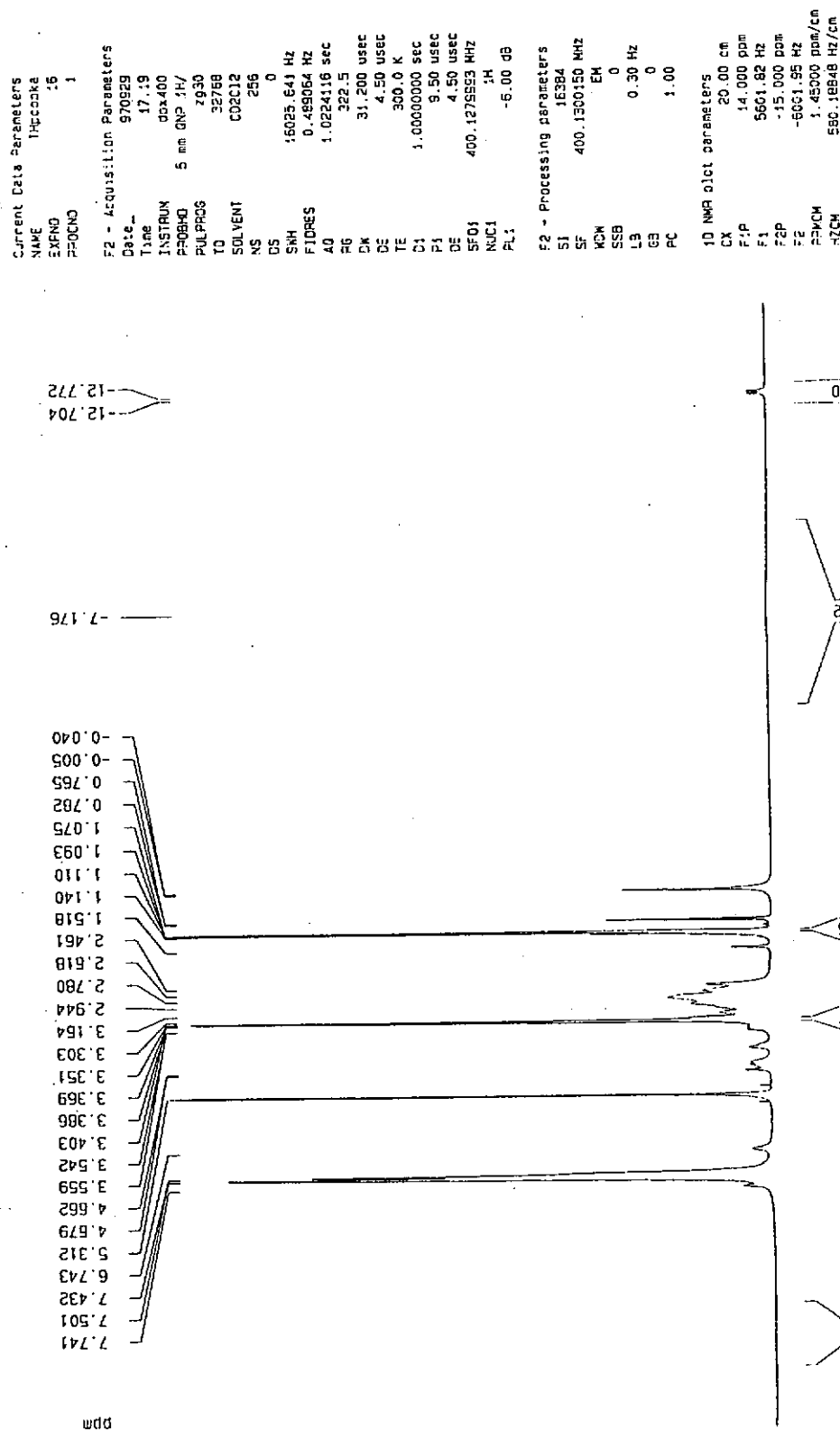


Figure 2.38. The <sup>1</sup>H-NMR spectra of [<sup>13</sup>C]nRuH(CO)(PPh<sub>3</sub>)<sub>2</sub>]BF<sub>4</sub> (2) and HBF<sub>4</sub>·Et<sub>2</sub>O in CD<sub>2</sub>Cl<sub>2</sub> -80 °C

MeCnRuH(dppe) + RuHCl(dppe)<sub>2</sub> in CD<sub>2</sub>Cl<sub>2</sub> after addition of  
1.5u) HBF<sub>4</sub> for 0.5hr

```

Current Data Parameters
NAME      Platadpe
EXPNO     5
PROCNO    1

F2 - Acquisition Parameters
Date_     970502
Time      16.14
INSTRUM   cp1400
PROBHD    5 mm QNP 1H/
PULPROG   zg30
TD         32768
SOLVENT   CD2C12
NS         1024
DS         0
SWH        16025.641 Hz
FIDRES     0.489064 Hz
AQ         1.0224116 sec
RG          161
CW         31.200 usec
DE         4.50 usec
TE         300.0 K
D1         1.00000000 sec
P1         9.50 usec
DE         4.50 usec
SFO1      400.1278993 MHz
NUC1       1H
PL1        -6.00 dB

F2 - Processing parameters
SI         16394
SF         400.1300140 MHz
WDW        EM
SSB        0
LB         0.30 Hz
GB         0
PC         1.00

1D NMR plot parameters
CX         20.00 cm
F1P        -8.000 ppm
F1         -3201.64 Hz
F2P        -20.000 ppm
F2         -8002.60 Hz
PQ/MCH     0.60000 ppm/cm
HZ/MCH     240.07800 Hz/cm
  
```

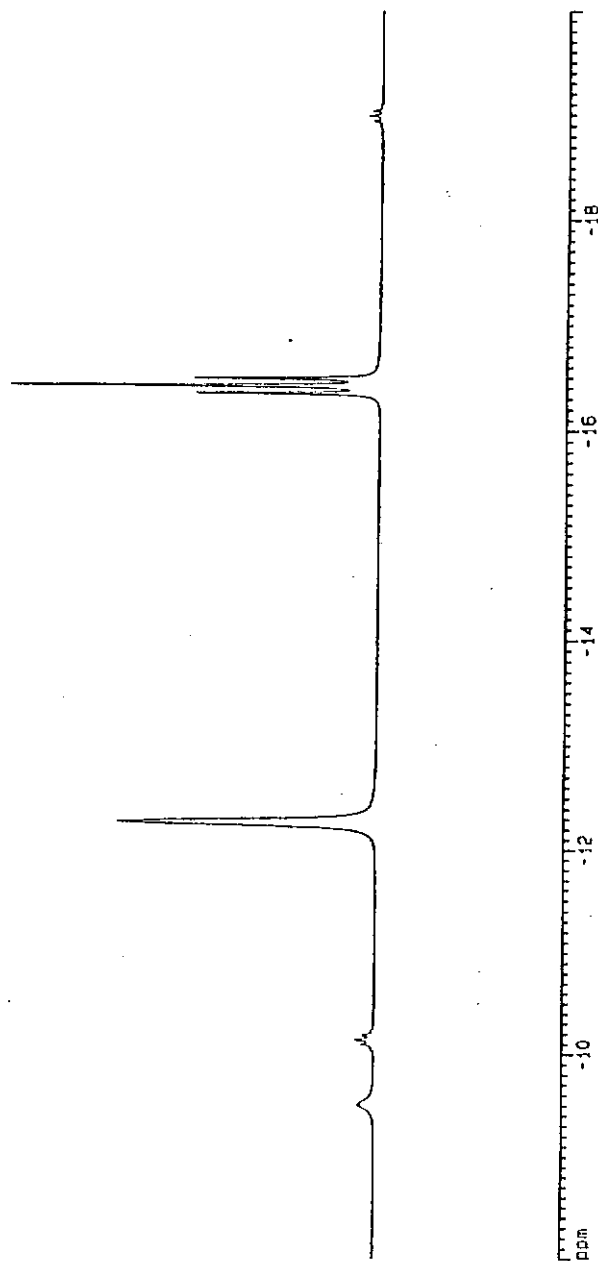


Figure 2.39. The <sup>1</sup>H-NMR spectra of [<sup>13</sup>CnRuH(dppe)](CF<sub>3</sub>SO<sub>3</sub>) (3) and RuHCl(dppe)<sub>2</sub> + HBF<sub>4</sub>·Et<sub>2</sub>O in CD<sub>2</sub>Cl<sub>2</sub>

MeCnRuHCO (ppm) + 4.5(J) HBF<sub>4</sub> in CD<sub>2</sub>Cl<sub>2</sub> at -30°C

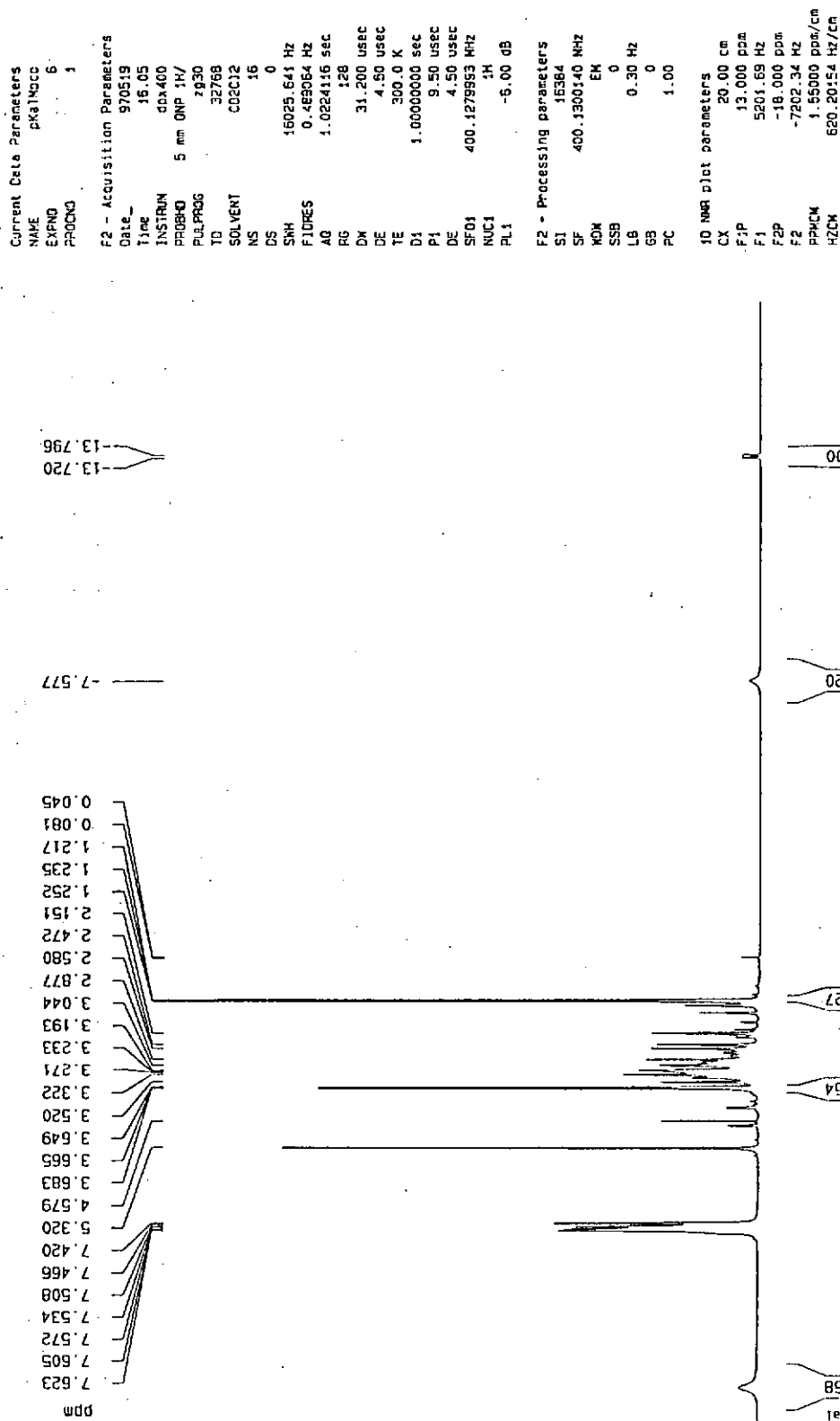


Figure 2.40. The <sup>1</sup>H-NMR spectra of [<sup>1</sup>H]CnRuH(CO)(PPh<sub>3</sub>)<sub>2</sub>]PF<sub>6</sub> (4) and HBF<sub>4</sub>.Et<sub>2</sub>O in CD<sub>2</sub>Cl<sub>2</sub> -30 °C



TpRuH(PPh<sub>3</sub>)<sub>2</sub> + CpRuH(dppm) + 2u1 HBF<sub>4</sub> in CD<sub>2</sub>Cl<sub>2</sub>

```

Current Data Parameters
NAME      : kkatapp2
EXPNO    : 2
PROCNO   : 1

F2 - Acquisition Parameters
Date_    : 9/11/8
Time     : 17.20
INSTRUM  : dx400
PROBHD   : 5 mm QNP 1H/
PULPROG  : zgpg
TD       : 2630
TO       : 32768
SOLVENT  : CD2Cl2
NS       : 128
DS       : 0
SWH      : 6025.541 Hz
FIDRES   : 0.4882064 Hz
AQ       : 1.028416 sec
RG       : 362
DN       : 31.200 usec
DE       : 4.50 usec
TE       : 300.0 K
D1       : 1.00000000 sec
P1       : 9.50 usec
DE       : 4.50 usec
SFO1     : 400.1279993 MHz
NUC1     : 1H
PL1      : -6.00 dB

F2 - Processing parameters
SI       : 16384
SF       : 400.1300140 MHz
WDW      : EM
SSB      : 0
LB       : 0.30 Hz
GB       : 0
PC       : 1.00

1D NMR plot parameters
CX       : 20.00 cm
F1P     : -6.052 ppm
F1      : -2421.49 Hz
F2P     : -15.988 ppm
F2      : -6401.37 Hz
P1MCM   : 0.49732 ppm/Hz
HZCM    : 95.93368 Hz/cm
  
```

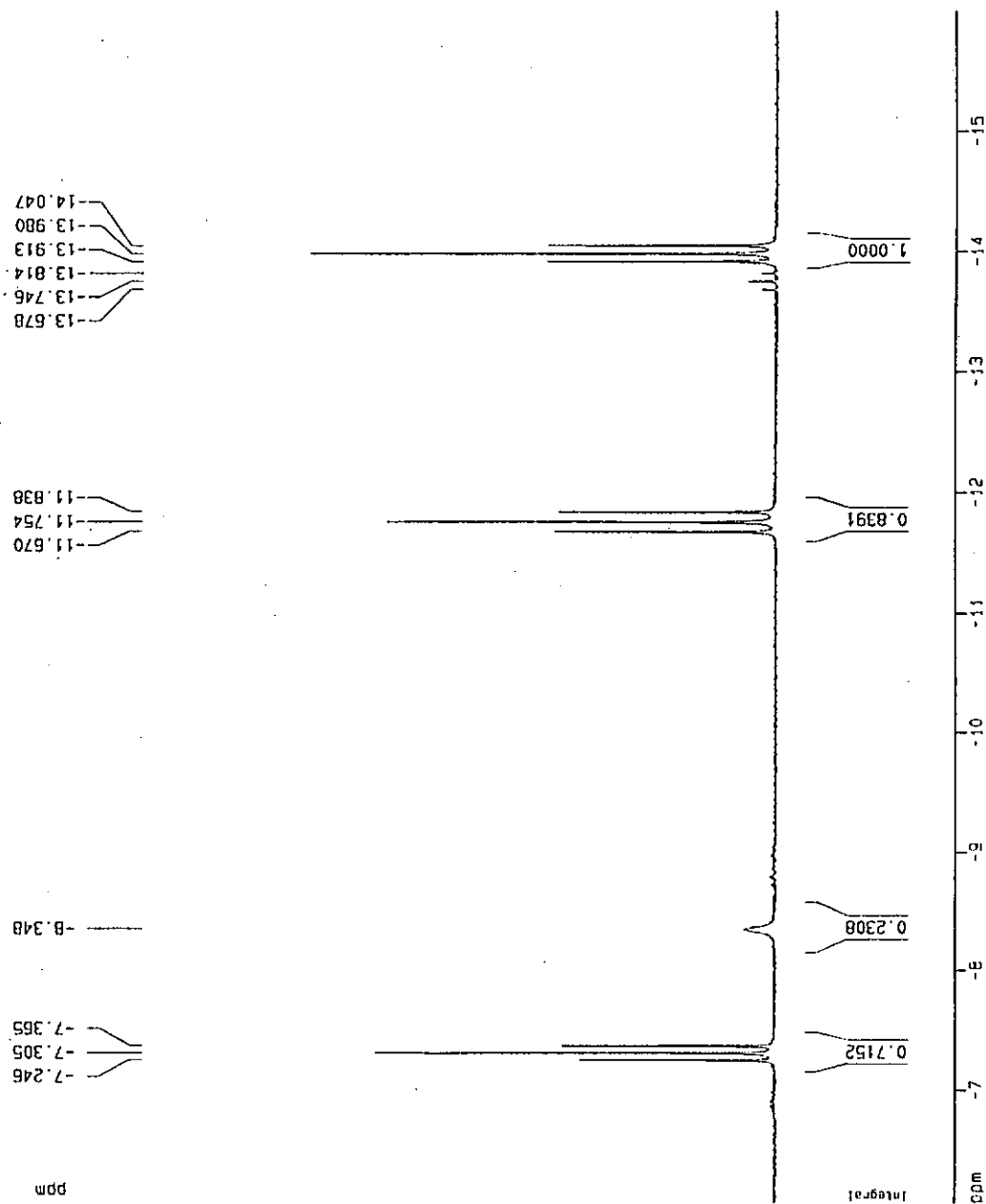


Figure 2.41. The <sup>1</sup>H-NMR spectra of TpRuH(PPh<sub>3</sub>)<sub>2</sub> (**12**) and CpRuH(dppm) + HBF<sub>4</sub>·Et<sub>2</sub>O in CD<sub>2</sub>Cl<sub>2</sub>

TpRuH(CH3CN)(PPh3)2 + CpRuH(PPh3)2 + 1.5 ul HBF4 in CD2Cl2  
at -35°C

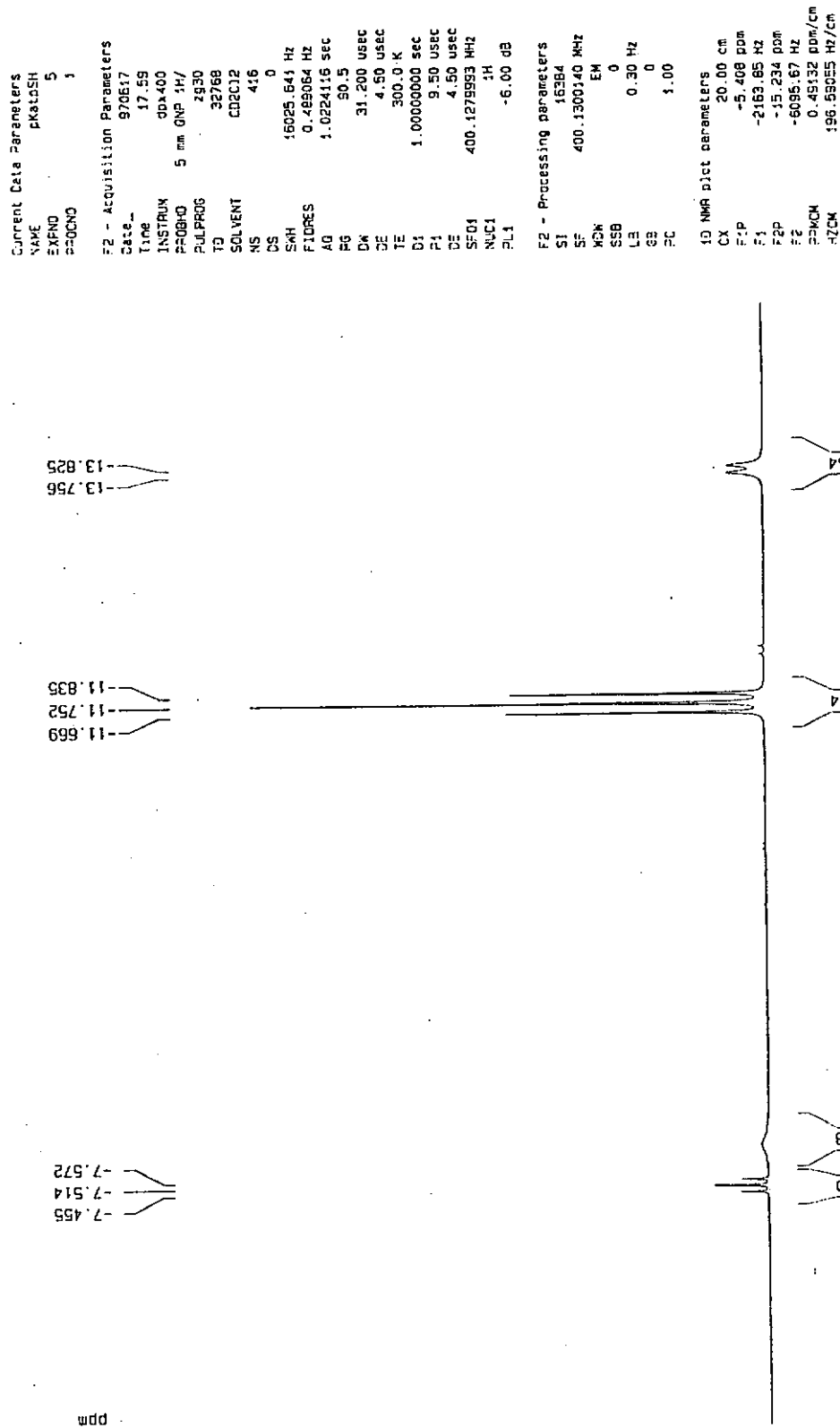


Figure 2.42. The  $^1\text{H}$ -NMR spectra of  $\text{TpRuH}(\text{CH}_3\text{CN})(\text{PPh}_3)_2$  (**13**) and  $\text{CpRuH}(\text{PPh}_3)_2 + \text{HBF}_4 \cdot \text{Et}_2\text{O}$  in  $\text{CD}_2\text{Cl}_2$  -35 °C

$\text{TpRuH}(\text{dppe}) + \text{CpRuH}(\text{dppm}) + 2 \text{ u} \text{ HBF}_4 \text{ in } \text{CD}_2\text{Cl}_2$

```

Current Data Parameters
NAME          PKatodpde
EXPNO         4
=====      1

F2 - Acquisition Parameters
Date_         970606
Time          16:58
INSTRUM      ddx400
PROBHD       5 mm QNP 1H/
PULPROG      zg30
TD            32768
SOLVENT      CD2Cl2
NS            256
DS            0
SWH           16025.841 Hz
FIDRES        0.489064 Hz
AQ            1.0224116 sec
RG            256
DK            31.200 usec
DE            4.50 usec
TE            300.0 K
D1            1.00000000 sec
D2            9.50 usec
D3            4.50 usec
SF01         400.1279993 MHz
NUC1          1H
PL1           -6.00 dB

F2 - Processing parameters
SI            16384
SF            400.1300150 MHz
RG            EM
SSB           0
LB            0.30 Hz
GB            0
PC            1.00

1D NMR plot parameters
CX            20.00 cm
F1P           -3.261 ppm
F1            -1304.75 Hz
F2P           -17.474 ppm
F2            -6891.63 Hz
=====      0.71065 ppm/cm
=====      264.35422 Hz/cm
  
```

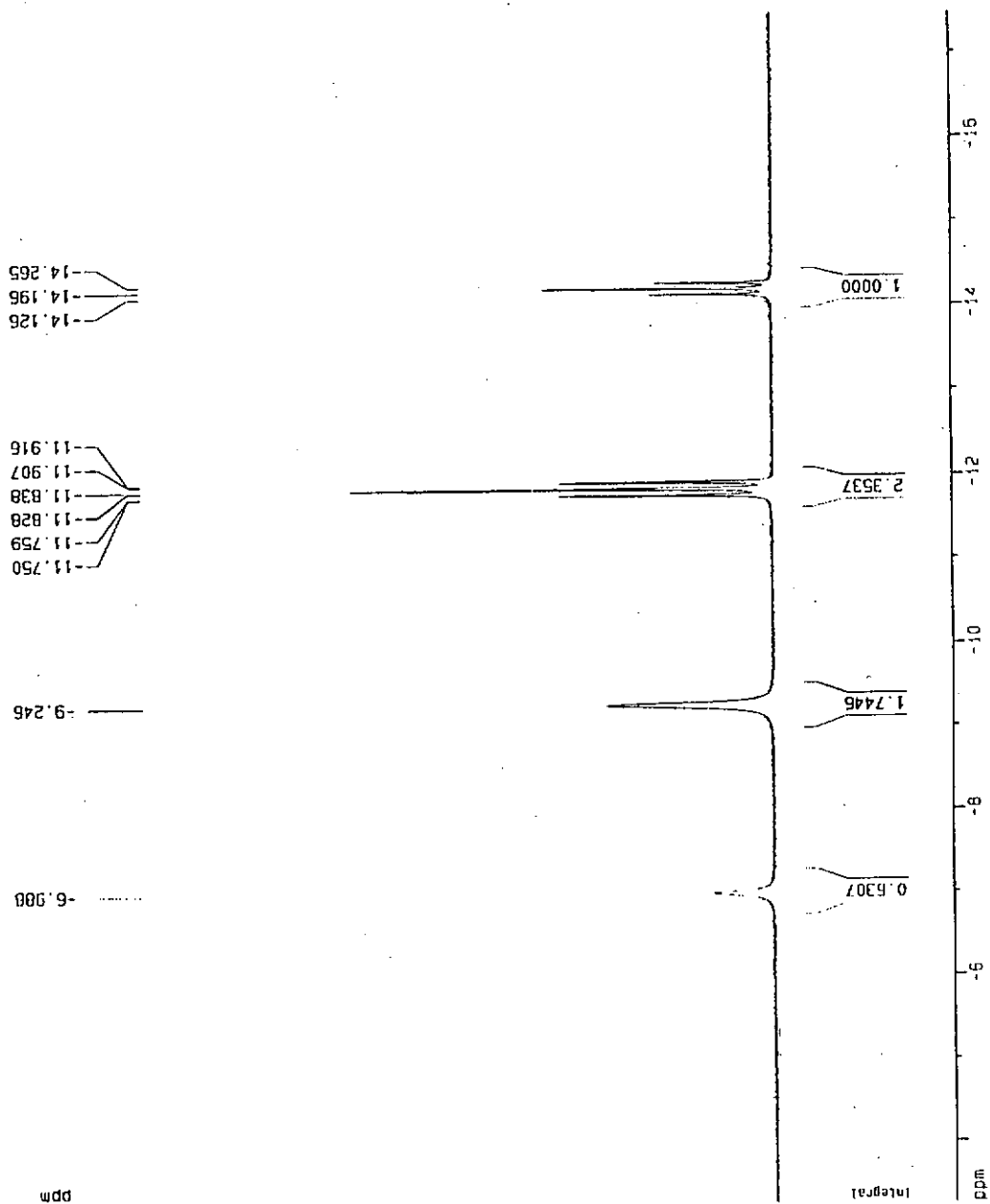


Figure 2.43. The  $^1\text{H}$ -NMR spectra of  $\text{TpRuH}(\text{dppe})$  (**14**) and  $\text{CpRuH}(\text{dppm}) + \text{HBF}_4 \cdot \text{Et}_2\text{O}$  in  $\text{CD}_2\text{Cl}_2$

HCnRuH(CO)(PPh<sub>3</sub>) + TpRuH(CO)(PPh<sub>3</sub>) + 0.6u1 HBF<sub>4</sub> in CD<sub>2</sub>Cl<sub>2</sub> at -80°C

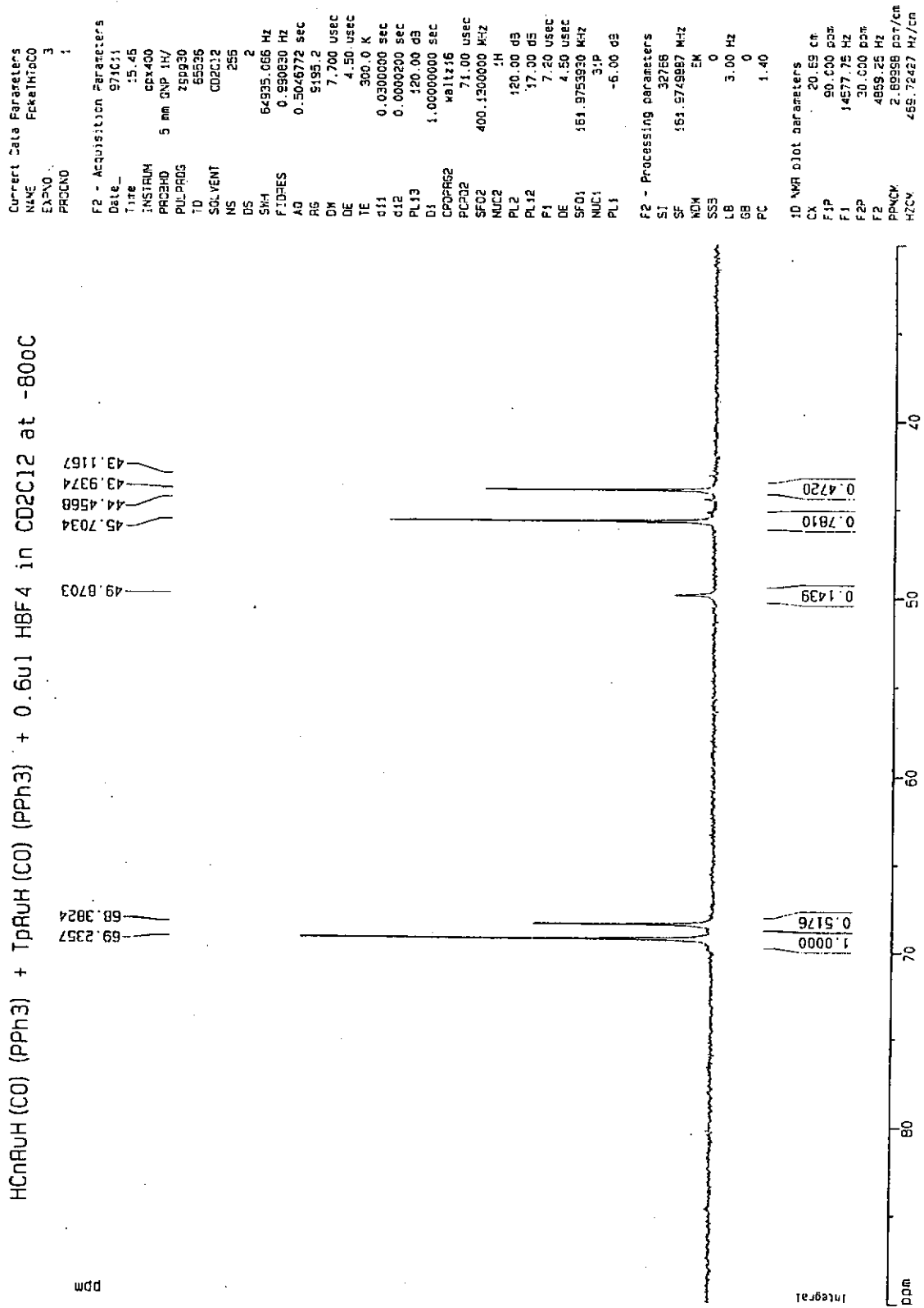


Figure 2.44. The <sup>31</sup>P{<sup>1</sup>H}-NMR spectra of TpRuH(CO)(PPh<sub>3</sub>) (15) and [<sup>1</sup>H]CnRuH(CO)(PPh<sub>3</sub>)<sub>2</sub>]PF<sub>6</sub> (4) + HBF<sub>4</sub>·Et<sub>2</sub>O in CD<sub>2</sub>Cl<sub>2</sub>

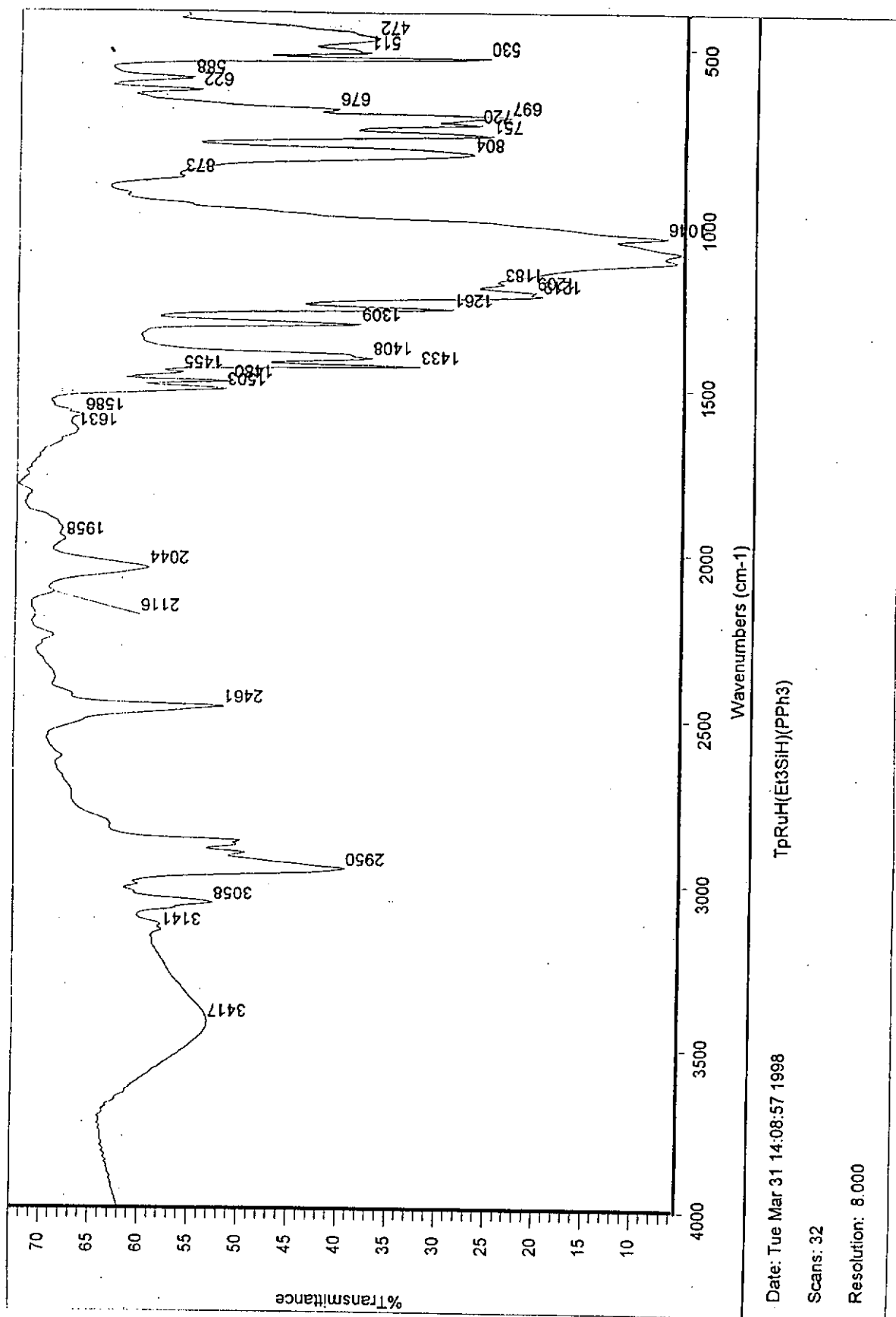


Figure 3.1. Infra-red spectrum of TpRuH(HSiEt<sub>3</sub>)(PPh<sub>3</sub>) (21a) in KBr disc

TpRuH(HSiEt<sub>3</sub>)(PPh<sub>3</sub>) in d<sub>6</sub>-tHF

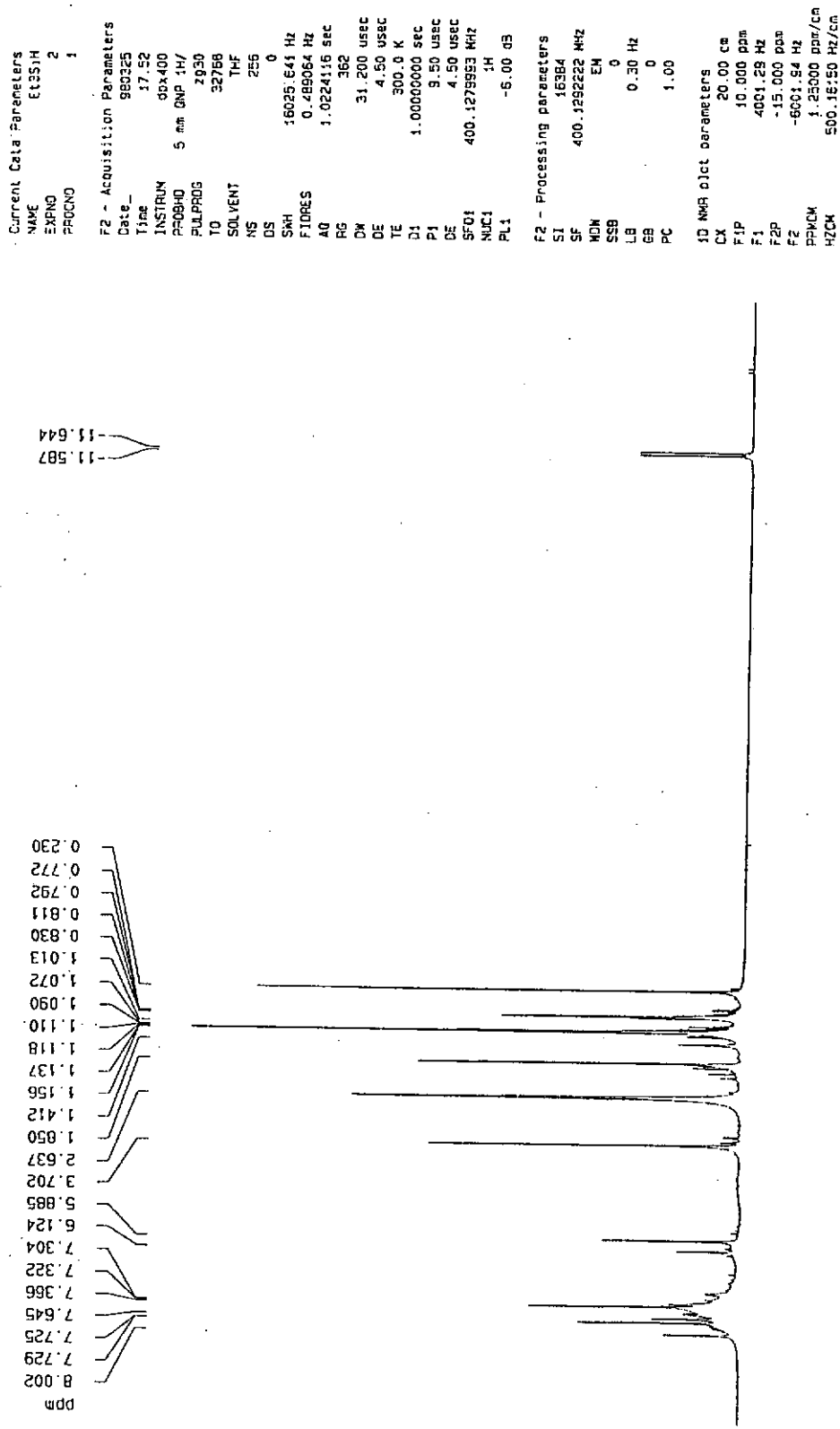


Figure 3.2(a). 400 MHz <sup>1</sup>H-NMR spectrum of TpRuH(HSiEt<sub>3</sub>)(PPh<sub>3</sub>) (21a)

TPRUH (HS)Et3 (PPH3) in d8-thf

Current Data Parameters  
 NAME ET3TH  
 EXPNO 2  
 PROCNO 1

F2 - Acquisition Parameters  
 Date\_ 980325  
 Time 17.52  
 INSTRUM dpx400  
 PROBHD 5 mm QNP 1H/  
 PULPROG zg30  
 TD 32768  
 SOLVENT THF  
 NS 256  
 DS 0  
 SWH 16025.641 Hz  
 FIDRES 0.489064 Hz  
 AQ 1.0224116 sec  
 RG 382  
 DK 31.200 usec  
 DE 4.50 usec  
 TE 300.0 K  
 D1 1.00000000 sec  
 P1 9.50 usec  
 DE 4.50 usec  
 SFO1 400.1279953 MHz  
 RUC1 1H  
 PL1 -6.00 dB

F2 - Processing parameters  
 SI 16384  
 SF 400.1262222 MHz  
 WDW EM  
 SSB 0  
 LB 0.30 Hz  
 GB 0  
 PC 1.00

1D NMR plot parameters  
 CX 20.00 cm  
 F1P -10.500 ppm  
 F1 -4201.35 Hz  
 F2P -12.500 ppm  
 F2 -5001.62 Hz  
 PPHCK 0.10000 ppm/cm  
 HZCK 40.01252 Hz/cm

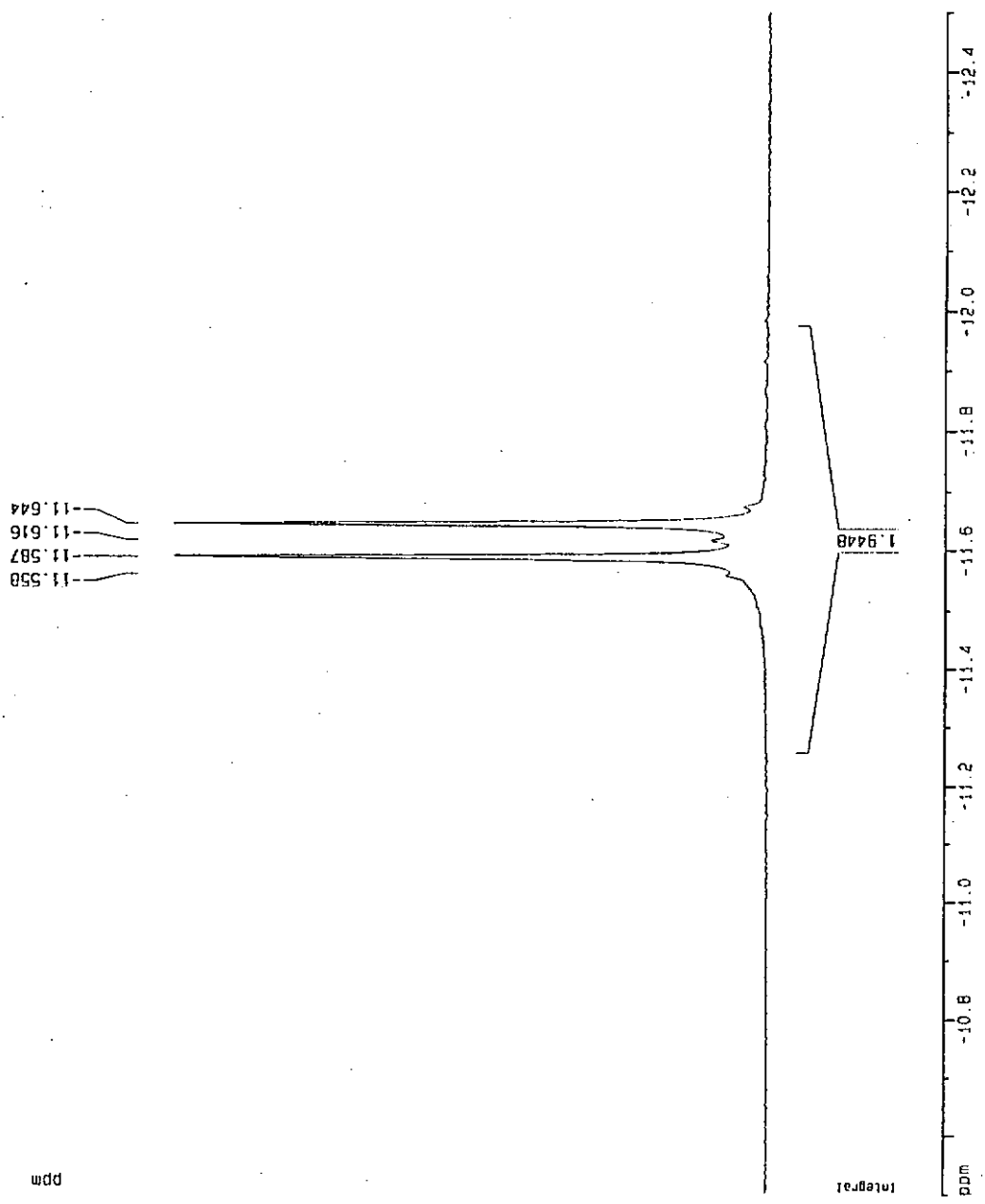


Figure 3.2(b). Expanded upfield region of Figure 3.2(a)

TpRuH(HSiEt<sub>3</sub>)(PPh<sub>3</sub>) in d<sub>8</sub>-thf

```

Current Data Parameters
NAME          TpRuH
EXPNO        2
PROCNO       1

F2 - Acquisition Parameters
Date_        960325
Time         17.40
INSTRUM      gpc400
PROBHD       5 mm QNP 1H/
PULPROG      zgpg30
TD           65536
SOLVENT      THF
NS           256
DS           2
SINH         64925.066 Hz
FIDRES       0.590630 Hz
AQ           0.504672 sec
RG           9195.2
DM           7.700 usec
DE           4.50 usec
TE           300.0 K
c11          0.0300000 sec
c12          0.0000200 sec
PL13         120.00 dB
D1           1.0000000 sec
CPDPRG2      waltz16
PCPD2        71.00 usec
SF02         400.1300000 MHz
NUC2         1H
PL2          120.00 dB
PL12         17.00 dB
P1           7.20 usec
DE           4.50 usec
SF01         161.9759930 MHz
NUC1         31P
PL1          -6.00 dB

F2 - Processing parameters
SI           32768
SF           161.9759935 MHz
WDW          EM
SSB          0
LB           3.00 Hz
GB           0
PC           1.40

ID NMR dict parameters
CX           20.55 CF
F1P          100.000 dBm
F1           16197.58 Hz
F2P          -50.000 dBm
F2           -6096.75 Hz
PP4CY       7.24995 dBm/CM
HZCY        1174.31666 Hz/CF
    
```

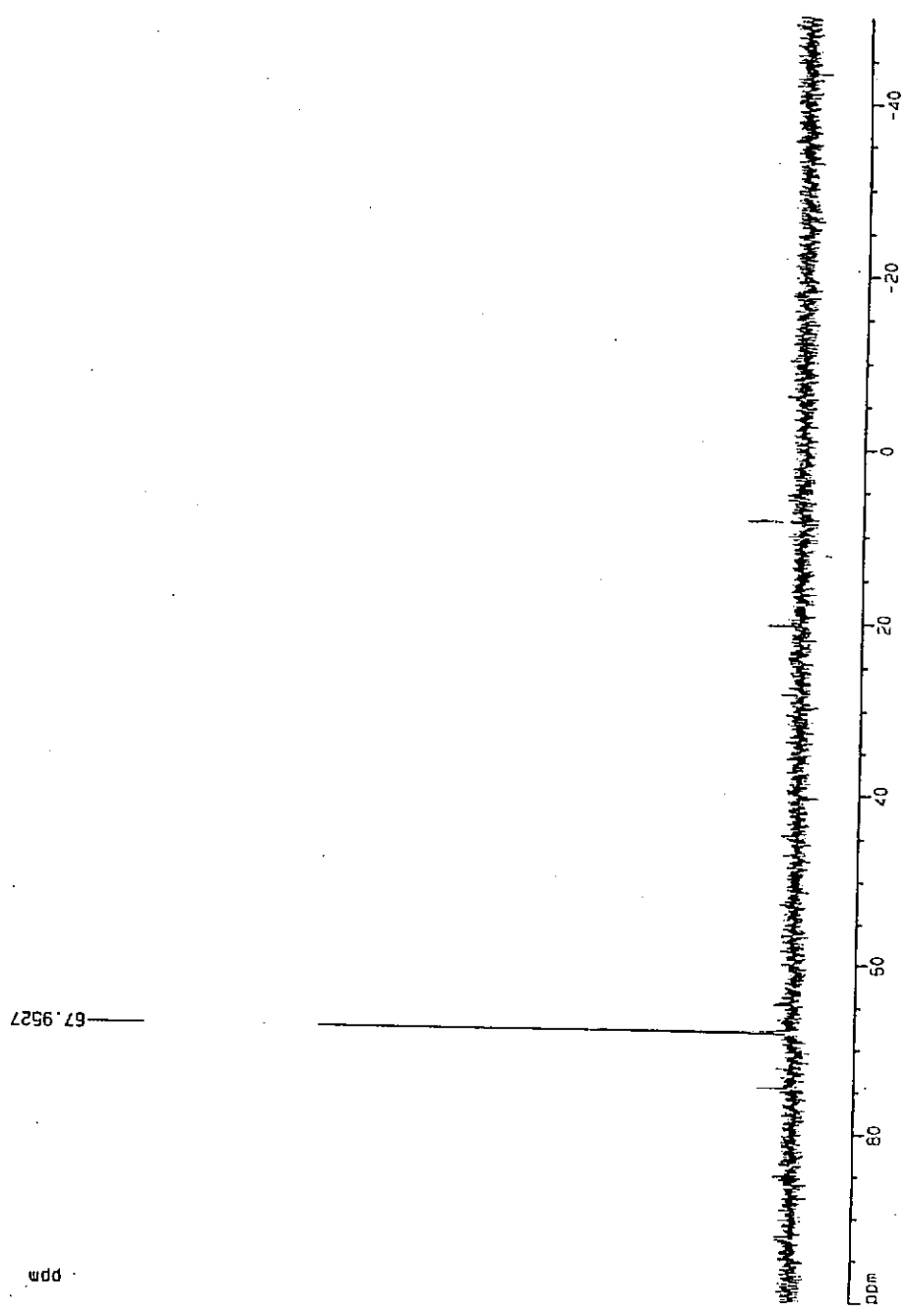


Figure 3.3. 161 MHz <sup>31</sup>P{<sup>1</sup>H}-NMR spectrum of TpRuH(HSiEt<sub>3</sub>)(PPh<sub>3</sub>) (21a)



TpRuH(HSiEt<sub>3</sub>)(PPh<sub>3</sub>) in d<sub>8</sub>-thf

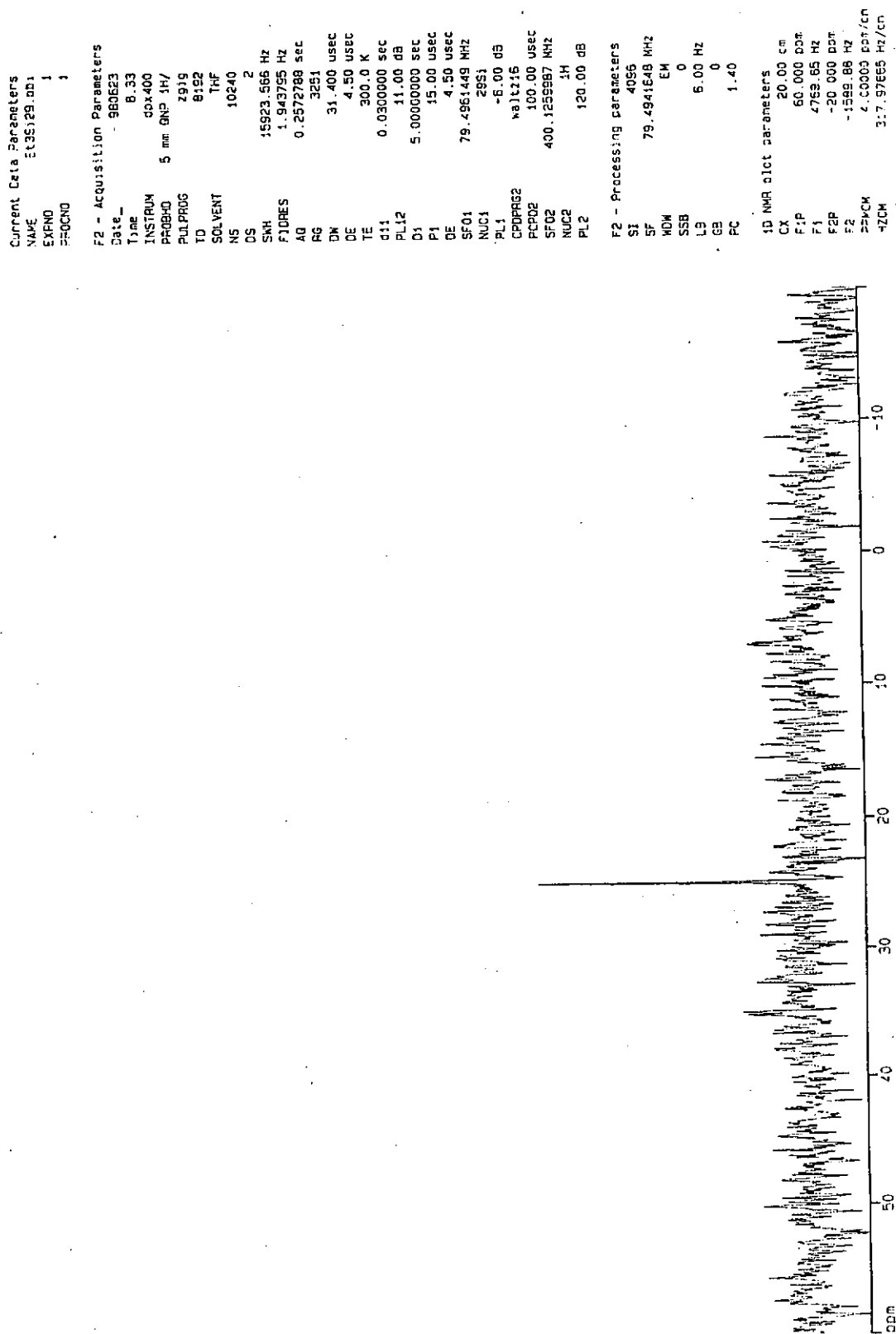


Figure 3.4. 79 MHz <sup>29</sup>Si{<sup>1</sup>H}-NMR spectrum of TpRuH(HSiEt<sub>3</sub>)(PPh<sub>3</sub>) (**21a**)

SPEC: 980618\_2  
 Samp: Et3SiH  
 Comm: nba as matrix  
 Mode: FAB +VE +LMR  
 Oper: 75.9  
 Base: 577.9  
 Norm: 2.00 mmu  
 Peak: 2 > 10  
 Accu:

18-Jun-98 Elapse: 01:16.3 1  
 Start : 14:15:52 19

BSCAN (EXP) UP LR NETCDF  
 Client: ng siu man  
 Inten : 229047  
 RIC : 1033675

Inlet :  
 Masses: 50 > 800  
 #peaks: 251

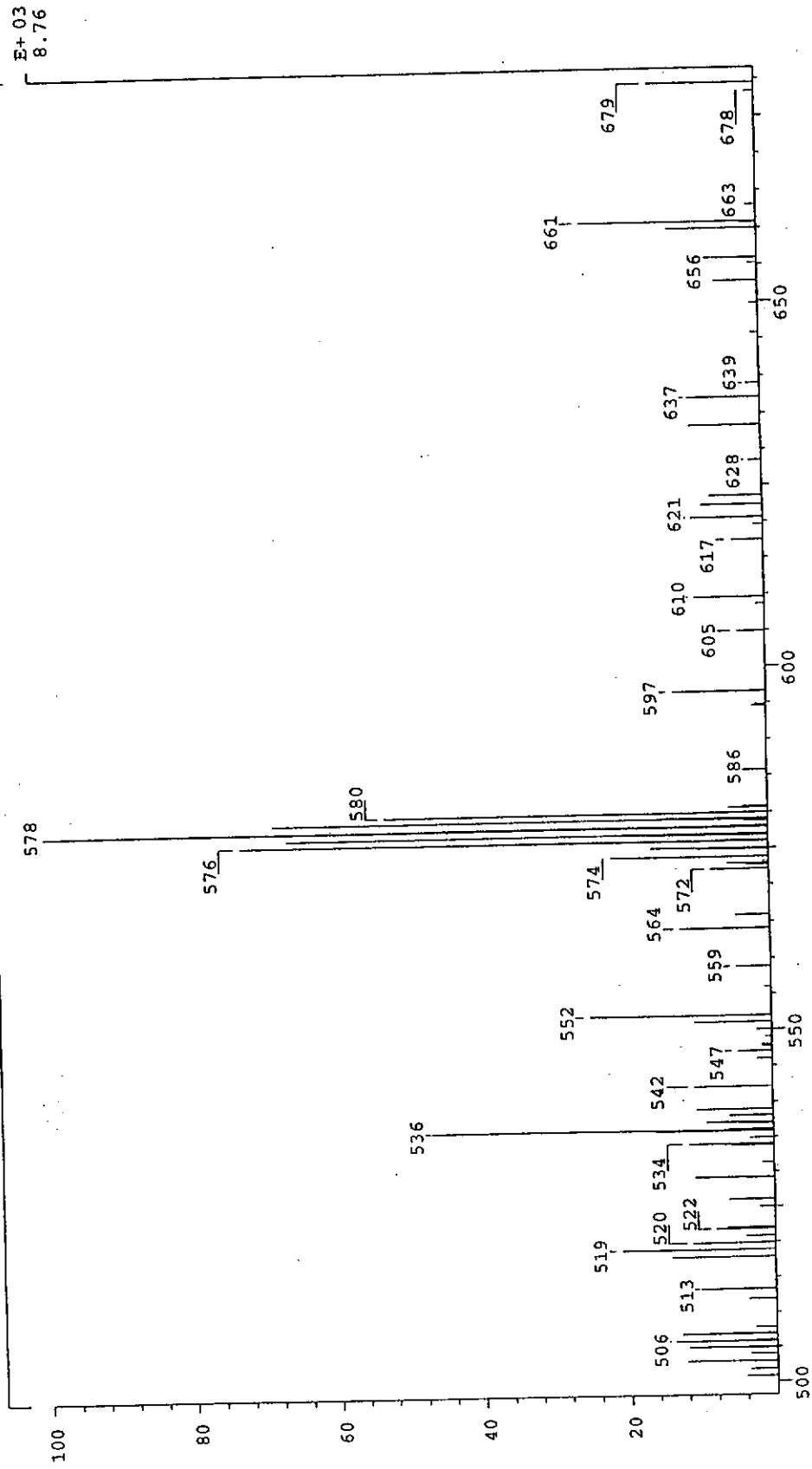


Figure 3.5. FAB mass spectrum of  $\text{TpRuH}(\text{HSiEt}_3)(\text{PPh}_3)$  (**21a**)

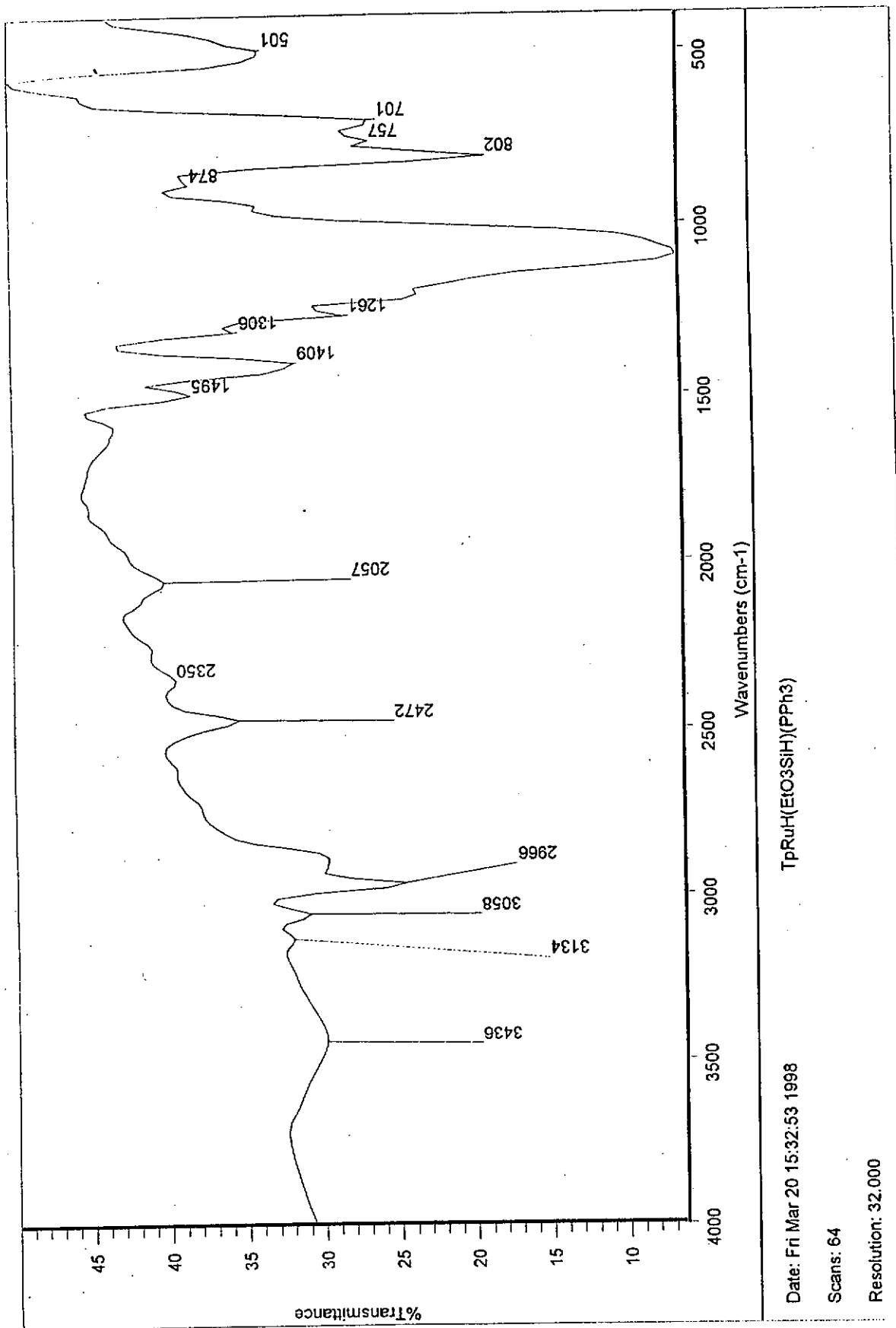


Figure 3.6. Infra-red spectrum of TpRuH(HSi(EtO)<sub>3</sub>)(PPh<sub>3</sub>) (21b) in KBr disc

TpRuH(HSi(EtO)<sub>3</sub>)(PPh<sub>3</sub>) d8-t17

```

Current Data Parameters
NAME      EtCS51H
EXPNO     2
PROCNO    1

F2 - Acquisition Parameters
Date_     990220
Time      17.32
INSTRUM   dx400
PROBHD    5 mm QNP 1H/
PULPROG   zg30
TD         32768
SOLVENT   THF
NS         256
DS         0
SWH        6025.841 Hz
FIDRES     0.489064 Hz
AQ         1.0224116 sec
RG         114
CW         31.200 usec
DE         4.50 usec
TE         300.0 K
D1         1.00000000 sec
P1         9.50 usec
DE         4.50 usec
SFO1      400.1279999 MHz
NUC1       1H
PL1        -5.00 dB

F2 - Processing parameters
SI         16384
SF         400.1299877 MHz
WDW        EM
SSB        0
LB         0.30 Hz
GB         0
PC         1.00

1D NMR dict parameters
CX         20.00 cm
F1P        10.000 ppm
F1         4001.30 Hz
F2P        -15.000 ppm
F2         -6001.95 Hz
PRMCM      1.25000 ppm/cm
HZCM       500.16248 Hz/cm
    
```

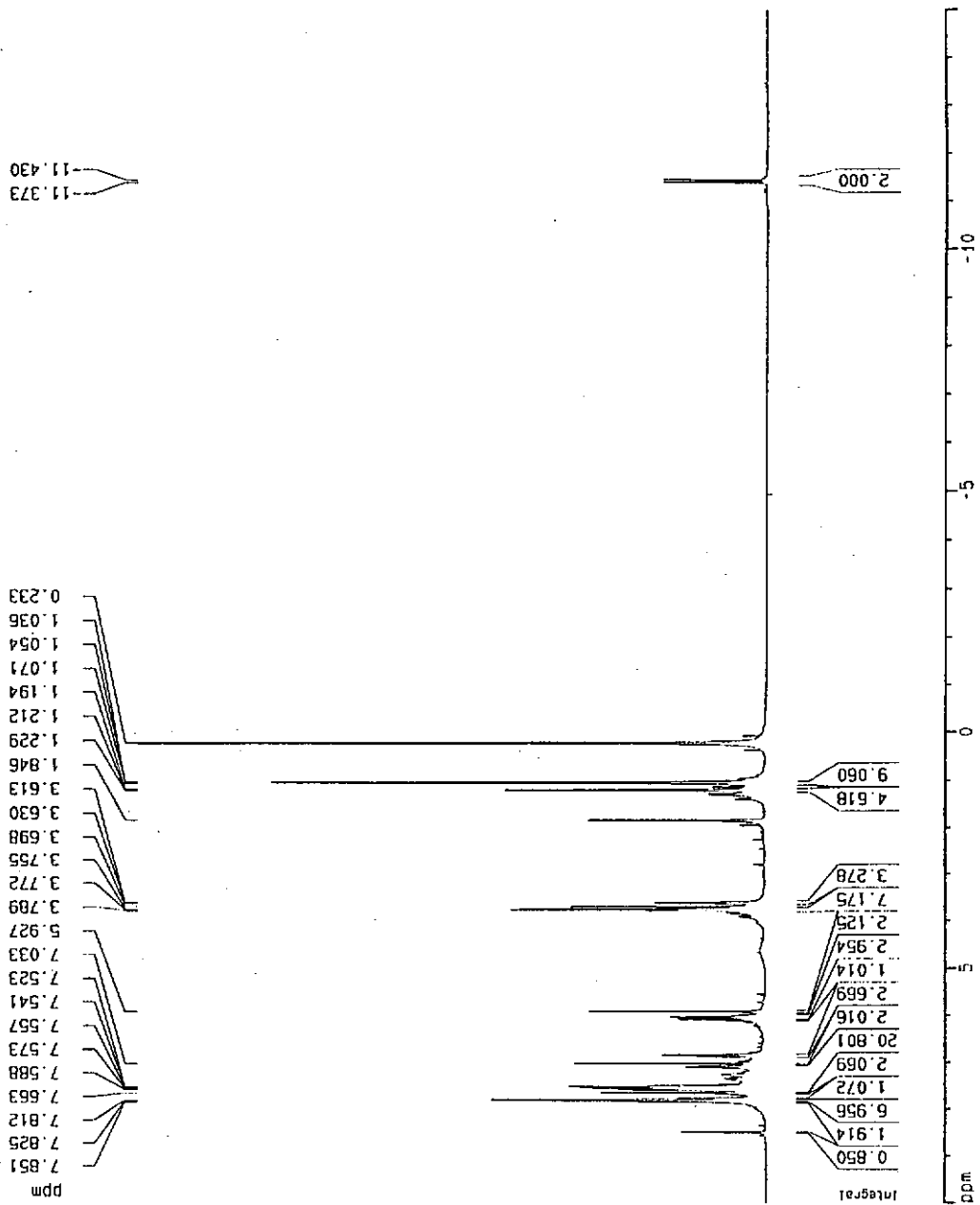


Figure 3.7(a). 400 MHz <sup>1</sup>H-NMR spectrum of TpRuH(HSi(EtO)<sub>3</sub>)(PPh<sub>3</sub>) (**21b**)

Current Data Parameters  
 NAME Et0351H  
 EXPNO 2  
 PROCNO 1

F2 - Acquisition Parameters  
 Date\_ 980220  
 Time 17.32  
 INSTRUM dx400  
 PROBHD 5 mm GNP 1H/  
 PULPROG zg30  
 TO 32769  
 SOLVENT THF  
 NS 256  
 DS 0  
 SWH 16025.641 Hz  
 FIDRES 0.489064 Hz  
 AQ 1.0224116 sec  
 RG 114  
 DM 31.200 usec  
 DE 4.50 usec  
 TE 300.0 K  
 D1 1.0000000 sec  
 F1 9.50 usec  
 DE 4.50 usec  
 SFO1 400.1279953 MHz  
 NUC1 1H  
 PL1 -6.00 dB

F2 - Processing parameters  
 SI 15364  
 SF 400.1299677 MHz  
 KCM EM  
 SSB 0  
 LB 0.30 Hz  
 GB 0  
 PC 1.00

1D NMR list parameters  
 CX 20.00 cm  
 F1P -11.000 ppm  
 F1 -4401.43 Hz  
 F2P -12.000 ppm  
 F2 -4801.56 Hz  
 FREQM 0.65000 ppm/cm  
 HZCM 20.60650 Hz/cm

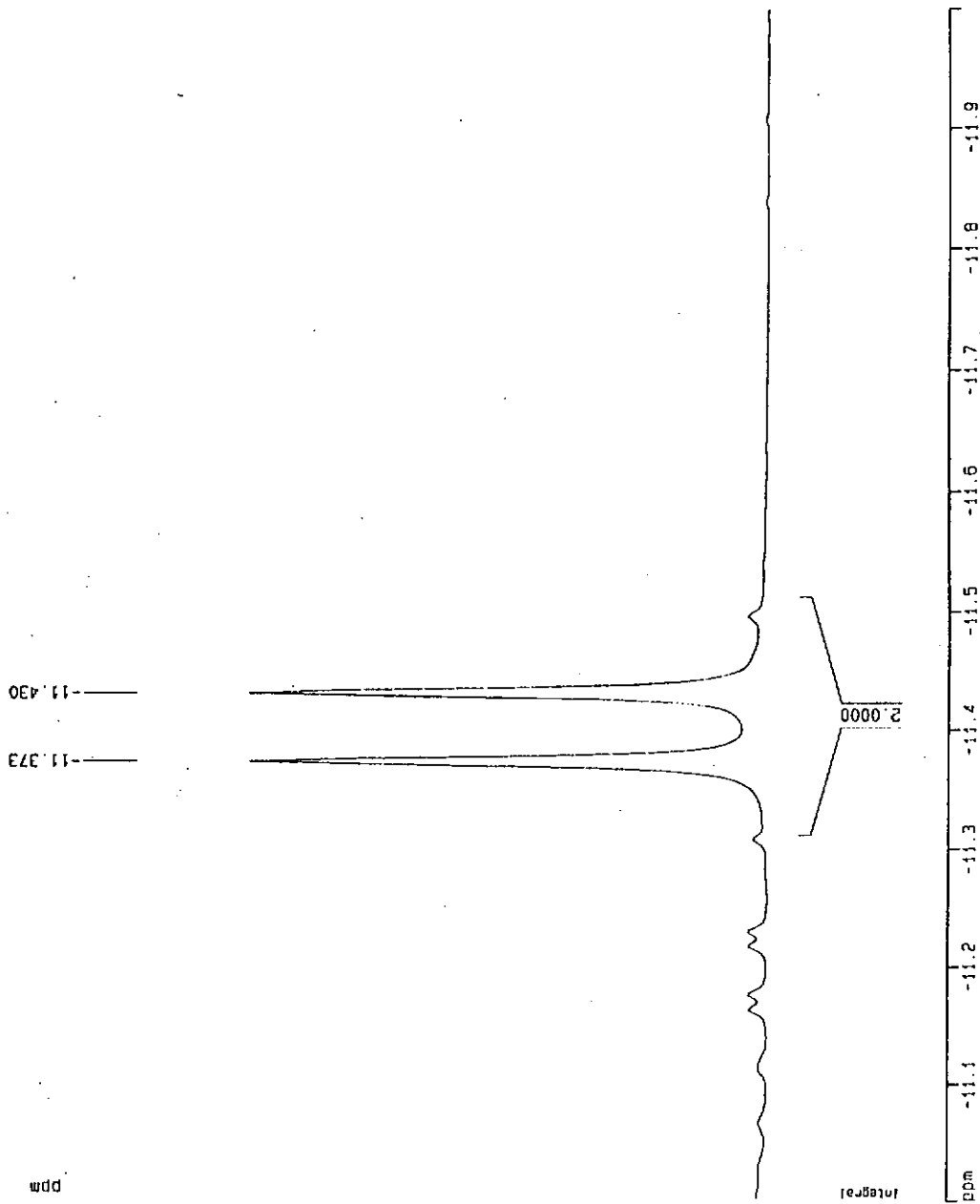


Figure 3.7(b). Expanded upfield region of Figure 3.7(a)

TPRuH (HSi (EtO)3) (PPh3) in d8-thf

```

Current Data Parameters
NAME      PE1035.H
EXPNO    2
PROCNO   1

F2 - Acquisition Parameters
Date_    980220
Time     17.49
INSTRUM  GPC400
PROBHD   5 mm QNP 1H/
PULPROG  zgpg30
TD        65536
SOLVENT  THF
NS        256
DS        2
SWH       64935.066 Hz
FIDRES    0.990630 Hz
AQ        0.5046772 sec
RG        9195.2
DM        7.700 USEC
DE        4.50 USEC
TE        300.0 K
C11       0.0300000 sec
C12       0.0000200 sec
PL13      120.00 dB
D1        1.0000000 sec
CPDPRG2  waltz16
PCPD2     71.00 USEC
SFO2      400.1300000 MHz
NUC2      1H
PL2       120.00 dB
PL12      17.00 dB
P1        7.20 USEC
DE        4.50 USEC
SFO1      161.975930 MHz
NUC1      31P
PL1       -6.00 dB

F2 - Processing parameters
SI        32768
SF        161.975935 MHz
AQ        5M
SSB       0
LB        3.00 Hz
GB        0
PC        1.40

1D NMR list parameters
CX        20.55 cm
F1P       100.000 ppm
F1        16197.56 Hz
F2P       -50.000 ppm
F2        -8098.76 Hz
PPMPPV    7.24555 ppm/cm
HZCV      174.31555 Hz/cm
    
```

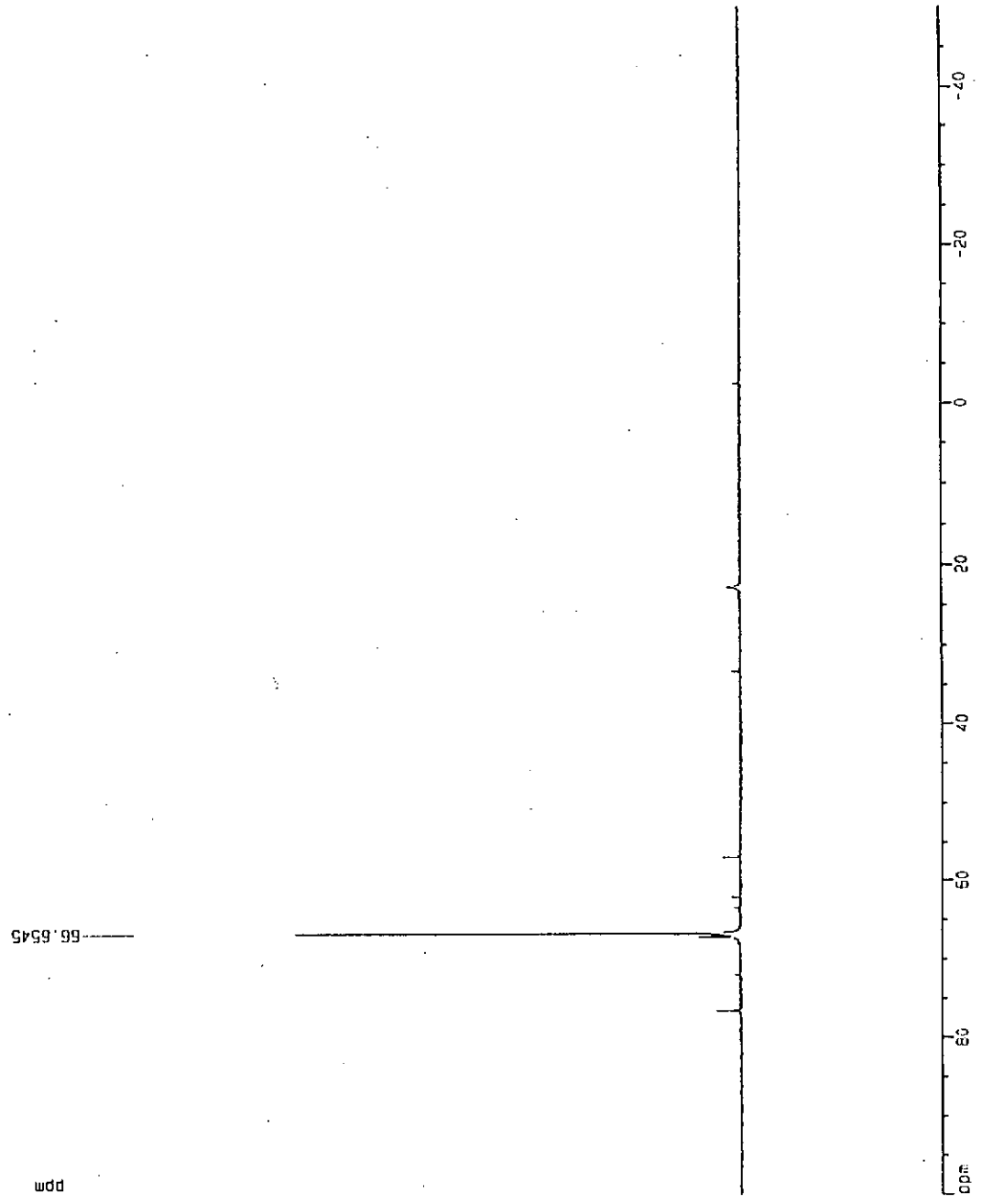


Figure 3.8. 161 MHz  $^{31}\text{P}\{^1\text{H}\}$ -NMR spectrum of  $\text{TPRuH}(\text{HSi}(\text{EtO})_3)(\text{PPh}_3)$  (**21b**)

TRRUH(HSi(EtO)<sub>3</sub>)(PPh<sub>3</sub>) in d<sub>8</sub>-thf

```

Current Data Parameters
NAME      ETC5129.D01
EXPNO     1
PROCNO    1

F2 - Acquisition Parameters
Date_     990920
Time      7.01
INSTRUM   dx400
PROBHD    5 mm QNP 1H/
PULPROG   zg30
TD         6552
SOLVENT   THF
NS         10240
DS         2
SWH        15923.566 Hz
FIDRES     1.943795 Hz
AQ         0.2572788 sec
RG          3251
DM         31.400 usec
DE         4.50 usec
TE         300.0 K
TE        0.0300000 sec
PL12       11.00 dB
D1         5.0000000 sec
F1         15.00 usec
DE         4.50 usec
SF01       75.4961449 MHz
NUC1       29Si
PL1        -6.00 dB
CPOPRG2   waltz16
PCPD2     100.00 usec
SF02       400.1265987 MHz
NUC2       1H
PL2        120.00 dB

F2 - Processing parameters
SI         4056
SF         75.4941648 MHz
WDW        EM
SSB        0
LB         5.00 Hz
GB         0
PC         1.40

1D NMR pict parameters
CX         20.00 cm
S:F        60.000 pps
F1         4768.65 Hz
F2P        -20.000 pps
F2         -1589.88 Hz
ZMCM       4.00000 pps/cm
AQDM       317.97665 Hz/cm
  
```

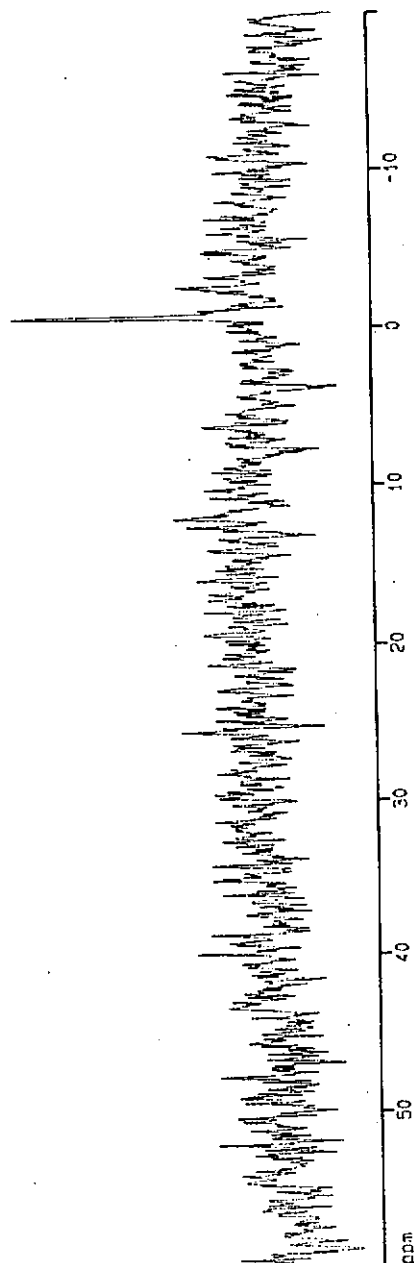


Figure 3.9. 79 MHz <sup>29</sup>Si{<sup>1</sup>H}-NMR spectrum of TpRuH(HSi(EtO)<sub>3</sub>)(PPh<sub>3</sub>) (**21b**)

SPEC: 980612\_2  
 Samp: (EtO)3SiH  
 Comm: nba  
 Mode: FAB +VE +LMR BSCAN (EXP) UP LR, NERCDF  
 Oper: Client: Ng Siu Man  
 Base: 576.2 Inten: 179281  
 Norm: 576.2 RIC: 1632900  
 Peak: 3000.00 mmu  
 Accu: 1 > 20

12-Jun-98 Elapse: 02:23.6 1  
 Start: 13:11:35 24

Inlet: 50 > 950  
 Masses: 50 > 950  
 #peaks: 807

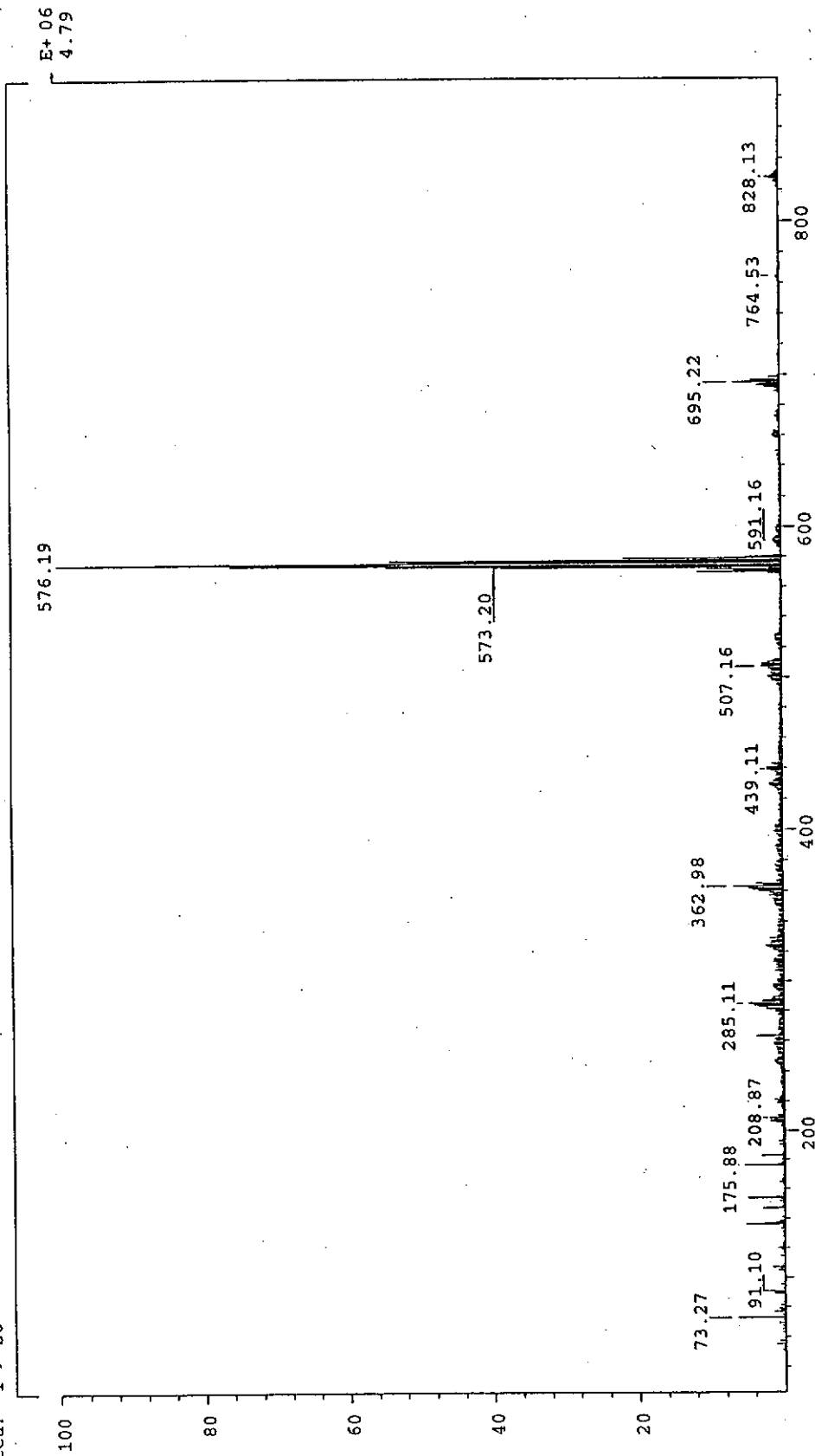


Figure 3.10. FAB mass spectrum of  $\text{TpRuH}(\text{HSi}(\text{EtO})_3)(\text{PPh}_3)$  (**21b**)



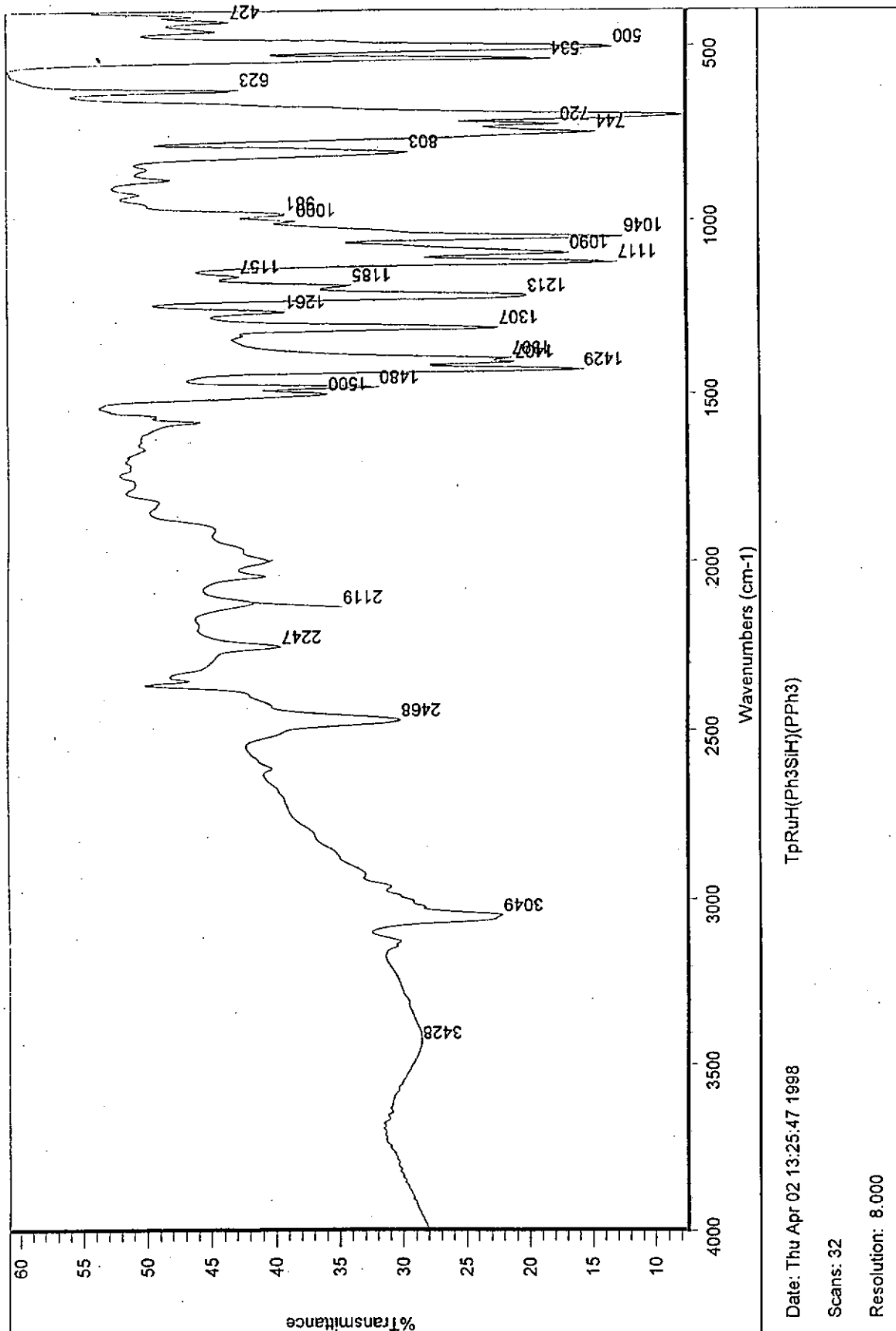


Figure 3.11. Infra-red spectrum of TpRuH(HSiPh<sub>3</sub>)(PPh<sub>3</sub>) (21c) in KBr disc

TpRuH(HSiPh<sub>3</sub>)(PPh<sub>3</sub>) in d<sub>8</sub>-THF

Current Data Parameters  
 NAME PHSJH  
 EXPNO 1  
 PROCNO 1

F2 - Acquisition Parameters  
 Date\_ 990215  
 Time 17:51  
 INSTRUM dax400  
 PROBHD 5 mm QNP 1H/  
 PULPROG zg30  
 TO 32768  
 SOLVENT THF  
 NS 256  
 DS 0  
 SWH 16025.641 Hz  
 FIDRES 0.469064 Hz  
 AQ 1.0224156 sec  
 RG 114  
 CW 31.200 usec  
 DE 4.50 usec  
 TE 300.0 K  
 D1 1.0000000 sec  
 P1 9.50 usec  
 DE 4.50 usec  
 SFO1 400.1279593 MHz  
 NUC1 1H  
 PL1 -5.00 dB

F2 - Processing Parameters  
 SI 16384  
 SF 400.1252656 MHz  
 MDX EH  
 SSB 0  
 LB 0.30 Hz  
 GB 0  
 PC 1.00

1D NMR data parameters  
 CX 20.00 cm  
 F1P 10.000 ppm  
 F2 400.130 Hz  
 F2P -15.000 ppm  
 ZF 24  
 ZF2 -6001.55 Hz  
 ZF3 1.25000 ppm/cm  
 ZF4 500.13248 Hz/cm

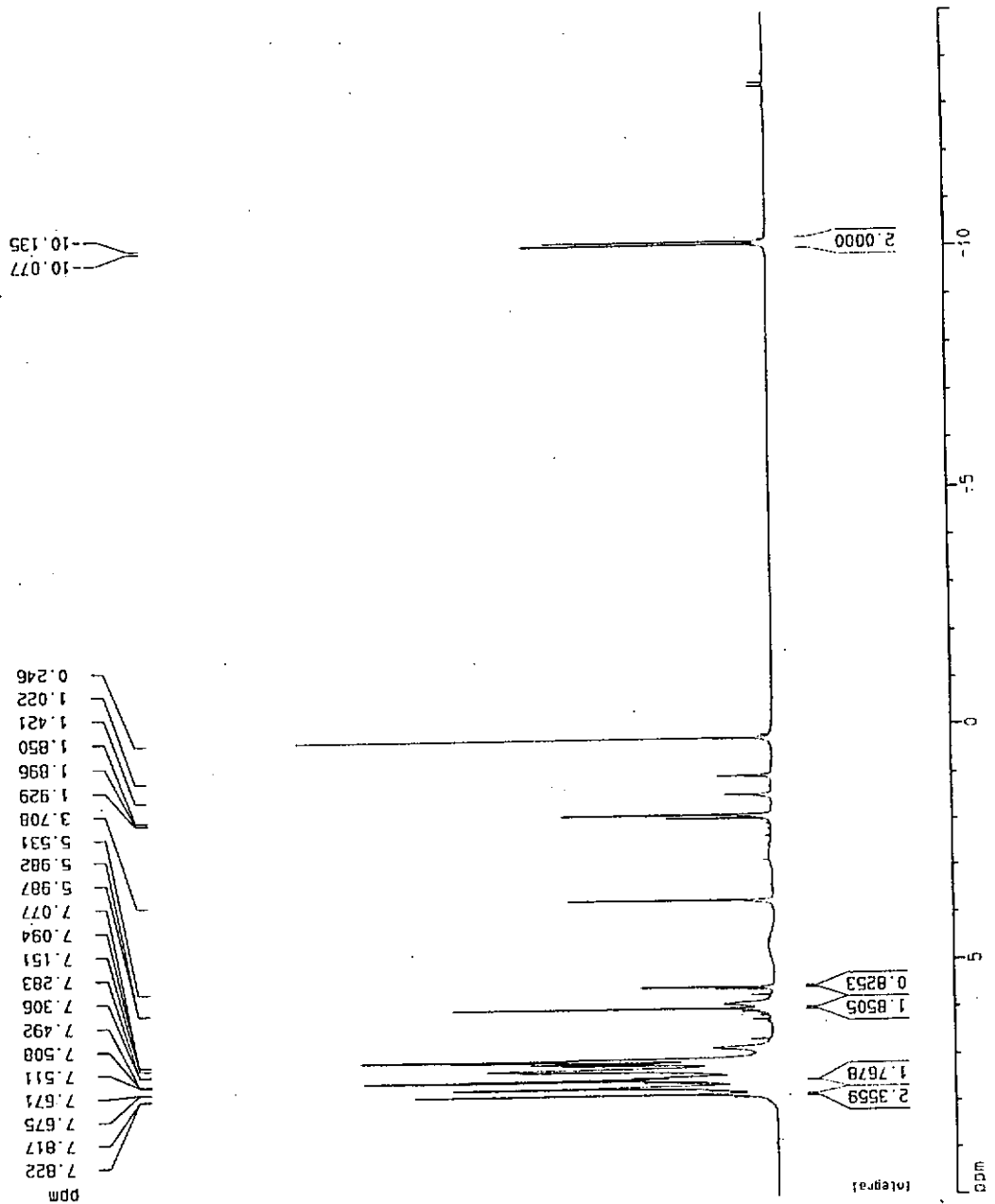


Figure 3.12(a). 400 MHz <sup>1</sup>H-NMR spectrum of TpRuH(HSiPh<sub>3</sub>)(PPh<sub>3</sub>) (21c)

TORUH (HS)Pn3 (Pn3) in d8-thf

```

Current Data Parameters
NAME      Pn35JH
EXPNO    1
PROCNO   1

F2 - Acquisition Parameters
Date_    990216
Time     17:51
INSTRUM  SDX400
PROBHD   5 mm QNP 1H/
PULPROG  zg30
TD        32768
SOLVENT  THF
NS        256
DS        0
SWH       16025.641 Hz
FIDRES    0.489064 Hz
AQ        1.0224115 sec
RG         114
DK        31.200 usec
DE        4.50 usec
TE        300.0 K
D1        1.0000000 sec
F1        9.50 usec
DE        4.50 usec
SFO1     400.1279953 MHz
NUC1      1H
P1        -5.00 dB

F2 - Processing parameters
SI        16384
SF        400.1299856 MHz
WDW       EM
SSB       0
LB        0.30 Hz
GB        0
PC        1.00

1D NMR plot parameters
CX        20.00 cm
F1P       -9.000 ppm
F1        -9601.17 Hz
F2P       -11.000 ppm
F2        -4401.43 Hz
PPMCH     0.10000 ppm/cm
HZCH      40.01300 Hz/cm
  
```

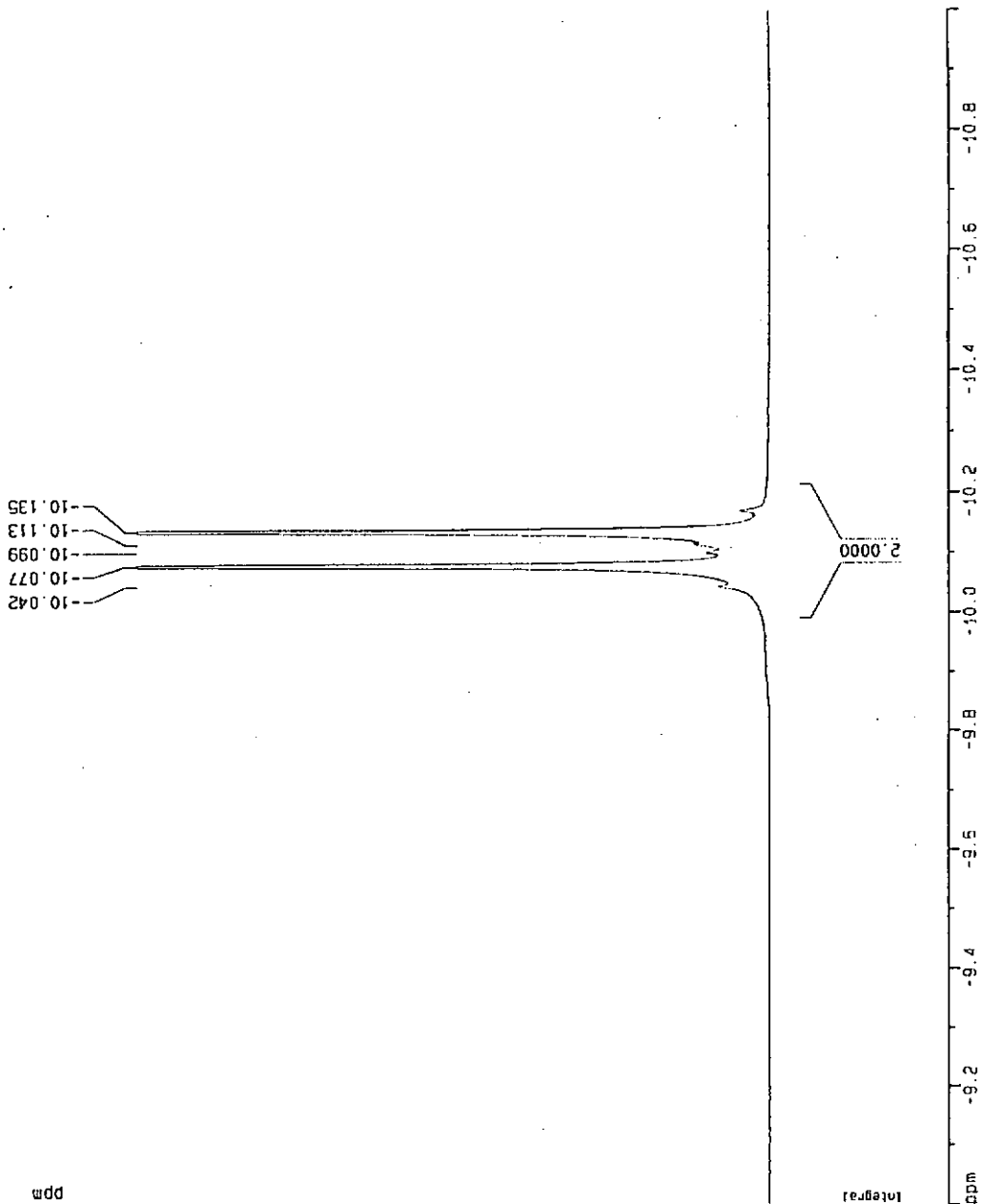


Figure 3.12(b). Expanded upfield region of Figure 3.12(a)

TPRUH(HSiPh3)(PPh3) in d8-thf

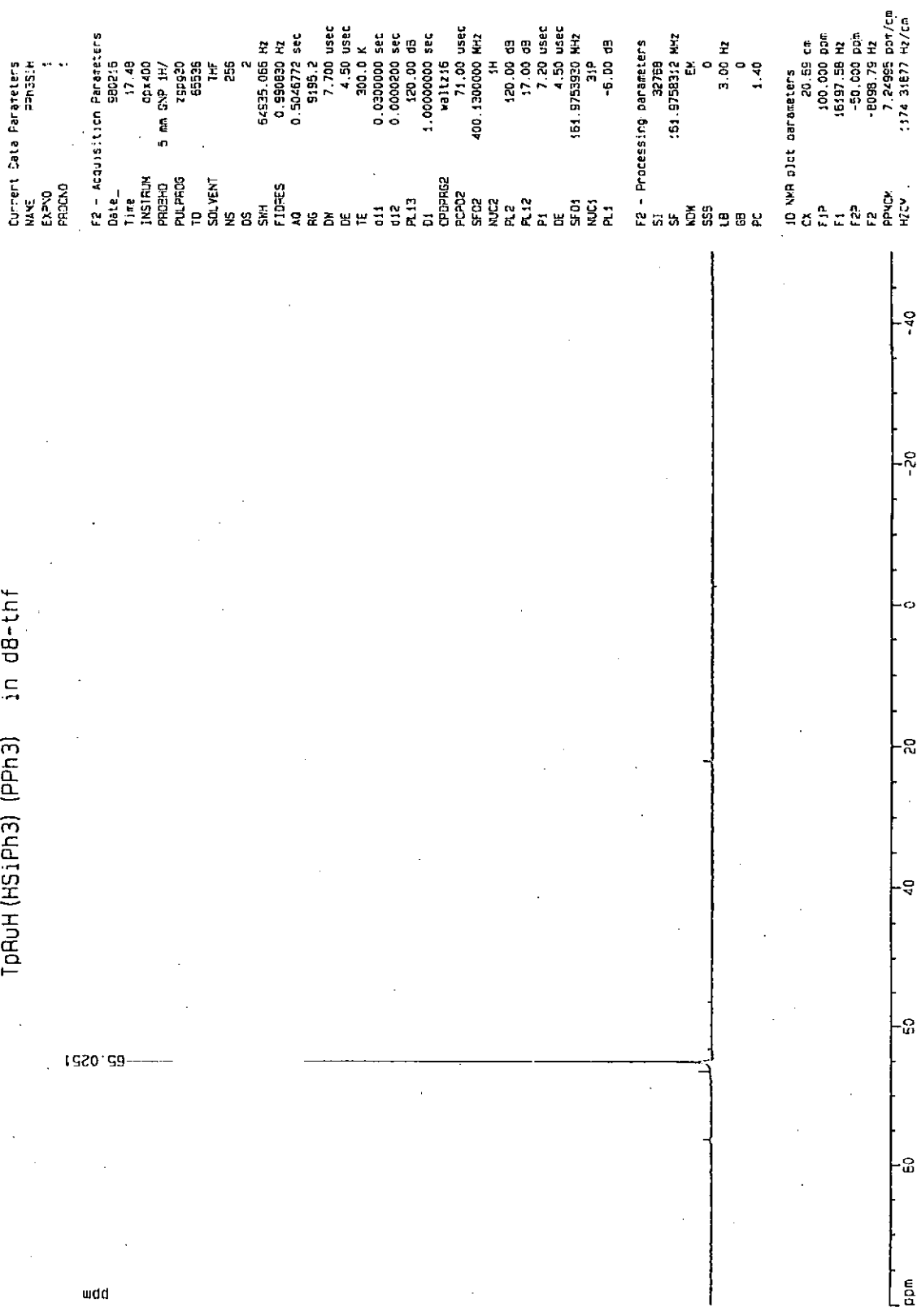


Figure 3.13. 161 MHz  $^{31}\text{P}\{^1\text{H}\}$ -NMR spectrum of TPRUH(HSiPh<sub>3</sub>)(PPh<sub>3</sub>) (21c)

TpRuH(HSiPh<sub>3</sub>)(PPh<sub>3</sub>) in d<sub>8</sub>-thf

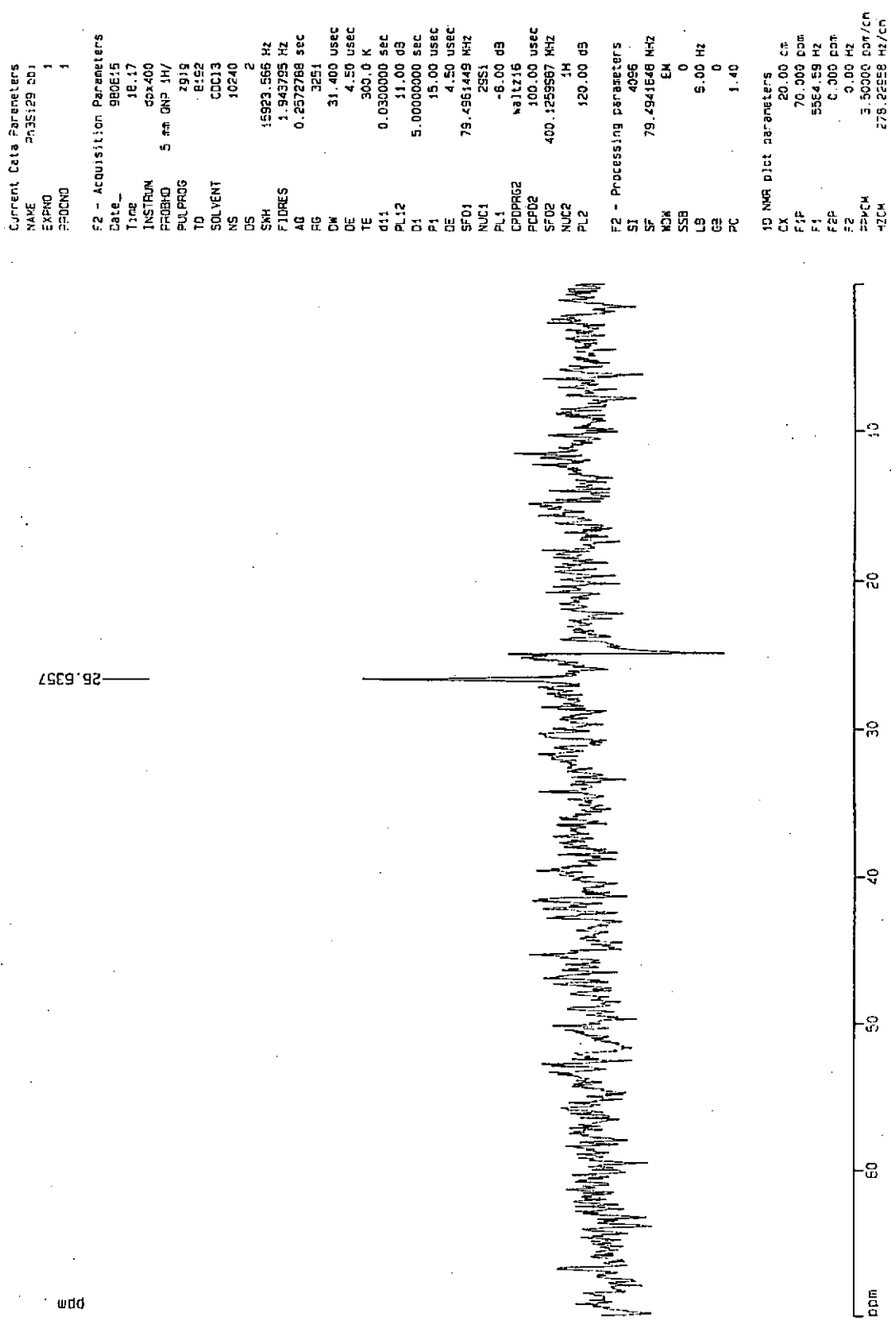


Figure 3.14. 79 MHz <sup>29</sup>Si{<sup>1</sup>H}-NMR spectrum of TpRuH(HSiPh<sub>3</sub>)(PPh<sub>3</sub>) (21c)

SPEC: cp980416\_4  
 Samp: nba as matrix  
 Comm: FAB, pos, 100-1000  
 Mode: FAB +VE +LMR ESCAN (EXP) UP LR NETCDF  
 Oper: Client: Ng siu man  
 Base: 154.2  
 Norm: 154.2  
 Peak: 3000.00 mmu  
 Accu: 2 > 15

16-Apr-98 Elapse: 02:44.8 1  
 Start : 17:19:58 16  
 Study : Ph3SiH  
 Inlet :  
 Masses: 100 > 1000  
 #peaks: 1078

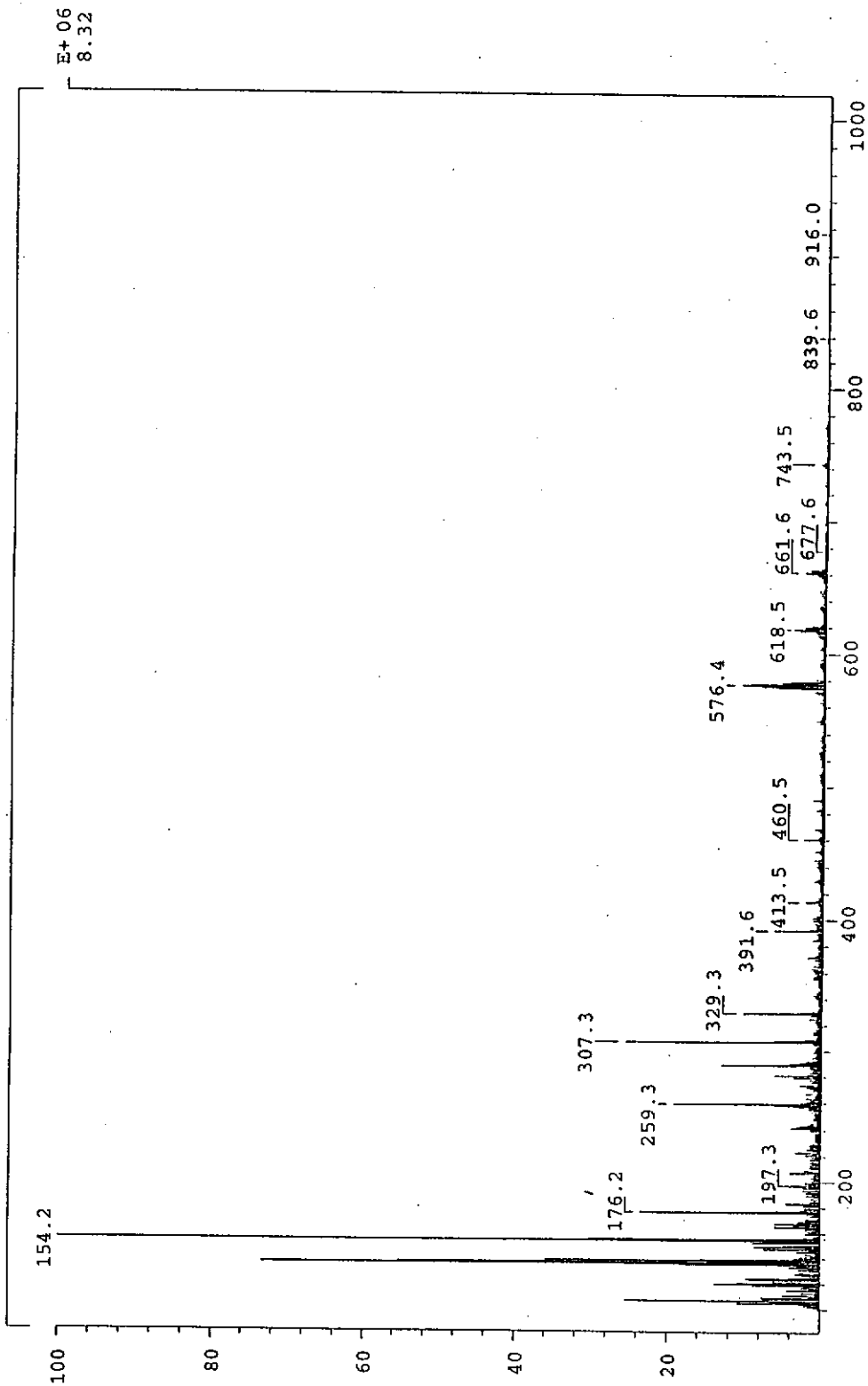


Figure 3.15. FAB mass spectrum of  $\text{TpRuH}(\text{HSiPh}_3)(\text{PPh}_3)$  (**21c**)

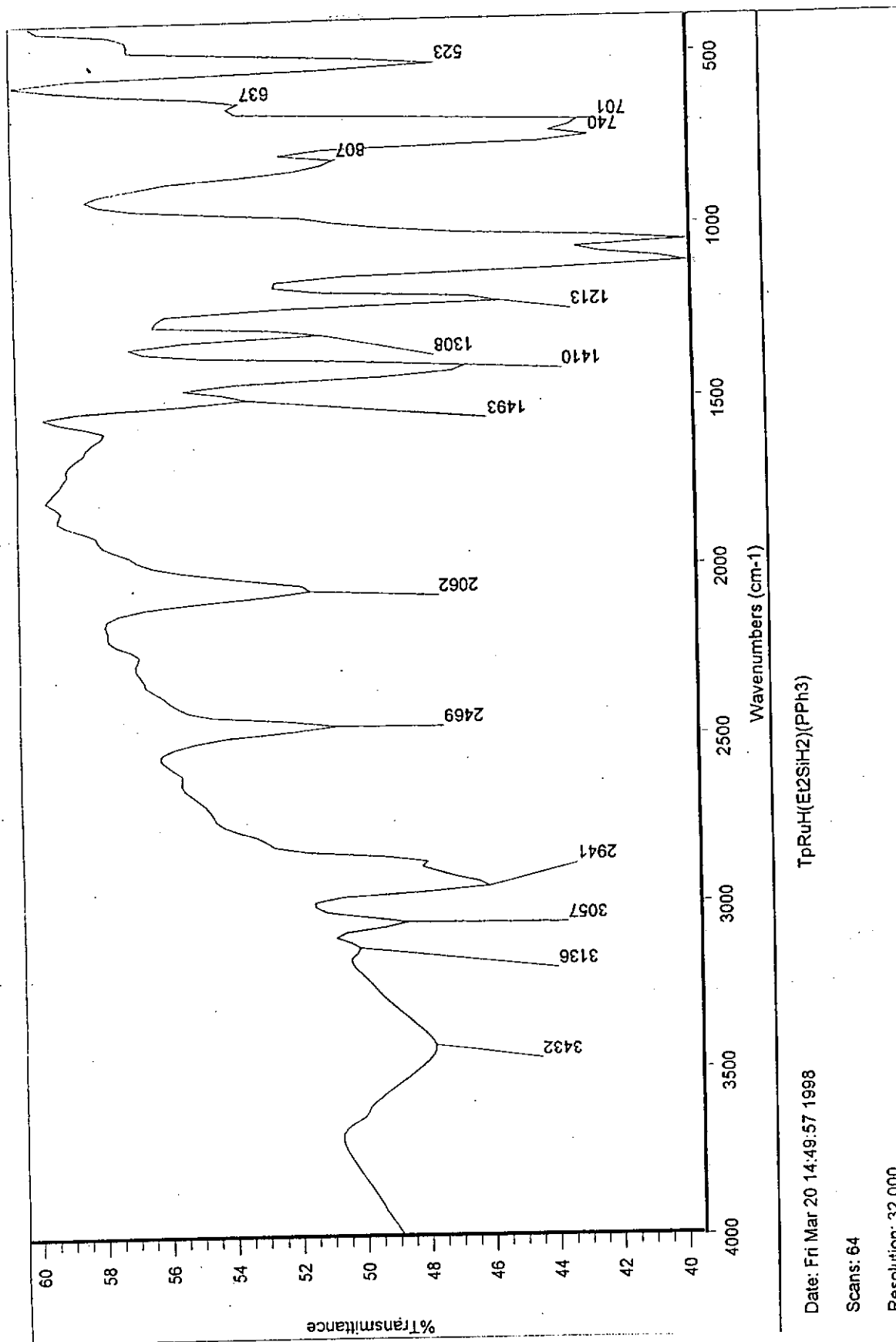


Figure 3.16. Infra-red spectrum of TpRuH(H<sub>2</sub>SiEt<sub>2</sub>)(PPh<sub>3</sub>) (21d) in KBr disc

[missing page]

Page 144



TpBuH (H2SiEt2) (PPh3) in d8-tmf

```

Current Data Parameters
NAME      EL2SIF2
EXPNO    7
PROCNO   1

F2 - Acquisition Parameters
Date_    990312
Time     15.42
INSTRUM  spect
PROBHD   5 mm QNP 1H/
PULPROG  zgpg30
TD        32768
SOLVENT  THF
NS        32
DS        0
SWH       16025.641 Hz
FIDRES    0.489064 Hz
AQ        1.022416 sec
RG         256
CK        31.200 usec
DE        4.50 usec
TE        300.0 K
D1        1.0000000 sec
P1        9.50 usec
DE        4.50 usec
SFO1     400.1279993 MHz
NUC1      1H
P11       -6.00 dB

F2 - Processing parameters
SI        16384
SF        400.1259656 MHz
XDK       EM
SSB       0
LB        0.30 Hz
GB        0
PC        1.00

ID NMR p1ct parameters
CX        20.00 cm
F1P       -10.600 ppm
F1        -4241.38 Hz
F2P       -11.200 ppm
F2        -4481.46 Hz
PPHMM     0.03500 ppm/cm
HZCM      12.00389 Hz/cm
  
```

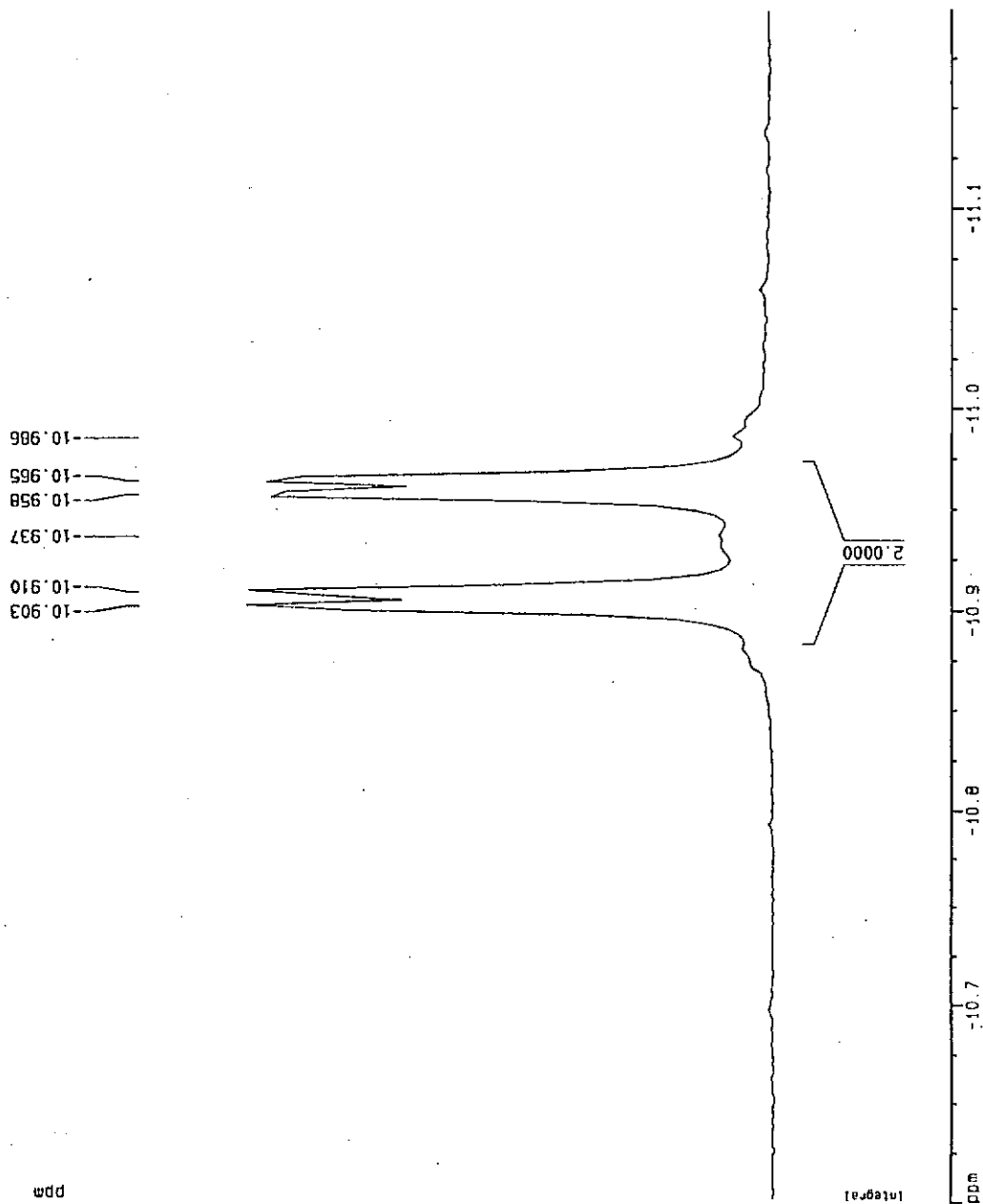


Figure 3.17(b). Expanded upfield region of Figure 3.17(a)

TPRuH(H<sub>2</sub>SiEt<sub>2</sub>)(PPh<sub>3</sub>) in d<sub>8</sub>-thf

Current Data Parameters  
 NAME P1251-2  
 EXPNO 3  
 PROCNO 1

F2 - Acquisition Parameters  
 Date\_ 960220  
 Time 16.31  
 INSTRUM dpx400  
 PROBRD 5 mm QNP 1H/  
 PULPROG zgpg30  
 TO 65535  
 SOLVENT THF  
 NS 128  
 DS 2  
 SWH 64935.066 Hz  
 FIDRES 0.590830 Hz  
 AQ 0.5046772 sec  
 RG 5195.2  
 DW 7.700 usec  
 DE 4.50 usec  
 TE 300.0 K  
 d11 0.0300000 sec  
 d12 0.0000200 sec  
 PL13 120.00 dB  
 DI 1.0000000 sec  
 CPDPRG2 waltz16  
 PCPD2 71.00 usec  
 SF02 400.1300000 MHz  
 NUC2 1H  
 PL2 120.00 dB  
 PL12 17.00 dB  
 P1 7.20 usec  
 DE 4.50 usec  
 SF01 161.975930 MHz  
 NUC1 31P  
 PL1 -6.00 dB

F2 - Processing parameters  
 SI 32768  
 SF 161.975935 MHz  
 NDM EK  
 SSB 0  
 LB 3.00 Hz  
 GB 0  
 PC 1.40

1D NMR plot parameters  
 CX 20.55 cm  
 F1P 100.000 ppm  
 F1 16197.58 Hz  
 F2P -50.000 ppm  
 F2 -8098.75 Hz  
 PPMCK 7.24995 ppm/cm  
 HZCV 1174.31655 Hz/cm

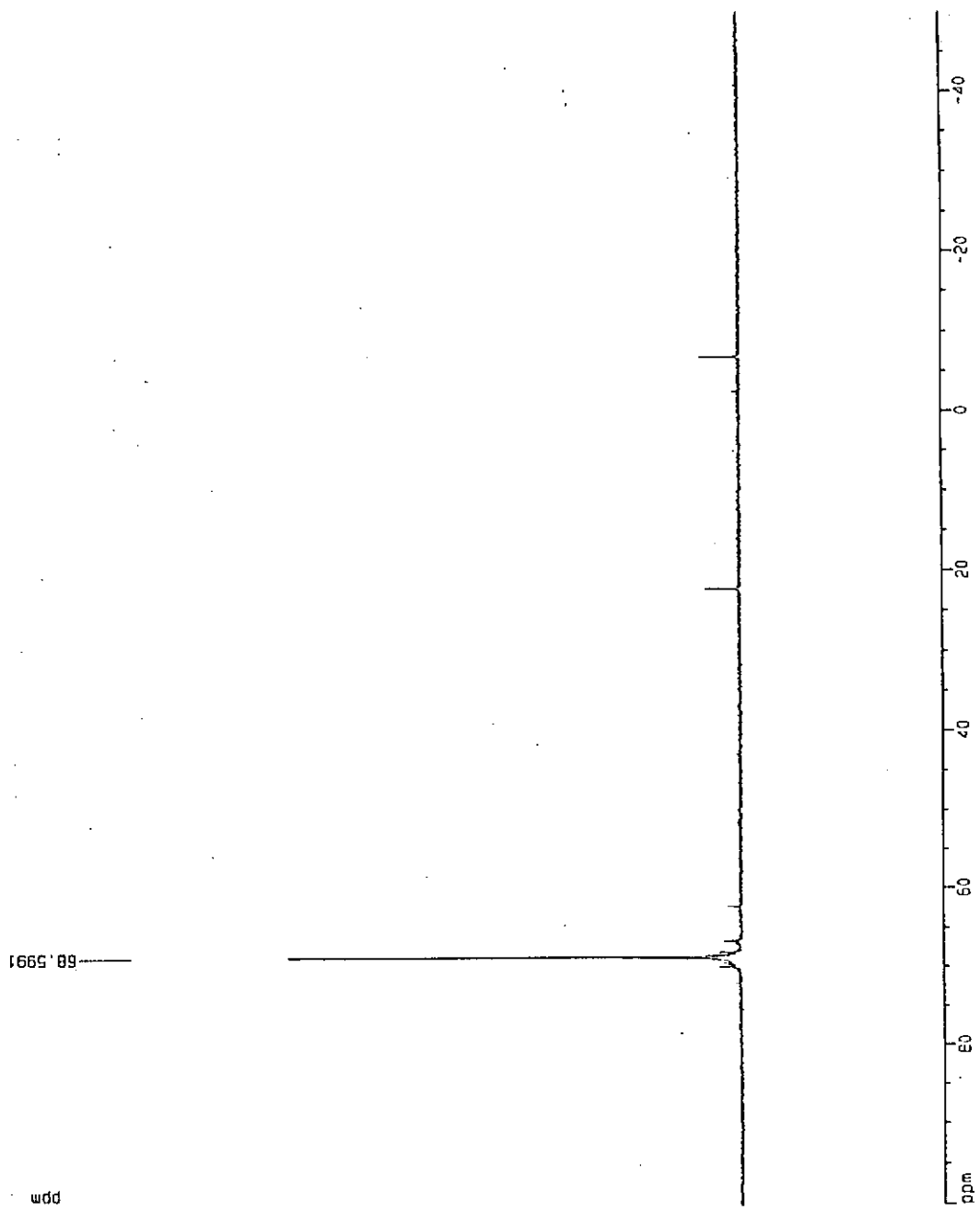
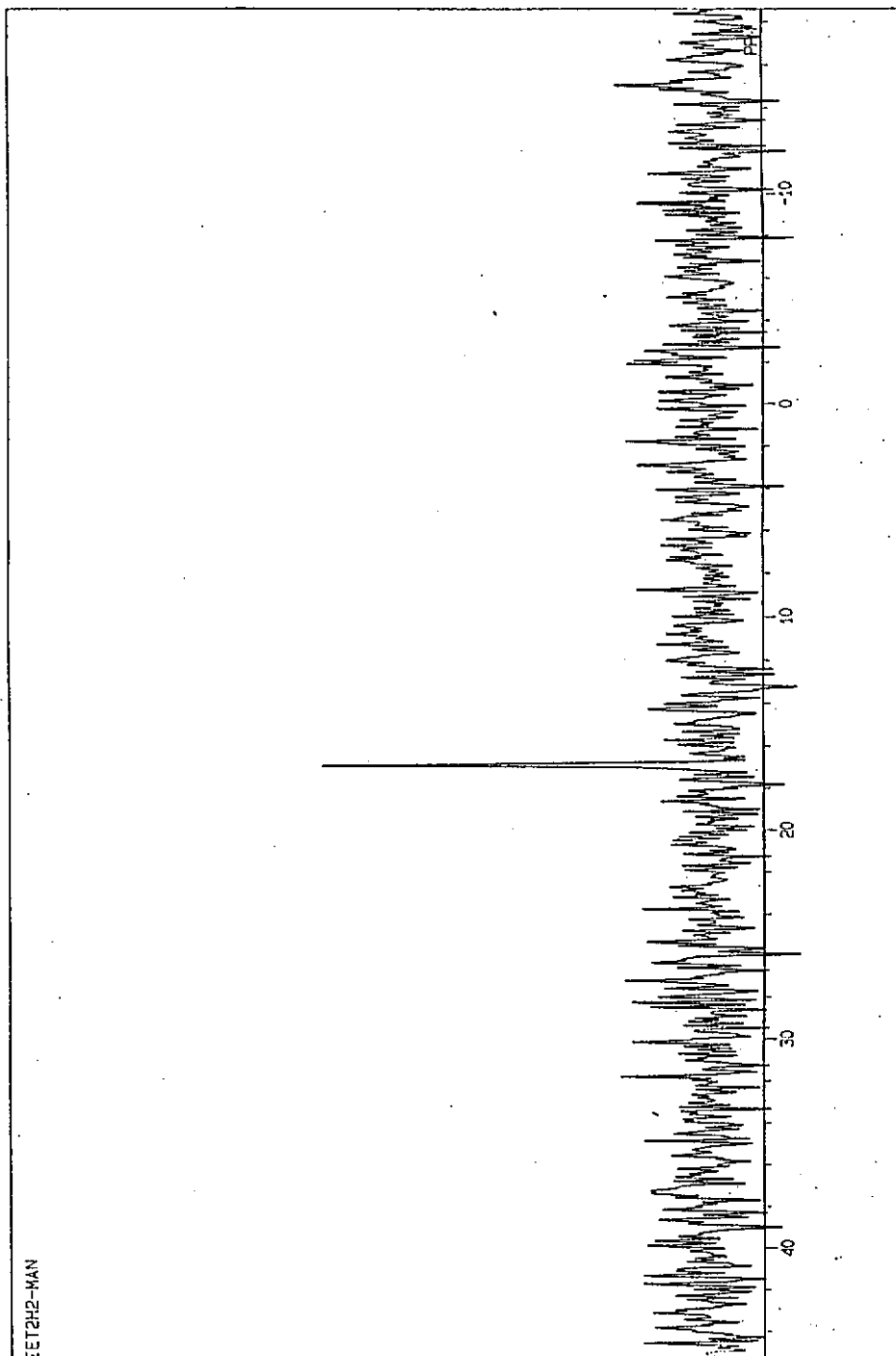


Figure 3.18. 161 MHz <sup>31</sup>P{<sup>1</sup>H}-NMR spectrum of TpRuH(H<sub>2</sub>SiEt<sub>2</sub>)(PPh<sub>3</sub>) (**21d**)

23-JUN-99 23:12:04  
 DFILF NC273  
 OBNUC 29SI  
 EXMOD DEPT  
 OFR 79.30 MHz  
 OBSET 115.00 kHz  
 OBFIN 13609.3 Hz  
 POINT 16384  
 FREGU 20000.0 Hz  
 SCANS 305  
 ACQTH 0.205 sec  
 PO 1.898 sec  
 PW1 11.2 US  
 IRNUC 1H  
 CTEMP 23.3 C  
 SLVNT C4080  
 EXREF 0.00 ppm  
 BF 2.00 Hz  
 RGAIN 28  
 OPERATOR : \_\_\_\_\_



ZET2H2-MAN

Figure 3.19. 79 MHz  $^{29}\text{Si}\{^1\text{H}\}$ -NMR spectrum of  $\text{TpRuH}(\text{H}_2\text{SiEt}_2)(\text{PPh}_3)$  (21d)

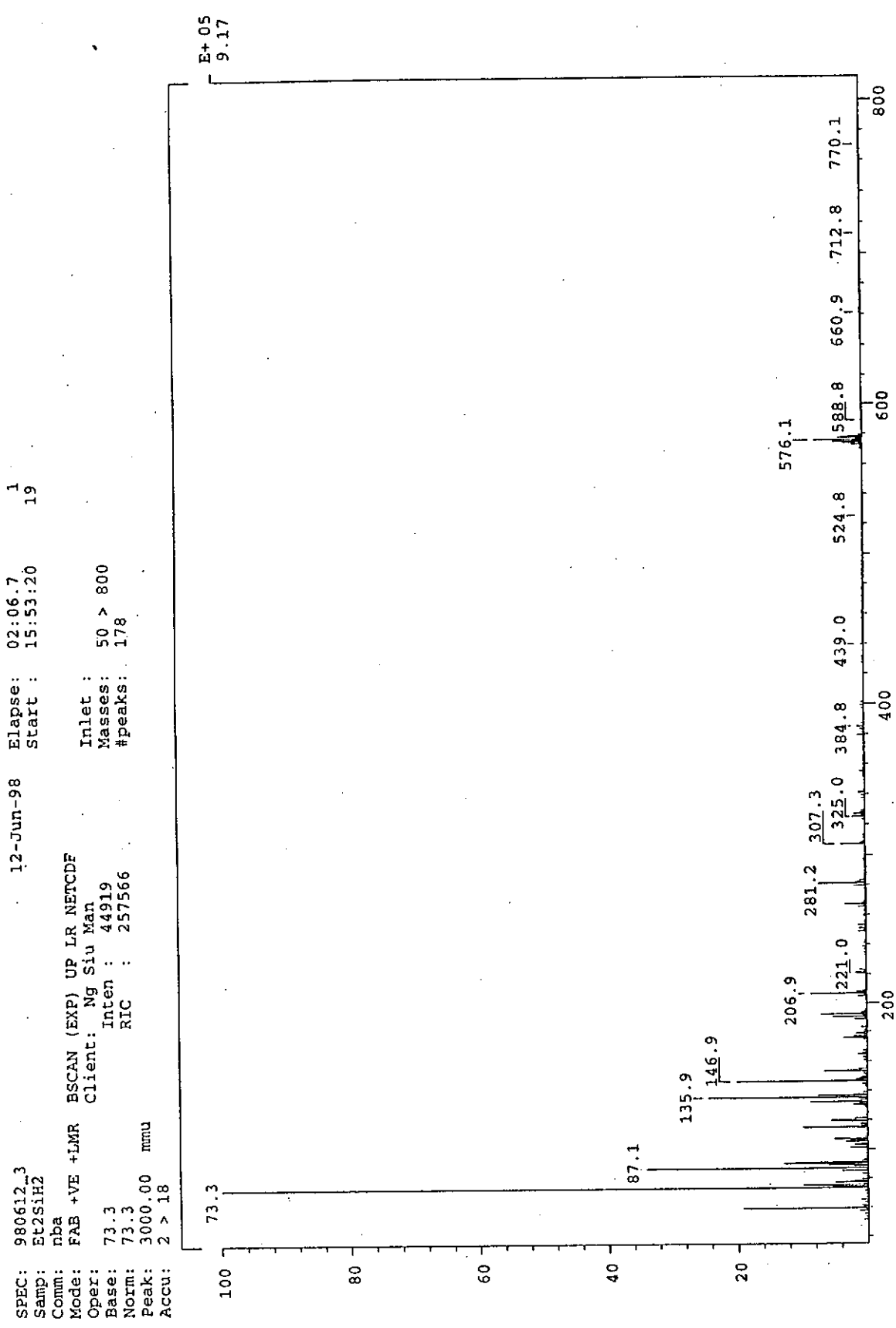


Figure 3.20. FAB mass spectrum of  $\text{TpRuH}(\text{H}_2\text{SiEt}_2)(\text{PPh}_3)$  (**21d**)

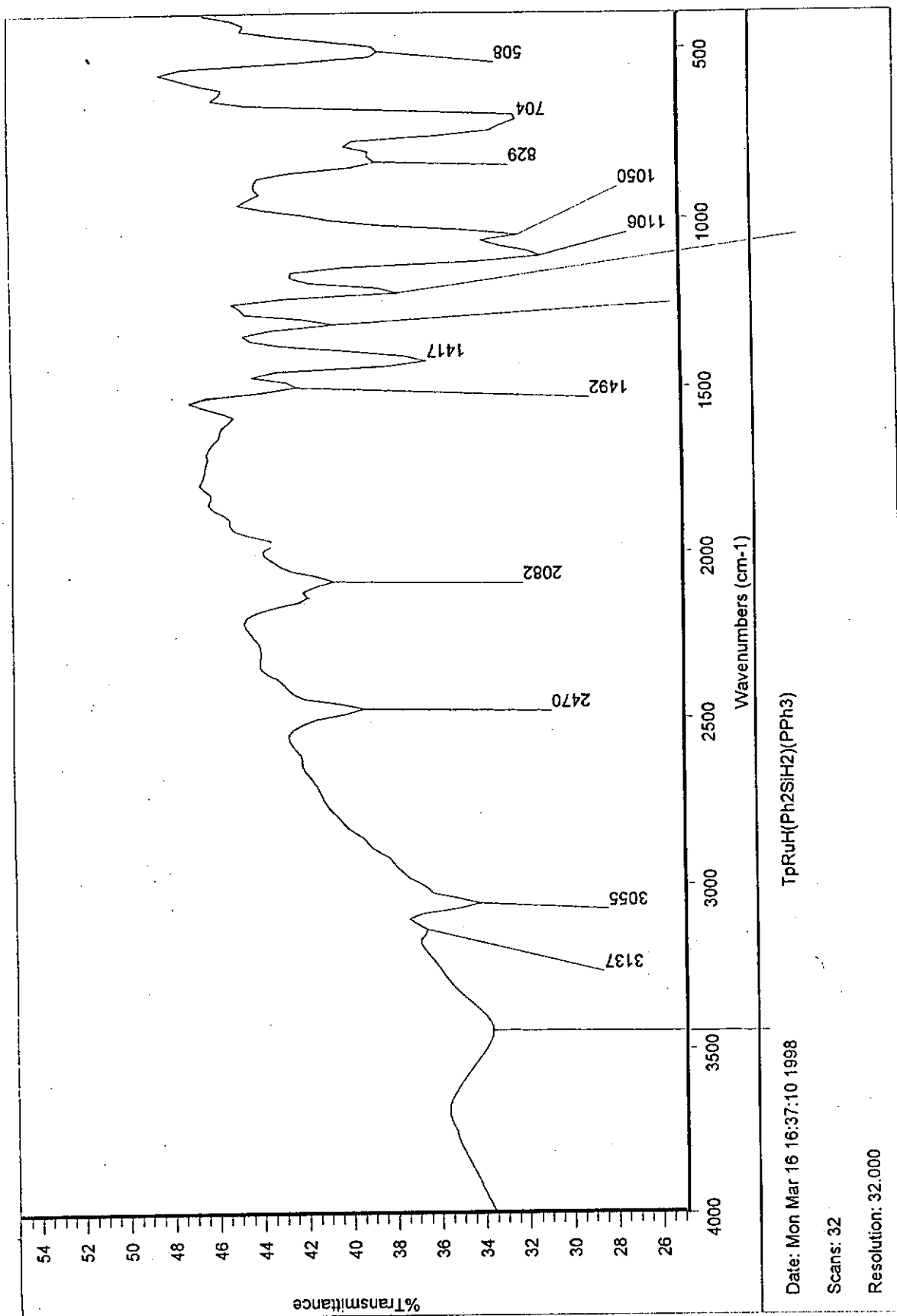


Figure 3.21. Infra-red spectrum of TpRuH(H<sub>2</sub>SiPh<sub>2</sub>)(PPh<sub>3</sub>) (21e) in KBr disc

TpRuH(H<sub>2</sub>SiPh<sub>2</sub>)(PPh<sub>3</sub>) in CD<sub>3</sub>Cl at R.T.

```

Current Data Parameters
NAME      PR251H2
EXPNO    1
PROCNO   1

F2 - Acquisition Parameters
Date_    980316
Time     14.37
INSTRUM  dx400
PROBHD   5 mm QNP 1H/
PULPROG  zg30
TD        32768
SOLVENT  THF
NS        64
DS        0
SWH       16025.641 Hz
FIDRES    0.489064 Hz
AQ        1.0224116 sec
RG         256
DM        31.200 usec
DE        4.50 usec
TE        300.0 K
P1        1.00000000 sec
P2        9.50 usec
P3        4.50 usec
SF01      400.1279593 MHz
NUC1      1H
PL1       -6.00 dB

F2 - Processing parameters
SI        16384
SF        400.1279593 MHz
WDW       EM
SSB       0
LB        0.30 Hz
GB        0
PC        1.00

ID NMR pict parameters
CX        20.00 cm
F1P       10.000 ppm
F1        4001.29 Hz
F2P       -15.000 ppm
F2        -6001.84 Hz
PPMCH     1.25000 ppm/cm
HZCM      500.18150 Hz/cm
  
```

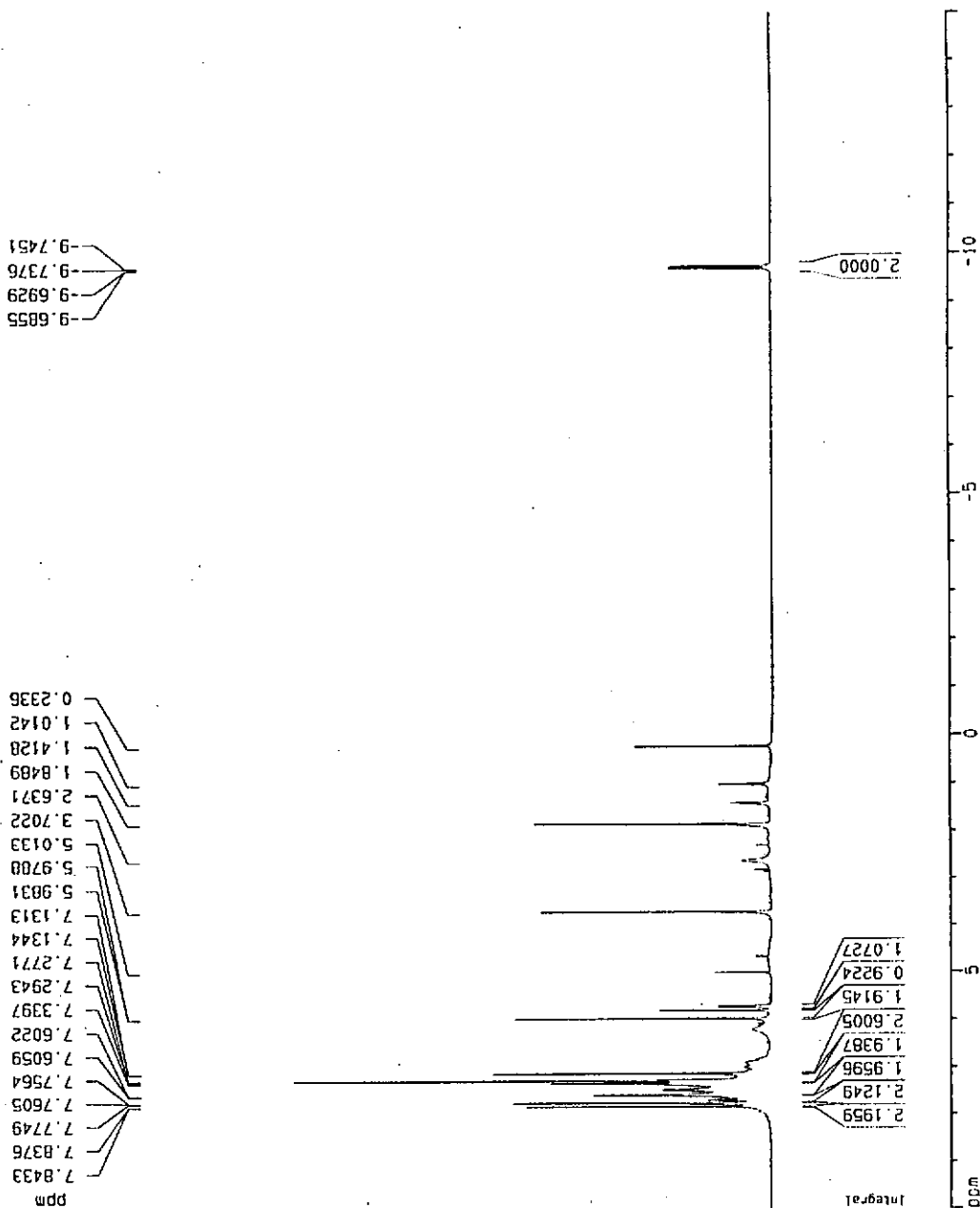


Figure 3.22(a). 400 MHz <sup>1</sup>H-NMR spectrum of TpRuH(H<sub>2</sub>SiPh<sub>2</sub>)(PPh<sub>3</sub>) (21e)

TORUH (H2S1P42) (PPH3) in d8-tmf at R.T.

```

Current Data Parameters
NAME      Ph2S1P2
EXPNO    1
PROCNO    1

F2 - Acquisition Parameters
Date_     980316
Time      14.37
INSTRUM   dx400
PROBHD    5 mm QNP 1H/
PULPROG   zg30
TD         32768
SOLVENT   THF
NS         64
DS         0
SINH       16025.141 Hz
FIDRES     0.489064 Hz
AQ         1.0224116 sec
RG         256
DK         31.200 usec
DE         4.50 usec
TE         300.0 K
D1         1.0000000 sec
F1         9.50 usec
DE         4.50 usec
SFO1       400.1279953 MHz
NUC1       1H
PL1        -6.00 dB

F2 - Processing parameters
SI         16384
SF         400.129222 MHz
RG         EM
SSB        0
LB         0.30 Hz
GB         0
PC         1.00

1D NMR plot parameters
CX         20.00 cm
F:P        -9.300 ppm
F1         -3721.20 Hz
F2P        -10.300 ppm
F2         -4121.33 Hz
FFTCM      0.05000 ppm/cm
HZCM       20.00546 Hz/cm
    
```

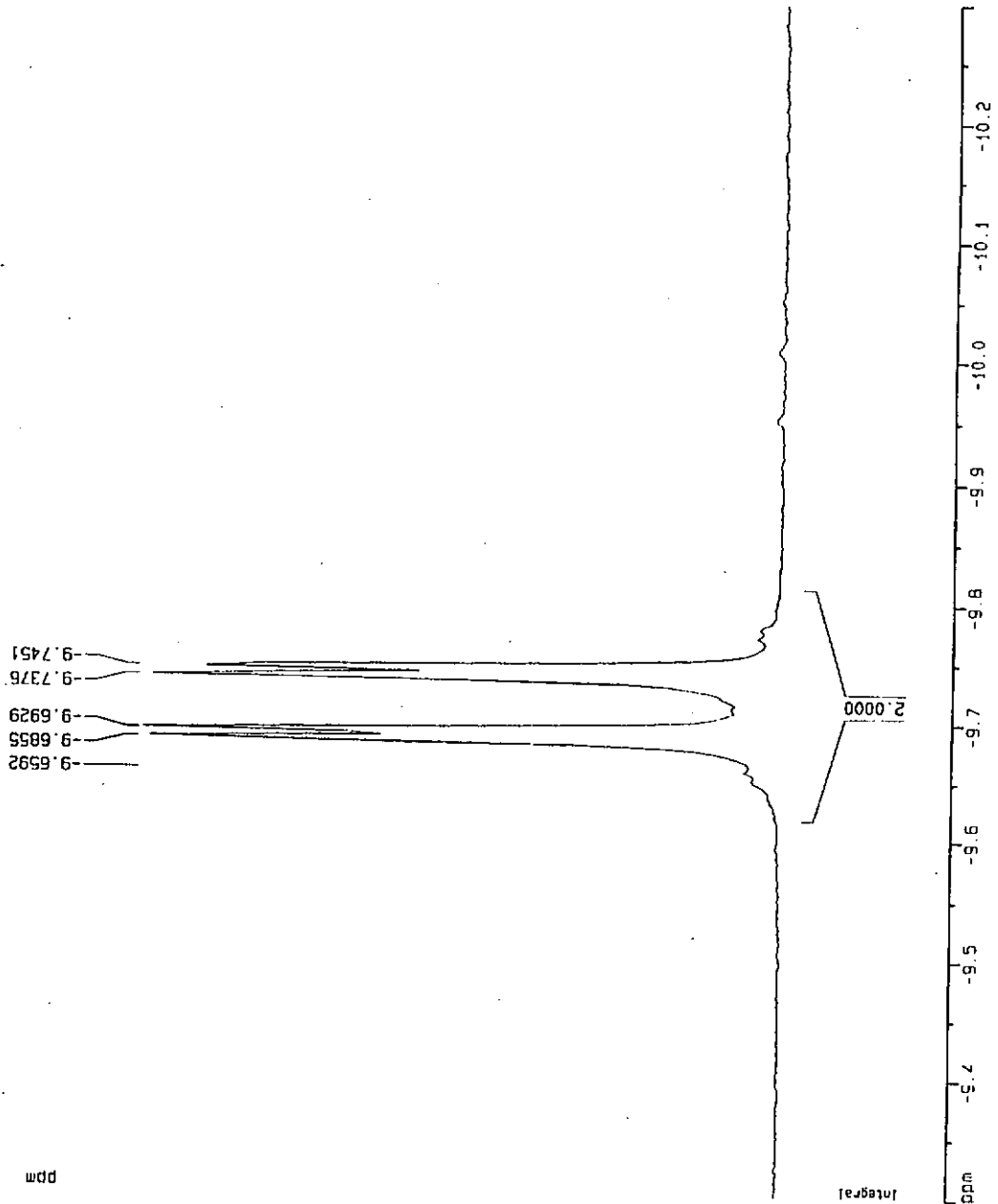


Figure 3.22(b). Expanded upfield region of Figure 3.22(a)

TPRuH(H<sub>2</sub>SiPH<sub>2</sub>)(PPh<sub>3</sub>) in d<sub>8</sub>-thf at R.T.

```

Current Data Parameters
NAME      PPh2SiH2
EXNO     1
PROCNO   1

F2 - Acquisition Parameters
Date_    980316
Time     14:39
INSTRUM  CPX400
PROBHD   5 mm QNP 1H/
PULPROG  zgpg30
TO       65536
SOLVENT  THF
NS       64
DS       2
SMH      64935.066 Hz
FIDRES   0.980830 Hz
AQ       0.5046772 sec
RG       9195.2
DM       7.700 usec
DE       4.50 usec
TE       300.0 K
SI       0.0300000 sec
Sf2      0.0000200 sec
PL13     120.00 dB
DI       1.00000000 sec
CPDPRG2  waltz16
PCPRG2   71.00 usec
SF02     400.1300000 MHz
NUC2     1H
PL2      120.00 dB
PL12     17.00 dB
P1       7.20 usec
DE       4.50 usec
SF01     161.9755930 MHz
NUC1     31P
PL1      -6.00 dB

F2 - Processing parameters
SI       32768
SF       161.9755935 MHz
WDW      EM
SSB      0
LB       3.00 Hz
GB       0
PC       1.40

1D NMR dict parameters
CX       20.65 cm
F1P      100.000 ppm
F1       16197.98 Hz
F2P      -50.000 ppm
F2       -8099.78 Hz
PPMCHK   7.24955 ppm/cm
HZCM     1174.31655 Hz/cm
  
```

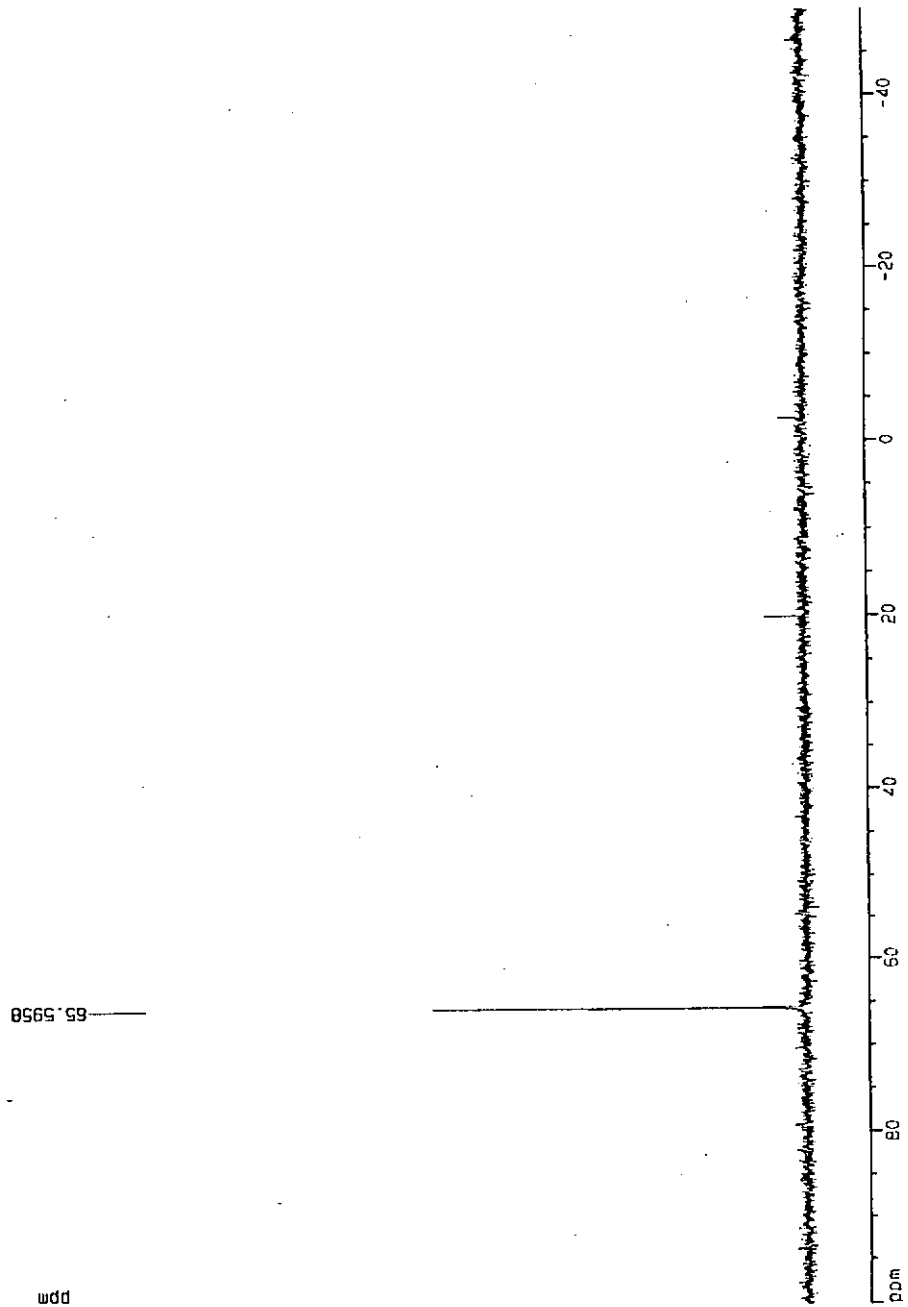


Figure 3.23. 161 MHz <sup>31</sup>P{<sup>1</sup>H}-NMR spectrum of TpRuH(H<sub>2</sub>SiPh<sub>2</sub>)(PPh<sub>3</sub>) (21e)



30-APR-98 10:02:49  
 DFIL ABC  
 06NUC 29SI  
 EXNOO DEPT  
 OFR 79.50 MHz  
 OBSET 125.00 KHZ  
 DBFIN 13609.3 Hz  
 POINT 16384  
 FREQU 20000.0 Hz  
 SCANS 17916  
 ADOTH 0.205 sec  
 PD 1.698 sec  
 PK1 11.2 JS  
 IRNUC 1H  
 CTEMP 21.7 c  
 SLVNT C-080  
 EXREF 0.00 ppm  
 BF 2.00 Hz  
 RGAIN 28  
 OPERATOR :

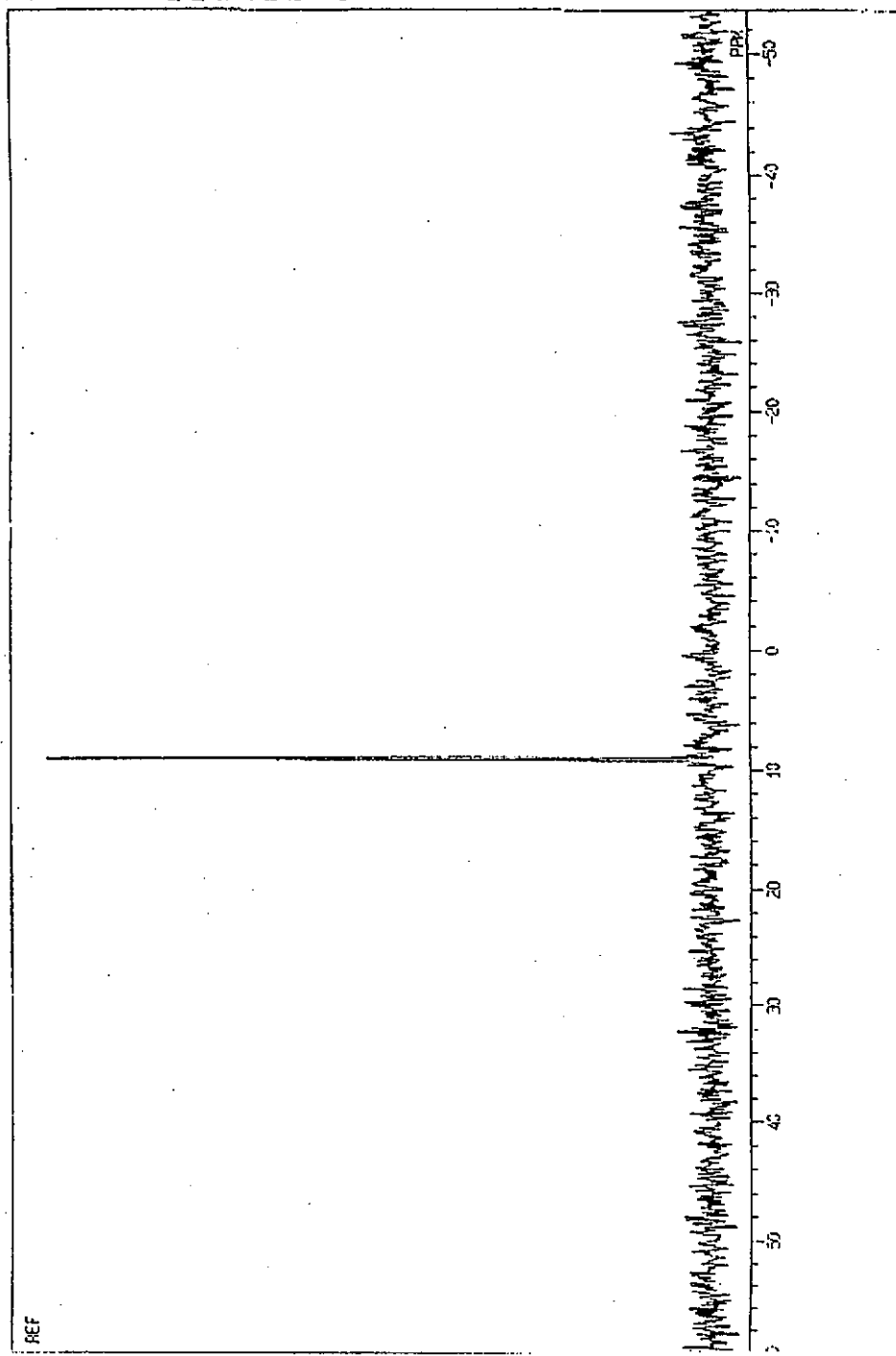


Figure 3.24. 79 MHz  $^{29}\text{Si}\{^1\text{H}\}$ -NMR spectrum of  $\text{TpRuH}(\text{H}_2\text{SiPh}_2)(\text{PPh}_3)$  (**21e**)

SPEC: cp980416\_5  
 Samp: nba as matrix  
 Conn: FAB, pos, 100-1000  
 Mode: FAB +VE +LMR BSCAN (EXP) UP LR NETCDF  
 Oper: Client: Ng siu man  
 Base: 183.2  
 Norm: 183.2  
 Peak: 3000.00 mmu  
 Accu: 2 > 16  
 16-Apr-98 Elapse: 03:03.9 1  
 Start : 17:31:37 19  
 Study : Ph2SiH2  
 Inlet :  
 Masses: 100 > 1000  
 #peaks: 975

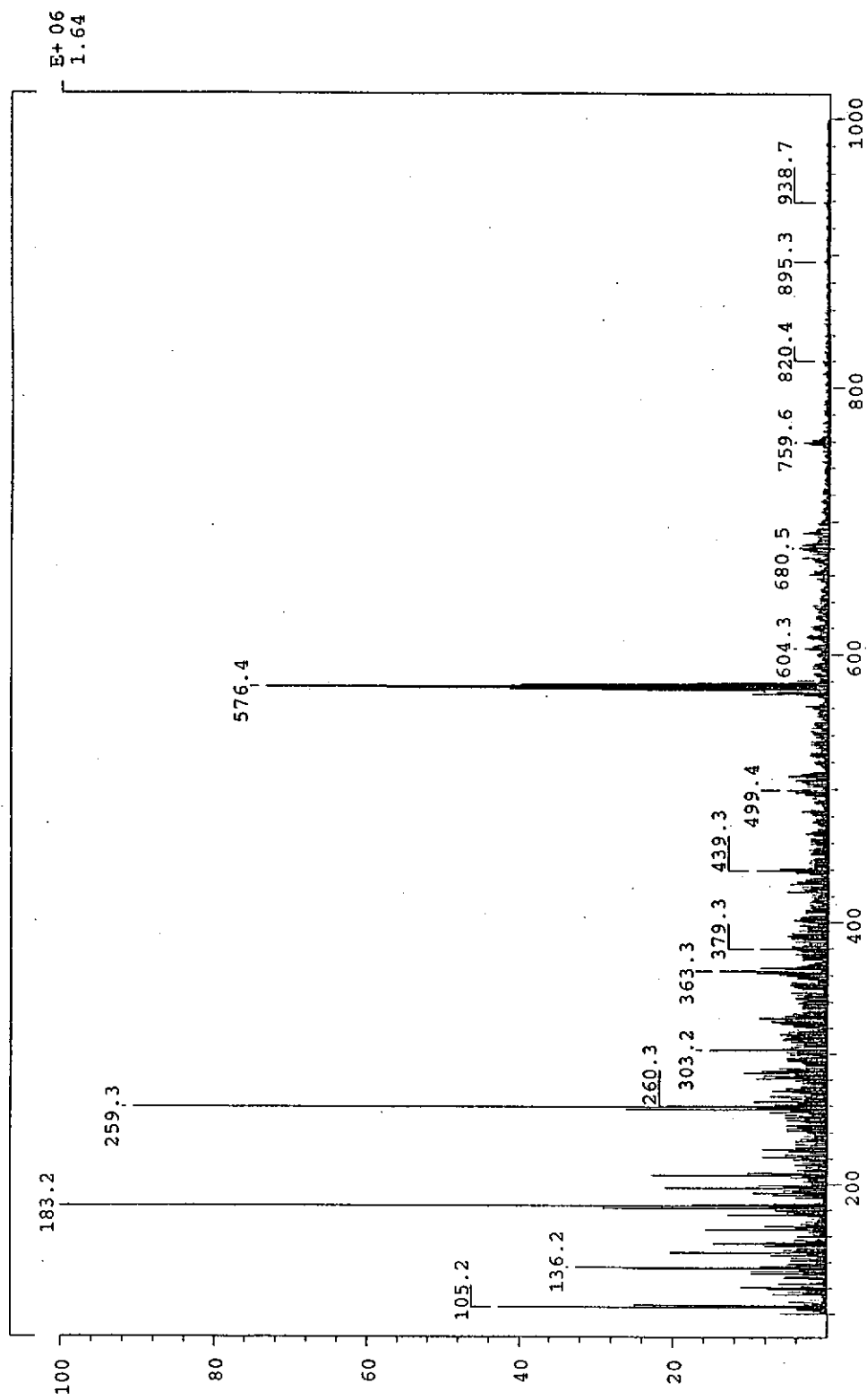


Figure 3.25. FAB mass spectrum of  $\text{TpRuH}(\text{H}_2\text{SiPh}_2)(\text{PPh}_3)$  (21e)

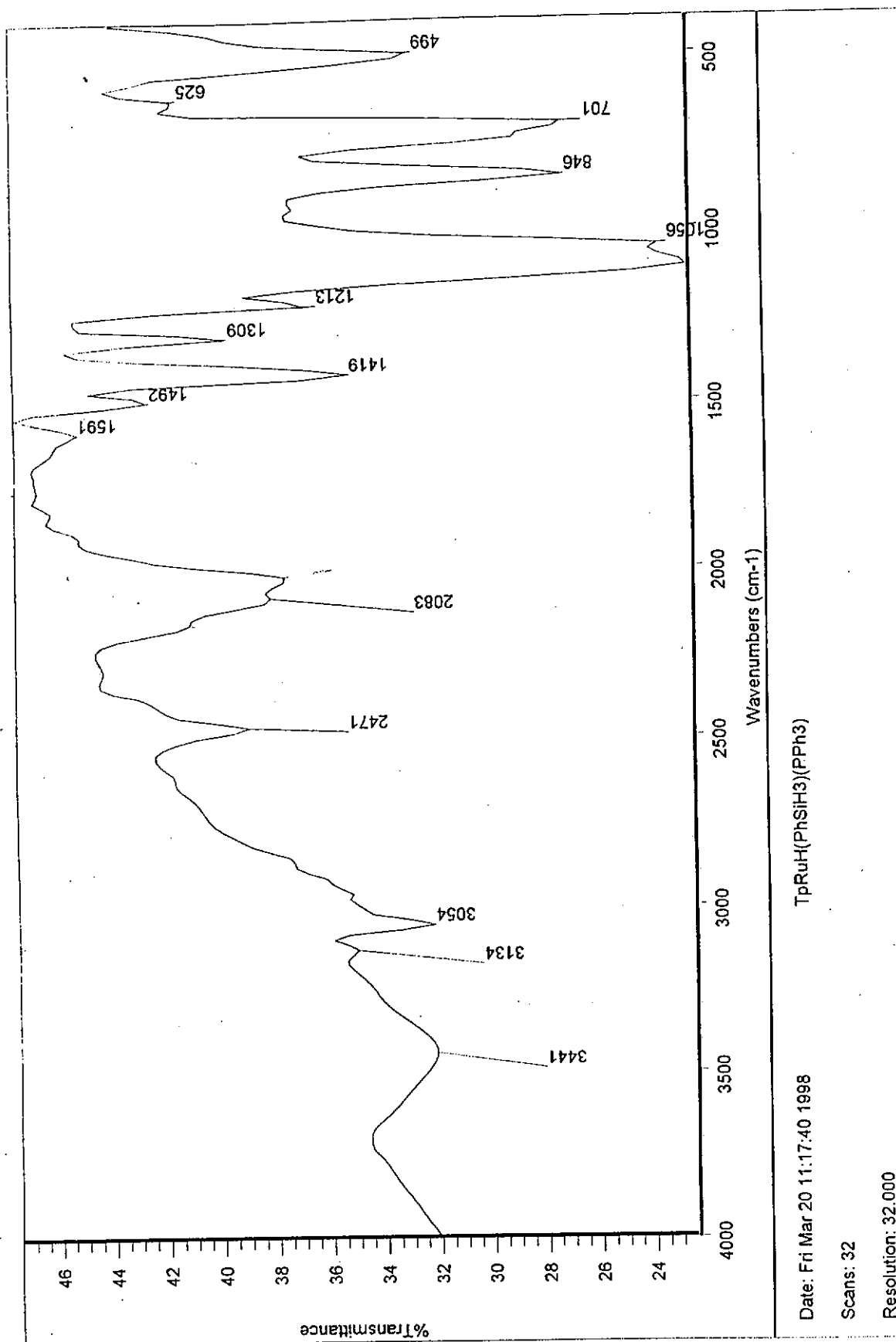


Figure 3.26. Infra-red spectrum of TpRuH(H<sub>3</sub>SiPh)(PPh<sub>3</sub>) (21f) in KBr disc

TpRuH(H<sub>3</sub>SiPh)(PPh<sub>3</sub>) in d8-tmf

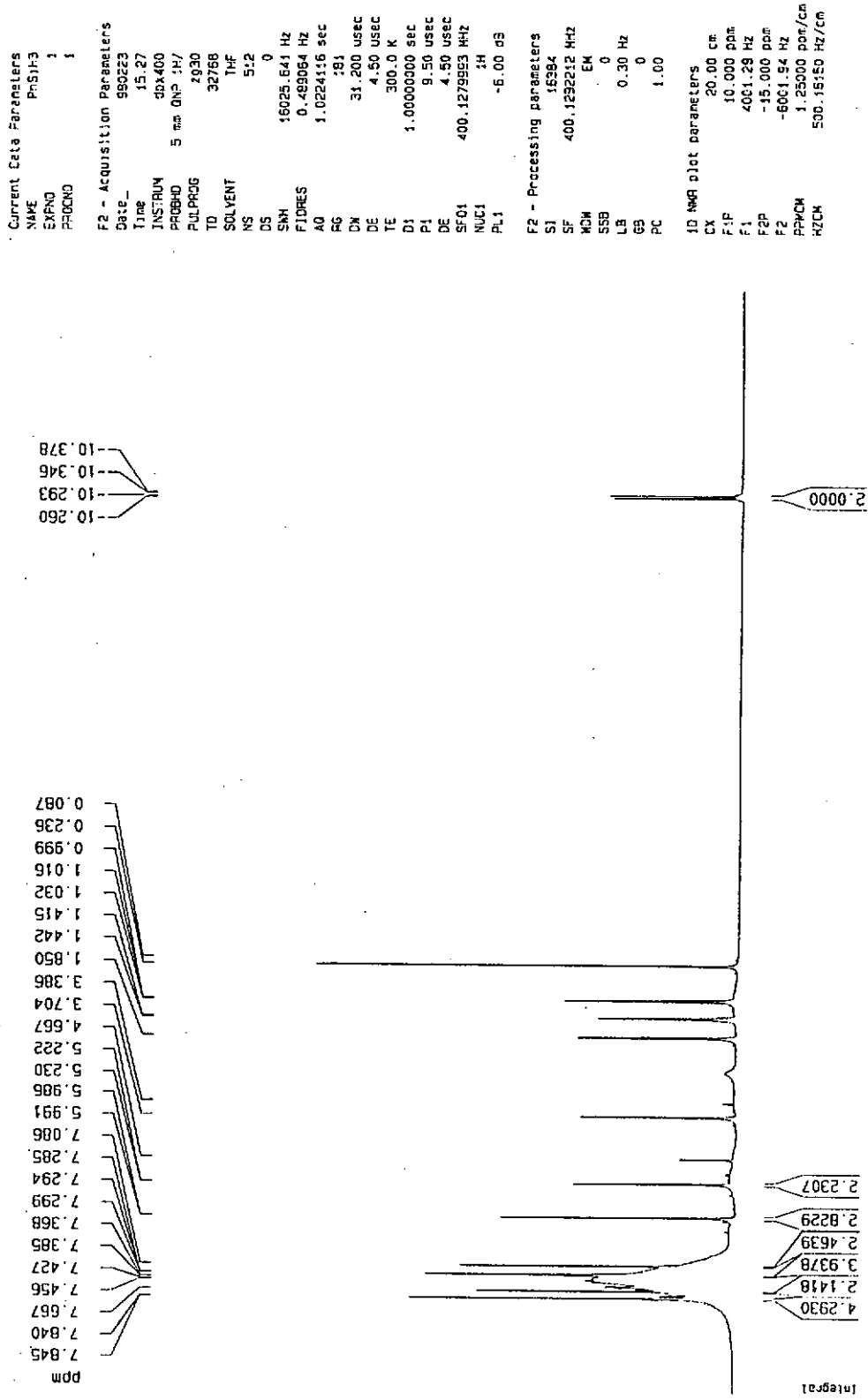


Figure 3.27(a). 400 MHz <sup>1</sup>H-NMR spectrum of TpRuH(H<sub>3</sub>SiPh)(PPh<sub>3</sub>) (**21f**)

TpRvH (H3S,Ph) (PPn2) in d8-tHf

```

Current Data Parameters
NAME          PnSjH3
EXPNO        1
PROCNO       1

F2 - Acquisition Parameters
Date_        990223
Time         15.27
INSTRUM      QNP400
PROBHD       5 mm QNP 1H/
PULPROG      zg30
TO           32766
SOLVENT      THF
NS           512
DS           0
SAH          16025.641 Hz
FIDRES       0.489064 Hz
AQ           1.0224116 sec
RG           181
CW           31.200 USEC
DE           4.50 USEC
TE           300.0 K
D1           1.00000000 sec
F1           9.50 USEC
DE           4.50 USEC
SFO1         400.1279993 MHz
NUC1         1H
PL1          -6.00 dB

F2 - Processing parameters
SI           16384
SF           400.125212 MHz
WDW          EM
SSB          0
LB           0.30 Hz
GB           0
PC           1.00

1D NMR list parameters
CX           20.00 cm
F1P          -9.500 ppm
F1           -981.23 Hz
F2P          -11.000 ppm
F2           -4461.42 Hz
PP4M        0.07500 ppm/cm
HZCM        30.00969 Hz/cm
  
```

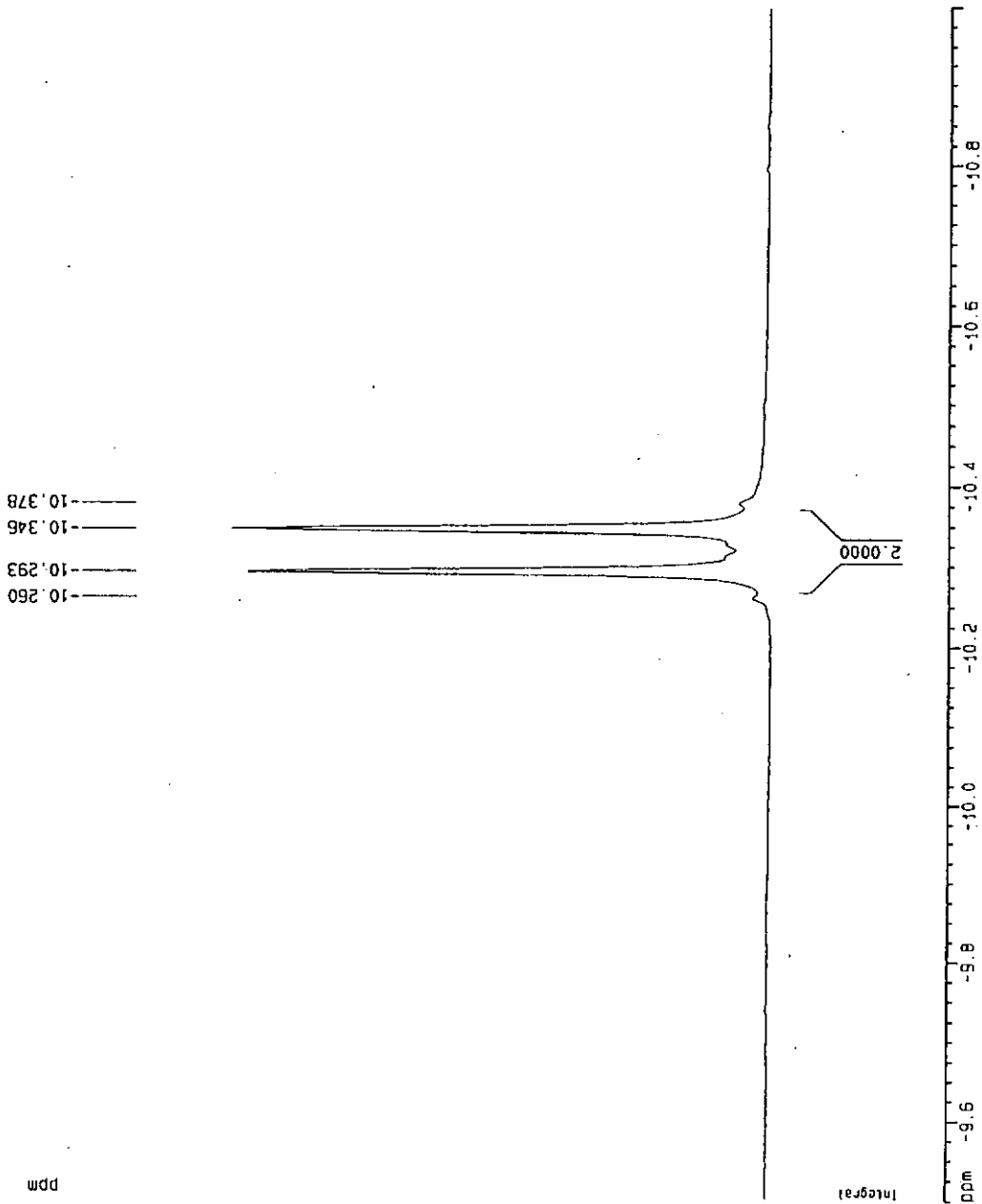
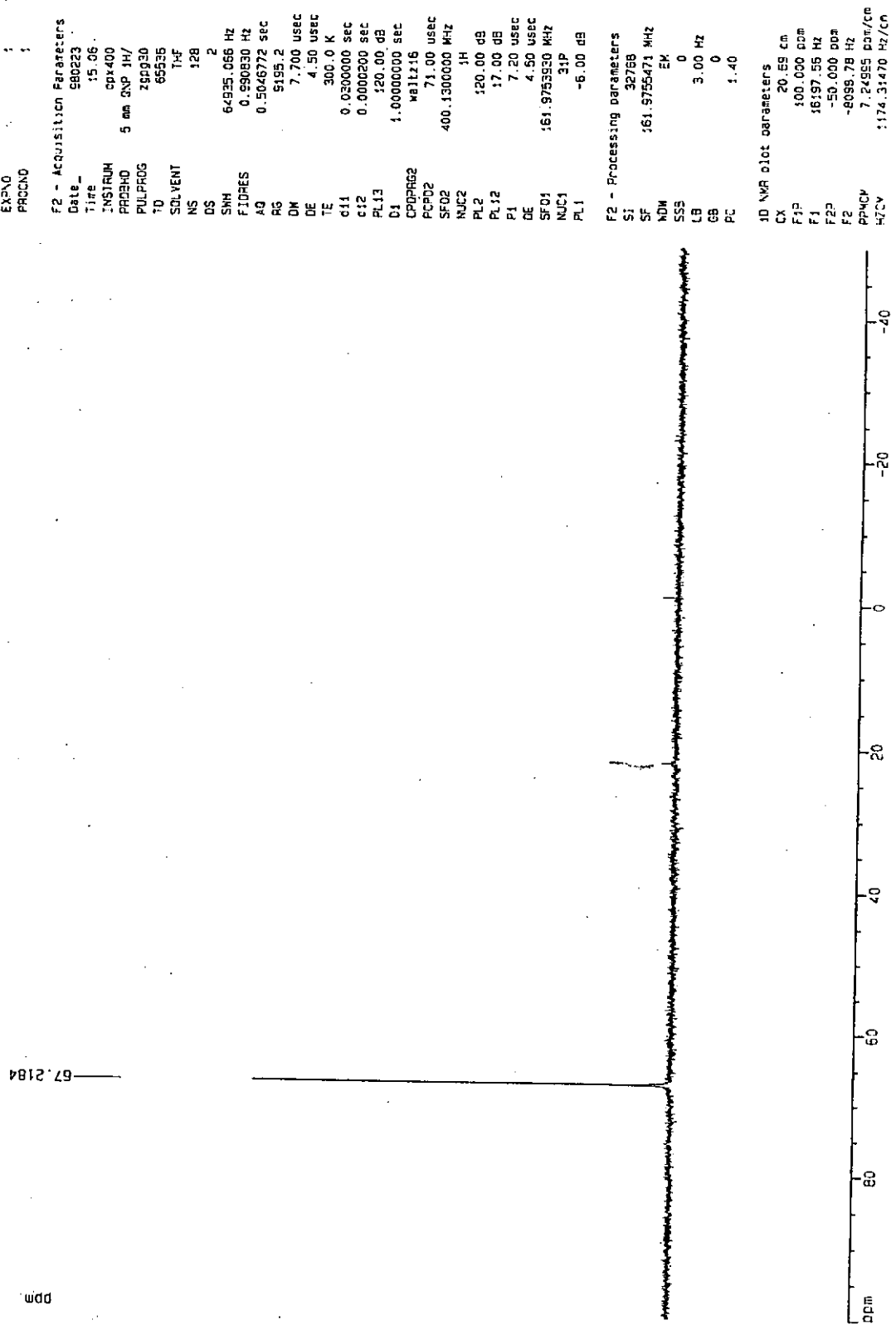


Figure 3.27(b). Expanded upfield region of Figure 3.27(a)

TpRuH(H3SiPh)(PPh3) in d8-thf



```

Current Data Parameters
NAME      PPH3H3
EXPNO    1
PROCNO   1

F2 - Acquisition Parameters
Date_    980223
Time     15.06
INSTRUM  gp400
PROBHD   5 mm QNP 1H/
PULPROG  zgpg30
TD        65536
SOLVENT  THF
NS        128
DS        2
SWH       64935.066 Hz
FIDRES    0.590830 Hz
AQ        0.5046772 sec
RG        5195.2
DM        7.700 USEC
DE        4.50 USEC
TE        300.0 K
c11       0.030000 sec
c12       0.000200 sec
PL13      120.00 dB
D1        1.0000000 sec
CPDPRG2  waltz16
PCPD2     71.00 usec
SF02      400.1300000 MHz
NUC2      1H
PL2       120.00 dB
PL12      17.00 dB
P1        7.20 usec
DE        4.50 USEC
SF01      161.9755320 MHz
NUC1      31P
PL1       -6.00 dB

F2 - Processing parameters
SI        32768
SF        161.9755471 MHz
EK        EM
SSS       0
LB        3.00 Hz
GB        0
PC        1.40

1D NMR plot parameters
CX        20.59 cm
F1P       100.000 02m
F1        16197.55 Hz
F2P       -50.000 00m
F2        -8088.78 Hz
PPHVCY   7.2495 02m/cm
HZCV      1174.31470 Hz/cm
    
```

Figure 3.28. 161 MHz  $^{31}\text{P}\{^1\text{H}\}$ -NMR spectrum of  $\text{TpRuH}(\text{H}_3\text{SiPh})(\text{PPh}_3)$  (**21f**)

21-MAY-99 23:50:14  
 CFIL 45C  
 DENUC 29SI  
 EXMOD DEPT  
 OFR , 79.30 MHz  
 OBSET 115.00 kHz  
 OBFIN 13609.3 Hz  
 POINT 15384  
 FREQ 20000.0 Hz  
 SCANS 17371  
 ACQTM 0.205 sec  
 PD 1.898 sec  
 PK1 11.2 us  
 IRNUC 1H  
 CTEMP 25.7 c  
 SLYNT C4080  
 EXREF 0.00 ppm  
 SF 2.00 Hz  
 RGAIN 30  
 OPERATOR :

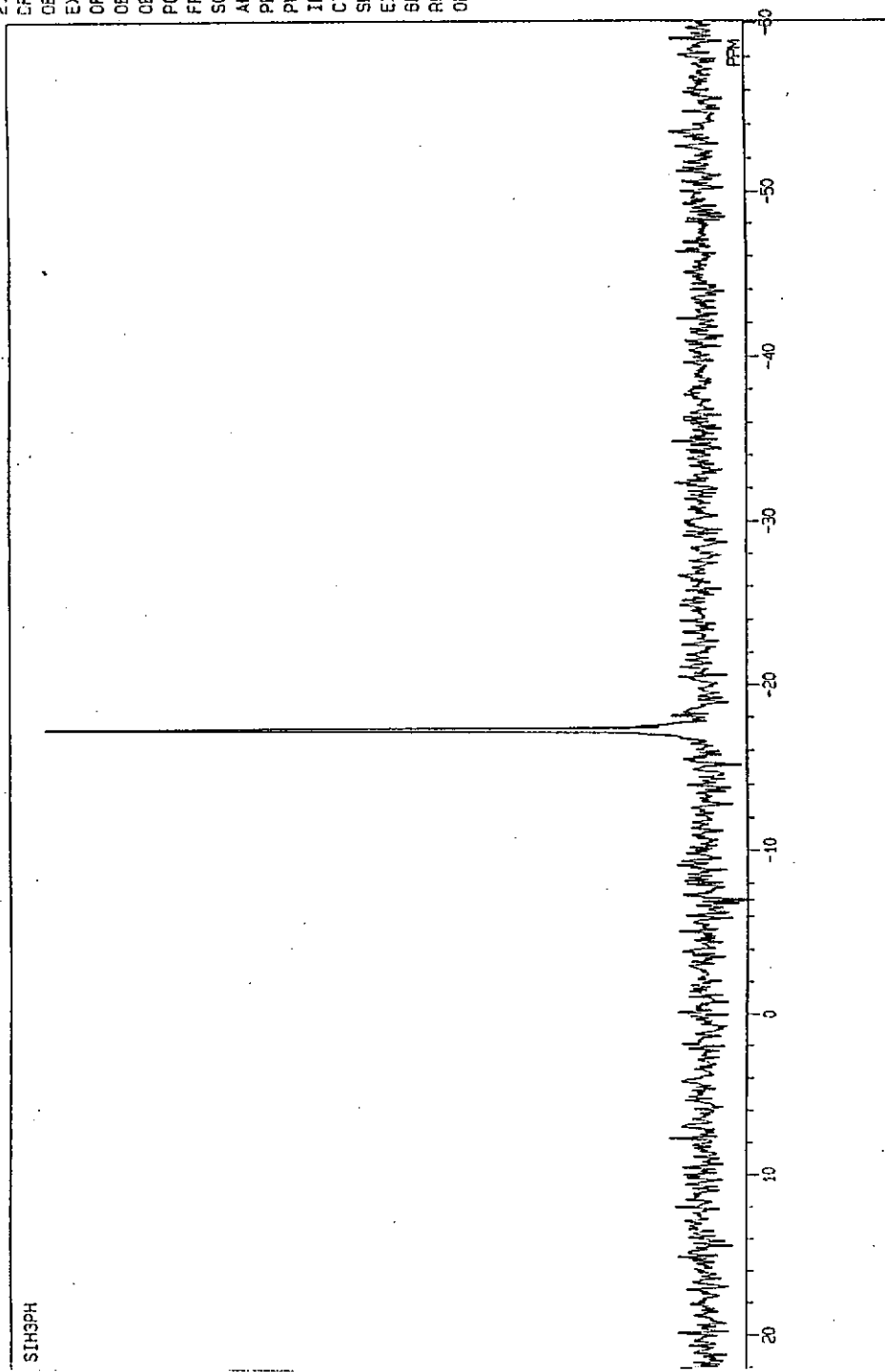


Figure 3.29. 79 MHz  $^{29}\text{Si}\{^1\text{H}\}$ -NMR spectrum of  $\text{TpRuH}(\text{H}_3\text{SiPh})(\text{PPh}_3)$  (**21f**)

SPEC: cp980416\_6  
 Samp: nba as matrix  
 Comm: FAB, pos, 100-1000  
 Mode: FAB +VE +LMR BSCAN (EXP) UP LR NETCDF  
 Oper: Client: Ng siu man  
 Base: 183.2 Inten: 25987  
 Norm: 183.2 RIC : 380186  
 Peak: 3000.00 mmu  
 Accu: 2 > 19

16-Apr-98 Elapse: 03:26.8 1  
 Start : 17:57:22 20

Study : PhSiH3  
 Inlet :  
 Masses: 100 > 1000  
 #peaks: 577

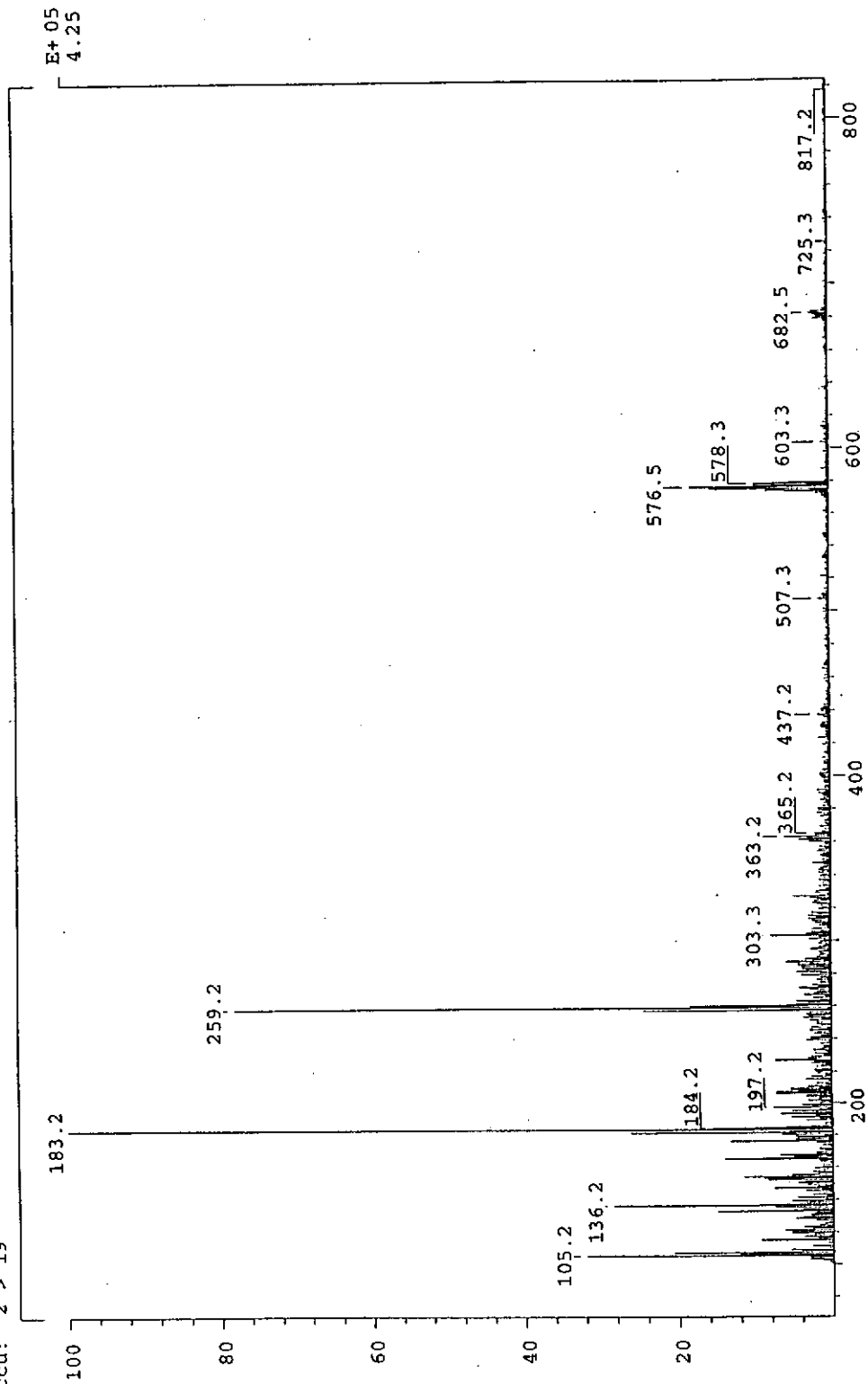


Figure 3.30. FAB mass spectrum of  $\text{TpRuH}(\text{H}_3\text{SiPh})(\text{PPh}_3)$  (21f)



## ***Publication***

1. Ng, S. M.; Fang, Y. Q.; Lau, C. P.; Wong, W. T.; Jia, G. 'Synthesis, Characterization, and Acidity of Ruthenium Dihydrogen Complexes with 1,4,7-Triazacyclononane, 1,4,7-Trimethyl-1,4,7-Triazacyclononane, and Hydrotris(pyrazolyl)borato Ligand' *Organometallics* **1998**, *17*, 2052-2059.
2. Chan, W. C.; Lau, C. P.; Chen, Y. Z.; Fang, Y. Q.; Ng, S. M.; Jia, G. 'Synthesis and Characterization of Hydrotris(1-pyrazolyl)borate of Dihydrogen Complexes of Ruthenium and Their Roles in Catalytic Hydrogenation Reactions' *Organometallics* **1997**, *16*, 34-44.